Mouse Models to Deplete or Label Dendritic Cells via Genetic Manipulation of the *Clec9a* Locus

Janneke Marije van Blijswijk

University College London
and
Cancer Research UK London Research Institute
PhD Supervisor: Dr. Caetano Reis e Sousa

A thesis submitted for the degree of
Doctor of Philosophy
University College London
September 2015

Declaration

I Janneke Marije van Blijswijk confirm that the work presented in this thesis is my own. Where information has been derived from other sources, I confirm that this has been indicated in the thesis.

Abstract

Dendritic cells (DCs) play important roles at the interface between innate and adaptive immunity by priming and directing T cell responses. Much of our current knowledge of DC biology has come from mouse models in which DCs can be genetically manipulated, labelled or ablated. Here, novel models are presented using a strategy that targets DC precursors via genetic editing of the *Clec9a* locus. While validating a novel mouse model to inducibly deplete DCs using diphtheria toxin receptor (DTR) expression driven by *Clec9a*, it became clear that these Clec9a$^{+/Cre}$ROSA^{iDTR} mice suffer from unexpected lymph node (LN) hypocellularity and reduced frequencies of DCs in LNs, even in the absence of diphtheria toxin (DT) injection. This phenotype turned out to be a common feature of other mouse models in which DTR is expressed on DCs (e.g. CD11c-DTR and Langerin-DTR mice) and raises questions about the interpretation of results obtained with such animals. Therefore, in an alternative approach, mice were developed to constitutively lack DCs by expressing the diphtheria toxin alpha (DTA) subunit under control of the *Clec9a* locus. Unfortunately, these mice still harboured DCs and only showed partial reduction of one DC subset.

Finally, seeding of tissues by DC precursors was examined. Clec9a$^{+/Cre}$ROSA$^{+/confetti}$ mice were generated in which DC precursors stochastically express one of four fluorescent proteins, which is inherited by its daughter cells. 8-Colour microscopy of tissue sections and histo-cytometry analysis of the images was developed to analyse these mice. This approach will be used to determine how many daughter cells are produced when a single DC precursor seeds the small intestine (clonal burst size), whether these daughters are found among different DC subsets and whether seeding changes during inflammation.

In summary, manipulation of the *Clec9a* locus proves to be an excellent way to study the DC lineage and DC precursor behaviour in the mouse.

Acknowledgement

Time flies when you're having fun, they say. And the past four years have definitely flown by. I thoroughly enjoyed my time in the lab, and never regretted starting a PhD.

I would like to thank all members, past and present, of the Immunobiology lab: Annemarthe, Barbara, Caetano, Delphine, Jan, Jan, Jatta, Julie, Kathryn, Naren, Neil, Oliver, Oliver, Paul, Pavel, Pierre, Safia, Santiago, Sonia, Sophie, Steve and Susan. You taught me everything I know about immunology and are never short of advice or a helping hand. You are also the people who give a heart and a soul to the lab and make it such a wonderful place to work. Without my colleagues and friends this thesis would never have existed!
A big thank you Barbara for teaching a non-immunologist everything about dendritic cell subsets and their seemingly endless list of markers, for showing how to find lymph nodes in a mouse (I managed!), for introducing me to the wonderful world of FACS, for spending numerous hours discussing my projects, for all the small talk, for… for… Now you are a world-class group leader yourself and I am sure you will do brilliantly!
Thanks to Sonia, Kat and Steve for being perfect lab managers and Alice and Helen for being awesome research administrators. I probably do not even fully realise how much easier you made my life. You managed to deal with even the most random issues without blinking an eye and are always available for a chat. I would also like to thank Neil here for making the mouse work in this thesis at all possible. Your knowledge of mice and mouse experiments is unprecedented.

Thank you to all my fellow PhD students (Aldona, Ania, Ichha, Justin, Kristyna, Marianne, Mauro, Molly, Nil, Pavel, Rute, Sakshi, Steffi, Yaiza…) for sharing this experience with me. During these four years you were not only here to discuss science and put lab life into perspective, but also to enjoy life in London.

I special thank you is in place for the organisations that funded and facilitated my PhD: Cancer Research UK London Research Institute (now the Francis Crick Institute) and the Boehringer Ingelheim Fonds. I would also like to mention all the core facilities in the institute for invaluable support, especially the members of the flow cytometry facility, the light microscopy facility, the transgenics facility and the animal facility.
I would like to thank my thesis committee, Adrian Hayday and Axel Behrens, for your constructive support and valuable advice, and my collaborators Ronald Germain, Michael Gerner, Erik Sahai and Robert Jenkins for your critical contributions to the 'Confetti project'.

Also a big thank you to my family, who continue to support me, who are mildly confused when I talk about my work and who still laugh at me when I am using English words when speaking Dutch.

And last but not least, I would like to thank Caetano for giving me the opportunity to do my research project in your lab and be part of this amazing group of people. You have been a great mentor during my PhD and always encouraged me to think independently and develop as a researcher and person.

Table of Contents

Abstract **3**
Acknowledgement **4**
Table of Contents **5**
Table of figures **7**
List of tables **10**
Abbreviations **11**
Chapter 1. Introduction **14**
1.1 Dendritic cells in the mouse **14**
1.1.1 Dendritic cell subsets 14
1.1.2 Cytokine and transcription factor dependency of dendritic cell subsets 31
1.1.3 Dendritic cell ontogeny 35
1.1.4 Functions of dendritic cells 41
1.2 Mouse models to study dendritic cells **58**
1.2.1 Introduction to Cre-loxP system 59
1.2.2 DTR-based mouse models to constitutively or inducibly deplete dendritic cells 60
1.2.3 Fluorescence-based models to track dendritic cells 66
1.2.4 Transcription factor knockout mice to study DC function 69
1.2.5 Chemokine (receptor) knockout mice to study DC function 71
1.2.6 Models to trace the dendritic cell lineage 73
1.3 Aims and objectives **74**
Chapter 2. Materials & Methods **76**
2.1 Mice **76**
2.1.1 Mouse strains used 76
2.1.2 Mouse generation 76
2.1.3 DT treatment 78
2.1.4 Tamoxifen treatment 78
2.1.5 Influenza Infection 79
2.1.6 CFA/OVA immunisation 79
2.1.7 Mixed BM chimeras 79
2.2 Flow cytometry **80**
2.2.1 Cell isolation 80
2.2.2 Counting of cell suspensions 81
2.2.3 MACS enrichment 81
2.2.4 Antibodies for Flow Cytometry 82
2.2.5 Flow Cytometry analysis 84
2.3 Microscopy **87**
2.3.1 Antibodies used for microscopy 87
2.3.2 Confocal microscopy 88
2.3.3 Fixation with PLP and staining of sections for histo-cytometry 88
2.3.4 Histo-cytometry 89
2.4 Miscellaneous **89**
2.4.1 IFNγ ELISA 89
2.4.2 Flt3L BMDC culture 90

2.4.3 Transwell Assay 91
2.4.4 Southern Blot 91
2.4.5 Semi-quantitative RT-PCR 93
2.4.6 Statistical analyses 94
Chapter 3. A Novel Mouse Model to Inducibly Deplete Dendritic Cells 95
3.1 Introduction 95
3.2 DT injection efficiently depletes DCs but no other cells in spleens of Clec9a$^{+/Cre}$ROSA^{iDTR} mice 96
3.3 LNs of Clec9a$^{+/Cre}$ROSA^{iDTR} mice show hypocellularity and reduced frequencies of DCs 99
3.4 In mixed bone marrow chimeras the phenotype of Clec9a$^{+/Cre}$ROSA^{iDTR} BM is dominant over WT BM 105
3.5 Other mice that express DTR on DCs also show LN hypocellularity and reduced DC frequencies 108
3.6 Mice that express DTR on B cells or Tregs do not show a profound LN hypocellularity or reduced DC frequencies 113
3.7 Clec9a$^{+/Cre}$ROSA^{iDTR} mice can mount normal immune responses upon immunisation or infection 115
3.8 What is the mechanism by which DTR expression confers LN abnormalities? 121
3.9 Discussion 126
Chapter 4. A Novel Mouse Model to Constitutively Ablate Dendritic Cells129
4.1 Introduction 129
4.2 Generation of Clec9a-DTA mice to constitutively ablate DCs 130
4.3 Characterisation of Clec9a-DTA mice 132
4.4 Discussion 138
Chapter 5. Fate Mapping of Single Dendritic Cell Precursors in the Small Intestine 140
5.1 Introduction 140
5.2 Generation of Clec9a-CreERT2 mice to allow for temporal control over Cre recombination 141
5.3 Characterisation of Clec9a-CreERT2 mice 145
5.4 Histo-cytometric analysis of DC precursor fate in the small intestine using Clec9a$^{+/Cre}$ROSA$^{+/confetti}$ mice 149
5.5 Discussion 165
Chapter 6. Discussion 170
6.1 How to classify mononuclear phagocytes? 170
6.2 The perfect mouse model to study dendritic cell biology 175
Chapter 7. Appendix 181
Reference List 182

Table of figures

Figure 1.1 Overview of mononuclear phagocytes in spleen and lymph node 19
Figure 1.2 Overview of mononuclear phagocytes in the skin 24
Figure 1.3 Overview of mononuclear phagocytes in the intestine 27
Figure 1.4 Overview of mononuclear phagocytes in the lung 30
Figure 1.5 Ontogeny of mononuclear phagocytes 39
Figure 2.1 Flow cytometry gating strategy to identify DCs in lymphoid organs 85
Figure 2.2 Flow cytometry gating strategy to identify DCs in non-lymphoid tissues 86
Figure 2.3 Flow cytometry gating strategy to identify DC progenitors in the BM 87
Figure 3.1 Efficient DC depletion in spleens of DT-injected Clec9a$^{+/Cre}$ROSA^{iDTR} mice 97
Figure 3.2 Clec9a$^{+/Cre}$ROSA^{iDTR} mice do not show neutrophilia or monocytosis upon DT injection 98
Figure 3.3 Other immune cells are not affected in the spleen of DT-injected Clec9a$^{+/Cre}$ROSA^{iDTR} mice 99
Figure 3.4 sdLNs of PBS-injected Clec9a$^{+/Cre}$ROSA^{iDTR} mice show a reduction in DCs 100
Figure 3.5 LNs but not spleen or thymus of Clec9a$^{+/Cre}$ROSA^{iDTR} mice display reduced DC frequencies 102
Figure 3.6 Epidermis, dermis, small intestine and Peyer's patches of Clec9a$^{+/Cre}$ROSA^{iDTR} mice do not have reduced frequencies of DCs 103
Figure 3.7 LNs, but not spleen or thymus, are hypocellular in Clec9a$^{+/Cre}$ROSA^{iDTR} mice 104
Figure 3.8 LNs of Clec9a$^{+/Cre}$ROSA^{iDTR} mice show an altered T/B cell ratio, but maintain LN organisation 104
Figure 3.9 Reduced migDC frequency in LNs and LN hypocellularity is maintained in old Clec9a$^{+/Cre}$ROSA^{iDTR} mice 105
Figure 3.10 In mixed BM chimeras the phenotype conferred by Clec9a$^{+/Cre}$ROSA^{iDTR} BM is dominant 106
Figure 3.11 LNs of mixed BM chimeras reconstituted with Clec9a$^{+/Cre}$ROSA^{iDTR} and WT BM show hypocellularity 107

Figure 3.12 Clec9a$^{+/cre}$ROSA^{YFP} mice do not show hypocellularity or reduced DC frequency of LNs 108
Figure 3.13 CD11c-Cre^{+ve}ROSA^{iDTR} mice show LN hypocellularity and reduced DC frequency in LNs 109
Figure 3.14 CD11c-DTR mice show LN hypocellularity and reduced DC frequency in LNs 110
Figure 3.15 Langerin-DTR mice show hypocellularity and reduced DC frequency only in sdLNs 111
Figure 3.16 CD11c-DOG mice do not show LN hypocellularity or reduced frequency of LN DCs 112
Figure 3.17 Expression of DTR on B cells does not lead to overall LN hypocellularity and reduced frequencies of LN DCs 114
Figure 3.18 Expression of DTR on Tregs does not lead to overall LN hypocellularity and reduced frequencies of LN DCs 115
Figure 3.19 sdLNs expand normally in CFA/OVA immunised Clec9a$^{Cre/Cre}$ROSA^{iDTR} mice 117
Figure 3.20 Clec9a$^{Cre/Cre}$ROSA^{iDTR} mice can mount a CD8^{+} T cell response upon CFA/OVA immunisation 118
Figure 3.21 MedLNs expand normally in influenza X-31 infected Clec9a$^{Cre/Cre}$ROSA^{iDTR} mice 119
Figure 3.22 Clec9a$^{Cre/Cre}$ROSA^{iDTR} and control mice mount similar CD8^{+} and CD4^{+} T cell responses upon influenza X-31 infection 120
Figure 3.23 DCs from sdLNs of Clec9a$^{+/Cre}$ROSA^{iDTR} mice show impaired migration towards the chemokine CCL21 122
Figure 3.24 DC subsets in sdLNs of Clec9a$^{+/Cre}$ROSA^{iDTR} mice do not show differential CCR7 or CD135 (Flt3) expression compared with controls 123
Figure 3.25 Clec9a$^{+/cre}$ROSA^{iDTR} mice appear to have normal HEVs, but may have an altered FRC network 125
Figure 4.1 Targeting strategy to generate Clec9a-DTA mice 130
Figure 4.2 Generation of Clec9a-DTA mice 131
Figure 4.3 Clec9a$^{+/DTA}$ and Clec9a$^{DTA/DTA}$ mice do not show signs of myeloproliferative disorder 133
Figure 4.4 Clec9a$^{+/DTA}$ and Clec9a$^{DTA/DTA}$ mice show a reduction in CD8α-like DCs, but have increased frequencies of CD11b^{+} DCs in spleen and mesLNs 134

Figure 4.5 MDPs, CDPs and preDCs are unaffected in BM of Clec9a$^{+/DTA}$ and Clec9a$^{DTA/DTA}$ mice 135
Figure 4.6 Old Clec9a$^{+/DTA}$ and Clec9a$^{DTA/DTA}$ mice show a similar phenotype as young mice 136
Figure 4.7 Clec9a$^{+/DTA}$ mice still express DNGR-1 137
Figure 5.1 Schematic representation of ROSA26-confetti mice 141
Figure 5.2 Targeting strategy to generate Clec9a-CreERT2 mice 142
Figure 5.3 Generation of Clec9a-CreERT2 mice 143
Figure 5.4 Tamoxifen-containing diet or oral gavage of tamoxifen does not induce labelling of DCs in the spleen of Clec9a$^{+/CreERT2}$ROSA$^{+/YFP}$ mice 146
Figure 5.5 I.p. or s.c. injection of tamoxifen does not induce labelling of DCs in the spleen of Clec9a$^{+/CreERT2}$ROSA$^{+/mTmG}$ mice 148
Figure 5.6 Treatment of Flt3l BMDC cultures from Clec9a$^{+/CreERT2}$ROSA$^{+/mTmG}$ BM with 4OH-tamoxifen does not induce labelling of DCs 149
Figure 5.7 Overview of fluorophores and microscope setup 151
Figure 5.8 Visualisation of confetti colours in small intestine and mesLN of Clec9a$^{+/Cre}$ROSA$^{+/confetti}$ mice 152
Figure 5.9 Analysis of small intestinal sections of Clec9a$^{+/Cre}$ROSA$^{+/confetti}$ mice for confetti colours, MHCII and E-cadherin 154
Figure 5.10 IRF8 and CD11b can be used to identify DC subsets in the small intestine by microscopy 157
Figure 5.11 8-Colour analysis of the small intestine of Clec9a$^{+/Cre}$ROSA$^{+/confetti}$ mice (1) 158
Figure 5.12 8-Colour analysis of the small intestine of Clec9a$^{+/Cre}$ROSA$^{+/confetti}$ mice (2) 159
Figure 5.13 Surface rendering on confetti channels by Imaris 162
Figure 5.14 Analysis of confetti surfaces based on the images in Figure 5.11 by FlowJo 163
Figure 5.15 Analysis of confetti surfaces based on the images in Figure 5.12 by FlowJo 164

List of tables

Table 1: Surface marker expression of DC subsets and LCs. 16
Table 2 Antibodies used for flow cytometry 83
Table 3 Antibodies used for microscopy 87
Table 4 Peptides used for restimulation 90
Table 5 Primers used for semi-quantitative RT-PCR 94

Abbreviations

Ab	antibody
APC	antigen-presenting cell
BEC	blood endothelial cell
BM	bone marrow
BrdU	5-bromo-2'-deoxyuridine
Cas9	CRISPR associated protein 9
CCL21	CC-chemokine ligand 21
CCR7	CC-chemokine receptor 7
CD	cluster of differentiation
CFA	complete Freund’s adjuvant
Clec9a	C-type lectin domain family 9, member A
CDP	common dendritic cell precursor
CFP	cyan fluorescent protein
CLR	C-type lectin receptor
cMoP	common monocyte progenitor
CRISPR	clustered regularly interspaced palindromic repeats
CTL	cytotoxic T lymphocyte
CTLA-4	cytotoxic T lymphocyte-associated antigen 4
DAMP	damage-associated molecular pattern
DC	dendritic cell
DNA	Deoxyribonucleic acid
DNGR-1	Dendritic cell NK lectin group receptor-1
DT	diphtheria toxin
DTA	diphtheria toxin alpha subunit
DTR	diphtheria toxin receptor
EAE	experimental autoimmune encephalomyelitis
EdU	5-Ethynyl-2´-deoxyuridine
EGF	epidermal growth factor
ELISA	enzyme-linked immunosorbent assay
FACS	fluorescence-activated cell sorting
FDC	follicular dendritic cell

Fl	floxed (flanked by loxP sites)
FRC	fibroblastic reticular cell
Flt3L	fms-related tyrosine kinase 3 ligand
GFP	green fluorescent protein
GM-CSF	granulocyte macrophage colony-stimulating growth factor
h	hour
HB-EGF	heparin-binding EGF-like growth factor
HEV	high endothelial venule
HSC	hematopoietic stem cell
HSV	herpes simplex virus
i.n.	intranasal
i.p.	intraperitoneal
i.v.	intravenous
IFA	incomplete Freund's adjuvant
IL	interleukin
ILC	innate lymphoid cell
INF	interferon
iNOS	inducible nitric oxide synthase
LC	Langerhans cell
LCMV	lymphocytic choriomeningitis virus
LEC	lymphatic endothelial cell
LMPP	lymphoid-primed multipotent progenitor
LN	lymph node
LPS	lipopolysaccharide
LT	lymphotoxin
MDP	macrophage and DC precursor
medLN	mediastinal lymph node
mesLN	mesenteric lymph node
MHCI	major histocompatibility complex class I
MHCII	major histocompatibility complex class II
migDC	migratory dendritic cell
min	minute
Neo	neomycin
NLR	NOD-like receptors

NOD	Nucleotide-binding oligomerisation domain-containing protein
OVA	ovalbumin
PAMP	pathogen-associated molecular pattern
PD-1	programmed cell death 1
pDC	plasmacytoid dendritic cell
pfu	plaque forming unit
PP	Peyer's patch
preDC	pre-dendritic cell
resDC	resident dendritic cell
RFP	red fluorescent protein
RLR	RIG-I-like receptor
RNA	ribonucleic acid
ROR	retinoic-acid-receptor-related orphan receptor
rpm	revolutions per minute
RT	room temperature
s	second
s.c.	subcutaneous
sdLN	skin-draining lymph node
SFB	segmented filamentous bacteria
SILT	solitary isolated lymphoid tissues
Tfh	follicular helper T cell
Th cell	T helper cell
TLR	toll-like receptor
TGF	transforming growth factor
TNF	tumour necrosis factor
Treg	regulatory T cell
WT	wild-type
YFP	yellow fluorescent protein

Chapter 1. Introduction

The mononuclear phagocyte system comprises monocytes, macrophages and dendritic cells that were historically thought to share morphological features, immune functions and ontogeny. The first mononuclear phagocyte to be discovered was the Langerhans cell in 1869, identified by and named after Paul Langerhans. Due to its dendritic morphology and resemblance to nerve cells, it was originally categorised as being part of the nervous system. In the late 19th century Ilya Metchnikoff described the process of phagocytosis and identified macrophages as key phagocytic cells, thereby starting the research on mononuclear phagocytes. However, it was only in the 1970s that Ralph Steinman and Zanvil Cohn discovered, described and named the dendritic cell (DC) in a series of seminal papers (Steinman and Cohn, 1973; Steinman, Lustig and Cohn, 1974; Steinman and Cohn, 1974; Steinman, Adams and Cohn, 1975). Ralph Steinman also identified the first functional properties of DCs by showing that DCs are the key inducers of mixed leukocyte reactions (Steinman and Witmer, 1978; Steinman et al., 1983). Research in the past forty years has greatly expanded our understanding of DC functions, ontogeny, localisation and marker expression, both in mice and humans. This introduction will discuss current knowledge on different murine DC subsets, their function and ontogeny and will pay special attention to transgenic mouse models that are used to study DC biology *in vivo*.

1.1 Dendritic cells in the mouse

1.1.1 Dendritic cell subsets

DCs are antigen-presenting cells with roles in innate and adaptive immune responses. They comprise a heterogeneous group of cells and, therefore, are commonly classified into subsets based on select functional attributes, differences in levels of expression of certain cell-surface markers, localisation in the body and ontogenetic relationships (Geissmann, Manz, *et al.*, 2010; Steinman and Idoyaga, 2010; Hashimoto, J. Miller and Merad, 2011; Merad *et al.*, 2013; Schraml and Reis e Sousa, 2014). DCs are generally characterised by expression of the integrin CD11c and major histocompatibility complex class II (MHCII), although these markers are not unique to DCs. DCs can be broadly subdivided into two main

groups: plasmacytoid DCs (pDCs), which are generally characterised by their rapid production of interferon-α upon Toll-like receptor (TLR) 7, 8 and 9 engagement; and conventional DCs (cDCs) that are superior in initiating and directing T cell responses (Geissmann, Manz, *et al.*, 2010; Steinman and Idoyaga, 2010; Hashimoto, J. Miller and Merad, 2011; Schraml *et al.*, 2013; Merad *et al.*, 2013). cDCs can be further divided into those normally resident at lymphoid tissues (resDCs) versus those that have immigrated from elsewhere (migDCs) (Geissmann, Gordon, *et al.*, 2010; Steinman and Idoyaga, 2010; Hashimoto, J. Miller and Merad, 2011; Merad *et al.*, 2013). The latter normally reside in non-lymphoid tissues but migrate to the draining LNs via afferent lymphatics in the steady state and, prominently, during inflammation. Both resDCs and migDCs are present in LNs, while other lymphoid structures, such as spleen, thymus and Peyer's patches only harbour resDCs, as these tissues lack an afferent lymph supply.

Both resDCs and migDCs consist of different subsets. The CD8α-like subset of cDCs comprises the $CD8\alpha^+$ resDCs in lymphoid organs and their $CD103^+$ $CD11b^-$ counterparts in tissues, which can migrate to LNs where they appear as $CD103^+$ $CD11b^-$ migDCs. These cells can additionally be characterised by their expression of Dendritic cell NK lectin group receptor-1 (DNGR-1, also called CLEC9A) and XCR1 (Sancho *et al.*, 2008; 2009; Crozat *et al.*, 2011; Bachem *et al.*, 2012; Becher *et al.*, 2014). CD8α-like DCs are thought to possess a superior capacity to cross-present exogenous antigens to $CD8^+$ T cells. They also share gene expression patterns and have similar transcription factor dependencies (Geissmann, Manz, *et al.*, 2010; Steinman and Idoyaga, 2010; Edelson *et al.*, 2010; Hashimoto, J. Miller and Merad, 2011; Merad *et al.*, 2013). Their counterparts are the more heterogeneous group of CD11b-expressing resDCs in lymphoid tissues and $CD11b^+$ DCs in non-lymphoid tissues that migrate to LNs, where they appear as $CD11b^+$ migDCs (Geissmann, Manz, *et al.*, 2010; Hashimoto, J. Miller and Merad, 2011; Merad *et al.*, 2013; Becher *et al.*, 2014). Langerhans cells (LCs) are often considered to be a subset of DCs. However, LCs differ considerably from DCs in terms of ontogeny, growth factor and transcription factor dependency, and should therefore be treated as a unique macrophage-type of cell that resides in the epidermis and migrates to skin-draining LNs (sdLNs) (Merad *et al.*, 2013; Malissen,

Tamoutounour and Henri, 2014). A table summarising surface marker expression of the different steady state DC subsets and LCs is included in Table 1.

DCs also share many traits with macrophages and monocytes, and especially in peripheral tissues and under inflammatory conditions the different mononuclear phagocytes can be hard to distinguish from one another. These difficulties have led to considerable debate in the field regarding the classification of certain cells as DCs, macrophages and/or monocyte-derived cells.

marker	**resDC**		**migDC**			**pDC**	**LC**
	CD8α$^+$	**CD11b$^+$**	**CD103$^+$ CD11b$^-$**	**CD103$^+$ CD11b$^+$ (intestinal)**	**CD103$^-$ CD11b$^+$**		
CD11c	++	++	++	++	++	+	++
MHCII	++	++	++	++	++	+	++
CD8α	+	-	-	-	-	subset	-
CD11b	-	++	-	++	++	-	+
CD103	subset	-	++	++	-	-	-
CD207 (Langerin)	subset	-	+	-	-	-	++
DNGR-1 (CLEC9A)	++	-	++	-	-	+	-
CD205 (DEC205)	subset	-	+	-	-	-	+
Xcr1	+	-	+	-	-	-	-
CD172a (Sirpα)	-	++	-	-	++	+	+
CD4	-	subset	-	-	-	+	?
B220	-	-	-	-	-	+	-
SiglecH	-	-	-	-	-	+	-

Table 1: Surface marker expression of DC subsets and LCs.

-: marker not expressed, +: marker expressed, ++: marker highly expressed, ?: not determined, subset: marker only expressed on a subset of population.
(Alvarez, Vollmann and Andrian, 2008; J. C. Miller *et al.*, 2012; Merad *et al.*, 2013)

1.1.1.1 Mononuclear phagocytes in the spleen and LNs

Since the discovery of DCs about forty years ago, most research in the mouse has focussed on spleen and LN DCs. These secondary lymphoid organs are relatively easy to obtain and process for analysis and exhibit the highest frequency of DCs relative to all nucleated cells. The spleen lacks an afferent lymph supply and filters

the blood for pathogens and senescent red blood cells. The red pulp comprises the largest part of the spleen and is the main site for red blood cell recycling. Lymphocytes cluster together in the white pulp of the spleen that is organised around arterioles. The white pulp contains distinct T cell and B cell areas, with T cells residing in the periarteriolar lymphoid sheath and B cells in the lymphoid follicles with the surrounding marginal zone. LNs have afferent lymph supply that delivers a continuous flow of lymph from the tissues to the LNs. The LN is also organised into B cell areas, called follicles that lie in the outer cortex, and a T cell area, called the T cell zone in the paracortical area. Naïve lymphocytes and other leukocytes enter the LN via specialised blood vessels called high endothelial venules (HEVs)

The spleen only harbours resident DCs, which express the prototypical DC markers CD11c and MHCII (Figure 1.1). Splenic DCs can be further divided into pDCs, $CD8\alpha^+$ DCs and $CD11b^+$ DCs. At steady state splenic pDCs express low levels of CD11c, MHCII and DNGR-1 and are positive for B220, Ly6c, SiglecH and PDCA-1 (Zhang et al., 2006; Blasius et al., 2006; Sancho et al., 2008). $CD8\alpha^+$ DCs express DNGR-1 and lack CD11b or CD4 expression and may be positive for langerin (Sancho *et al.*, 2008; J. C. Miller *et al.*, 2012; Becher *et al.*, 2014). Although most $CD8\alpha^+$ DCs are $CD103^+$ $CD205^+$ and negative for the chemokine receptor CX3CR1, a smaller population lacks CD103 and CD205 expression, but are positive for CX3CR1 (Bar-On et al., 2010). These latter cells were reported to functionally and phenotypically resemble pDCs rather than CD8α-like DCs, although more recent studies have questioned this conclusion, based on lineage tracing data (Bar-On et al., 2010; Satpathy, KC, et al., 2012; Schraml et al., 2013). $CD11b^+$ DCs in the spleen lack CD8α and CD103 expression and a subset expresses CD4 (J. C. Miller *et al.*, 2012; Becher *et al.*, 2014). CD4 has been used to identify a $CD4^+$ DC population in the spleen, however, both older and more recent data indicate that CD4 expression is not discriminatory, and $CD11b^+$ $CD4^+$ DCs and $CD11b^+$ $CD4^-$ DCs are highly similar in expression levels of other DC markers and in transcription factor dependencies (Edwards et al., 2003; Becher et al., 2014). ESAM expression also identifies two different $CD11b^+$ DC subsets in the spleen, and in this case $ESAM^{hi}$ and $ESAM^{low}$ $CD11b^+$ DCs do show differential expression of various other markers such as CD4, CD11c, CX3CR1 and Flt3, show differences in Notch2 and

lymphotoxin β receptor dependency and are functionally distinct (Lewis et al., 2011). In the original report it was suggested that ESAM^{hi} but not ESAM^{low} CD11b^{+} DCs develop from committed DC precursors, although more recent lineage tracing data suggest that committed DC precursors can give rise to both subsets (Lewis et al., 2011; Schraml et al., 2013). In the spleen CD11b^{+} DCs are located in the T cell zone of the white pulp, while CD8α^{+} DCs reside both in the white pulp and the marginal zone (Nolte et al., 2000; Qiu et al., 2009; Idoyaga et al., 2009).

ResDCs in the LNs show a similar organisation as splenic DCs and are divided into pDCs, CD8α^{+} resDCs and CD11b^{+} resDCs, which largely express the same surface markers as their splenic equivalents (Figure 1.1). In addition, LNs contain migDCs that have migrated from peripheral tissues. The exact composition of the migDC compartment depends on what sites the LN is draining. However, in general migDCs contain a CD8α-like subset and a CD11b^{+} subset. A more detailed description of migDCs originating from the skin, intestine and lung is given in subsequent sections (1.1.1.2, 1.1.1.3 and 1.1.1.4). CD8α^{+} resDCs localise predominantly to the T cell zone in LNs, while CD11b^{+} resDCs tend to be found around lymphatic regions (Gerner et al., 2012; Gerner, Torabi-Parizi and Germain, 2015). CD103^{+} migDCs also tend to be found in the T cell zone, while CD11b^{+} migDCs cluster in the interfollicular areas (Gerner *et al.*, 2012).

The marginal zone of the spleen contains two macrophage populations, the marginal zone macrophages and the metallophilic macrophages. A third macrophage population, the red pulp macrophage, can be found in the red pulp of the spleen (Haan and Kraal, 2012). Marginal zone macrophages lack MHCII and F4/80 expression, but do express CD68, SIGN-R1 and MARCO and are large phagocytic cells (Hashimoto, J. Miller and Merad, 2011; Davies *et al.*, 2013). Metallophilic macrophages also lack F4/80 expression but can be identified via CD169 and CD68 expression and are not very phagocytic (Hashimoto, J. Miller and Merad, 2011; Davies *et al.*, 2013). Red pulp macrophages express high levels of F4/80, the mannose receptor (CD206) and are low for CD11b, MHCII and CD169 (Hashimoto, J. Miller and Merad, 2011; Davies *et al.*, 2013).
In the LN, macrophage populations can be found lining the subcapsular sinus and the medullar sinus. Subcapsular sinus macrophages are low for F4/80 and CD11c

and express CD11b, CD169 and MARCO. Medullar sinus macrophages express high levels of F4/80, low levels of CD11c and are positive for CD169, CD11b and MARCO (Hashimoto, J. Miller and Merad, 2011; Gray and Cyster, 2012).

The spleen harbours one of the largest monocyte pools of the body (Swirski et al., 2009). These monocytes express CD11b and CD115 and can be divided into a Ly6c^{hi} and Ly6c^{low} subset. They are located in the cords of the subcapsular red pulp and can be released into the blood in response to an inflammatory stimulus (Swirski et al., 2009). Steady state LNs contain hardly any monocytes.

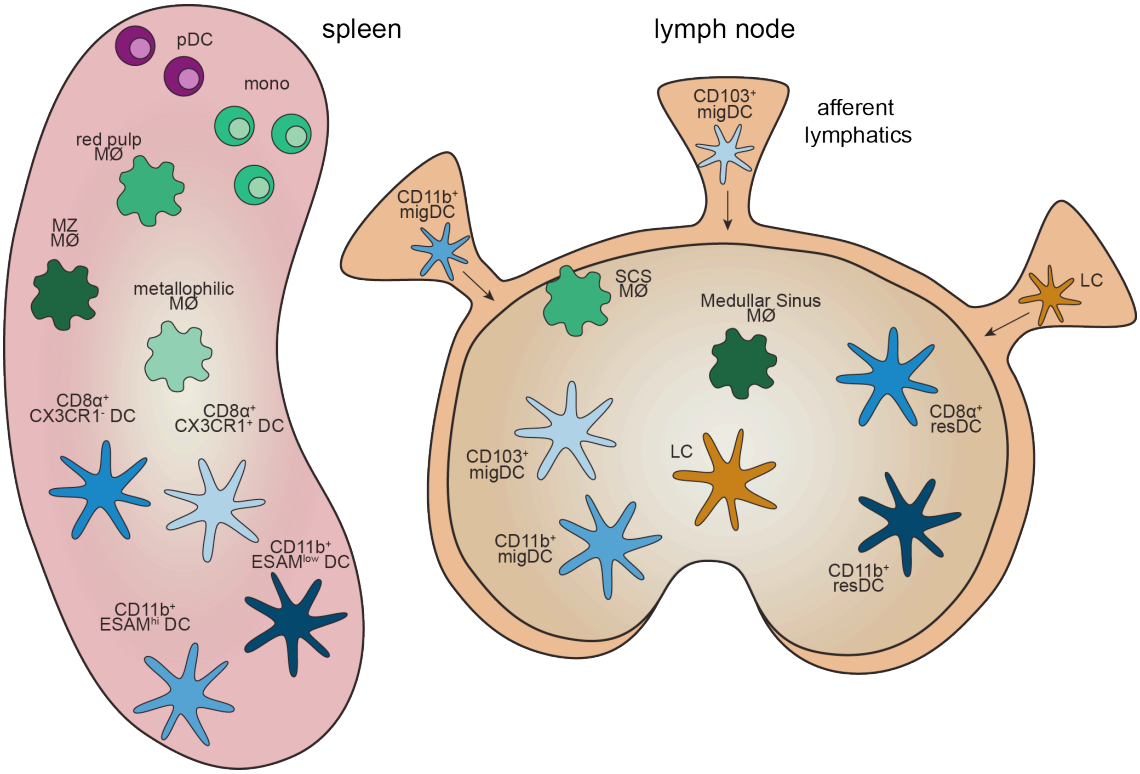

Figure 1.1 Overview of mononuclear phagocytes in spleen and lymph node

Schematic illustration of mononuclear phagocyte subsets in steady state spleen and LN. DC: dendritic cell, LC: Langerhans cell, MØ: macrophage, MZ MØ: marginal zone macrophage, mono: monocyte, pDC: plasmacytoid DC, SCS MØ: subcapsular sinus macrophage.

Inflammation can change surface marker expression of mononuclear phagocytes in spleen and LN and may also prompt the appearance of novel subsets of mononuclear phagocytes. Upon systemic infection with *Listeria monocytogenes*

monocytes differentiate into DC-like cells that have been called TNF/iNOS-producing DCs (Tip DCs), although these cells do not belong to the DC lineage (Serbina, Salazar-Mather, et al., 2003; Serbina, Kuziel, et al., 2003). They express CD163 and Ly6c and intermediate levels of MHCII, CD11c and CD11b, and they produce high amounts of TNFα and iNOS (Serbina, Kuziel, et al., 2003). Similar cells were found upon systemic infection with *Brucella melitensis* (Copin et al., 2007).

Systemic LPS challenge leads to the appearance in skin-draining LNs (sdLNs) of a monocyte-derived cell with DC-like properties that expresses CD11c, MHCII, the C-type lectin DC-SIGN (CD209) and the mannose receptor (CD206) (Cheong et al., 2010). Like resDCs, these DC-SIGN^{+} cells located to the T cell zone in LNs (Cheong et al., 2010). Although it was shown that DC-SIGN^{+} cells derive from monocytes, they failed to develop in Flt3l$^{-/-}$ mice and expressed the transcription factor Zbtb46, which are considered to be properties of DCs (Meredith, Liu, Darrasse-Jeze, et al., 2012). *Leishmania major* infection in the footpad also leads to the appearance of a monocyte-derived cell resembling the splenic Tip DCs found upon systemic *Listeria monocytogenes* infection (De Trez et al., 2009). These cells in the LNs are positive for CD11c, MHCII, CD11b and Ly6c, and produce iNOS and to a lesser extend TNFα (De Trez et al., 2009). Although most inflammatory monocytes in LN are thought to have migrated from peripheral sites, inflammatory monocytes can also enter LNs directly from the blood (Nakano et al., 2009). In germinal centres a special type of macrophage, termed the tangible body macrophage, can be found that clears up apoptotic cells during the germinal centre reaction and expresses CD68 (Haan and Kraal, 2012).

1.1.1.2 Mononuclear phagocytes in the skin

The skin comprises an epidermal and dermal layer. The epidermis is a stratified squamous epithelium and is mainly composed of keratinocytes that proliferate and differentiate into an enucleated, organised structure that protects from the external environment. The epidermis does not contain blood and lymph vessels. A basement membrane separates the epidermis from the dermis. The dermis is made of connective tissue and does contain blood vessels, lymphatics and nerve

endings. Hair follicles are also present in the skin and are the production sites of hair, sweat and sebum.

In the steady state epidermis only a population of well-characterised Langerhans cells (LCs) is found (Figure 1.2). LCs are radioresistant cells that express Epithelial-cell adhesion molecule (EpCAM), the C-type lectin langerin (CD207) and Birkbeck granules that can be identified microscopically and whose formation is induced by langerin (Birbeck, Breathnach and Everall, 1961; Wolff, 1967; Valladeau et al., 2000). LCs migrate from the epidermis, via the dermis into afferent lymphatics that take them to draining sdLNs. In order to migrate, LCs downregulate E-cadherin expression to relieve homotypic interactions with E-cadherin molecules on keratinocytes in the epidermis (A. Tang *et al.*, 1993; Jakob and Udey, 1998). LCs also produce enzymes that facilitate the degradation of the basement membrane that separates epidermis from dermis, such as matrix metalloproteinases (MMP) 2 and 9 (Y. Kobayashi *et al.*, 1999; Ratzinger *et al.*, 2002). In addition, the chemokine receptor CXCR4 expressed on LCs and it ligand CXCL12 are critical for LC migration from the epidermis to the dermis (Ouwehand *et al.*, 2008). Once in the dermis, migration to the draining LNs is predominantly dependent on the chemokine receptor CCR7, which can bind both CCL19 and CCL21 (Ohl *et al.*, 2004), while the CXCR4-CXCL12 chemokine receptor-chemokine pair has also been shown to contribute to the migration of LCs in the dermis (Kabashima et al., 2007).

Various radiosensitive DC subsets can be found in the dermis, in addition to the radioresistant LCs that are in transit from the epidermis to dermal lymphatics, as well as monocytes and a macrophage population (Figure 1.2) (Malissen, Tamoutounour and Henri, 2014). The dermis contains a subset of DCs that expresses langerin, which has been overlooked for a long time, as langerin was thought to be an exclusive marker for LCs (Poulin et al., 2007; Bursch et al., 2007; Henri et al., 2010). These cells correspond to the CD8α-like subset of DCs in the skin and express CD103 in addition to langerin, while lacking CD11b expression. They will be called $CD103^+$ dermal DCs here. In addition, the dermis contains a large $CD11b^+$ dermal DC population that lacks expression of CD103 and langerin, and a DC population that is negative for CD103 and langerin and expresses very little to no CD11b (Henri *et al.*, 2010; Tamoutounour *et al.*, 2013; Mollah *et al.*,

2014). At least some of the CD11b$^+$ dermal DCs express the C-type lectin CD301b (Kumamoto et al., 2009). However, interpretation of many studies on the latter two subsets has been complicated by the fact that CD11b$^+$ dermal DC and marker-negative dermal DC populations are often contaminated with monocytes and macrophages (Tamoutounour et al., 2013). Recent advancements in identifying additional surface markers to separate monocytes and macrophages from DCs have shown that dermal DCs are negative for Ly6c, CD64 and MerTK, while monocytes and macrophages express varying amounts of at least one of these markers (Tamoutounour et al., 2013). These observations should aid future studies of CD11b$^+$ dermal DCs and marker-negative dermal DCs.
Henri et al. (Henri et al., 2010) identified a fourth DC population in the dermis that is radiosensitive and positive for langerin, expresses low levels of CD11b but is negative for CD103 and negative to low for EpCAM. The difference between this subset and the CD103$^+$ dermal DCs is solely based on differential CD103 expression, while expression of additional markers for the CD8α-like subset of DCs, such as DNGR-1 or XCR1, was not assessed. Furthermore, CD103 expression on CD8α-like DCs is regulated by GM-CSF and correlates with cross-presentation ability of the cells (Zhan et al., 2011). CD103$^+$ dermal DCs (which are langerin$^+$) and langerin$^+$ CD103$^-$ dermal DCs may therefore both represent the CD8α-like DCs in the dermis, at different stages of maturation.

Migration of dermal DCs from the skin to draining sdLNs is well studied due to the good accessibility of both the non-lymphoid tissue (skin) and the draining LNs *in vivo*. Dermal DCs migrate from the skin to the draining sdLNs via lymphatics in a manner that is largely dependent on CCR7 and its ligands CCL19 and CCL21. In addition to CCR7-CCL19/21, CXCR4-CXCL12 has also been implicated in aiding DC migration towards LNs (Kabashima et al., 2007). Soluble CCL19 and haptotactic CCL21 gradients provide directional cues for dermal DCs to migrate towards the blind-ended tips of lymphatic vessels (Robbiani *et al.*, 2000; Ohl *et al.*, 2004; Tal *et al.*, 2011; Weber *et al.*, 2013). The basal membrane of the ends of lymphatic vessels is discontinuous and the gaps, named portals, can serve as entry points for migrating DCs (Pflicke and Sixt, 2009). These portals are coated with immobilised CCL21 that likely aids the docking and transmigration of DCs into the vessel (Tal et al., 2011). Once inside the initial lymphatics, crawling of DCs on the

endothelial cells is facilitated by the C-type lectin receptor CLEC2 on DCs and its ligand podoplanin that is expressed on the endothelial cells (Acton et al., 2012), while directionality is provided by CCL19 and the lymph flow in the vessel (Tal et al., 2011). In the larger collecting lymphatics migrating DCs are transported by the lymph flow in a passive way (Miteva *et al.*, 2010; Tal *et al.*, 2011).

Both monocytes and macrophages can be found at steady state in the dermis of the skin (Figure 1.2). Monocytes express low to intermediate levels of CD64 and are positive for CCR2. When expression of Ly6c is plotted against MHCII expression, dermal monocytes show a classical 'monocyte waterfall' distribution, with cells that are $Ly6c^{hi}$ $MHCII^{-}$, $Ly6c^{hi\text{-}int}MHCII^{+}$ and $Ly6c^{low}$ $MHCII^{+}$ (Tamoutounour *et al.*, 2012; 2013; Bain *et al.*, 2013). These cells show close developmental relationships, with blood $Ly6c^{hi}$ monocytes generating subsequently $Ly6c^{hi}$ $MHCII^{-}$, $Ly6c^{hi\text{-}int}MHCII^{+}$ and $Ly6c^{low}$ $MHCII^{+}$ cells (Tamoutounour *et al.*, 2013). One study has shown that monocytes can acquire a DC-like transcriptional signature in addition to the monocyte signature (Tamoutounour *et al.*, 2013), while another study did not find the DC signature (Jakubzick *et al.*, 2013). In addition, a small fraction of the dermal monocytes can migrate to draining sdLNs, but under steady state conditions they are vastly outnumbered by dermal DCs (Tamoutounour *et al.*, 2013; Jakubzick *et al.*, 2013). Dermal macrophages are large and highly autofluorescent, express high levels of CD64 and are positive for MerTK, while they express low levels of CD11b and Ly6c (Tamoutounour et al., 2013; Jakubzick et al., 2013). Macrophages do not migrate to draining sdLNs.

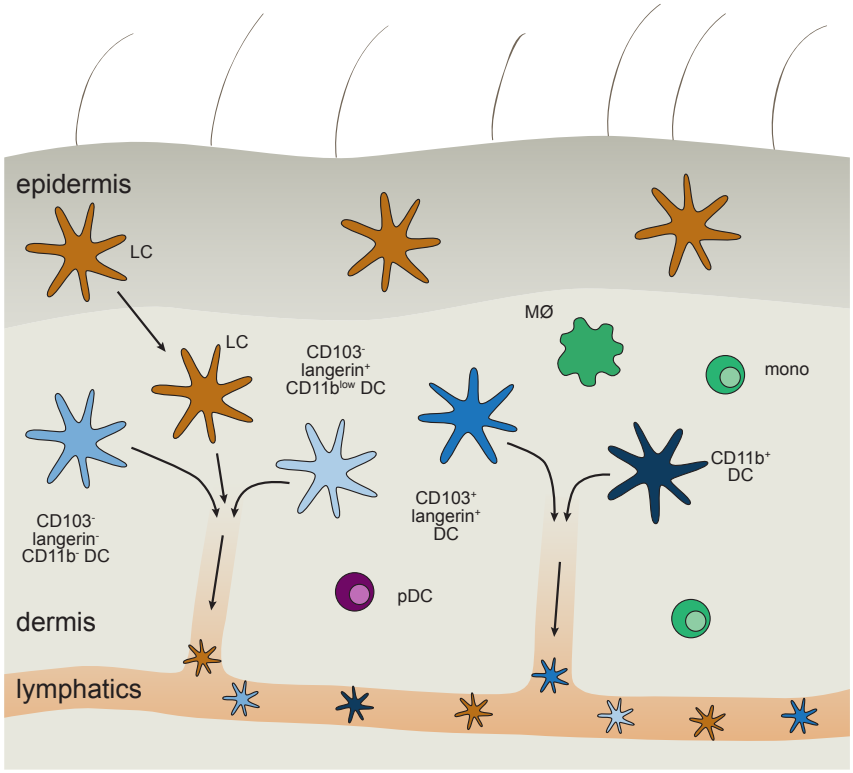

Figure 1.2 Overview of mononuclear phagocytes in the skin

Schematic illustration of mononuclear phagocyte subsets in the steady state skin. DC: dendritic cell, LC: Langerhans cell, MØ: macrophage, mono: monocyte, pDC: plasmacytoid DC.

Inflammatory conditions induce the influx of monocytes into the skin in a CCR2-dependent manner (Rodero et al., 2014). These monocytes can replenish the LC pool in the epidermis, but not the macrophage pool in the dermis, and can also differentiate into a DC-like cell (Ginhoux *et al.*, 2006; León, López-Bravo and Ardavín, 2007; Eidsmo *et al.*, 2009; Tamoutounour *et al.*, 2013). The latter are often called monocyte-derived DCs or inflammatory DCs, although they do not originate from a DC precursor, which makes this nomenclature confusing (Guilliams et al., 2014) (a more detailed description of the ontogeny of DCs and monocytes can be found in 1.1.3). At least in a model for allergic contact dermatitis these cells continue to express varying levels of Ly6c and CD64, which distinguishes them from dermal DCs that remain negative for Ly6c and CD64 under inflammatory conditions (Tamoutounour *et al.*, 2013). Inflammation may also attract pDCs, a DC population normally not present in the steady state skin (Farkas *et al.*,

2001; Wollenberg *et al.*, 2002; Nestle *et al.*, 2005; van der Fits *et al.*, 2009). pDCs express the pDC markers SiglecH and PDCA-1 and low levels of CD11c. Inflammation induces the migration of dermal DCs and LCs from the skin to the draining sdLNs. Dermal DCs arrive in the LNs with faster kinetics than LCs, and dermal DC numbers peak at day 2, while LC numbers peak at day 4 after the induction of skin inflammation (Kissenpfennig et al., 2005). DC-like monocytes can also migrate to draining sdLNs during inflammation, although their migratory capacity is clearly inferior to dermal DCs and LCs, while dermal macrophages fail to migrate altogether (Tamoutounour et al., 2013). Therefore, most monocytes that enter the skin during inflammation remain tissue-resident, as the dermal macrophages.

1.1.1.3 Mononuclear phagocytes in the intestine

The intestine is anatomically organised into the duodenum, jejunum and ileum, which together form the small intestine, and the large intestine comprising the caecum and colon. The small intestine displays villi, which extend into the lumen and increase the surface area of the intestine many fold, while the large intestine lacks these structures. A layer of columnar epithelial cells forms the lining of the intestine and separates the lumen from the loose connective tissue, termed lamina propria. The epithelium is largely protected from the intestinal microbiota by a layer of mucus produced by goblet cells. Crypts are found along the whole intestine and are the home of stem cells that repopulate the epithelial layer. In the small intestine, but not colon, organised lymphoid structures can be found that are termed Peyer's patches. Specialised cells called M cells sample the lumen for antigens and microorganisms for presentation to the mucosal immune system of the Peyer's patch. Smaller clusters of immune cells termed solitary isolated lymphoid tissues (SILT) can be found throughout the small intestine and colon and range in size from small cryptopatches to isolated lymphoid follicles. Additionally, many immune cells can be found dispersed throughout the lamina propria and epithelium. Lymphatic vessels are dispersed throughout the intestine and transport antigens and immune cells to draining LNs. The mesenteric lymph nodes (mesLNs) drain the majority of the intestine, but small LNs in the pancreas and the caudal LN also drain part of the intestine (Carter and Collins, 1974).

The intestine contains three subsets of DCs, namely $CD103^+$ $CD11b^-$ DCs, $CD103^-$ $CD11b^+$ DCs and $CD103^+$ $CD11b^+$ DCs (Figure 1.3). All three subsets express CD11c, MHCII and CD24, but lack CD64 and MerTK expression and are negative or low for CX3CR1 (Tamoutounour et al., 2012; Schlitzer et al., 2013). The $CD103^+$ $CD11b^-$ DC subset represents the CD8α-like DCs in the intestine (Olga Schulz *et al.*, 2009; Crozat *et al.*, 2011; Satpathy, KC, *et al.*, 2012). Like in the dermis, $CD103^-$ $CD11b^+$ DCs are more heterogeneous and are likely to be contaminated with cells with a monocytic origin if additional markers such as CD64 are not used to select against the latter (Bogunovic *et al.*, 2009; Satpathy, KC, *et al.*, 2012; Tamoutounour *et al.*, 2012; Cerovic *et al.*, 2013; Schlitzer *et al.*, 2013). $CD103^+$ $CD11b^+$ DCs are unique to the intestine and are more closely related to $CD11b^+$ DCs than to CD8α-like DCs (Satpathy, KC, *et al.*, 2012; Persson, Uronen-Hansson, *et al.*, 2013; Schlitzer *et al.*, 2013). All three intestinal DC subset migrate to the draining mesLNs and are therefore represented in mesLN migDC subsets (Johansson-Lindbom, 2005; Olga Schulz *et al.*, 2009; Cerovic *et al.*, 2013). Like for skin DC subsets, CCR7 is essential for migration of intestinal DCs to mesLNs (Johansson-Lindbom, 2005; Jang *et al.*, 2006; Bogunovic *et al.*, 2009). However, details of this migratory process are less well studied for intestinal DCs compared with skin DCs, due to the relative inaccessibility of the intestine to experimental techniques like intravital microscopy.

A large pool of intestinal macrophages is present in the lamina propria of the small intestine and colon (Figure 1.3). These cells express CD11c and CD11b, but also the macrophage markers CD64, F4/80 and MerTK and high levels of CX3CR1, show an anti-inflammatory phenotype and do not normally migrate to the mesLNs, although they can upregulate CCR7 and migrate under certain conditions (Olga Schulz *et al.*, 2009; Tamoutounour *et al.*, 2012; Rivollier *et al.*, 2012; Zigmond *et al.*, 2012). Monocytes are continuously recruited to the lamina propria and express intermediate levels of CX3CR1, CD11b and are low to intermediate for CD64 (Tamoutounour et al., 2012). They show the characteristic 'monocyte waterfall', with $Ly6c^{hi}$ $MHCII^-$, $Ly6c^{hi\text{-}int}MHCII^+$ and $Ly6c^{low}$ $MHCII^+$ cells that are developmentally linked (Tamoutounour et al., 2012). In addition to DCs, monocytes and macrophages, a steady state population of pDCs is also present in the

intestine and these cells can be found in both the epithelium and lamina propria, and in the Peyer's patches (Wendland et al., 2007).

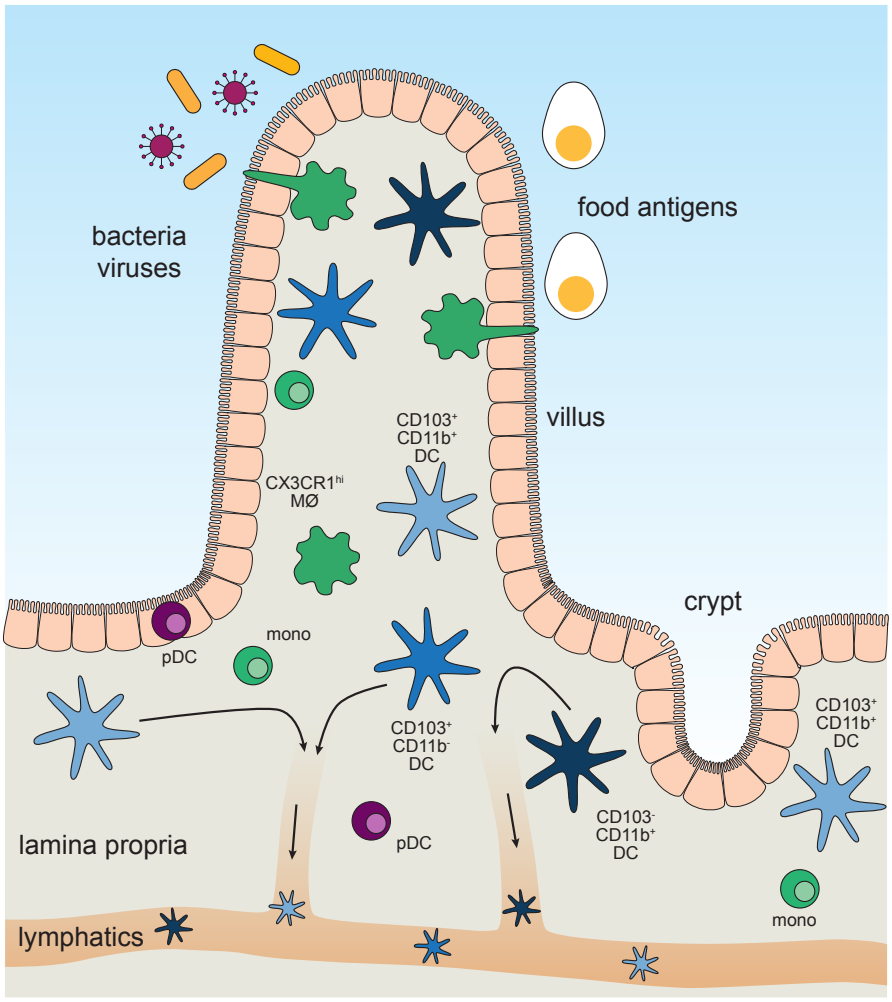

Figure 1.3 Overview of mononuclear phagocytes in the intestine

Schematic illustration of mononuclear phagocyte subsets in the steady state intestine. DC: dendritic cell, MØ: macrophage, mono: monocyte, pDC: plasmacytoid DC.

The lamina propria contains $CD103^+$ $CD11b^-$ DCs, most of the $CD103^-$ $CD11b^+$ DCs and $CD103^+$ $CD11b^+$ DCs and all macrophages, while these cells are normally not found in the epithelium (Bogunovic *et al.*, 2009; Rivollier *et al.*, 2012). The abundance of macrophages and $CD103^+$ $CD11b^-$ DCs progressively increases from the duodenum to the colon, while the $CD103^+$ $CD11b^+$ DC frequency decreases when moving down the intestinal tract (Denning et al., 2011; Mowat and Agace, 2014). Peyer's patches and isolated lymphoid follicles contain a CD8α-like

DC population that expresses both CD8α and CD103, but lacks CD11b expression, and a CD11b DC population that lacks CD8α expression but may express CD103 (Iwasaki and Kelsall, 2000; Anjuère *et al.*, 2004; Jang *et al.*, 2006; Bogunovic *et al.*, 2009; Rivollier *et al.*, 2012).

Under inflammatory settings extravasated monocytes differentiate into pro-inflammatory macrophages expressing CD64 and intermediate levels of CX3CR1 and into cells with a DC-like phenotype expressing CD11c and CD11b, intermediate levels of CX3CR1 and low levels of Ly6c (Zigmond et al., 2012; Tamoutounour et al., 2012; Rivollier et al., 2012). The latter can migrate to draining mesLNs, while the former are tissue resident (Zigmond *et al.*, 2012; Tamoutounour *et al.*, 2012; Rivollier *et al.*, 2012). In addition, inflammation increases the influx of $CD103^+$ $CD11b^-$ DCs, $CD103^-$ $CD11b^+$ DCs and $CD103^+$ $CD11b^+$ DC into the lamina propria and also causes their mobilisation (Anjuère *et al.*, 2004; Denning *et al.*, 2011). pDC influx into the lamina propria and epithelium is also increased in response to inflammatory stimuli (Wendland et al., 2007).

1.1.1.4 Mononuclear phagocytes in the lung and airways

The airway system can be divided into the conducting airways comprising nose, pharynx, larynx, trachea, bronchi and bronchioles, and the lung parenchyma where the gas exchange takes place. Alveoli of the lung parenchyma are lined with an epithelial layer of pneumocytes that is separated from the endothelial cells of the blood capillaries by a basement membrane. The lymphatic network in the lung drains to the mediastinal LN (medLN).

Lung DCs express CD11c, MHCII and CD24, lack CD64, F4/80 and MerTK expression, and can be divided into a CD103-expressing subset and a CD11b-expressing subset (Figure 1.4) (Schlitzer *et al.*, 2013; Becher *et al.*, 2014). $CD103^+$ lung DCs express langerin and CD24, do not express CD11b and form the CD8α-like DC population of the lung, while $CD11b^+$ lung DCs are a classical CD11b-expressing DC population and some of these cells express CD24 (Sung *et al.*, 2006; del Rio *et al.*, 2007; Schlitzer *et al.*, 2013). However, as is the case in the skin and intestine, lung $CD11b^+$ DCs may be contaminated with monocyte-derived

cells if additional markers like CD64 and MerTK are not used to exclude the latter (Gautier et al., 2012). pDCs expressing low levels of CD11c, SiglecH and PDCA-1 are also found in steady state lungs (de Heer, 2004). $CD103^+$ DCs are present in the epithelium of the conducting airway, while $CD11b^+$ DCs reside in the lamina propria below the basement membrane (Sung et al., 2006). Both DC subsets and pDCs can be found in the lung interstitium from where they access the alveolar lumen to sample antigen (de Heer, 2004; Sung et al., 2006). In addition, $CD103^+$ DCs and $CD11b^+$ DCs can be found lining the bronchioles and vessel walls. pDCs are also present in the conducting airways (GeurtsvanKessel et al., 2008).

Monocytes enter the lung during steady state conditions and can differentiate into a cell with DC-like properties that resembles $CD11b^+$ lung DCs (Figure 1.4) (Plantinga et al., 2013). This small population of monocyte-derived cells is positive for CD64 and the high-affinity IgE receptor FcεRIα chain and may express Ly6c, while $CD11b^+$ lung DCs are negative for these surface markers (Plantinga et al., 2013). At least three types of macrophages can be found in the lung. Alveolar macrophages are located in the air space of the alveoli, interstitial macrophages reside in the interstitium between alveoli and bronchial macrophages are found in the bronchi. All lung macrophages express F4/80 and MerTK. Alveolar macrophages are positive for CD11c, express low levels of MHCII and CD11b, are highly autofluorescent and express the lectin SiglecF, while interstitial macrophages express CD11c, are high for MHCII and CD11b, but are negative for SiglecF and CD24 (Becher et al., 2014).
Of all mononuclear phagocytes found in the lung, only $CD103^+$ DCs and $CD11b^+$ DCs migrate from the lung to the medLN in a CCR7-dependent manner under steady state conditions (del Rio *et al.*, 2007; Plantinga *et al.*, 2013). Other factors that have been implicated in DC migration from the lung to the medLN are prostaglandin D_2 and the D prostanoid receptor 1, Chemokine CC motif receptor-like 2 (CCRL2) and CCR8 (Hammad *et al.*, 2003; Jakubzick *et al.*, 2006; Otero *et al.*, 2010).

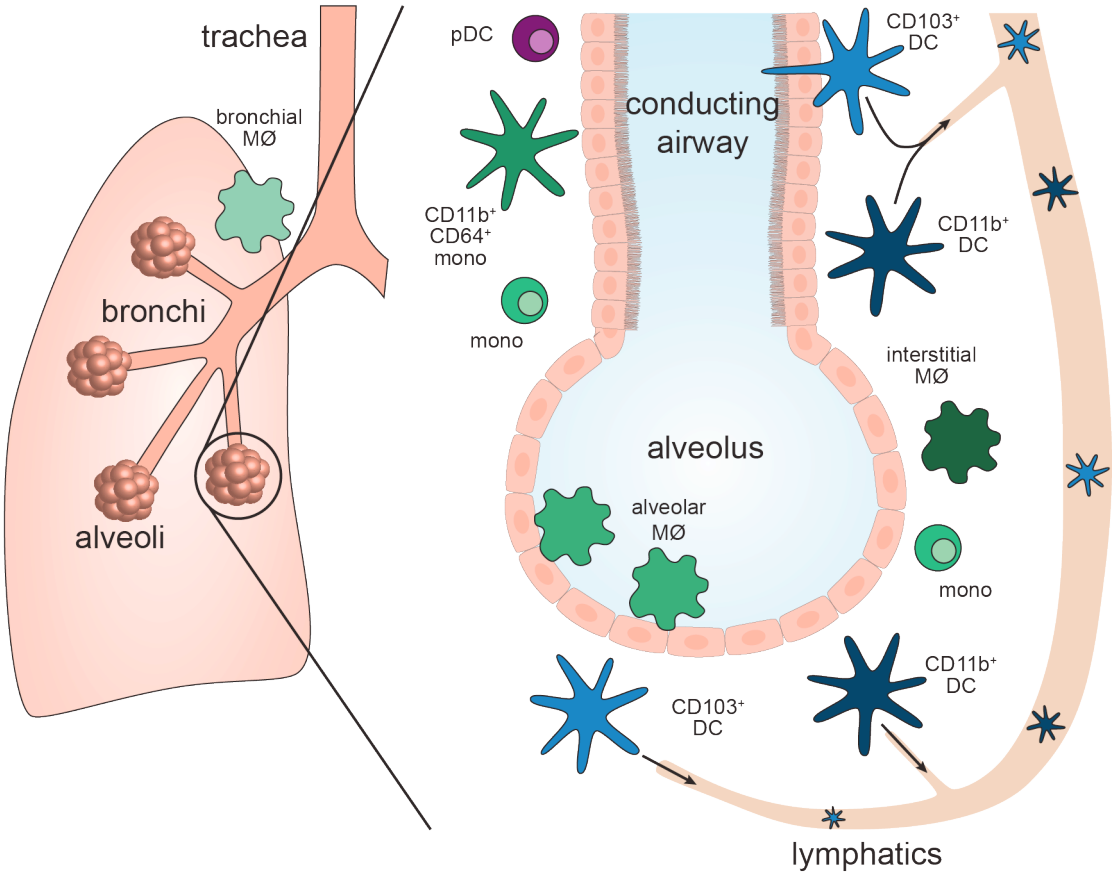

Figure 1.4 Overview of mononuclear phagocytes in the lung

Schematic illustration of mononuclear phagocyte subsets in the steady state lung. DC: dendritic cell, MØ: macrophage, mono: monocyte, pDC: plasmacytoid DC.

Airway inflammation, such as during *Mycobacterium tuberculosis*, influenza A or fungal infections, induce the differentiation of monocytes into inflammatory monocytes that can acquire DC-like properties (Aldridge *et al.*, 2009; Osterholzer *et al.*, 2009; Mayer-Barber *et al.*, 2011; Fei *et al.*, 2011). Monocyte-derived cells can still be discerned from CD11b$^+$ DCs by virtue of CD64, FcεRIα chain and sometimes Ly6c expression (Plantinga et al., 2013). In addition, inflammation induces the migration of these cells to the medLN (Plantinga et al., 2013). CD103$^+$ DC, CD11b$^+$ DC and pDC numbers also increase in the lung upon exposure to inflammatory stimuli, with a greater accumulation of CD11b$^+$ DCs than CD103$^+$ DCs (GeurtsvanKessel *et al.*, 2008; Plantinga *et al.*, 2013). Both DC subsets show increased migratory kinetics to the draining medLN during the early stages of inflammation, with migration rates returning to baseline level at later stages (Legge and Braciale, 2003).

1.1.2 Cytokine and transcription factor dependency of dendritic cell subsets

The process of distinguishing DCs from other mononuclear phagocytes and demystifying the relationships among DC subsets found in different tissues has greatly benefited from work mapping the dependency of DCs on specific cytokines and transcription factors, akin to using transcription factor dependency to define T cell subtypes. Indeed, in certain cases the transcription factor has become synonymous to a DC subset, as is the case for 'Batf3 DCs' that is synonymous with CD8α-like DCs.

1.1.2.1 Cytokine control of DC development

The key growth factor and regulator of lineage commitment for DCs is Flt3l, which binds the receptor Flt3 (CD135). pDCs, CD11b-like DCs as well as CD8α-like DCs can be generated *in vitro* when total BM is cultured with Flt3l (Brasel *et al.*, 2000; Naik *et al.*, 2005). Flt3 is expressed on differentiated DCs and on restricted DC progenitors (CDP and preDC) (Karsunky et al., 2003; Onai et al., 2007; Naik et al., 2007; K. Liu et al., 2009). Interestingly, Flt3 is also expressed at earlier stages of haematopoiesis, such as on early HSCs and MDPs, but is absent from progenitors that have lost the ability to generate DCs (Adolfsson *et al.*, 2001; Karsunky *et al.*, 2003; Waskow *et al.*, 2008). Flt3 signalling is crucial for the development and maintenance of DCs *in vivo* and loss of Flt3 or Flt3l results in a severe reduction of total DCs, while injection or overexpression of Flt3l greatly expands the DC population (Maraskovsky *et al.*, 1996; McKenna *et al.*, 2000; Manfra *et al.*, 2003; Waskow *et al.*, 2008; Kingston *et al.*, 2009). Interestingly, $Flt3^{-/-}$ and $Flt3l^{-/-}$ mice show subtle differences in phenotype, as $Flt3l^{-/-}$ but not $Flt3^{-/-}$ mice have reduced leukocytes and B cell progenitors in the bone marrow and a deficiency in NK cells in the spleen (Mackarehtschian *et al.*, 1995; McKenna *et al.*, 2000; Sitnicka *et al.*, 2002; Waskow *et al.*, 2008).

GM-CSF is important for myeloid lineage commitment, but can also act on differentiated mononuclear phagocytes, and several DC subsets express the receptor for GM-CSF (Metcalf, 2008; Kingston *et al.*, 2009; Greter, Helft, *et al.*, 2012). Indeed, GM-CSF is widely used to differentiate $MHCII^{+}$ $CD11c^{+}$ cells from total BM in *in vitro* cultures (Inaba et al., 1992; Lutz et al., 1999). However, this culture method generates a more heterogeneous cell population than the Flt3l

cultures, including granulocytes, macrophages, monocytes and DC-like cells that can be traced back to distinct precursors (Helft et al., 2015). A lack of GM-CSF signalling has little effect on lymphoid DC subsets *in vivo* though, but does impact on CD8α-like DCs and CD11b$^+$ DCs in peripheral tissues (Kingston *et al.*, 2009; King, Kroenke and Segal, 2010; Greter, Helft, *et al.*, 2012). Furthermore, GM-CSF signalling induces CD103 expression on CD8α-like DCs and is thought to promote the cross-presenting capabilities of these cells (Zhan et al., 2011; Sathe et al., 2011).

LC development is independent of both Flt3l and GM-CSF, but requires IL-34 signalling via the M-CSFR (CD115) and autocrine TGFβ1 production, which are dispensable for cDC homeostasis (Borkowski *et al.*, 1996; Kaplan *et al.*, 2007; Y. Wang *et al.*, 2012; Greter, Lelios, *et al.*, 2012). The development of splenic ESAM^{hi} CD11b$^+$ DCs is dependent on lymphotoxin α1β2 signalling via the lymphotoxin β receptor and the transcription factor RelB, as mice lacking either one of these components have reduced ESAM^{hi} CD11b$^+$ DCs in the spleen (L. Wu *et al.*, 1998; Q. Wu *et al.*, 1999; Y.-G. Wang *et al.*, 2005; Kabashima *et al.*, 2005; Lewis *et al.*, 2011). The influence of lymphotoxin signalling on CD11b$^+$ DCs outside of the spleen remains to be investigated.

1.1.2.2 Transcription factor control of DC development

Transcription factor expression and dependency have emerged as powerful tools to define DC subsets across tissues. Although a substantial number of subset-specific transcription factors have been described over the years, surprisingly few specific pan-DC transcription factors have been identified. Loss of Gfi1, Ikaros, Pu.1, STAT3 and Runx1 and Cbfβ negatively impact on DC development, but absence of these transcription factors also affects many other hematopoietic lineages (L. Wu *et al.*, 1997; Anderson *et al.*, 2000; Laouar *et al.*, 2003; Rathinam *et al.*, 2005; Carotta *et al.*, 2010; Satpathy *et al.*, 2014). More recently, expression of the transcription factor L-Myc has been implicated in regulating DC homeostasis (Kc et al., 2014). Within the immune compartment L-Myc expression is specific for the DC lineage. Its expression is driven by IRF8 and mice lacking L-Myc show reductions in certain DC subsets, such as CD103$^+$ DCs in the lung (Kc et al., 2014). Zbtb46 (Btbd4,

zDC) was identified as a transcription factor specifically expressed in cDCs and pre-DCs (but not pDCs and LCs), although its expression was also found to be induced in activated monocytes (Meredith, Liu, Darrasse-Jeze, et al., 2012; Satpathy, KC, et al., 2012). However, contrary to expectations, deletion of Zbtb46 does not affect DC development *in vivo* (Satpathy, KC, et al., 2012; Meredith, Liu, Kamphorst, et al., 2012). Instead, Zbtb46 appears to be a negative regulator of DC maturation and is rapidly downregulated upon TLR stimulation (Meredith, Liu, Kamphorst, et al., 2012).

The development of pDCs is critically dependent on the transcription factor E2-2 and a constitutive loss of E2-2 in the haematopoietic system results in the absence of pDCs, while deletion of E2-2 from mature pDCs induces spontaneous differentiation into a cDC-like cell, probably via the derepression of the transcription factor Id2 (Cisse et al., 2008; Ghosh et al., 2010). Furthermore, E2-2 shows haploinsufficiency and heterozygous E2-2$^{+/-}$ animals harbour reduced pDC numbers and the remaining pDCs show impaired IFN responses and aberrant surface marker expression (Cisse et al., 2008).

CD8α-like DCs rely on Id2, IRF8, Nfil3 and Batf3 for their development and deletion of any of these transcription factors results in the loss of all CD8α-like DCs, while CD11b^{+} DCs are spared (Aliberti *et al.*, 2003; Hacker *et al.*, 2003; Hildner *et al.*, 2008; Ginhoux *et al.*, 2009; Kashiwada *et al.*, 2011). In addition to a loss of CD8α-like DCs, Id2$^{-/-}$ mice also lack LCs, NK cells and certain secondary lymphoid tissues (Yokota *et al.*, 1999; Hacker *et al.*, 2003). Nfil3$^{-/-}$ also exhibit a defect in NK cell development and show a B cell intrinsic impairment in IgE class switching (Gascoyne *et al.*, 2009; Kamizono *et al.*, 2009; Kashiwada *et al.*, 2010). Although Batf3 is expressed in all cDCs, only CD8α-like DCs are negatively affected in Batf3$^{-/-}$ mice (Hildner et al., 2008). The effect of Batf3 deletion on CD8α-like DCs depends on the background strain of the mice, as the Batf3$^{-/-}$ 129S6/SvEv strain has a more complete reduction of CD8α-like DCs than Batf3$^{-/-}$ on the C57Bl/6 background (Hildner *et al.*, 2008; Edelson *et al.*, 2010; 2011). Furthermore, infection with intracellular pathogens such as *Toxoplasma gondii* can induce CD8α^{+} DC development independently of Batf3 (Tussiwand et al., 2012). It was subsequently shown that Batf and Batf2, which are members of the same family of

transcription factors, can compensate for Batf3 loss under certain conditions (Tussiwand et al., 2012).

Loss of IRF8 not only leads to a complete absence of CD8α-like DCs, but also of pDCs, and causes a myeloproliferative disorder due to a bias towards granulocyte production at the expense of other myeloid lineages (Holtschke *et al.*, 1996; Tamura *et al.*, 2000; Tsujimura *et al.*, 2002; Tsujimura, Tamura and Ozato, 2003). Interestingly, mice that harbour a spontaneous point mutation in the gene encoding IRF8 also show a loss of CD8α-like DCs and develop a myeloproliferative disorder, but unlike $IRF8^{-/-}$ mice have normal pDC numbers (Tailor et al., 2008). IRF8 deficiency not only impacts on cell development, but also on function, as a lack of IRF8 results in impaired migration of LCs and other dermal myeloid cells (Schiavoni et al., 2004).

Although $Id2^{-/-}$ mice, $Nfil3^{-/-}$ mice and $Batf3^{-/-}$ mice show a more pronounced reduction of CD8α-like DCs, these DCs can still develop from BM in short-term *in vitro* or *in vivo* experiments in the absence of Id2, Nfil3 or Batf3, while $IRF8^{-/-}$ BM completely fails to generate CD8α-like DCs in any setting (Seillet et al., 2013). These results indicate that IRF8 is probably the main transcription factor driving CD8α-like DC development, acting upstream of Id2, Nfil3 and Batf3.

Transcription factors implicated in the development and homeostasis of $CD11b^+$ DCs include RelB, TRAF6, Notch, RBP-J, IRF2, IRF4 and Klf4 (L. Wu *et al.*, 1998; T. Kobayashi *et al.*, 2003; Ichikawa *et al.*, 2004; Suzuki *et al.*, 2004; Caton, Smith-Raska and Reizis, 2007; Lewis *et al.*, 2011; Persson, Scott, *et al.*, 2013; Schlitzer *et al.*, 2013; Tussiwand *et al.*, 2015). Mice deficient in either RelB or TRAF6 show a phenotype similar to lymphotoxin β receptor knockout mice with reduced $CD11b^+$ DCs, but not $CD8\alpha^+$ DCs, in the spleen (L. Wu *et al.*, 1998; T. Kobayashi *et al.*, 2003; Kabashima *et al.*, 2005). As the lymphotoxin β receptor signals through RelB and TRAF6, it is likely that deficiency in RelB, TRAF6 and lymphotoxin β receptor all affect the same pathway in $CD11b^+$ DC development. Signalling via the Notch-RBP-J pathway is also important for $CD11b^+$ DC development and mice lacking RBP-J in $CD11c^+$ cells show reduced $CD11b^+$ splenic DCs, while in mice lacking Notch in $CD11c^+$ cells the lack of $CD11b^+$ DCs is confined to the $ESAM^{hi}$ subset in the spleen and $CD103^+$ $CD11b^+$ DCs in the intestine (Caton, Smith-Raska and Reizis, 2007; Lewis *et al.*, 2011). However, absence of Notch signalling in all

hematopoietic cells not only affects $CD11b^+$ DCs but also many other leukocyte populations, such as T cells and B cells (Maillard, Fang and Pear, 2005). $CD11b^+$ DCs are reduced in the spleen of $IRF2^{-/-}$ mice and in addition these mice display defects in LCs and NK cells (Ichikawa et al., 2004). IRF4 is another member of the IFN-regulatory factor family involved in $CD11b^+$ DC development and function. $IRF4^{-/-}$ mice have reduced $CD11b^+$ DCs in the spleen, and defects in the T cell and B cell lineages (Suzuki et al., 2004). More recently it was shown that IRF4 is also important for the development and survival of $CD103^+$ $CD11b^+$ DCs in the intestine and $CD11b^+$ DCs in the lung (Persson, Uronen-Hansson, et al., 2013; Schlitzer et al., 2013). Additionally, IRF4 has been implicated in promoting migration of $CD11b^+$ DCs and modulating their ability to prime Th2 responses via increased MHCII antigen presentation and cytokine production (Bajana *et al.*, 2012; Williams *et al.*, 2013; Vander Lugt *et al.*, 2014). IRF4-expressing DCs, including $CD11b^+$ splenic DCs, $CD103^+$ $CD11b^+$ intestinal DCs and $CD11b^+$ lung DCs, are also reduced in mice that lack the transcription factor Klf4 in the hematopoietic system or in CD11c-expressing cells (Tussiwand et al., 2015).

1.1.3 Dendritic cell ontogeny

In the mouse the hematopoietic system develops in two waves. The first one starts around embryonic day 7 (E7) in the yolk sack and is called primitive haematopoiesis. A first wave of macrophage progenitors is formed from the primitive ectoderm around this time, together with nucleated erythrocytes. Definitive haematopoiesis originates from the aorta-gonad-mesonephros in the embryo itself and is initiated at E10.5. These stem cells subsequently move to the foetal liver where the haematopoietic stem cells (HSCs) expand and produce erythrocytes, lymphocytes and myeloid cells. At around E13-14 the HSCs temporarily move to the spleen and just before birth HSCs finally colonise the bone marrow (BM) where they maintain haematopoiesis throughout life.

In recent years several lines of research have greatly expanded our knowledge on the ontogeny of different mononuclear phagocytes. One major paradigm shift is the notion that many macrophage populations in adult tissues do not necessarily rely on monocytic input from the BM for their homeostasis, but originate from embryonic

populations that are maintained locally. Indeed, the earliest macrophages appear around E9 in the yolk sac, without the need for a monocytic intermediate and colonise the embryo upon establishment of the blood circulation (McGrath et al., 2003; C Schulz et al., 2012). These cells also colonise the brain, epidermis and liver and exclusively give rise to F4/80^{hi} CD11b^{low} microglia in the brain that remain of yolk sac origin throughout life (Alliot, Godin and Pessac, 1999; Ginhoux et al., 2010; C Schulz et al., 2012). F4/80^{hi} CD11b^{low} macrophages in other adult tissues such as the spleen, kidney, lung and heart are likely a mixture of yolk sac-derived cells and foetal liver-derived cells that may gradually replace the former ones over time (Ginhoux *et al.*, 2010; C Schulz *et al.*, 2012; Epelman *et al.*, 2014). Two more recent studies further refined this view on macrophage ontogeny by showing that yolk sac-derived progenitors can colonise the foetal liver and continue to contribute to embryonic tissue macrophages independent of HSCs until at least E16.5 (Perdiguero *et al.*, 2014; Hoeffel *et al.*, 2015). Early yolk-sac derived erythro-myeloid progenitors seed the embryo with macrophages, without a monocytic intermediate, while a later wave of yolk-sac derived erythro-myeloid progenitors colonise the fetal liver and give rise to embryonic macrophages via a monocytic intermediate (Hoeffel *et al.*, 2015). However, an even more recent study challenged this idea, claiming that the second wave of macrophage precursors is not yolk sac-derived, but originates from very early HSCs (Sheng, Ruedl and Karjalainen, 2015). All three studies agreed that microglia in the brain remain of early yolk-sac derived erythro-myeloid progenitor origin throughout adult life. Kupffer cells, alveolar macrophages and red pulp macrophages in the adult originate from later embryonic progenitors that are derived from either a second wave of yolk-sac progenitors, or early HSCs (Perdiguero *et al.*, 2014; Hoeffel *et al.*, 2015; Sheng, Ruedl and Karjalainen, 2015). Adult LCs predominantly originate from this later wave of yolk sac-derived or HSC-derived embryonic progenitors, although a minority of adult LCs may originate from early yolk sac progenitors. (Perdiguero *et al.*, 2014; Hoeffel *et al.*, 2015; Sheng, Ruedl and Karjalainen, 2015). Microglia, Kupffer cells, red pulp macrophages and LCs are only marginally replaced by HSC-derived cells during adult life (Perdiguero *et al.*, 2014; Hoeffel *et al.*, 2015; Sheng, Ruedl and Karjalainen, 2015). Alveolar macrophages are predominantly yolk sac-derived in young adults, but may be slowly replaced by HSC-derived cells during life (Perdiguero et al., 2014).

A second type of macrophage is F4/80^{low} CD11b^{hi}, can be found in many organs such as spleen, liver and lung and depends on definitive haematopoiesis for their development (C Schulz et al., 2012). Another fate-mapping study revealed that under steady-state conditions most tissue-resident macrophage populations are established before birth (either from primitive or definitive haematopoiesis) and do not require input from monocytes to maintain homeostasis (Yona et al., 2012). This notion was further supported by parabiosis experiments showing that BM-derived cells do not substantially contribute to adult tissue-resident macrophages (Hashimoto et al., 2013). For LCs it has been suggested that the epidermal LC network is maintained by local precursors that replenish terminally differentiated LCs (Ghigo et al., 2013). Furthermore, even after a substantial reduction of local macrophages, for example upon irradiation, tissue-resident macrophages can have the ability to repopulate the tissue via self-renewal without the requirement for BM input (Hashimoto et al., 2013). However, the ability to self renew may depend on the specific inflammatory setting, as for LCs both local self renewal and replacement by BM-derived cells has been reported under inflammatory conditions (Merad *et al.*, 2002; Ginhoux *et al.*, 2006; Chorro *et al.*, 2009; Nagao *et al.*, 2012; Ghigo *et al.*, 2013). Interestingly, intestinal macrophages appear to be the exception to the rule that tissues macrophages are maintained by self-renewal under steady-state conditions (Bain et al., 2014). The intestine of neonatal mice is seeded by embryonic macrophages, but they are steadily replaced by monocyte-derived cells in a process that is dependent on the microbiota, so that in the adult intestine virtually all macrophages are of monocytic origin (Bain et al., 2014).

Adult haematopoiesis relies on HSCs in the BM, whose daughter cells expand and gradually lose their multipotency and become more restricted to certain lineages. Lymphoid-primed multipotent progenitors (LMPPs) still share the ability to generate both lymphoid and myeloid lineages, but have lost the ability to generate erythroid and megakaryocyte cells (Adolfsson et al., 2005). Mononuclear phagocytes share a common precursor called the macrophage and DC precursor (MDP) that only gives rise to monocytes, DCs and macrophages and has lost the potential to generate other leukocyte populations (Figure 1.5) (Fogg, 2006; Varol, Mildner and Jung, 2015). MDPs further differentiate in the BM into a monocyte and macrophage restricted progenitor called the common monocyte progenitor (cMoP), which

subsequently generates Ly6c^{hi} monocytes that can exit the BM in a CCR2-dependent manner (Hettinger et al., 2013). Both in BM and in blood Ly6c^{hi} monocytes give rise to Ly6c^{low} monocytes (Yona et al., 2012). In addition, Ly6c^{hi} monocytes are recruited to peripheral tissues where they differentiate into effector cells that may resemble monocytes, DC-like cells or macrophages, depending on the local environment (Varol, Mildner and Jung, 2015).

MDPs also differentiate into common dendritic cell precursors (CDPs), which are the earliest precursors fully committed to the DC lineage and were initially reported to generate both pDCs and cDCs (Figure 1.5) (K. Liu et al., 2009). Interestingly, expression of the transcription factor Zbtb46 or the C-type lectin DNGR-1 on a subpopulation of CDPs seems to identify a precursor population that is restricted to the cDC lineage (Satpathy, KC, et al., 2012; Schraml et al., 2013). Conversely, a precursor population with a predominant pDC potential has been described that, contrary to MDPs and CDPs, does not express M-CSFR (CD115) but does express Flt3 (Onai et al., 2013).

CDPs give rise to preDCs that subsequently leave the BM and travel via the blood to peripheral tissues, where they differentiate into DC subsets (Naik et al., 2006; K. Liu et al., 2009). Interestingly, preDCs already appear to commit in the BM to differentiate into a specific DC subset when they later reach the periphery. PreDCs in the BM can be divided into two subpopulations based on transcriptional signatures and surface marker expression, and this division is maintained in preDCs in the spleen (Naik et al., 2006; Grajales-Reyes et al., 2015; Schlitzer, McGovern and Ginhoux, 2015). When isolated and cultured *in vitro* with Flt3l or transferred into mice, these preDC subpopulations either exclusively give rise to CD8α-like DCs, or to CD11b^{+} DCs, indicating that the preDC can be divided into a CD8α-committed preDC and a CD11b-committed preDC and that lineage commitment takes place in the BM (Naik *et al.*, 2006; Schlitzer, McGovern and Ginhoux, 2015; Grajales-Reyes *et al.*, 2015).

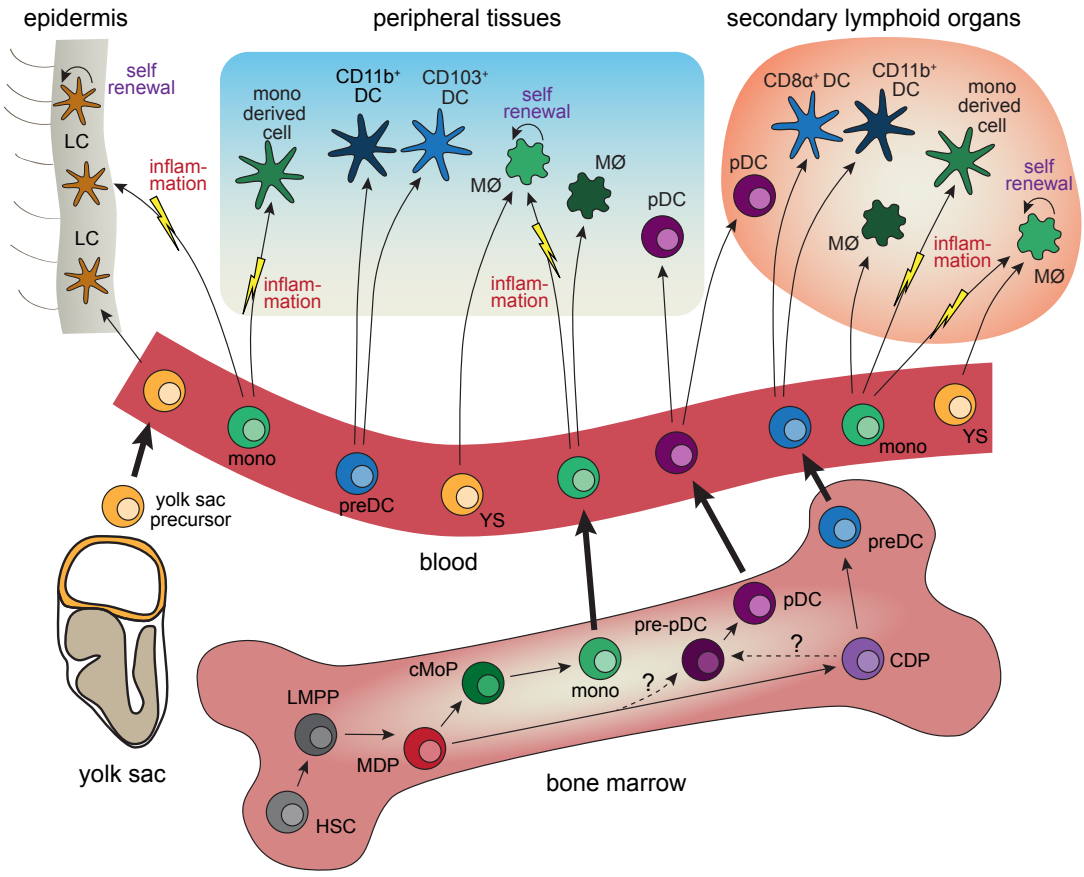

Figure 1.5 Ontogeny of mononuclear phagocytes

Schematic illustration of mononuclear phagocyte ontogeny. cMoP: common monocyte progenitor, DC: dendritic cell, HSC: haematopoietic stem cell, LC: Langerhans cell, LMPP: lymphoid-primed multipotent progenitor, MDP: macrophage and DC precursor, MØ: macrophage, mono: monocyte, pDC: plasmacytoid DC, YS: yolk sac precursor.

Although the ‘conventional’ ontogonetic model in which uncommitted HSCs develop into CDPs and preDCs or cMoPs and monocytes via an MDP intermediate is currently most widely accepted, recent studies have challenged this view. Specifically, tracing the fate of single HSCs and LMPPs via a barcoding strategy revealed that although most HSCs still retained true multipotency on a single cell basis, LMPPs are a highly heterogeneous population with many single cells already showing lineage bias (Naik et al., 2013; Perié et al., 2014). These findings may indicate that lineage commitment occurs much earlier than in the conventional ontogenetic model, where single precursors already start to commit to certain lineages after the HSC stage.

Another recent study questioned the existence of the MDP on a single cell basis (Sathe et al., 2014). By combining data from adoptive transfer experiments, clonal assays and limiting dilution assays it was shown that the BM fraction commonly identified as MDP mainly contained monocyte and macrophage restricted precursors, some DC-restricted precursors and a small fraction of multipotent progenitors that also gave rise to granulocytes, but no cells with restricted monocyte/macrophage and DC potential. (Sathe et al., 2014).
Collectively, these studies suggest that monocyte/macrophage or DC commitment takes place earlier during haematopoiesis than currently thought, starting at the HSC to LMPP transition. Precursor commitment may initially be quite weak and easily overcome by extrinsic factors, but could grow stronger during precursor development and differentiation. Although this alternative view of haematopoiesis is attractive to explain the barcoding results and does not require a committed MDP, more research on single cell progenitors is warranted to establish the early commitment of precursors.

PreDCs have a very short half-life in the blood and quickly exit circulation to seed tissues (K. Liu et al., 2007). Therefore, preDCs show incomplete equilibration in parabiosis experiments that plateaus at around 15-30%, even after prolonged parabiosis (K. Liu et al., 2007; Ginhoux et al., 2009). In line with these findings, DCs in spleen and LNs show a similar degree of exchange in parabionts and also reach about 15-30% chimaerism after three weeks (Kabashima *et al.*, 2005; K. Liu *et al.*, 2007; Ginhoux *et al.*, 2009). Separation of the parabionts revealed that pDCs have a very short half-life of 1-2 days and cDCs in lymphoid organs, liver and kidney have a half life of 5-7 days (K. Liu et al., 2007). Interestingly, the life span of DCs in the lung was much longer, with a half-life of around 15 days for $CD11b^+$ DCs and about 30 days for $CD103^+$ DCs (Ginhoux et al., 2009).
BrdU labelling experiments have revealed that DCs rapidly turn over for most tissues and that at any given moment about 5% of all cDCs are cycling or originate from a recently divided precursor (Kamath *et al.*, 2002; Kabashima *et al.*, 2005; K. Liu *et al.*, 2007; Waskow *et al.*, 2008; Ginhoux *et al.*, 2009; C. L. Scott *et al.*, 2015). Furthermore, for a given tissue different cDC subsets show similar labelling kinetics, which indicate similar proliferation rates (C. L. Scott et al., 2015). One exception is the kidney, where $CD11b^+$ DCs incorporated BrdU with slower kinetics than

$CD103^+$ DCs, although contamination of the $CD11b^+$ DC subset with monocytes or macrophages cannot be ruled out (Ginhoux et al., 2009). Specifically, BrdU pulse-chase experiments suggest a short half-life for all DC subsets in the small intestine and mesLNs (Jaensson *et al.*, 2008; C. L. Scott *et al.*, 2015). Intestinal macrophages have a half life of around three weeks, which is uniquely short compared with other macrophage subsets (Samokhvalov, Samokhvalova and Nishikawa, 2007; Jaensson *et al.*, 2008; Varol *et al.*, 2009).

1.1.4 Functions of dendritic cells

Historically, one of the defining features of DCs as compared to other mononuclear phagocytes is their superior ability to initiate T cell responses. However, with the advancement of knowledge on DC biology, it has become clear that DCs are not only critically involved in directing CD8 T cell responses and inducing CD4 T cell differentiation, but also in mediating immune tolerance via the regulation of Tregs. In addition to these 'classical' T cell mediated functions, DCs can influence functions of other innate immune cells and interact with non-immune cells in tissues, modulating their behaviour.

To appropriately perform all these classical and non-classical functions, DCs are equipped with a wealth of receptors to recognise both pathogen-associated molecular patterns (PAMPs) and damage-associated molecular patterns (DAMPs). Such receptors expressed by DCs include toll-like receptors (TLRs), NOD-like receptors (NLRs), C-type lectin receptors (CLRs) and RIG-I-like receptors (RLRs). The distribution of these receptors differs among DC subsets and may additionally change during inflammatory settings. In the mouse, most TLRs are found in all DC subsets in the spleen. However, $CD8\alpha^+$ DCs selectively lack TLR5 and TLR7 expression, but instead preferentially express TLR3 (Edwards *et al.*, 2003; Reis e Sousa, 2004; Luber *et al.*, 2010). Furthermore, $CD8\alpha^+$ DCs express lower levels of the RLRs RIG-I and MDA-5 compared to other splenic DC populations (Luber et al., 2010). CLRs are widely expressed among mononuclear phagocytes, however, the expression pattern of a given CLRs is often confined to specific cell types. These CLRs are frequently used as surface markers to identify different mononuclear phagocytes. For example, the expression of the CLR DNGR-1 is

confined to CD8α-like DCs, pDCs and DC precursors, while the CLR langerin is found on LCs and on some CD8α-like DCs.

1.1.4.1 Regulation of T cell responses

DCs are specialised in taking up exogenous antigen, and processing and presenting both exogenous and endogenous antigen via major histocompatibility complex class I (MHCI) and MHCII to $CD8^+$ T cells and $CD4^+$ T cells, respectively. Contrarily to most other phagocytes, DCs can control and delay lysosomal degradation of antigen to preserve peptides for presentation to T cells (Savina et al., 2006). Activation of DCs via for example TLR stimulation temporarily enhances macropinocytosis and accelerates antigen degradation (Trombetta *et al.*, 2003; West *et al.*, 2004). Furthermore, inflammatory stimuli boost MHCII synthesis in antigen presenting cells and increase cell surface expression of peptide-loaded MHCII (Cella et al., 1997; Pierre et al., 1997).
MHCII expression is restricted to antigen presenting cells that endocytose extracellular antigen, which is then digested in lysosomes to facilitate peptide loading on MHCII, before the MHCII molecules are transported to the cell surface. On the contrary, nearly every nucleated cell can present cytosolic antigens, whether endogenous or exogenous (e.g. following direct viral infection) via MHCI. DCs are no exception in this respect and can readily present cytosolic antigens to $CD8^+$ T cells via MHCI. However, DCs employ a second mechanism, called cross-presentation, in which exogenous antigen is either shuttled from endosomes and phagosomes into the cytoplasm for presentation on MHCI, or, alternatively, exogenous antigen is degraded in the phagosome where the peptides are directly loaded onto MHCI. The major cross-presenting cells *in vivo* are DCs. Direct infection of DCs with a pathogen allows for direct presentation of pathogen-derived antigens, in addition to cross-presentation. For example, for vaccinia virus infection it was shown that cross presentation is dispensable for $CD8^+$ T cell activation when DCs are directly infected with the virus (Xu et al., 2010). A third mechanism, besides direct presentation and cross-presentation, by which DCs can stimulate memory $CD8^+$ T cell responses is via the acquisition of pre-loaded peptide-MHCI complexes from other infected cells via membrane exchange, which is called cross-dressing (Wakim and Bevan, 2011).

When naïve T cells recognise their cognate antigen in the context of MHCI or MHCII and the right combination of co-stimulatory molecules and cytokines is present, the T cells start proliferating and differentiate into effector T cells. Upon removal of the antigenic source the antigen-specific T cell pool contracts substantially and the remaining cells persist as memory T cells. Thus far, three types of memory T cells have been identified: central memory T cells, effector memory T cells and tissue-resident memory T cells. Central memory T cells home to the T cell zones of secondary lymphoid organs, ready to proliferate when activated with cognate antigen. Effector memory T cells are the only memory cells recirculating through the body and migrate to inflamed tissues to provide immediate protection. Tissue resident memory T cells were discovered relatively recently and are non-circulating cells that reside in tissues where they respond rapidly to cognate antigen.

T cells primed in LNs in response to a local challenge in the draining tissue should exit these LNs and preferentially migrate back to that same tissue. T cells use specific homing receptors to accomplish this task and DCs have been shown to be key regulators of this process. DCs that originate from the intestine express retinoid dehydrogenase enzymes that convert vitamin A into retinoic acid, which is a main driver of CCR9 and integrin $\alpha_4\beta_7$ expression on T cells, which in turn impose gut tropism on the T cells (Mora *et al.*, 2003; Johansson-Lindbom, 2005; Jaensson *et al.*, 2008). Interestingly, it seems that retinoic acid in the bile is responsible for the induction of retinoid dehydrogenase enzymes specifically in intestinal DCs and therefore for the ability of these DCs to induce gut homing molecules on T cells (Jaensson-Gyllenbäck et al., 2011). In a similar fashion DCs originating from the skin induce the skin-homing molecules E-selectin ligand and P-selectin ligand on T cells (D. J. Campbell and Butcher, 2002; Dudda, Simon and Martin, 2004).

1.1.4.1.1 $CD8^+$ T cells

Cross-presentation of cognate antigen to cytotoxic $CD8^+$ T cells is a key function of DCs and in most tissues the CD8α-like subset of DCs is superior to any other

mononuclear phagocyte in generating effector CTL responses. CD8α$^+$ DCs in the spleen are particularly well-equipped in taking up dead cell-associated antigens for cross-presentation, as CD8α$^+$ DCs express receptors such as DNGR-1 that specifically recognise dead cells (Oliver Schulz and Reis e Sousa, 2002; Iyoda et al., 2002; Schnorrer et al., 2006; Sancho et al., 2009). Additionally, even when the antigen is delivered in a form that permits similar uptake by all DC subsets, for example coupled to beads, splenic CD8α$^+$ DCs are still superior at cross-presentation in an *in vitro* setting, possibly because CD8α-like DCs express higher levels of components of the MHCI processing machinery than CD8α$^-$ DCs (Schnorrer et al., 2006; Dudziak et al., 2007). Furthermore, *in vivo* CD8α$^+$ DCs appear to be the most efficient DC subset to take up and cross-present antigen in the spleen (Haan, Lehar and Bevan, 2000; Pooley, Heath and Shortman, 2001; Schnorrer *et al.*, 2006; Dudziak *et al.*, 2007). While delaying lysosomal degradation and reducing lysosomal acidification are essential for CD8α$^+$ DCs to cross-present, these features also render CD8α$^+$ DCs susceptible to infection with pathogens. Indeed, the intracellular bacterium *Listeria monocytogenes* highjacks CD8α$^+$ DCs in the spleen to migrate into deeper splenic regions and establish infection, hence mice lacking splenic CD8α$^+$ DCs are protected from *Listeria monocytogenes* infection (Edelson *et al.*, 2011).

Activation of DCs induces the expression of chemokine receptors that prompts DCs to migrate to the T cell zones in secondary lymphoid structures, upregulates the expression of costimulatory molecules such as CD80 and CD86 and promotes cytokine production and release. In particular, IL-12 and IL-15 are important cytokines in the differentiation of CTLs and CD8α-like DCs are key producers of these two cytokines (Reis e Sousa *et al.*, 1997; Maldonado-López *et al.*, 1999; Mattei *et al.*, 2001; Farrand *et al.*, 2009). Recognition by naïve CD8$^+$ T cells of their cognate antigen in the context of MHCI, leads in combination with these costimulatory molecules and cytokines to the generation of effector CTLs that have the ability to eliminate infected or transformed cells.

Mice that lack the CD8α-like subset of DCs due to Batf3 deficiency are severely impaired in cross-presentation and the generation of effector CTL responses (Hildner et al., 2008). Batf3$^{-/-}$ mice show a significantly impaired CTL response in the spleen upon subcutaneous West Nile Virus infection and also fail to generate a

memory $CD8^+$ T cell response against the virus (Hildner et al., 2008). Furthermore, CTL responses are compromised in $Batf3^{-/-}$ mice infected intranasally with influenza or Sendai virus and upon systemic infection with *Toxoplasma gondii* (Edelson *et al.*, 2010; Mashayekhi *et al.*, 2011; Waithman *et al.*, 2013). In addition to impaired CTL responses to infections, $Batf3^{-/-}$ mice fail to mount an effector $CD8^+$ T cell response to reject syngeneic fibrosarcoma tumour cells (Hildner et al., 2008). Furthermore, deletion of the CD8α-like subset of DCs in XCR1-DTR mice leads to reduced CTL responses against cell-associated antigen, soluble antigen with poly I:C immunisation, or systemic *Listeria monocytogenes* infection (Yamazaki et al., 2013).

During initial cutaneous HSV-1 infection via skin scarification, $CD8\alpha^+$ resDCs in draining sdLNs are the dominant cell type driving CTL responses (Allan *et al.*, 2006; Bedoui, Whitney, *et al.*, 2009). However, upon viral recrudescence both $CD103^+$ dermal DCs migrating to draining sdLNs and $CD8\alpha^+$ resDCs are capable of cross-presenting antigen to $CD8^+$ T cells (Allan *et al.*, 2006; Bedoui, Whitney, *et al.*, 2009). In line with these results in the skin, migratory $CD103^+$ DCs in the lung are the key inducers of $CD8^+$ T cell responses in the draining medLN upon intranasal influenza infection, in addition to $CD8\alpha^+$ resDCs in the medLNs that can also contribute to $CD8^+$ T cell responses (GeurtsvanKessel *et al.*, 2008; Helft *et al.*, 2012; Waithman *et al.*, 2013).

Although the CD8α-like subset of DCs is the key inducer of $CD8^+$ T cell responses in most settings, $CD11b^+$ DCs have also been reported to prime $CD8^+$ T cells in certain inflammatory contexts. In an *in vitro* culture system splenic $CD8\alpha^-$ DCs were shown to be superior to $CD8\alpha^+$ DCs in activating OT-I $CD8^+$ T cells when incubated with ovalbumin (OVA)-expressing *Saccharomyces cerevisiae* (Backer et al., 2008). Furthermore, $MHCII^+$ $CD11b^+$ $CD103^-$ cells (either genuine DCs and/or monocyte-derived cells) isolated from medLNs from influenza-infected mice were reported to be capable of driving $CD8^+$ T cells proliferation *ex vivo*, albeit less efficiently than $CD103^+$ migDCs (Kim and Braciale, 2009). Ballesteros-Tato et al. (Ballesteros-Tato et al., 2010) also reported on the ability of $MHCII^+$ $CD11b^+$ $CD103^-$ migratory cells in medLNs (probably monocyte-derived, as they also express Ly6c) to drive $CD8^+$ T cell responses upon influenza infection. Interestingly, these authors found that the $CD11b^+$ cells were more efficient than $CD103^+$ migDCs in medLNs in activating

$CD8^+$ T cells (Ballesteros-Tato et al., 2010). These findings are in apparent contradiction with reports that have described the $CD103^+$ migDCs and/or $CD8\alpha^+$ resDCs in medLNs from influenza infected mice to be main drivers of $CD8^+$ T cells proliferation *ex vivo* and with the fact that mice that lack CD8α-like DCs have severely impaired CTL responses upon influenza infection (GeurtsvanKessel *et al.*, 2008; Helft *et al.*, 2012; Waithman *et al.*, 2013). These differences may be explained by different time points upon infection looked at, the influenza strain used or the source of the $CD8^+$ T cells (TCR transgenic T cells or natural T cells). However, whether $CD11b^+$ cells play a role in priming $CD8^+$ T cells *in vivo* during infections remains to be determined and most likely awaits mouse models to selectively ablate these cells. Furthermore, it remains to be elucidated whether $CD11b^+$ DCs utilise direct presentation, cross-presentation and/or cross-dressing to generate peptide-loaded MHCI molecules and drive $CD8^+$ T cell activation. In any case, even though $CD11b^+$ DCs may induce $CD8^+$ T cell responses under certain conditions, CD8α-like DCs have emerged as the main antigen presenting cell to prime $CD8^+$ T cells.

In the absence of activating stimuli, $CD8\alpha^+$ DCs can induce peripheral $CD8^+$ T cell tolerance, instead of promoting cytotoxic $CD8^+$ T cell reactions. In a process called cross-tolerance, $CD8\alpha^+$ DCs cross-present antigen to self-reactive $CD8^+$ T cells and promote their activation and proliferation followed by apoptosis-mediated deletion (Kurts *et al.*, 1998; Hawiger *et al.*, 2001; Davey *et al.*, 2002; Belz *et al.*, 2002; Bonifaz *et al.*, 2002). These processes take place in the LN draining the site where the self-antigen is expressed (Scheinecker et al., 2002). However, most of these studies relied on the adoptive transfer of transgenic T cells into mice expressing a model antigen, usually OVA, under control of the rat insulin promoter, while it has been shown that the frequency of antigen-specific $CD8^+$ T cells can have a profound influence on the outcome (tolerance or activation) of the immune response (Kurts et al., 1997; Morgan, Kreuwel and Sherman, 1999). In a different approach by Probst et al. (Probst et al., 2003) LCMV epitopes could be inducibly expressed in a small fraction of DCs, allowing for the assessment of cross-tolerance of endogenous $CD8^+$ T cells. Indeed, in the absence of activatory signals from DCs, cross-tolerance of endogenous $CD8^+$ T cells was induced upon LCMV epitope expression, while cross-priming could be induced in the same mouse strain

by activating DCs with poly I:C or anti-CD40 antibody treatment while expressing the viral epitopes (Probst et al., 2003). In the same mouse model it was shown that cross-tolerance induced by DCs depended on PD-1 and CTLA-4 expression on $CD8^+$ T cells (Probst, McCoy, et al., 2005).

Primary encounter of an antigen usually not only generates and effector T cell response, but also a memory T cell response and many of the latter cells remain in peripheral tissues. Here, memory $CD8^+$ T cells can be reactivated when cognate antigen is present. In the case of HSV-1 infection it was show that the reactivation occurs locally and is dependent on both resident $CD4^+$ T cell and recruited inflammatory monocytes (Wakim et al., 2008).

1.1.4.1.2 $CD4^+$ T cells

Naïve $CD4^+$ T cells can differentiate into distinct Th cell subsets upon recognition of their cognate antigen in the context of MHCII. Decision of T cell fate is mainly guided by environmental clues and DCs play major roles in both antigen presentation on MHCII and the direction of Th cell differentiation. Initially two Th cell subsets were identified: Th1 and Th2 cells. Th1 cell differentiation is regulated by the master transcription factor T-bet and these cells tend to produce IFNγ, lymphotoxin and IL-2. Th2 cells depend on the transcription factor Gata3 and produce IL-4, IL-5 and IL-13. More recently other $CD4^+$ T cell subsets have been defined, like Tregs, Th17 cells, Tfh cells and other less-well defined Th cell subsets. Tregs can be induced in the thymus (natural or nTregs) or in the periphery (induced or iTregs) and both rely on the transcription factor FoxP3 and produce IL-10 and TGFβ. On the other hand, the key transcription factor for Th17 cells is Rorγt and these cells produce IL-17A and IL-17F. Tfh cells depend on Bcl-6 and secrete IL-21.

In general, $CD11b^+$ DCs are better equipped for antigen presentation on MHCII than CD8α-like DCs, as they express higher levels of components of the MHCII processing machinery (Dudziak et al., 2007). *Ex vivo* $CD4^+$ T cell stimulation assays with DCs isolated from immunised or infected mice also revealed that in most cases $CD11b^+$ DCs are superior to CD8α-like DCs in driving $CD4^+$ T cell

responses (Dudziak *et al.*, 2007; Bedoui, Prato, *et al.*, 2009; Plantinga *et al.*, 2013). However, many studies did not address which Th subtype was induced in these *ex vivo* experiments. Results are also more mixed than with $CD8^+$ T cell responses, and both $CD11b^+$ DCs and CD8α-like DCs are likely to be involved in driving $CD4^+$ T cell responses, depending on the setting and the type of Th cell induced. Importantly, a confounding factor in many of these studies is the presence of monocytes with a DC-like phenotype in the $CD11b^+$ DC population, especially in models where inflammation is present, which complicates the attribution of certain functions to either monocytes or $CD11b^+$ DCs, or both.

Generation of Th1 responses is thought to depend on DCs. The Th1 response and control of parasitaemia upon systemic infection with *Plasmodium chabaudi* is dependent on CD11c-expressing cells (Borges da Silva et al., 2015). Furthermore, depletion of all DCs in genetically engineered zDC-DTR mice (see 1.2.2) leads to severely hampered Th1 responses to antigens targeted to CD205 or Treml4 and upon *Toxoplasma gondii* or *Citrobacter rodentium* infection (Meredith, Liu, Darrasse-Jeze, et al., 2012; Schreiber et al., 2013).
Th1 cell differentiation is dependent on the cytokines IL-12 and IFNγ (Hsieh et al., 1993; Lighvani et al., 2001) and CD8α-like DCs can produce substantial amounts of IL-12 (Reis e Sousa *et al.*, 1997; Maldonado-López *et al.*, 1999; O Schulz *et al.*, 2000; Farrand *et al.*, 2009). Furthermore, splenic $CD8\alpha^+$ DCs, but not $CD8\alpha^-$ DCs, pulsed *ex vivo* with KLH and transferred back into the footpad of a naïve mouse induce $CD4^+$ T cell proliferation and Th1 cytokine production in the draining popliteal LN (Maldonado-López et al., 1999). Targeting of antigen to CD8α-like DCs via an anti-DNGR-1 antibody also induces a potent Th1 response when combined with poly I:C as adjuvant (Joffre et al., 2010). Likewise, similar results were obtained when antigen is coupled to an anti-XCR1 antibody or to XCL1, which both target XCR1 on CD8α-like DCs (Hartung *et al.*, 2015; Fossum *et al.*, 2015; Terhorst *et al.*, 2015). Finally, CD8α-like DCs can be targeted via antibodies recognising CD205, although CD205 is also expressed on other antigen presenting cells, such as LCs. Antigen delivery via an anti-CD205 antibody induced $CD4^+$ T cell proliferation and Th1 polarisation when administered together with adjuvant (Bonifaz *et al.*, 2004; Boscardin *et al.*, 2006; Idoyaga *et al.*, 2011).

In the context of HSV-1 infection it was shown that T cell help is essential for the generation of a CTL response and it was suggested that splenic $CD8\alpha^+$ DCs have to directly present cognate antigen to $CD4^+$ T cells via MHCII for the licencing of the DC to happen (C. M. Smith et al., 2004). However, other $MHCII^+$ cells, like $CD11b^+$ DCs, may have initially activated the $CD4^+$ T cells before licensing occurred. Interestingly, in a model for topical *Candida albicans* infection $CD103^+$ dermal DCs are required for the proliferation of TCR-transgenic $CD4^+$ T cells and the generation of IFNγ-expressing Th1 cells *in vivo*. In the absence of the $CD103^+$ dermal DCs Th1 cell differentiation is abrogated (Igyarto et al., 2011; Kashem et al., 2015). Similarly, in an EAE autoimmunity model $CD103^+$ dermal DCs were shown to be necessary for Th1 cell differentiation, as the Th1 response is diminished and autoimmunity is delayed and less severe when $CD103^+$ dermal DCs are depleted by DT injection of WT mice reconstituted with Langerin-DTR BM (King, Kroenke and Segal, 2010). However, these findings did not reproduce in $Batf3^{-/-}$ mice that constitutively lack $CD103^+$ dermal DCs, as $Batf3^{-/-}$ mice are as sensitive as WT mice to EAE and have normal Th1 responses (Edelson *et al.*, 2011). It is unclear why these two studies report differential involvement of $CD103^+$ dermal DCs in Th1 cell generation and EAE induction, although these contradictory findings may relate to the different mouse models used, as the former study employs irradiation chimeras and a DTR-based transgenic model, while the latter relies on a transcription factor knockout model and constitutive loss of $CD103^+$ dermal DCs.

In the context of cutaneous HSV-1 infection $CD8\alpha^+$ resDCs, $CD103^+$ dermal migDCs, $CD11b^+$ migDCs as well as LCs sorted from the draining LN are capable of driving $CD4^+$ T cell proliferation and the induction of Th1 cytokines in an *ex vivo* setting (Bedoui, Whitney, et al., 2009). As all three DC subsets and LCs are capable of inducing a Th1 response in this context, it seems likely that the local environment created by the HSV-1 infection is more important than the specifics of the antigen presenting cell in driving $CD4^+$ T cell polarisation. A similar finding was reported in an intranasal influenza infection model, where both $CD11b^+$ migDCs and $CD103^+$ migDCs sorted from medLNs of infected mice can induce $CD4^+$ T cell proliferation and IFNγ production in an *ex vivo* setting (Kim et al., 2010).

Upon subcutaneous immunisation with antigen, $CD11b^+$ $CD11c^+$ cells were shown to be the major cell type to present antigen locally in the skin to previously activated

$CD4^+$ T cells and induce IFNγ production from $Foxp3^-$ T cells and IL-10 production from $Foxp3^+$ Tregs (McLachlan et al., 2009). As these $CD11b^+$ $CD11c^+$ cells also express F4/80 and are present in an inflammatory environment, the majority of these cells are probably derived from infiltrating monocytes, with little input from DCs.

In sum, both CD8α-like DCs and $CD11b^+$ DCs, and probably monocyte-derived cells, have been shown to be capable of inducing Th1 responses. However, which subset(s) is dominant in a certain setting is likely to be context-specific, depending on factors such as the site of Th1 generation (e.g. spleen versus LN), the type of antigen, and the type and route of immunisation or infection.

Factors involved in the generation of a Th2 response are less clear than those leading to a Th1 response. DCs are generally thought to play a key role in Th2 differentiation via MHCII antigen presentation and cytokine secretion. Mice in which all CD11c-expressing cells are depleted during helminth infection show reduced Th2 responses (Phythian-Adams *et al.*, 2010; K. A. Smith *et al.*, 2011; 2012). Also, in an asthma model $CD11c^+$ cell depletion diminishes the Th2 response and reduces clinical signs of asthma (van Rijt et al., 2005). These findings are in line with studies showing that the induction of Th2 immunity is abrogated when mice lacking $CD11c^+$ cells are immunised with antigen and a NOD1 or NOD2 ligand, or with antigen and the cysteine protease papain (H. Tang et al., 2010; Magalhaes et al., 2011). However, in other settings, like vesicular stomatitis virus infection, the Th2 response is not affected by the absence of all $CD11c^+$ cells (Ciavarra et al., 2006).

Attempts to determine which mononuclear phagocyte subsets are involved in driving Th2 responses have been hampered by problems to phenotypically distinguish different subsets during inflammation, especially $CD11b^+$ DCs and monocyte-derived cells. Nonetheless, several studies have looked into this question utilising both *in vitro* and *in vivo* approaches. When splenic $CD8\alpha^-$ DCs (corresponding to $CD11b^+$ DCs) and $CD8\alpha^+$ DCs are pulsed *ex vivo* with antigen and returned to the footpad of naïve mice, both DC subsets induce $CD4^+$ T cell proliferation in the draining LN, but only $CD8\alpha^-$ DCs generate a Th2 cytokine response (Maldonado-López et al., 1999). Also, when cells from GM-CSF BM cultures are pulsed with soluble egg antigen from *Schistosoma mansoni*, they

induce a Th2 response both *in vitro* and *in vivo* (MacDonald et al., 2001). However, the soluble egg antigen is a potent Th2 inducer by itself and in this study the GM-CSF cultures were not compared with DC subsets. It is therefore not possible to distinguish the Th2-inducing potency of the antigen preparation from that of the antigen presenting cell.

In a model of house dust mite-driven asthma it was shown that under (physiological) conditions of low allergen availability the $CD11b^+$ lung DCs that migrate to the medLN are necessary and sufficient to induce a Th2 allergic response. On the contrary, when allergen is abundantly present both $CD11b^+$ lung DCs and inflammatory monocytes that migrated to the medLN can drive the Th2 response (Hammad *et al.*, 2010; Mesnil *et al.*, 2012; Plantinga *et al.*, 2013). Furthermore, during contact hypersensitivity $CD11b^+$ dermal DCs that express the C-type lectin CD301b were shown to induce a Th2 response *in vivo* (Kumamoto *et al.*, 2009; Murakami *et al.*, 2013). Corroborating these results that $CD11b^+$ DCs and possibly inflammatory monocytes are key inducers of Th2 responses, are findings that Th2 immunity is impaired in mice that lack the transcription factor IRF4, which is important for $CD11b^+$ DC development (Suzuki et al., 2004). Mice that had IRF4 deleted in CD11c-expressing cells show a lack of $CD11b^+$ DCs and severely reduced Th2 responses to immunisation with antigen and papain, antigen and incomplete Freund's adjuvant and nematode infection (Gao et al., 2013; Vander Lugt et al., 2014). In a cross of a different CD11c-Cre mouse line with $IRF4^{fl/fl}$ mice that deletes IRF4 later in DC development, $CD11b^+$ DCs are not ablated, however, these mice still show impaired Th2 responses in the lung upon house dust mite challenge, indicating that IRF4 is not only important for $CD11b^+$ DC development, but also for Th2 induction (Williams et al., 2013). Interestingly, in the context of nematode infection, both DCs and $CD4^+$ T cells express CXCR5 and locate close to the B cell follicles, and this localisation is essential for the generation of a Th2 response against the nematode (León et al., 2012).

Development of Th17 cells depends on TGFβ and IL-6, which induce the master regulator of Th17 development RORγt. In the steady state Th17 development has mainly been studied in the intestine and associated mesLN. There, Th17 cells are induced by the microbiota with a dominant role for SFBs. Indeed, the presence of SFBs in the microbiota correlates with increased Th17 cells and colonisation of

mice with SFBs is sufficient to induce Th17 development (Ivanov *et al.*, 2009; Gaboriau-Routhiau *et al.*, 2009; Schnupf *et al.*, 2015). The induction of SFB-specific Th17 cells is dependent on MHCII expression on $CD11c^+$ cells, although mice lacking MHCII on $CD11c^+$ cells still harbour a population of Th17 cells that do not recognise SFBs (Goto et al., 2014). Furthermore, deletion of $CD11c^+$ cells in the lamina propria largely abrogates the generation of a Th17 response (Denning et al., 2011).

In one study only sorted $CD103^-$ $CD11b^+$ DCs, and not $CD103^+$ $CD11b^+$ DCs or $CD103^+$ $CD11b^-$ DCs, from the mesLN were capable of inducing Th17 responses *in vitro* when cultured with OT-II cells and OVA (Cerovic et al., 2013). However, in other studies that used sorted populations from the lamina propria, the $CD103^+$ $CD11b^+$ DCs were the most efficient in driving Th17 responses *in vitro*, although $CD103^-$ $CD11b^+$ DCs were not included in the analysis (Uematsu *et al.*, 2008; Denning *et al.*, 2011; Fujimoto *et al.*, 2011). Interestingly, a recent study reported that the $CD103^-$ $CD11b^+$ DCs from the lamina propria can be divided into a larger $CCR2^-$ fraction and a smaller $CCR2^+$ fraction, with the $CCR2^+$ fraction being superior in driving Th17 differentiation *in vitro* (C. L. Scott et al., 2015). The same study also reported that this effect is masked when total $CD103^-$ $CD11b^+$ DCs are used, which may explain the lack of Th17 induction by $CD103^-$ $CD11b^+$ DCs in previous studies. Furthermore, when intestinal macrophages are added to the DC and T cell co-cultures, the induction of Th17 cells is inhibited, suggesting a regulatory role for intestinal macrophages on Th17 development (Denning et al., 2011). Although in the aforementioned studies $CD103^+$ $CD11b^-$ intestinal DCs failed to elicit any Th17 responses *ex vivo*, direct targeting of antigen to CD8α-like DCs via anti-DNGR-1 antibodies results in *in vivo* Th17 generation, but only when curdlan is co-administered as adjuvant with the antibody treatment (Joffre et al., 2010).

In the intestine the $CD103^+$ $CD11b^+$ DCs are thought to be the main drivers of Th17 responses, as mice that lack IRF4 in $CD11c^+$ cells harbour a reduction in $CD103^+$ $CD11b^+$ DCs and have a diminished Th17 population in steady state (Schlitzer et al., 2013). $CD103^+$ $CD11b^+$ DCs may regulate Th17 responses via the production of IL-6 and IL-23, although other mechanisms cannot be excluded (Persson, Uronen-Hansson, et al., 2013; Schlitzer et al., 2013). Mice with a deletion of Notch2 in CD11c-expressing cells also have reduced $CD103^+$ $CD11b^+$ DCs in both lamina

propria and mesLNs and show a defect in intestinal Th17 cells under steady state conditions (Lewis et al., 2011). Additionally, mice that express DTA under control of the human *langerin* promoter completely lack $CD103^+$ $CD11b^+$ DCs in the lamina propria and have greatly reduced steady state Th17 cells, indicating that $CD103^+$ $CD11b^+$ DCs are required for Th17 development *in vivo* Altogether, these studies suggest that $CD103^+$ $CD11b^+$ DCs are important inducers of Th17 responses in the intestine. It is possible that the role for these cells might be indirect as MHCII expression on $CD103^+$ $CD11b^+$ DCs is dispensable for Th17 generation (Welty *et al.*, 2013). Notably, these results do not exclude a role for $CD103^-$ $CD11b^+$ DCs and $CD103^+$ $CD11b^-$ DCs in intestinal Th17 responses, although lack of a Th17 phenotype in $Batf3^{-/-}$ mice, in which $CD103^+$ $CD11b^-$ DCs are absent, suggests that $CD103^+$ $CD11b^-$ DCs are dispensable for Th17 development (Welty et al., 2013). Furthermore, Th17 induction is not necessarily confined to LNs, as experiments in mice that lack secondary lymphoid organs show that the priming of Th17 cells can take place locally in the lamina propria (Goto et al., 2014; Lécuyer et al., 2014). Although most studies have focussed on Th17 generation in the intestine, mice that lack IRF4 in CD11c-expressing cells have a severely reduced $CD11b^+$ DC population in the lung and also show a reduction in steady state Th17 cells (Schlitzer et al., 2013). Furthermore, Th17 production upon challenge with the fungus *Aspergillus fumigatus* is reduced in these mice, indicating a role for $CD11b^+$ lung DCs in Th17 generation (Schlitzer et al., 2013). Epicutaneous infection with *Candida albicans* yeast induces a strong protective Th17 response, the generation of which depends on recognition of *Candida albicans* by LCs in the epidermis (Igyarto *et al.*, 2011; Kashem *et al.*, 2015). LCs recognise *Candida albicans* via Dectin-1, which induces to the production of IL-6 that is essential for driving the Th17 response (Kashem et al., 2015).

In sum, $CD103^-$ $CD11b^+$ DCs and $CD103^+$ $CD11b^+$ DCs appear to be the dominant drivers of Th17 responses *in vivo*, while intestinal macrophages dampen this response, although other antigen-presenting cells are capable of inducing Th17 cells under specific conditions (for example LCs in *Candida albicans* skin infection).

Both Tregs derived in the thymus (nTregs) and in the periphery (iTregs) rely on the transcription factor FoxP3 and a lack of Tregs leads to spontaneous autoimmunity. iTregs are generated when naïve $CD4^+$ T cells are activated in the presence of

TGFβ and IL-2. To assess if DCs are crucial in Treg formation and the control of spontaneous autoimmunity, two groups have crossed CD11c-Cre mice to two different strains of ROSA26-DTA mice, generating mice in which CD11c-expressing cells are ablated through expression of DTA (Birnberg *et al.*, 2008; Ohnmacht *et al.*, 2009). Intriguingly, only one of these crosses developed spontaneous autoimmunity, while the other cross showed unaffected T cell homeostasis under steady-state conditions (Birnberg et al., 2008; Ohnmacht et al., 2009). This discrepancy may be due to the different ROSA26-DTA strains used, be related to the environment the mice were housed in, or have a yet undefined cause. Furthermore, by using a Cre recombinase driven by CD11c, other cells in addition to DCs are ablated in these mice, which further complicates interpreting these experiments.

In the periphery the expression of aldehyde dehydrogenase (which metabolises vitamin A into retinoic acid) by DCs is essential for the induction of Tregs (Sun et al., 2007; Coombes et al., 2007; Mucida et al., 2007). In the intestine and mesLN $CD103^+$ $CD11b^+$ DCs express high levels of aldehyde dehydrogenase and are efficient inducers of Tregs (Sun et al., 2007; Coombes et al., 2007). In addition to $CD103^+$ $CD11b^+$ DCs, intestinal macrophages also express considerable amounts of aldehyde dehydrogenase and are potent inducers of Treg responses (Denning et al., 2007). Furthermore, $CX3CR1^+$ macrophages in the lamina propria are driving local expansion of Treg cells and deletion of CX3CR1 impairs local Treg expansion and oral tolerance (Hadis et al., 2011). In the skin and sdLNs a considerable fraction of the $CD11b^+$ dermal DCs express aldehyde dehydrogenase and can convert OT-II cells into Tregs in *in vitro* culture setting (Guilliams et al., 2010). In the intestine it was shown that Wnt-signalling-induced β-catenin activation in DCs is mediating the expression of aldehyde dehydrogenase (and IL-10 and TGFβ), which subsequently drives Treg development (Manicassamy et al., 2010).

CD8α-like DCs can induce Treg formation when antigen is directly and specifically delivered to these DCs by coupling of the antigen to an anti-DNGR-1 antibody (Joffre et al., 2010). Furthermore, inducible depletion of $CD205^+$ $CD8\alpha^+$ DCs confers an impairment in the generation of Tregs from OT-II cells in the spleen upon subcutaneous immunisation with OVA protein in CFA (Fukaya et al., 2012).

Tfh cells are specialised in promoting the formation of germinal centres and are essential for the generation of high-affinity long-lived plasma cells and memory B cells. Although antigen presentation by B cells to Tfh cells is essential for Tfh differentiation and a proper germinal centre response, DCs are crucial for the initial activation of $CD4^+$ T cells and Tfh cell commitment in an antigen-dependent manner (Poholek *et al.*, 2010; Choi *et al.*, 2011; Goenka *et al.*, 2011). Research into the role of different DC subsets in the generation of Tfh cells is still in its infancy. In the skin both LCs and $CD103^+$ dermal DCs are capable of inducing Tfh responses under steady state conditions when antigens are directly targeted to these cells via antibodies, with LCs being more efficient than $CD103^+$ dermal DCs in generating Tfh responses (Yao et al., 2015). Additionally, targeting of antigen to CD8α-like DCs via an anti-DNGR-1 antibody can induce potent humoral responses, although the requirement for adjuvants depends on the antibody used (Caminschi *et al.*, 2008; Joffre *et al.*, 2010; Li *et al.*, 2015). The response is dependent on T helper cells, and antibody targeting to DNGR-1 induces the differentiation of OT-II cells into Tfh cells (Caminschi et al., 2008; Lahoud et al., 2011). So, based on the limited data currently available, it seems that LCs and CD8α-like DCs can induce Tfh responses, at least as long as antigen is targeted directly to these cells. However, the role of $CD11b^+$ DCs, the prototypical $CD4^+$ T cell inducers, remains to be determined.

1.1.4.2 Innate functions of DCs

Since their discovery more than forty years ago, most of the research on DC function has focussed on their interaction with T cells. However, more recently the roles of DCs and DC subsets in directing innate immunity are being appreciated. Although many aspects of innate functions of DCs are still underexplored, DCs are appearing to not only orchestrate adaptive immunity, but also innate immunity. Especially the cytokines produced by DCs can instruct other types of innate immune cells.

Early control of *Toxoplasma gondii* infection is critically dependent on IL-12-mediated IFNγ production by NK cells and $CD8\alpha^+$ splenic DCs are excellent producers of IL-12 in response to *T. gondii* (Gazzinelli et al., 1993; Reis e Sousa et al., 1997). Indeed, mice that are depleted for DCs (via DT injection of CD11c-DTR

mice) show a high mortality during early *T. gondii* infection, which can be rescued by adoptively transferring WT DCs, but not IL-12 deficient DCs (C.-H. Liu et al., 2006). Furthermore, Batf3$^{-/-}$ mice that lack CD8α-like DCs, show a similar high susceptibility to early *T. gondii* infection that can be rescued by the administration of IL-12 (Mashayekhi et al., 2011). These reports indicate a crucial innate role for CD8α-like DCs in early *T. gondii* infection via the production of IL-12.

DCs present glycolipid antigens on CD1d to invariant NKT cells (Kawano et al., 1997). It has been shown that splenic CD8α^{+} DCs are crucial for invariant NKT cell responses and Batf3$^{-/-}$ mice show increased bacterial burden upon infection with *Streptococcus pneumonia*, the clearance of which depends on invariant NKT cells (Arora et al., 2014).

TLR5 activation by flagellin induces high IL-23 production by CD103^{+} CD11b^{+} intestinal DCs, which leads to IL-22-driven production of the antimicrobial peptide RegIIIγ by epithelial cells that is important for barrier integrity in the intestine (Kinnebrew et al., 2012). IL-22 is critical for controlling *Citrobacter rodentium* infection and lack of Notch2-dependent CD103^{+} CD11b^{+} DCs in the intestine leads to high susceptibility to oral *Citrobacter rodentium* infection, due to a lack of IL-23 and consequently IL-22 (Satpathy et al., 2013). Conversely, these results could not be reproduced in huLangerin-DTA mice that also lack intestinal CD103^{+} CD11b^{+} DCs (Welty et al., 2013). The discrepancy between these studies is currently unresolved, but could be caused by (subtle) differences in DC subsets affected. Moreover, a recent study reported CD11c^{+} CX3CR1^{+} mononuclear phagocytes in the intestine to be the source of IL-23 that drives IL-22 production during *Citrobacter rodentium* infection (Longman et al., 2014). Although this finding does not preclude a crucial and non-redundant role for both CD11c^{+} CX3CR1^{+} cells and CD103^{+} CD11b^{+} DCs in producing IL-23 during *Citrobacter rodentium* infection, these conflicting results do warrant for a more detailed characterisation of the intestinal mononuclear phagocytes capable of producing IL-23. DCs also produce IL-23p19 in response to the detection of *Candida albicans* via CLRs and Syk signalling, and in this case IL-23p19 promotes GM-CSF production by NK cells, which in turn fully activates infiltrating neutrophils to kill the *Candida* (Whitney et al., 2014). Indeed, mice that harbour a specific deletion of Syk in DCs are more susceptible to systemic *Candida albicans* infection, due to a lack of NK cell-mediated neutrophil activation (Whitney et al., 2014). Furthermore, DCs also

directly influence NK cell homeostasis and function via the production of IL-15 and depletion of DCs results in reduced homeostatic proliferation of NK cells *in vivo* and reduced effector function upon TLR stimulation (Hochweller et al., 2008).

During a local inflammatory response migDCs accumulate in the subcapsular sinus of LNs, Here, they are involved in temporarily disrupting the layer of subcapsular sinus macrophages, leading to impaired B cell responses to a subsequent challenge (Gaya et al., 2015). TLR signalling via MyD88 in migDCs is required for the disruption of macrophage organisation, but at present it is unknown whether DCs directly interact with the subcapsular sinus macrophages, or indirectly via an intermediate cell type, and what signalling molecules are involved in this interaction.

1.1.4.3 Interactions of dendritic cells with stromal cells

The stromal compartment has long been regarded as essential to provide structure to lymphoid structures, but otherwise not involved in immune responses. However, stromal cells are now acknowledged for actively taking part in immunological processes. Most of our current knowledge comes from studying the stromal compartment in LNs, where fibroblastic reticular cells (FRCs) in the T cell zone and follicular dendritic cells (FDCs) in the B cell follicles form a dense network that facilitates leukocyte trafficking and the transportation of antigens and signalling molecules. FRCs and FDCs also produce different sets of chemokines that are crucial for attracting lymphocytes and organising the B cell and T cell areas. Other major stromal compartments of LNs are blood endothelial cells (BECs) that form the vasculature and lymphatic endothelial cells (LECs) that form the lymphatic network.

A few key publications have recently highlighted that DCs actively engage with stromal cells in LNs and modulate their functions to appropriately orchestrate an immune response. Naïve lymphocytes and other leukocytes enter the LN via specialised blood vessels called high endothelial venules (HEVs). Interestingly, DCs are crucial in maintaining HEV function and in the absence of DCs HEVs loose their ability to support leukocyte trafficking into the LN (Moussion and Girard, 2011; Wendland et al., 2011). Mechanistically it is thought that DCs form a crucial source of LTβ receptor ligands that are essential for HEV homeostasis, and

vascular endothelial growth factor, which induces HEV proliferation (Moussion and Girard, 2011; Wendland et al., 2011; Chyou et al., 2011).
Besides interacting with HEVs, DCs were recently also shown to control FRC function via CLEC2-podoplanin interactions (Acton *et al.*, 2014; Astarita *et al.*, 2015). FRCs form a dense and contractile network in a steady-state LN that needs to expand during an inflammatory response to allow for LN swelling and accommodate lymphocyte influx. FRCs accomplish this task by stretching during the early phase of an immune response, followed by subsequent proliferation if the immune response is prolonged. In steady state podoplanin expression on FRCs promotes FRC contractility and tension throughout the FRC network. During an inflammatory response the accumulation of CLEC2-expressing DCs causes increased binding of podoplanin on FRCs to CLEC2 on DCs, leading to the inhibition of podoplanin-mediated contractility in FRCs (Acton *et al.*, 2014; Astarita *et al.*, 2015). Importantly, in mice that lack CLEC2 expression on DCs, LN expansion is severely impaired, while administration of soluble CLEC2 facilitates LN expansion in response to inflammation (Acton *et al.*, 2014; Astarita *et al.*, 2015). In addition to this well-documented role for DCs in FRC stretching, DCs have also been linked to the regulation of FRC proliferation, as DC depletion in CD11c-DTR mice abrogated inflammation-induced FRC proliferation (Chyou et al., 2011; Yang et al., 2014). However, although these changes in LN swelling mediated by DCs are likely to have an impact on T cell and B cell response, these implications have not been formally addressed yet.

1.2 Mouse models to study dendritic cells

Transgenic mouse models have proven to be indispensable tools to study all aspects of DC biology. These models have allowed for the identification of DC subsets and delineation of DC ontogeny, and have provided a wealth of information on DC function, to name but a few. Among the models most frequently used are mice that express Cre recombinase in DCs, knockout mice for transcription factors involved in DC development, mice in which DCs can be inducibly depleted and mice in which DCs are labelled with fluorescent proteins.

1.2.1 Introduction to Cre-loxP system

The Cre recombinase-loxP system was first discovered in a bacteriophage in 1981, used some years later to recombine DNA in a mammalian cell line, and has since been used extensively for genome manipulation in many organisms (Sternberg and Hamilton, 1981; Sauer and Henderson, 1988). The system relies on the Cre recombinase enzyme that recognises specific 34-base pair sequences called loxP sites that consist of a 8-base pair spacer and two 13-base pair palindromic sequences (Sternberg and Hamilton, 1981). When two such sites are recognised, recombination of the DNA takes place, the outcome of which depends on the orientation of the loxP sites. A stretch of DNA within the genome that is flanked by two loxP sites in the same orientation will be circularised, leading to the loss of the loxP-flanked DNA fragment from the genome and one intact loxP site ending up in the circular DNA fragment and one intact loxP site remaining in the genome. Two loxP sites oriented in opposite directions promote a Cre-mediated inversion of the flanked DNA fragment without the loss of any DNA from the genome, while preserving both loxP sites. Finally, when two loxP sites are located on different chromosomes the action of Cre recombinase will lead to chromosomal translocation.

In transgenic mice the gene encoding Cre recombinase can be expressed under the control of a generic promoter that allows for widespread Cre-mediated loxP recombination, or under the control of tissue specific, cell specific or otherwise restricted promoters to achieve loxP recombination only in cells or tissues of interest. Additionally, a split-Cre system has been developed consisting of two inactive Cre fragments that form a functional Cre recombinase when expressed in the same cell (Hirrlinger, Scheller, et al., 2009; P. Wang et al., 2012). The two split-Cre fragments can be expressed by two different promoters, allowing for more precise targeting of Cre activity to the desired cells (Hirrlinger, Scheller, et al., 2009; P. Wang et al., 2012). Furthermore, various modified Cre recombinases have been generated that are non-functional unless a certain compound is introduced to activate the recombinase activity. One major group consists of Cre recombinase fused to a mutated from of the hormone-binding domains of the estrogen receptor (ER). CreER, or the improved CreERT2, is normally sequestered in the cytoplasm where it is inactive. Upon binding of the ligand 4OH-tamoxifen to the mutated ER

domain, the CreER or CreERT2 enzyme translocates to the nucleus where recombination of loxP sites can take place. Analogous to the split-Cre system, a split-CreERT2 system has also been developed that allows for a more targeted expression of functional CreERT2 (Hirrlinger, Requardt, et al., 2009). As 4OH-tamoxifen has poor bioavailability, the prodrug tamoxifen is normally used for *in vivo* studies and can be administered systemically via oral or parental routes, but is also amenable to local topical application.

1.2.2 DTR-based mouse models to constitutively or inducibly deplete dendritic cells

Our knowledge of DC biology has greatly benefited from the introduction of mouse models that allow for specific depletion of DCs. Most such models make use of the diphtheria toxin receptor (DTR) system. DTR is a membrane-anchored protein that is also called heparin-binding EGF-like growth factor (HB-EGF) and is targeted by diphtheria toxin (DT), a toxin produced by *Corynebacterium diphtheriae* (Higashiyama et al., 2008). Fragment B of the toxin binds the receptor, which results in receptor-mediated endocytosis of the toxin and subsequent translocation of the A fragment (DTA) into the cytosol. DTA inactivates the polypeptide chain elongation factor 2, which leads to the inhibition of protein synthesis and cell death (Saito et al., 2001). Mice are naturally resistant to DT intoxication due to a low binding affinity of DT for murine HB-EGF, which is about 10^5 times lower than the affinity of DT for simian or human HB-EGF (Saito et al., 2001). Therefore, expression of primate DTR on murine cells by transgenesis renders these cells highly susceptible to DT intoxication and cell death, while not affecting the rest of the mouse.

The first DTR model to inducibly deplete DCs used a minimal CD11c promoter to drive a DTR-GFP fusion protein (Jung et al., 2002). In these mice cDCs, pDCs and LCs express DTR and are ablated upon a single DT injection (Jung et al., 2002). However, longer term DC depletion is not possible, as CD11-DTR mice die upon multiple DT injections, probably because of aberrant DTR expression on epithelial cells of the gut (Zaft et al., 2005). Long-term DC depletion can only be achieved in radiation chimeras in which WT mice are reconstituted with CD11c-DTR BM.

Radioresistant cells such as LCs remain of host origin in irradiation chimeras and are therefore not depleted upon DT injection, which can be exploited, but may also be a limitation of this experimental setup. To circumvent the necessity to generate irradiation chimeras for longer-term DC depletion, another mouse model was developed that used a bacterial artificial chromosome approach to express DTR, a fragment of the OVA protein and GFP regulated by the CD11c locus control region (Hochweller et al., 2008). Unlike CD11c-DTR mice, these CD11c-DOG mice do not die upon repeated DT injections. However one major limitation of both CD11c-DTR and CD11c-DOG mice is that CD11c expression is not constrained to DCs, but is also found on some macrophages, plasmablasts, activated T cells, NK cells and Ly6c^{low} monocytes, and many of these cell populations are depleted in both CD11c-DTR and CD11c-DOG mice upon DT injection (Jung *et al.*, 2002; Probst, Tschannen, *et al.*, 2005; Hochweller *et al.*, 2008). Therefore, results obtained in these mice are difficult to firmly attribute to DCs, as other immune cell populations are also affected. Furthermore, both CD11c-DTR and CD11c-DOG mice exhibit neutrophilia and monocytosis upon DT injection, which may confound results obtained, especially when bacterial or viral infections are examined (Hochweller *et al.*, 2008; Tittel *et al.*, 2012; van Blijswijk, Schraml and Reis e Sousa, 2013). For example, one study observed improved bacterial clearance in DC-depleted CD11c-DTR and CD11c-DOG mice in a bacterial pyelonephritis model, which turned out to be caused by neutrophilia and not by DC depletion per se (Tittel et al., 2012). CD11c-DTR and CD11c-DOG mice display an early wave of neutrophilia that is manifest 24h after DT injection and a late wave beginning at 72h after DT injection. The early neutrophilia is due to the release of neutrophils from the bone marrow in response to chemokines CXCL1 and CXCL2 and is mouse model dependent (Tittel et al., 2012). Indeed, the more recently generated CD11c-LuciDTR mice that express DTR, GFP, luciferase and Cre recombinase under control of the CD11c locus control region do not show the early neutrophilia (Tittel et al., 2012). In contrast, the late neutrophilia is a consequence of increased granulopoiesis, likely caused by increased levels of Flt3l and is present in all mice in which DCs are depleted (Tittel et al., 2012).

DTR expression is not restricted to cDCs when expressed under control of the CD11c locus control region or minimal promoter. Therefore, mice were generated that use the expression pattern of the transcription factor Zbtb46 to drive DTR

expression on cDCs (Meredith, Liu, Darrasse-Jeze, et al., 2012). Within the immune system Zbtb46 expression is restricted to cDCs, some activated monocytes and monocytes cultured *in vitro* with GM-CSF and IL-4, but is absent from pDCs and LCs, and hence DTR expression in these zDC-DTR mice is fairly restricted to cDCs, though monocytes may also express DTR (Meredith, Liu, Darrasse-Jeze, et al., 2012; Satpathy, KC, et al., 2012). However, outside of the immune system Zbtbt46 is also expressed in committed erythroid progenitors and endothelial cells, leading to death of zDC-DTR mice upon DT injection (Satpathy, KC, et al., 2012). Consequently, zDC-DTR mice can only be used as radiation chimeras generated by reconstitution of wild type mice with zDC-DTR bone marrow. In a different approach a loxP-flanked stop-cassette followed by the gene encoding simian DTR was inserted into the first intron of the *Itgax* locus (encoding CD11c) (Okuyama et al., 2010). In these CD11c-iDTR mice DTR is only expressed from the CD11c locus control region when the loxP-flanked stop-cassette is excised by Cre recombinase. Therefore, depending on the Cre transgenic line used, only a subset of CD11c-expressing cells will express DTR and will be sensitive to DT-mediated depletion. To demonstrate proof-of-principle, CD11c-iDTR mice were crossed with CAG-Cre mice, which ubiquitously express Cre recombinase (Okuyama et al., 2010). In this cross all CD11c-expressing cells in the spleen were depleted upon DT injection, demonstrating the feasibility of this approach (Okuyama et al., 2010).

In addition to transgenic mice that aim for the depletion of all DCs, several mouse models have been generated to only deplete certain DCs subsets. The expression pattern of langerin has been used to try and generate mice to specifically and inducibly deplete LCs. Two groups independently generated mice to inducibly deplete langerin$^+$ cells by placing DTR and GFP expression under the control of the langerin promoter, either via a knock-in approach or insertion into the 3' untranslated region of the langerin locus (Bennett et al., 2005; Kissenpfennig et al., 2005). Initially it was thought that langerin is exclusively expressed on LCs, and that therefore only LCs would be depleted in Langerin-DTR mice. Although LCs are efficiently depleted in these mice upon DT administration, more recent studies have shown that the CD103$^+$ dermal DCs also express langerin, as well as some CD8α$^+$ DCs in the spleen and LNs, and these DCs are also depleted in Langerin-DTR mice injected with DT (Poulin et al., 2007; Bursch et al., 2007; Henri et al., 2010).

As LCs remain depleted for much longer than the langerin$^+$ DCs after a single dose of DT (around 2 weeks versus 5 days), clever timing of experiments can allow for specific assessment of the effect of LC depletion (Kissenpfennig et al., 2005; Bursch et al., 2007). Alternatively, radiation chimeras can be generated in which Langerin-DTR mice are reconstituted with WT BM, taking advantage of the radioresistance of LCs (Kautz-Neu et al., 2011). Apart from the Langerin-DTR mice, transgenic mice were developed that express DTR under control of the human langerin regulatory elements, the huLangerin-DTR mice (Bobr et al., 2010). Interestingly, in these mice the human langerin regulatory elements only drive DTR expression in LCs and not in CD103$^+$ dermal DCs, and consequently only LCs are depleted in huLangerin-DTR mice injected with DT (Bursch *et al.*, 2007; Bobr *et al.*, 2010).
In addition to these inducible depletion systems, huLangerin-DTA mice were generated that constitutively lack LCs due to the expression of DTA (and immediate cell death) under control of the human langerin regulatory elements (Kaplan et al., 2005). As with huLangerin-DTR mice, dermal CD103$^+$ DCs are unaffected in huLangerin-DTA mice (Bursch et al., 2007). Interestingly, murine intestinal DCs do not express langerin, while human intestinal DCs do (Welty et al., 2013). In huLangerin-DTA mice DTA is also expressed in CD103$^+$ CD11b$^+$ DCs in the intestine and these cells are indeed absent from these mice (Welty et al., 2013).

Inducible depletion of pDCs can be achieved by using the promoter of human blood dendritic cell antigen 2 (BDCA-2, CLEC4C), which is exclusively expressed on pDCs in humans, or by exploiting the expression pattern of SiglecH in the mouse (Swiecki et al., 2010; Takagi et al., 2011; Swiecki et al., 2014). Although BDCA-2 is not present in the mouse, transgenic huBDCA-2-DTR mice exclusively express DTR on pDCs (Swiecki et al., 2010) and DT treatment of BDCA-2-DTR mice leads to efficient and specific mouse pDC depletion (Swiecki et al., 2010). Two transgenic mice have been generated to express DTR from the SiglecH locus control region (Takagi et al., 2011; Swiecki et al., 2014). In the first model DTR and GFP transgenes were inserted into the 3' untranslated region of the *Siglech* gene, while the second one made use of a bacterial artificial chromosome approach (Takagi et al., 2011; Swiecki et al., 2014). SiglecH is highly expressed on pDCs, but is also found on a fraction of CDPs and preDCs, cDCs and certain macrophages (Zhang

et al., 2006; Blasius, 2006; Swiecki *et al.*, 2010; Satpathy, KC, *et al.*, 2012; Swiecki *et al.*, 2014). It was initially reported that DT administration to SiglecH-DTR mice selectively depleted pDCs without affecting other immune cells, but a subsequent study showed that also other SiglecH-expressing cells are eliminated (Takagi et al., 2011; Swiecki et al., 2014). Furthermore, although the insertion of the transgene into the 3' untranslated region was intended not to interfere with SiglecH expression, homozygous mice turned out to be deficient in SiglecH expression, altering the phenotype and function of pDCs in SiglecH-DTR mice (Takagi et al., 2011; Swiecki et al., 2014).

A few different approaches have been taken to inducibly deplete CD8α-like DCs in the mouse. The Clec9a-DTR model uses a bacterial artificial chromosome to express DTR under the control of the *Clec9a* locus (Piva et al., 2012). DNGR-1, the product of the *Clec9a* locus, is expressed on $CD8\alpha^+$ DCs in the spleen and these cells are depleted in Clec9a-DTR mice upon DT treatment (Piva et al., 2012). Given that DNGR-1 is also expressed on CD8α-like DCs in other tissues, these cells are expected to be depleted in Clec9a-DTR mice as well, although this remains to be demonstrated. pDCs express low levels of DNGR-1 and are partially reduced by DT treatment in Clec9a-DTR mice (Piva et al., 2012). Moreover, more recent research has shown that DNGR-1 is expressed on CDP and preDC populations, which suggest that these precursor populations may also be affected by DT injection of Clec9a-DTR mice (Schraml et al., 2013). If CDPs and preDCs are reduced by DT treatment, this may result in quantitative and qualitative differences in other cDC populations that do not express DNGR-1.
Another C-type lectin receptor whose expression is relatively restricted to CD8α-like DCs is CD205 (DEC-205), although LCs, dermal DCs and thymic epithelial cells also express CD205 (Jiang et al., 1995; Kissenpfennig et al., 2005). CD205-DTR mice were generated by inserting a DTR transgene fused to GFP into the 3' untranslated region of the CD205 gene (Fukaya et al., 2012). As CD205-DTR mice die upon DT injection, irradiated WT mice reconstituted with CD205-DTR BM have to be used for depletion studies (Fukaya et al., 2012). In these irradiation chimaeras DT injection depletes $CD205^+$ DCs, but not LCs and thymic epithelial cells, which are radioresistant (Fukaya et al., 2012).

Finally, XCR1-DTR mice have been developed that harbour a *Dtr* and *Venus* gene knocked into the *Xcr1* locus, replacing the entire *Xcr1* coding region (Yamazaki et al., 2013). XCR1 is selectively expressed on CD8α-like DCs and DT injection of XCR1-DTR mice depletes $CD8\alpha^+$ DCs in spleen and LNs and $CD103^+$ migDCs in LNs, but does not affect other leukocyte populations (other tissues were not analysed) (Yamazaki et al., 2013).

Unfortunately at present no transgenic mouse exists that allows for inducible depletion of $CD11b^+$ DCs. The reason is probably that $CD11b^+$ DCs are a more heterogeneous group of DCs than CD8α-like DCs or pDCs and that it has proven to be difficult to find a marker that is selectively expressed on $CD11b^+$ DCs. CD11b-DTR mice exist that use the CD11b promoter to express both DTR and GFP (Duffield et al., 2005). However, $CD11b^+$ DC depletion has not been assessed in these mice and more importantly, CD11b is also expressed on many other myeloid cells such as monocytes, macrophages and granulocytes, rendering these mice not useful to study $CD11b^+$ DC biology. In theory, a more specific way to inducibly deplete $CD11b^+$ DCs is by crossing the CD11c-iDTR mice that harbour a loxP-flanked stop-cassette followed by the gene encoding simian DTR with CD11b-Cre mice (Ferron and Vacher, 2005; Boillée *et al.*, 2006; Okuyama *et al.*, 2010). This cross should only induce DTR expression on $CD11c^+$ cells that have expressed CD11b at some point during their life, which is true for $CD11b^+$ DCs, but also for certain macrophages and monocytes. It therefore remains to be seen which cell populations would be depleted in these mice. Both CD11c-iDTR and CD11b-Cre mice are available, but such cross has not been published yet.

In summary, many DTR- and DTA-based mouse strains are available to inducibly or constitutively deplete all DCs or DC subsets *in vivo*. However, although these mouse models are useful tools to study DC biology, other cell populations than the one intended may be affected, which complicates the interpretation of experiments. Furthermore, at least the CD11c-based DTR models have been shown to suffer from neutrophilia and monocytosis upon DT injection, which must be taken into account when interpreting results. Unfortunately, the induction of neutrophilia and monocytosis has not been formally examined in other models. Moreover, some DTR-based models such as zDC-DTR mice and CD205-DTR mice die upon DT

injection and may only be used as irradiation chimaeras. Finally, mouse models have been developed to deplete LCs, pDCs and CD8α-like DCs, but no model exists to inducibly deplete $CD11b^+$ DCs, hampering the study of this subset.

1.2.3 Fluorescence-based models to track dendritic cells

Besides mouse models to deplete DCs, another powerful tool to study DC biology *in vivo* is to use mice that harbour fluorescently labelled DCs. Many DTR-based mouse models express a fluorescent protein (usually GFP) in addition to the DTR transgene, like CD11c-DTR and langerin-DTR mice (Jung *et al.*, 2002; Bennett *et al.*, 2005; Kissenpfennig *et al.*, 2005). The fluorescent protein expression is not only useful to track DT-mediated ablation and subsequent recovery of the DTR-expressing DC population in these mice, but can also be used to visualise the labelled cells in the absence of DT treatment. In addition to the mouse models that combine DTR expression with fluorescent protein expression, transgenic mice have also been developed that exclusively express fluorescent proteins. For example, in CD11c-YFP mice YFP-Venus expression is controlled by the CD11c promoter and cells with high CD11c expression are high YFP^{bright}, while in cells with lower CD11c expression YFP is dimmer (Lindquist et al., 2004). CD11c is also expressed on other cells than DCs, but in many tissues the majority of the $CD11c^{hi}$, and therefore YFP^{bright}, cells are often DCs. CD11c-YFP mice are therefore very useful for microscopy-based approaches. Confocal microscopy on tissue sections from CD11c-YFP mice readily shows the localisation and dendritic morphology of DCs in for example LNs and spleen (Lindquist et al., 2004; Gerner, Torabi-Parizi and Germain, 2015). Moreover, the YFP signal in DCs is bright enough to allow for the detection of DCs by intravital microscopy and track their behaviour *in vivo*. In this respect CD11c-YFP mice have for example been used to visualise the uptake of beads, bacteria and malaria sporozoites by DCs in LNs, DC migration in the afferent lymphatics of mesLNs, or antigen sampling in the intestine (Chieppa *et al.*, 2006; Olga Schulz *et al.*, 2009; McDole *et al.*, 2012; Radtke *et al.*, 2015; Gerner, Torabi-Parizi and Germain, 2015).

Zbtb46-GFP mice harbour the gene encoding GFP in the endogenous *Zbtb46* locus, which allows for selective GFP expression in cDCs, some activated monocytes, committed erythroid progenitors and endothelial cells (Satpathy, KC, et

al., 2012; Meredith, Liu, Darrasse-Jeze, et al., 2012). In irradiation chimeras in which WT mice are reconstituted with Zbtb46-GFP BM, endothelial cells are of WT origin and not labelled, allowing for the visualisation of cDCs (and maybe activated monocytes, depending on the experimental setup). These irradiation chimeras have a more restricted fluorescent protein expression than the CD11c-YFP mice and can be a useful alternative to visualise cDCs in tissue sections or by intravital microscopy.

Several mouse models exist to visualise specific DC subsets, analogous to the subset-specific DTR-based mouse models as discussed in 1.2.2. Langerin-GFP mice contain the gene encoding GFP in the 3' untranslated region of the *langerin* locus, resulting in GFP expression in LCs, $CD103^+$ dermal DCs and some $CD8\alpha^+$ DCs in the spleen and LNs (Kissenpfennig et al., 2005; Bursch et al., 2007). Additionally, both Langerin-DTR strains also express GFP in the same cell types (Kissenpfennig *et al.*, 2005; Bennett *et al.*, 2005; Bursch *et al.*, 2007). All these mice can be used to visualise LCs in epidermal sheets and $langerin^+$ cells in tissue sections (Kissenpfennig *et al.*, 2005; Bennett *et al.*, 2005; Bursch *et al.*, 2007). CD205-DTR mice express GFP as well and may be used to visualise CD8α-like DCs, although some other cell types are also labelled (Fukaya et al., 2012). However, whether GFP expression in these mice is bright enough for microscopy experiments remains to be established. DNGR-1 (or CLEC9A) is expressed on CD8α-like DCs and at lower levels on pDCs. Clec9a-GFP mice express GFP under control of the *Clec9a* locus and both CD8α-like DCs and pDCs express GFP in these mice, although GFP levels are lower in pDCs (Sancho et al., 2009). XCR1 expression is specific for CD8α-like DCs and both XCR1-DTR and XCR1-Venus mice express the fluorescent protein Venus from the endogenous *Xcr1* locus (Yamazaki et al., 2013). Venus is selectively expressed in CD8α-like DCs in both lymphoid and non-lymphoid tissues and can be used to visualise these cells by confocal microscopy (Yamazaki et al., 2013). These mice will be a useful tool to study CD8α-like DCs by intravital microscopy or in tissue sections.

In the above-mentioned mouse models fluorescent protein expression is directly driven by a DC-restricted promoter. Alternatively, mouse lines that express Cre recombinase in DCs crossed to fluorescent reporter mice can be used to visualise

DCs *in vivo* or in tissue sections. Using the Cre-loxP system to fluorescently label DCs has advantages over using direct fluorescent protein expression driven by a DC-restricted promoter. Firstly, a Cre mouse line regulated by a given promoter may label different cell populations than a mouse line expressing a fluorescent protein regulated by the same promoter, as the Cre-mediated excision of loxP sites is irreversible and inheritable by daughter cells. Secondly, the Cre-loxP system is more versatile, as many different fluorescent reporter mouse lines exist that express different fluorescent proteins. Finally, if a mouse line expressing an inducible Cre recombinase is available, not only spatial control but also temporal control over fluorescent protein expression can be achieved.

CD11c-Cre mice will recombine loxP sites in any CD11c-expressing cell, and when these mice are crossed to a reporter mouse DCs are labelled, but also many macrophages and some other immune cells such as T cells and B cells (Caton, Smith-Raska and Reizis, 2007). As many macrophages are labelled in CD11c-Cre mice crossed to the ROSA26-LSL-YFP reporter line, these mice have been used to visualise alveolar macrophages by intravital microscopy (Westphalen et al., 2014). However, to visualise DCs, CD11c-Cre mice crossed to a fluorescent reporter line are less useful. Interestingly, CD11c-CreERT mice have been generated that express an inducible form of Cre recombinase under the control of the CD11c promoter (Probst et al., 2003). When these mice are crossed with a GFP reporter line and tamoxifen is administered, about 4-8% of DCs in lymphoid organs turn GFP^+ (Probst et al., 2003). Although the recombination frequency is relatively low, it should label enough DCs for microscopy-based experiments. Furthermore, recombination only takes place during a relatively short time frame, which should limit the labelling of non-DCs.

Another useful Cre mouse line are the Clec9a-Cre mice, which express Cre recombinase under control of the *Clec9a* locus (Schraml et al., 2013). In these mice Cre is expressed at the CDP and preDC stage, as well as in CD8α-like DCs and pDCs. As DC precursors express Cre and loxP excision is irreversible, all DCs are labelled in Clec9a-Cre mice crossed to the ROSA26-LSL-YFP reporter line and can be visualised by microscopy (Schraml et al., 2013).

The only two transgenic mouse lines currently available to express Cre recombinase in a subset of DCs are the Langerin-Cre mice that have the gene encoding Cre recombinase knocked into the murine *langerin* locus and the

huLangerin-Cre mice that express Cre under control of the human langerin regulatory elements (Kaplan *et al.*, 2007; Zahner *et al.*, 2011). Langerin-Cre mice express Cre in LCs and other langerin$^+$ DCs, and when crossed to a RFP reporter strain all these cells are RFP$^+$ (Zahner et al., 2011). As the human langerin regulatory elements were used to generate huLangerin-Cre mice, Cre is only active in LCs and probably in intestinal CD103$^+$ CD11b$^+$ DCs (Bursch et al., 2007; Welty et al., 2013). When huLangerin-Cre mice are crossed to a GFP reporter mouse strain LCs are specifically GFP$^+$ (Kaplan et al., 2007).

In summary, multiple fluorescence-based mouse models to visualise DCs *in vivo* and in tissue sections are available. CD11c-YFP, Zbtbt46-GFP and Clec9a-Cre mice crossed to a reporter strain all label DCs with fluorescent proteins, but do not distinguish between subsets. Subset-specific labelling can be achieved with Langerin-GFP, XCR1-GFP, Clec9a-GFP and huLangerin-Cre mice crossed to a reporter strain, and with several of the DTR strains that express a fluorescent protein in addition to DTR. Unfortunately, only one mouse strain, the CD11c-CreERT mouse, currently exists that expresses an inducible Cre recombinase and therefore allows for temporal control over labelling of DCs *in vivo*. It will be very useful for the study of DCs and DC subsets if other inducible Cre mice are developed.

1.2.4 Transcription factor knockout mice to study DC function

Besides mice that allow for constitutive or inducible depletion of DCs and mice in which DCs are fluorescently labelled, another group of mice to study DC biology is mice that lack a transcription factor. These mice can be full knockouts, affecting not only DCs but all cells in the body, but may also contain DC-specific deletions. In the latter case parts of the gene of interest are flanked by loxP sites and DC-specific Cre expression is used to generate a DC-specific knockout.

A detailed overview of transcription factor expression and dependency is given in 1.1.2.2. Although full knockout mice for various transcription factors have been instrumental to delineate transcription factor dependency of DCs, most are not useful to study other aspects of DC biology. The main reason is that transcription

factors are usually expressed in and important for many other cell types in addition to DCs. Full knockout mice lack the transcription factor of interest in all cells, which complicates the interpretation of results obtained in these mice. The main exception are Batf3$^{-/-}$ mice, which have a selective deficiency in CD8α-like DCs (Hildner et al., 2008; Edelson et al., 2010). Therefore, Batf3$^{-/-}$ mice are often used to study immune responses in the absence of CD8α-like DCs, for example in the context of *Listeria monocytogenes, Toxoplasma gondii*, influenza or West Nile virus infection, contact hypersensitivity and tumour rejection. However, Batf3 is not only expressed in CD8α-like DCs, but in all cDC subsets, Th1 cells and at lower levels in Th2 and Th17 cells, although these cells do not rely on Batf3 for their development and survival (Hildner et al., 2008). It is therefore conceivable that the function of DCs still present in Batf3$^{-/-}$ mice and Th1, Th2 and Th17 cells is altered due to the lack of Batf3 in these cells, which should be taken into account when interpreting results.

The transcription factor E2-2 is essential for pDCs, but is also involved in development and E2-2$^{-/-}$ mice die at birth (Cisse et al., 2008). This lethal phenotype can be overcome by generating conditional knockout mice by crossing E2-2$^{fl/fl}$ mice with CD11c-Cre mice. These conditional E2-2 knockout mice show about a 3-fold reduction in pDC numbers and the remaining pDCs are functionally impaired, which may be sufficient to show a phenotype in certain experimental settings, but not in all (Cisse et al., 2008).

IRF4$^{-/-}$ mice show impaired CD11b^{+} DC development. However, IRF4 is also important for the function and homeostasis of T cells and B cells, which makes it difficult to determine which cell type(s) is responsible for observed immune defects in these mice (Mittrücker *et al.*, 1997; Suzuki *et al.*, 2004). To circumvent the effects of IRF4 deficiency on lymphocytes, IRF4$^{fl/fl}$ mice were crossed with CD11c-Cre mice to generate mice in which IRF4 deficiency is confined to DCs (Persson, Uronen-Hansson, et al., 2013; Schlitzer et al., 2013). Indeed, these conditional IRF4 knockout mice show a specific impairment in development and function of intestinal CD103^{+} CD11b^{+} DCs and CD11b^{+} DCs in the lung (Persson, Uronen-Hansson, et al., 2013; Schlitzer et al., 2013). Similarly, mice that are deficient in Notch2 signalling in DCs, via conditional deletion of Notch2 or the downstream

transcription factor RBP-J by CD11c-Cre, have reduced $CD11b^+$ DCs in the spleen (Caton, Smith-Raska and Reizis, 2007; Lewis *et al.*, 2011). In the case of Notch2 it was shown that a specific subset of splenic $CD11b^+$ DCs, the $ESAM^{hi}$ cells, were selectively missing (Lewis et al., 2011). $CD103^+$ $CD11b^+$ DCs in the intestine were also lost in mice that lacked Notch2 in DCs, while this subset was not investigated in the RBP-J conditional knockout mice (Caton, Smith-Raska and Reizis, 2007; Lewis *et al.*, 2011).

So, although deficiency in many transcription factors leads to a (partial) loss of DCs or impaired DC functionality, only a few of these models may be useful to study DC function beyond the direct effects of transcription factor loss. Of the models discussed here only $Batf3^{-/-}$ are widely used to study immune responses in the absence of CD8α-like DCs.

1.2.5 Chemokine (receptor) knockout mice to study DC function

Analogous to mice lacking transcription factors, mice that lack chemokines or chemokine receptors are also useful tools to study DC biology. The chemokine receptor CCR7 and its ligands CCL19 and CCL21 are essential for DC, T cell and B cell migration and positioning within tissues (Förster *et al.*, 1999; Förster, Davalos-Misslitz and Rot, 2008). CCL19 and CCL21 are expressed on HEVs and by FRCs in the T cell zone of LNs. CCL21 is also expressed in lymphatic vessels, lymphoid and non-lymphoid organs (Förster, Davalos-Misslitz and Rot, 2008). Due to a gene duplication event mice have two genes encoding CCL21, CCL21-Leu and CCL21-Ser, that differ by one amino acid and show differential expression patterns (Förster, Davalos-Misslitz and Rot, 2008). *Plt/plt* mice have a spontaneous deletion in the gene loci encoding CCL19 and CCL21-Ser, without affecting CCL21-Leu. These mice still express CCL21-Leu in lymphatic vessels of non-lymphoid tissues, but completely lack the expression of CCL19 and CCL21 in lymphoid organs (Vassileva *et al.*, 1999; Luther *et al.*, 2000; Nakano and Gunn, 2001).
Loss of CCR7 expression on T cells leads to homing defects of these T cells to LNs and to the white pulp in the spleen, and impairs migration within lymphoid organs (Förster et al., 1999; Worbs et al., 2007). A similar phenotype is observed in *plt/plt*

mice, which also show impaired T cell homing (Gunn et al., 1999). Migration of DCs from peripheral tissues to LNs is also crucially dependent on CCR7. Full knockout mice for CCR7 or mice that lack CCR7 on all cells except for T cells show impaired DC migration from peripheral tissues to LNs and harbour severely reduced DC numbers in their LNs (Ohl *et al.*, 2004; Wendland *et al.*, 2011). DC migration is also reduced in *plt/plt* mice, even though CCL21-Leu is still expressed on the lymphatics in peripheral tissues (Gunn et al., 1999).

Migration of DCs from peripheral tissues to LNs is considered to be a defining property of DCs. As CCR7 is crucial for DC migration, CCR7 expression and CCR7-dependent migration to LNs are often used to help classify myeloid cells in peripheral tissues as DCs. However, LCs and certain monocyte-derived cells also express CCR7 and migrate towards LNs, and therefore CCR7-dependent migration is not a unique feature of DCs (Ohl *et al.*, 2004; Zigmond *et al.*, 2012; Tamoutounour *et al.*, 2013). Besides the use of $CCR7^{-/-}$ mice to assess CCR7-dependent migration of myeloid cells, these mice are also used to study the effects of antigen delivery by migDCs (and other migrating myeloid cells) on immune responses. A local inflammation or infection in peripheral tissues generally leads to antigen-specific T cell responses in the draining LNs and migDCs are in most cases crucial for the transportation of antigen to the LNs (Ohl *et al.*, 2004; Plantinga *et al.*, 2013). The accumulation of antigen in LNs is abolished in $CCR7^{-/-}$ mice, leading to impaired immune responses (Ohl *et al.*, 2004; Tamoutounour *et al.*, 2012; Plantinga *et al.*, 2013). However, a major limitation of using $CCR7^{-/-}$ mice for these studies is that not only DC migration is impaired, but also T cell homing and migration, which in itself impacts immune responses. One way to overcome this limitation is to adoptively transfer $CCR7^{-/-}$ T cells or DCs into a WT host (or suitable transgenic host). More recently a conditional proficient CCR7 transgenic mouse was developed (Wendland et al., 2011). In these mice the endogenous *Ccr7* locus is disrupted by insertion of a loxP flanked *neomycin* gene, followed by a gene encoding the human CCR7 protein, which is not transcribed when the *neomycin* cassette is present. Effectively these mice are a full knockout for CCR7, but Cre-mediated recombination can induce human CCR7 expression on specific cells. When these mice are crossed to a T cell-specific Cre mouse strain, such as CD4-Cre that was used in the original paper describing these mice, T cells express

human CCR7 and regain full functionality (Wendland et al., 2011). However, CD4 is also expressed on certain DC subsets that consequently may also express human CCR7 when CD4-Cre mice are used. Nonetheless, such crosses will be very useful to dissect the contribution of CCR7-dependent antigen delivery to LNs on immune responses.

Egress of Ly6c^{hi} monocytes from the bone marrow is critically dependent on the chemokine receptor CCR2 (Serbina and Pamer, 2006). CCR2$^{-/-}$ mice show accumulation of Ly6c^{hi} monocytes in the bone marrow and reduced frequencies of Ly6c^{hi} monocytes in the blood and of monocyte-derived cells in tissues, both under steady state conditions and during inflammation (Boring *et al.*, 1997; Kuziel *et al.*, 1997; Serbina and Pamer, 2006). CCR2$^{-/-}$ mice have therefore proven to be a useful tool to show monocytic origin of myeloid cell populations in tissues and to study immune responses in the absence of inflammatory monocytes (Serbina, Salazar-Mather, *et al.*, 2003; Ginhoux *et al.*, 2007; Tamoutounour *et al.*, 2012; 2013; Satpathy *et al.*, 2013). Interestingly, a recent study reported that a fraction of preDC-derived CD11b^{+} DCs in the intestine and mesLN express CCR2 and is reduced in CCR2$^{-/-}$ mice (C. L. Scott et al., 2015). These results highlight that caution is warranted when using CCR2$^{-/-}$ mice to address the origin and function of myeloid cells.

1.2.6 Models to trace the dendritic cell lineage

Tracing of daughter cells of progenitors is a powerful tool to establish lineage relationships and can be used to classify various mononuclear phagocytes into DCs, monocytes and macrophages (Guilliams et al., 2014; Schraml and Reis e Sousa, 2014; Poltorak and Schraml, 2015). One method to establish a precursor-product relationship is to sort the precursors, adoptively transfer them into a congenic host and retrieve and analyse the donor-derived cells at a defined time point after transfer. However, this method is not always feasible, as precursors tend to be rare cell populations and enough cells need to be sorted in order to retrieve donor cells from the host. Furthermore, it is not always clear when to analyse the hosts and if the wrong time point is chosen, certain products of progenitors may be missed. Finally, these types of experiments may require sublethal irradiation of the

host to ensure engraftment of donor cells and always involve intravenous injection of precursors, which may lead to results that are not reflective of the physiological behaviour of precursors.

Alternatively, a genetic approach based on the Cre-loxP system can be taken to fate map precursors *in vivo*. In this case a transgenic mouse line expressing a constitutive or inducible Cre in the precursor of interest is crossed to a fluorescent reporter strain. Cre-mediated expression of the fluorescent protein is induced in the precursor and is inherited by all daughter cells. Analysis of the labelled cells then identifies precursor-derived cells.
The only mouse model available to trace the dendritic cell lineage are Clec9a-Cre mice that express Cre recombinase in CDPs and preDCs (Schraml et al., 2013). When Clec9a-Cre mice are crossed to a ROSA26-LSL-YFP reporter line, DCs are labelled with YFP both in steady state and during inflammation (Schraml et al., 2013). However, Clec9a-Cre mice are not perfect as lineage tracers, as CD8α-like DCs and pDCs also express DNGR-1 (or CLEC9A) and therefore will express YFP irrespective of precursor origin. Furthermore, the labelling penetrance is not complete, so some CDP- and preDC-derived cells do not express YFP (Schraml et al., 2013). Identification of genes whose expression is restricted to CDPs and/or preDCs should aid in the generation of Cre mouse lines that will overcome these limitations. Furthermore, the development of mice that express an inducible version of Cre recombinase specifically in CDPs and/or preDCs will allow for temporal control over the lineage tracing of DCs.

1.3 Aims and objectives

DCs comprise a heterogeneous group of innate immune cells, unified by a shared developmental origin, overlapping surface marker expression, morphology and functions. Many different subsets of DCs have been identified over the years, which can be stratified into pDCs and cDCs, the latter of which consists of the CD8α-like subgroup of DCs and CD11b-expressing DCs. Alternatively, cDCs can be separated into DCs resident in lymphoid tissues (resDCs) and DCs that populated peripheral tissues from where they migrate to LNs (migDCs).

The field of DC biology has greatly benefited from transgenic mouse models to genetically manipulate DCs. Examples are mice that lack transcription factors, growth factors or chemokines essential for DC development or function, mice in which DCs can be inducibly depleted, or mice that have their DCs labelled with fluorescent proteins. However, although these models have greatly contributed to our understanding of DC biology, there are still many open questions that await novel mouse models to be answered.

In this thesis novel mouse models are presented to study DCs *in vivo*. All these mice target DC precursors via genetic editing of the *Clec9a* locus, thereby manipulating the DC lineage. Chapter 3 discusses the validation of a novel mouse model to inducibly deplete DCs *in vivo* via expression of DTR on DCs, and general limitations of this type of model to study DC biology. In Chapter 4 the generation and validation of a transgenic mouse engineered to constitutively lack DCs is presented. Finally, Chapter 5 discusses how DC precursors seed tissues by making use of novel mouse models and advanced microscopy techniques.

Chapter 2. Materials & Methods

2.1 Mice

2.1.1 Mouse strains used

Clec9a-Cre (Schraml et al., 2013), ROSA26-LSL-iDTR (Buch et al., 2005), CD11c-Cre (Caton, Smith-Raska and Reizis, 2007), CD11c-DTR (Jung et al., 2002), CD11c-DOG (Hochweller et al., 2008), Langerin-DTR (Kissenpfennig et al., 2005), CD19-Cre (Rickert, Roes and Rajewsky, 1997), DEREG (Lahl et al., 2007), ROSA26-YFP (Srinivas et al., 2001), ROSA26-mTmG (Muzumdar et al., 2007), ROSA26-dTomato (Madisen et al., 2010), ROSA26-confetti (Snippert et al., 2010), C57BL/6J and B6.SJL mice were bred at Cancer Research UK in specific pathogen-free conditions. All transgenic mouse lines were on a C57BL/6J background and were maintained by Neil Rogers. CD11c-DTR mice (Jung et al., 2002) on a C57BL/6J background were a kind gift from Giovanna Lombardi, Langerin-DTR mice (Kissenpfennig et al., 2005) on a C57BL/6J background were a kind gift from Clare Bennett and ROSA26-CreERT2 mice (Ventura et al., 2007) on a C57BL/6J background were a kind gift from Dinis Calado. All were bred at Cancer Research UK in specific pathogen-free conditions.
Six to Twenty week old mice were used in all experiments, unless otherwise specified. All animal experiments were performed in accordance with national and institutional guidelines for animal care and were approved by the London Research Institute Animal Ethics Committee and by the UK Home Office.

2.1.2 Mouse generation

Clec9a-DTA and Clec9a-CreERT2 mice were generated using a modified version of the targeting vector pFloxRI-C9a-EGFP that was used to generate Clec9a-GFP mice (Sancho et al., 2009). The DTA gene was amplified by PCR from a pMC1DT-A vector provided by Axel Behrens using the primers AAA**GTCGAC**ATGGACCCTGATGATGTTGTTGATTCT and AAA**GGATCC**TTAGAGCTTTAAATCTCTGTAGGTA (bold nucleotides indicate SalI and BamHI restriction sites, underlined nucleotide indicates silent mutation to remove BamHI site) using the expand high fidelity PCR system (Roche). Both the

pFloxRI-C9a-EGFP vector and the DTA PCR product were digested with SalI and BamHI (NEB) and purified on agarose gel. The DTA gene was ligated into the cut vector using T4 ligase (NEB). The resulting pFloxRI-C9a-DTA vector was sequenced to confirm correct cloning, linearized using NotI (NEB) digestion and transfected into C57BL/6-derived embryonic stem (ES) cells (PRXB6N, Primogenix) by electroporation. Cells were selected in medium containing G418 and gancyclovir and clones were picked after selection. Clones were screened for successful targeting by PCR with the PCR primers TCTGAGAGCTCCCTGGCGAAT and TCTCTTAGCCCTATTTCCACCACA using LA taq DNA polymerase (TaKaRa). Clones positive by PCR were additionally screened by Southern blot for correct targeting. Correctly targeted ES cell clones were injected into blastocyst donors, which were transferred back into pseudo-pregnant females. Chimeric males were mated with C57BL/6J females. Germline transmission of correctly targeted clones was confirmed by PCR with the PCR primers AAAAGTTCCACTTTCTGGATGATGA and AGATCGCCTGACACGATTTCCTG for the targeted allele and AAAAGTTCCACTTTCTGGATGATGA and TCACTTACTCCTCCATGCTGACG for the WT allele using GoTAQ Flexi DNA polymerase system (Promega).

The CreERT2 gene was amplified from a pCre-ERT2 vector (Indra et al., 1999) provided by Taija Makinen using the primers AAA**GTCGAC**ATGTCCAATTTACTGACCGTACACC and AAA**GTTAAC**TCAAGCTGTGGCAGGGAAACC (bold nucleotides indicate SalI and HpaI restriction sites) with the expand high fidelity PCR system (Roche). The pFloxRI-C9a-EGFP vector was cut with BamHI (NEB), treated with large klenow fragment DNA polymerase I (NEB) to generate a blunt end and then cut with SalI (NEB). The CreERT2 PCR product was first cut with SalI (NEB) and subsequently with HPAI (NEB). The CreERT2 gene was ligated into the cut vector using T4 ligase (NEB), using the SalI site and blunt end ligation. The resulting pFloxRI-C9a-CreERT2 vector was sequenced to confirm correct cloning, linearized using NotI (NEB) digestion and transfected into C57BL/6-derived ES cells (PRXB6N, Primogenix) by electroporation. Cells were selected in medium containing G418 and gancyclovir and clones were picked after selection. Clones were screened for successful targeting by PCR with the PCR primers

TCTGAGAGCTCCCTGGCGAAT and TCTCTTAGCCCTATTTCCACCACA using LA taq DNA polymerase (TaKaRa). Clones positive by PCR were additionally screened by southern blot for correct targeting. Correctly targeted ES cell clones were injected into blastocyst donors, which were transferred back into pseudo-pregnant females. Chimeric males were mated with C57BL/6J females. Germline transmission of correctly targeted clones was confirmed by PCR with the PCR primers AAAAGTTCCACTTTCTGGATGATGA and CCCAGAAATGCCAGATTACG for the targeted allele and AAAAGTTCCACTTTCTGGATGATGA and TCACTTACTCCTCCATGCTGACG for the WT allele using GoTAQ Flexi DNA polymerase system (Promega).

The neomycin cassette was removed by crossing Clec9a-DTA or Clec9a-CreERT2 mice with PGK-Cre mice (Lallemand et al., 1998).

2.1.3 DT treatment

To deplete DCs in Clec9a$^{+/Cre}$ROSA^{iDTR} mice, mice were injected i.p. with 12ng/g body weight diphtheria toxin (Sigma Aldrich) in PBS and analysed 24 hours later.

2.1.4 Tamoxifen treatment

Tamoxifen diet (TAM400) was purchased from Harlan. Mice were changed from normal diet to TAM400 diet ad libitum for six days before analysis.
Tamoxifen was purchased from Sigma Aldrich (T5648) and always protected from light. For oral gavage, tamoxifen was dissolved in 100% EtOH at 2g/ml and diluted 50 times with peanut oil (Sigma Aldrich) to a final concentration of 40mg/ml. Mice were gavaged with 100µl of 40mg/ml tamoxifen for four consecutive days.
Tamoxifen was dissolved in peanut oil at 80mg/ml for s.c. injections and 20mg/ml for i.p. injections by rotating the suspension at 56°C in a hybridisation oven, protected from light, until the tamoxifen was dissolved. Aliquots were kept at 4°C for the duration of the experiment and warmed to 37°C before injection. For s.c. injections mice were injected with 100µl on day 1, 3 and 5 (8mg tamoxifen per injection). For i.p. injections mice were injected daily with 5µl/g body weight (100µg tamoxifen/g body weight) for five consecutive days.

2.1.5 Influenza Infection

Mice were anaesthetised via an i.p. injection of ketamine/xylasine. Mice were infected i.n. with $1x10^4$ pfu influenza A HK31 (ATCC, strain A/Hong Kong/8/68) in PBS. Mice were monitored daily for weight loss and signs of infection. Mice were sacrificed at day 9 post infection.

2.1.6 CFA/OVA immunisation

CFA/OVA emulsion was prepared by sonicating equal volumes of 2mg/ml EndoFit Ovalbumin (Invivogen) in PBS with Complete Freund's Adjuvant (Sigma Aldrich) until an emulsion was formed. The emulsion was tested by floating a drop on PBS and only used when the emulsion did not dissolve into the PBS. Mice were immunised s.c. draining to the inguinal lymph node with 50µl CFA/OVA emulsion (50µg OVA per injection). Mice were sacrificed at day 12 post infection.

2.1.7 Mixed BM chimeras

BM was isolated from femur, tibia and ilium. Bones were flushed with ice-cold 5% foetal calf serum in PBS, centrifuged for 4min/1400rpm/4°C and resuspended in 2ml PBS. Cell suspensions were counted and adjusted to $1x10^7$ cells/ml. For mixed BM chimeras BM from both donors was combined in a 1:1 ratio.
Hosts were treated with 0.043% HCl (Sigma Aldrich) in their drinking water ad libitum, starting 7 days before irradiation and continuing up to 10 weeks after irradiation. Host mice were irradiated twice with 6.6 Gray, separated by 4 hours. Hosts were injected i.v. 24 hours after the last irradiation with $2x10^6$ total BM donor cells.
Peripheral blood was collected via tail vein bleed into heparinised tubes to assess reconstitution after a minimum of eight weeks after BM transfer.

2.2 Flow cytometry

2.2.1 Cell isolation

Inguinal lymph nodes were used for analysis of skin draining lymph nodes. Spleens, lymph nodes, thymus and Peyer's patches were cut into small pieces and digested with Collagenase IV (200U/ml, Worthington) and DNase I (0.2mg/ml, Roche) in RPMI for 30 min at 37°C. Digested tissues were strained through a 70µm cell strainer (BD Bioscience) and washed with FACS buffer (3% foetal calf serum, 5mM EDTA, 0.02% sodium azide in PBS). For spleens, red blood cells were lysed with Red Blood Cell Lysis Buffer (2 min at RT; Sigma). For flow cytometry analysis cells were resuspended in FACS buffer.

For small intestines (SI) Peyer's patches and connective tissue were removed. Connective tissue was removed from colons. SI or colons were cut open longitudinally and rinsed with PBS. The tissue was cut in 0.5cm long pieces and incubated in 20ml of RMPI with 25mM HEPES, L-glutamine, Penicillin/Streptomycin, 50µM β-mercaptoethanol, 5mM EDTA (all Gibco), 3% foetal calf serum and 0.145mg/ml DL-dithiothreitol (Sigma) for 20min at 37°C with shaking. SI or colons were subsequently vortexed for 30s and strained through a fine mesh kitchen strainer. Pieces were washed three times in 10ml of RMPI with 25mM HEPES, L-glutamine, Penicillin/Streptomycin, 50µM β-mercaptoethanol and 2mM EDTA (all Gibco), while vortexing in between each washing step to remove intraepithelial lymphocytes. SI or colon pieces were digested with Collagenase IV (200U/ml, Worthington) and DNase I (0.2mg/ml, Roche) in 10 ml RPMI medium for one hour at 37°C. Digested tissues were strained through a 70µm cell strainer (BD) and washed with FACS buffer.
For the analysis of dermis and epidermis both ears were collected and split into dorsal and ventral halves. Split ears were then incubated for 1 hour at 37°C, while floating dermis-down on 2U/ml Dispase II (Roche) in PBS. Epidermis and dermis were subsequently separated and digested separately with Collagenase IV (200U/ml; Worthington) and DNase I (0.2mg/ml, Roche) in RPMI for 1 hour at 37°C. Digested tissues were strained through a 70µm cell strainer (BD) and washed with FACS buffer.

For the SI, colon, dermis and epidermis leukocytes were enriched by Percoll gradient centrifugation (GE Healthcare). 9 Parts Percoll were combined with 1 part 10x PBS to obtain 100% Percoll. Cells were resuspended in 70% Percoll in PBS or HBSS, overlaid with 37% and 30% Percoll and centrifuged at room temperature for 30min at 2000rpm without braking. Cells were collected at the 70/37% interface.

2.2.2 Counting of cell suspensions

10µl of a sample was combined with 5000 nominal 10µm latex beads (Beckman Coulter) and 5ng/ml propidium iodide in FACS buffer, in a total volume of 100µl. This sample was analysed on a BD FACS Calibur (BD Biosciences) and the cell number was calculated with the formula: cells acquired/beads acquired*50.

2.2.3 MACS enrichment

Single cell suspensions from one spleen were resuspended in 180µl MACS buffer (5% foetal calf serum, 2mM EDTA in PBS, degassed) and 20µl CD11c microbeads (Miltenyi Biotec) was added. Samples were incubated for 15min at 4°C, washed by adding 10ml MACS buffer and resuspended in 500µl MACS buffer.
LS MACS columns (Miltenyi Biotec) were prepared by attaching them to the MACS magnet and rinsing with 3ml MACS buffer, after which the cell suspension was applied. The column was washed three times with 3ml MACS buffer. Columns were removed from the MACS magnet and $CD11c^+$ cells were eluted with 5ml MACS buffer.

2.2.4 Antibodies for Flow Cytometry

Target	Fluorophore	Clone	Company	Final concentration
CD3ε	APC	145-2C11	BD Bioscience	2μg/ml
CD3ε	FITC	145-2C11	BD Bioscience	5μg/ml
CD3ε	PE	145-2C11	BD Bioscience	2μg/ml
CD4	FITC	RM4-5	BD Bioscience	2.5μg/ml
CD4	Pacific Blue	RM4-5	Biolegend	1.25μg/ml
CD8α	eFluor 605nc	53-6.7	eBioscience	1:20
CD8α	BV605	53-6.7	Biolegend	10μg/ml
CD8α	FITC	53-6.7	BD Bioscience	5μg/ml
CD8α	Pacific Blue	53-6.7	Biolegend	1.25μg/ml
CD11b	AF700	M1/70	eBioscience	1μg/ml
CD11b	APC eFluor780	M1/70	eBioscience	1μg/ml
CD11b	eFluor450	M1/70	eBioscience	1μg/ml
CD11b	eFluor 605nc	M1/70	eBioscience	1:20
CD11c	APC eFluor780	N418	eBioscience	1μg/ml
CD11c	FITC	HL3	BD Bioscience	2.5μg/ml
CD11c	PercpCy5.5	N418	Biolegend	1μg/ml
CD16/32 (Fc block)		2.4G2	BD Bioscience	2.5μg/ml
CD19	PeCy7	1D3	eBioscience	1μg/ml
CD19	V450	1D3	BD Bioscience	0.5μg/ml
CD24	BV605	M1/69	BD Bioscience	10μg/ml
CD24	eFluor 605nc	M1/69	eBioscience	1:20
CD24	FITC	M1/69	BD Bioscience	5μg/ml
CD45.1	eFluor 605nc	A20	eBioscience	1:20
CD45.1	FITC	A20	BD Bioscience	2.5μg/ml
CD45.1	PeCy7	A20	eBioscience	2μg/ml
CD45.1	PercpCy5.5	A20	eBioscience	1μg/ml
CD45.2	FITC	104	BD Bioscience	2.5μg/ml
CD45.2	PeCy7	104	Biolegend	1μg/ml
CD45R (B220)	eFluor450	RA3-6B2	eBioscience	2μg/ml
CD45R (B220)	FITC	RA3-6B2	BD Bioscience	1.25μg/ml
CD45R (B220)	PE	RA3-6B2	BD Bioscience	0.5μg/ml
CD64	AF647	X5-4/7.1	Biolegend	2μg/ml
CD64	PE	X5-4/7.1	Biolegend	1μg/ml
CD103	APC	2E7	eBioscience	2μg/ml
CD103	PE	2E7	eBioscience	1μg/ml
CD103	PercpCy5.5	2E7	Biolegend	4μg/ml
CD115	AF488	AFS98	eBioscience	1.67μg/ml
CD115	Percp eFluor710	AFS98	eBioscience	1μg/ml
CD117	PeCy7	2B8	Biolegend	1μg/ml
CD135	APC	A2F10	Biolegend	2μg/ml
CD172α	APC	P84	BD Bioscience	2μg/ml
CD197 (CCR7)	PE	4B12	eBioscience	4μg/ml

CD205	APC	NLDC-145	Biolegend	1µg/ml
CD207 (Langerin)	AF488	929F3.01	Dendritics	2.5µg/ml
CD207 (Langerin)	AF647	929F3.01	Dendritics	2.5µg/ml
CD326 (Ep-CAM)	AF647	G8.8	Biolegend	1.25µg/ml
CD326 (Ep-CAM)	Percp eFluor710	G8.8	eBioscience	1µg/ml
DNGR-1 (CLEC9A)	PE	1F6	Biolegend	5µg/ml
F4/80	AF647	C1:A3-1	Biolegend	2.5µg/ml
hHB-EGF (DTR)	biotinylated	polyclonal	R&D	2µg/ml
I-A/I-E (MHCII)	APC eFluor-780	M5/114.15.2	eBioscience	0.4µg/ml
I-A/I-E (MHCII)	AF647	M5/114.15.2	Biolegend	0.5µg/ml
I-A/I-E (MHCII)	AF700	M5/114.15.2	eBioscience	1µg/ml
IRF8	APC	V3GYWCH	eBioscience	2µg/ml
Ly6c/Ly6g (Gr-1)	FITC	RB-8C5	BD Bioscience	0.5µg/ml
Ly6c/Ly6g (Gr-1)	PercpCy5.5	RB-8C5	Biolegend	2µg/ml
Ly6g	AF700	RB-8C5	eBioscience	0.67µg/ml
NK1.1	APC	PK136	eBioscience	2µg/ml
NK1.1	Pacific Blue	PK136	Biolegend	2.5µg/ml
SiglecH	AF647	440c	eBioscience	4µg/ml
SiglecH	PE	440c	eBioscience	2µg/ml
TER-119	Pacific Blue	TER-119	Biolegend	5µg/ml
Rat IgG1 isotype control	PE		BD Bioscience	

Table 2 Antibodies used for flow cytometry

Abbreviations: AF (Alexa Fluor), APC (Allophycocyanin), BV (Brilliant Violet), Cy (Cyanide), FITC (Fluorescein isothiocyanate), nc (Nanocrystal), PE (Phycoerythrin), PerCp (Peridinin-chlorophyll-protein)
Final concentrations are given in µg/ml when available. Otherwise the dilution is stated.

When staining for precursors in the BM, the following lineage cocktail was used: CD45R (B220) eFluor450, CD4 Pacific Blue, CD8α Pacific Blue, CD11b eFluor450, NK1.1 Pacific Blue, Ter119 Pacific Blue and CD19 V450.

2.2.5 Flow Cytometry analysis

For extracellular staining up to 4 million cells were blocked with anti-CD16/32 in FACS buffer (3% foetal calf serum, 5mM EDTA, 0.02% sodium azide in PBS) for 10min at 4°C and then stained for 20min at 4°C with the staining cocktail in FACS buffer in the presence of anti-CD16/32. Samples were washed three times with FACS buffer. For biotinylated antibodies, the extracellular antibody staining was followed by a 20min staining with streptavidin-PE diluted 1:1200 in FACS buffer (BD Biosciences), after which samples were washed three times with FACS buffer.

Peripheral blood samples were fixed and red blood cells lysed with BD FACS lysing solution (BD Biosciences) for 5-10min at RT after extracellular staining.

PE-SIINFEKL and PE-SSLENFRAYV (both Proimmune) pentamers were used for CFA/OVA immunisation and influenza infection, respectively. One million cells were stained with 7.5µl pentamer in 25µl FACS buffer (without sodium azide) for 15min at RT. Samples were washed three times with FACS buffer, after which the extracellular staining protocol was followed.
Dapi was used to exclude dead cells, except for when cells were fixed and/or stained intracellularly with anti-CD207 or anti-IRF8. In the latter case dead cells were excluded by live/dead fixable violet dye (Invitrogen). For intracellular staining, cells were stained for surface markers, followed by staining with the fixable live/dead dye. fFxation and intracellular staining were performed with FIX&PERM (ADG) according to the manufacturer's protocol.
Samples were collected on a LSR Fortessa flow cytometer (BD Biosciences) and analysed using FlowJo 9 software (TreeStar Inc.). Gating strategies to identify DCs in lymphoid organs, non-lymphoid tissues and DC progenitors in the BM are shown in Figure 2.1, Figure 2.2 and Figure 2.3 respectively.

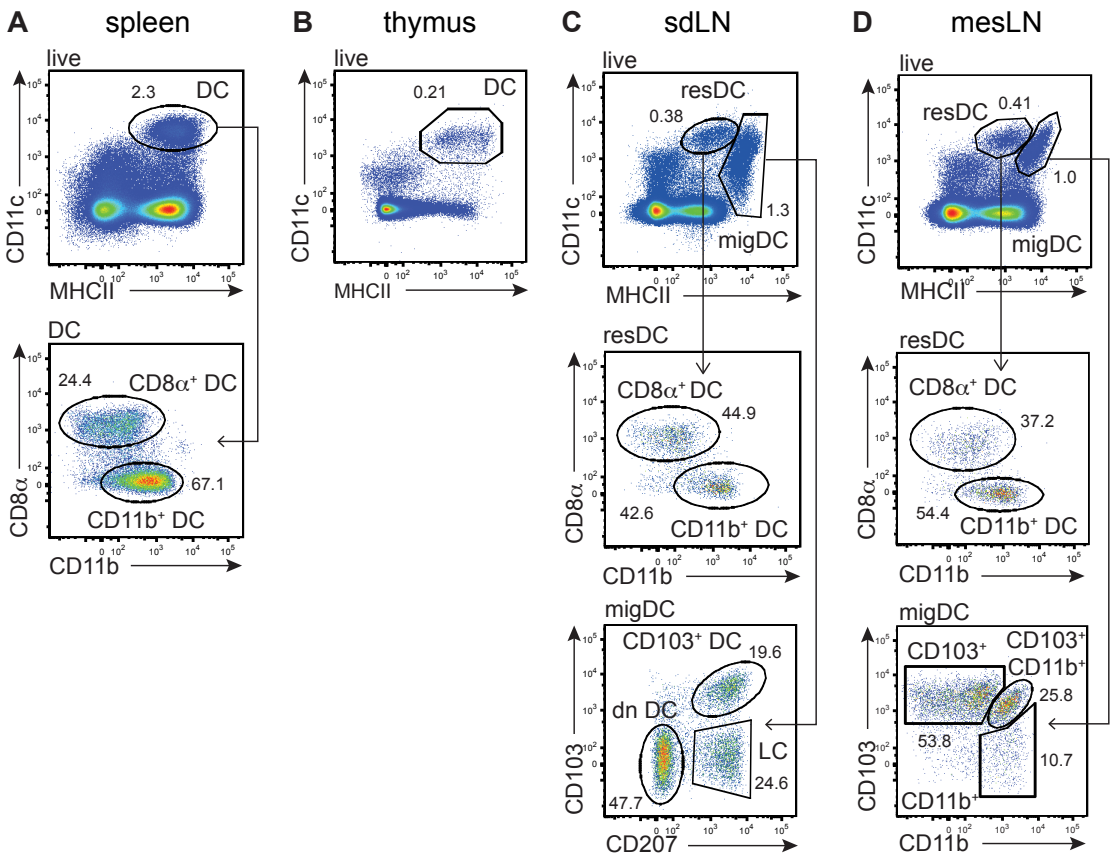

Figure 2.1 Flow cytometry gating strategy to identify DCs in lymphoid organs

The gating strategies to identify DCs in spleen (A), thymus (B), sdLN (C) and mesLN (D) are shown. Numbers indicate gate frequencies.

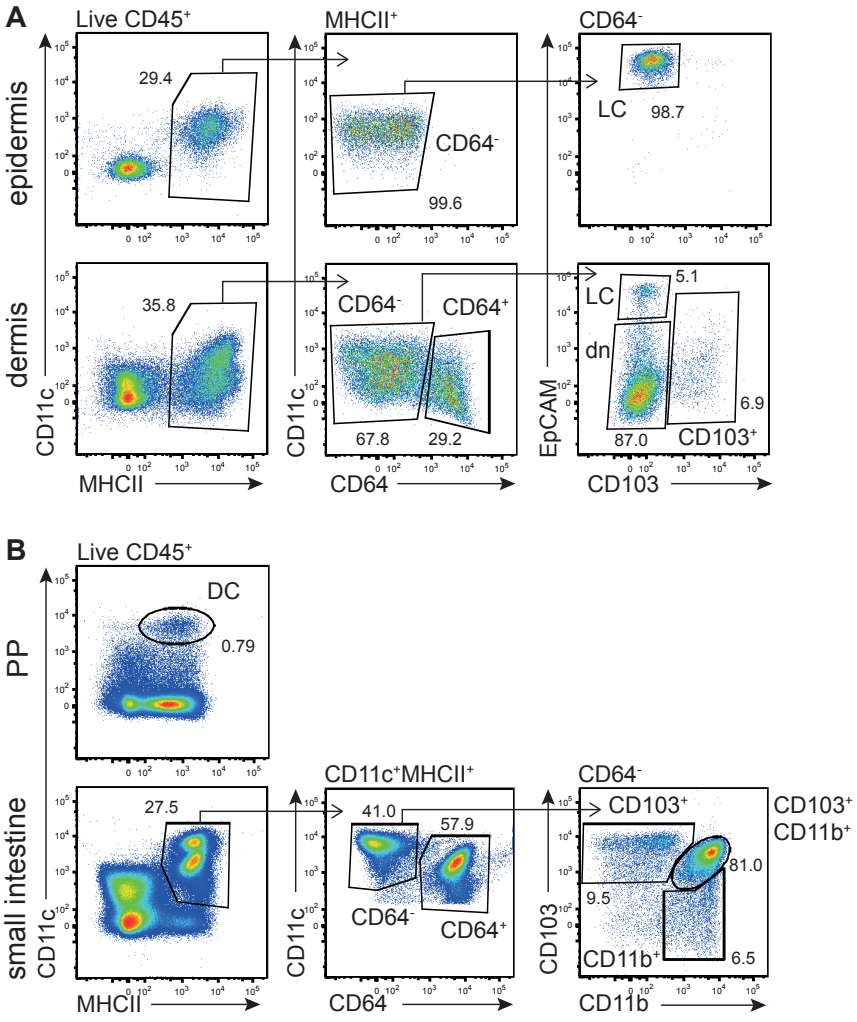

Figure 2.2 Flow cytometry gating strategy to identify DCs in non-lymphoid tissues

The gating strategies to identify DCs in epidermis and dermis (A) and Peyer's patches (PP) and small intestine (B) are shown. Numbers indicate gate frequencies.

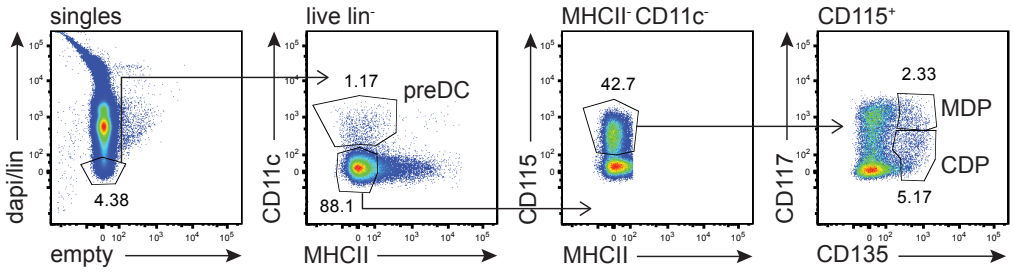

Figure 2.3 Flow cytometry gating strategy to identify DC progenitors in the BM

The gating strategy to identify DC progenitors the BM is shown. Numbers indicate gate frequencies and 'lin' denotes lineage cocktail (CD45R (B220), CD4, CD8α, CD11b, NK1.1, Ter119 and CD19).

2.3 Microscopy

2.3.1 Antibodies used for microscopy

Target	Fluorophore	Clone	Company	Final concentration
CD3ε	FITC	145-2C11	BD Bioscience	4µg/ml
CD11b	AF594	M1/70	eBioscience	10µg/ml
CD31	AF647	MEC13.3	Biolegend	0.8µg/ml
CD45R (B220)	eFluor450	RA3-6B2	eBioscience	2µg/ml
CD324 (E-cadherin)	AF594	DECMA-1	Biolegend	1µg/ml
CD326 (EpCAM)	BV421	G8.8	Biolegend	0.5µg/ml
CCL21 Goat anti-rabbit	- AF555	Polyclonal rabbit polyclonal	Peprotech Invitrogen	1:100 10µg/ml
ER-TR7	AF488	Sc-73355	Santa Cruz	0.25µg/ml
I-A/I-E (MHCII)	AF647	M5/114.15.2	Biolegend	2µg/ml
I-A/I-E (MHCII)	AF700	M5/114.15.2	eBioscience	2µg/ml
IRF8	APC	V3GYWCH	eBioscience	1µg/ml
MECA79	AF488	MECA-79	eBioscience	10µg/ml

Table 3 Antibodies used for microscopy

Abbreviations: AF (Alexa Fluor), APC (Allophycocyanin), BV (Brilliant Violet)
Final concentrations are given in µg/ml when available. Otherwise the dilution is stated.

2.3.2 Confocal microscopy

Inguinal lymph nodes were frozen in OCT (Tissue-TEK) and 10µm sections were cut on a cryostat. Sections were air dried, fixed for 10min in 2% paraformaldehyde (Electron Microscopy Sciences) and washed in PBS. Blocking was performed for 30min at room temperature in 10% goat serum (Sigma) in PBS. Sections were stained for 1 hour at room temperature with the indicated antibodies in blocking buffer. Slides were washed in PBS and mounted in Fluoromount-G (Southern Biotech). Images were acquired on a LSM710 upright confocal microscope (Zeiss) using a 10x dry objective and analysed with Bitplane Imaris software. Images are maximum intensity projections of tile scans and z-stacks.

2.3.3 Fixation with PLP and staining of sections for histo-cytometry

Desired tissues were dissected and SI and colons were flushed with ice-cold PBS. To preserve fluorescence, tissues were treated according to the PLP protocol (Bajénoff, Granjeaud and Guerder, 2003; Gerner et al., 2012). All tissues except SI and colons were fixed overnight at 4°C in 1% paraformaldehyde (Electron Microscopy Sciences), 75mM L-lysine (Sigma) and 2.12mg/ml $NaIO_4$ (Sigma) in 0.1M P-buffer (phosphate buffer, pH7.4). SI and colon were fixed for 2-3 hours at 4°C in the paraformaldehyde-containing buffer, after which they were cut open longitudinally and rolled into Swiss rolls. Rolls were secured with a pin and placed back in the paraformaldehyde-containing buffer to fix overnight at 4°C.
Tissues were washed in 0.1M P-buffer, transferred to 30% w/v sucrose (Fisher Scientific) in 0.1M P-buffer and incubated overnight at 4°C. SI and colon rolls were transferred into OCT (Tissue-TEK) and incubated overnight at room temperature with gentle shaking. Tissues were frozen in OCT and cut on a cryostat.
Tissue sections were rehydrated for 10min in 0.1M Tris pH7.4 and either mounted in Vectashield hard set (Vector labs) or stained with antibodies. For staining, slides were blocked for 30min at RT in 1% foetal calf serum, 0.3% Triton X-100 (Sigma) and 1% mouse serum (Sigma) in 0.1M Tris pH7.4. Primary antibodies were diluted in the blocking buffer and sections were incubated 16-48h at 4°C in a humidified chamber. Sections were washed in 0.1M Tris pH7.4 and mounted in Mowiol (5g Mowiol (Merck), 12ml H_2O, 12g glycerol and 24ml of 200mM Tris pH8.5).

2.3.4 Histo-cytometry

The histo-cytometry protocol presented here was developed in collaboration with Ronald Germain and Michael Gerner (National Institutes of Health). Stained and mounted tissue sections were analysed on a LSM880 invert confocal microscope with a 25x oil objective (Zeiss). Lasers 405nm, 458nm, 514nm, 561nm and 633nm were used to excite the flourophores with a 458/514/561/633 dichroic and a plate for the 405nm laser (to attenuate the laser power reaching the sample). Lambda mode scanning (detecting 410-687nm) was used to detect BV421, CFP, GFP, YFP, RFP, AF594 and AF647 or APC. AF700 was detected in a separate channel collecting 686-735nm. For all images tile scans and z-stacks were acquired and for the z-stack the optimal step size for a pinhole of 1 airy unit was chosen. Images were taken at 1024x1024 voxel density with a line averaging of 8. The fluorophores were unmixed into separate channels using the unmixing algorithm of the Zen software (Zeiss). Single-stained slides were used to obtain the reference spectra of the different fluorophores. Images are maximum intensity projections of tile scans and z-stacks.
Images were analysed using Bitplane Imaris software, as previously described (Gerner et al., 2012). 3D volumetric surface objects were created on the confetti channels using the surface rendering module in Imaris. Surface parameters (intensities of separate channels and location) were exported to Excel (Microsoft) as comma-separated files, which could then be imported into FlowJo 10 (TreeStar Inc.) to perform gating.

2.4 Miscellaneous

2.4.1 IFNγ ELISA

$5x10^5$ Cells/well were plated in round-bottom 96-well tissue culture plates in 200µl R10 medium with 10µg/ml CD4 peptides or 5µg/ml CD8 peptides (Table 4). Cultures were incubated overnight in a 37°C 5% CO_2 incubator. The next day cultures were centrifuged 1400rpm/4°C/4min and supernatants were transferred to a new 96-well tissue culture plate. Supernatants were frozen at -20°C until analysis. IFNγ was detected using the BD OptEIA Set Mouse IFNγ (BD Biosciences). NUNC immuno Maxisorb 96-well plates (Thermo Scientific) were coated with the capture

antibody diluted 1:250 in 100μl coating buffer (0.1 M Sodium Carbonate, 7.13g/l NaHCO , 1.59g/l NaCO ; pH9.5) overnight at 4°C. Plates were washed 5 times with ELISA wash (0.05% Tween20 in PBS) and blocked in 10% foetal calf serum in PBS for 1 hour at room temperature. Plates were subsequently washed 5 times with ELISA wash, after which 50μl supernatant or 5μl supernatant in 45μl R10 medium was added. A standard curve of recombinant IFNγ was also included. Samples were incubated for 2 hours at room temperature. Plates were washed 5 times with ELISA wash and 100μl detection antibody diluted 1:250 and streptavidin-horse radish peroxidase diluted 1:250 in 10% foetal calf serum in PBS was added to each well. Plates were incubated for 1 hour at room temperature. Plates were subsequently washed 10 times with ELISA wash and 50μl tetramethylbenzidine /hydrogen peroxide substrate solution (BD Biosciences) was added to each well. Plates were incubated for 30min at room temperature in the dark. 50μl Stop solution was added to each well and absorbance was read at 450nm on a Molecular Devices microplate reader.

Name	**CD4/CD8**	**Peptide sequence**
$HA_{211-225}$	CD4	YVQASGRVTVSTRRS
$NP_{276-290}$	CD4	LPACVYGPAVASGYD
$PA_{224-233}$	CD8	SSLENFRAYV
$NP_{366-374}$	CD8	ASNENMETM
$PB1_{703-711}$	CD8	SSYRRVPGI
$NS2_{114-121}$	CD8	RTFSFQLI

Table 4 Peptides used for restimulation

Peptides were generated by the LRI Peptide Chemistry Core Facility.

2.4.2 Flt3L BMDC culture

Both femurs and tibiae from one mouse were collected and flushed with R10 medium (10% foetal calf serum, L-glutamine, Penicillin/Streptomycin in RPMI). Red blood cells were lysed with Red Blood Cell Lysis Buffer for 1min on ice (Sigma Aldrich). 20ml R10 was added and cells were centrifuged 1400rpm/4°C/4min. The pellet was resuspended in 24ml R10 with 150ng/ml Flt3L (R&D Systems) and cells

were seeded in a 6-well plate with 4ml cell suspension/well or in 96-well flat bottom plates with 250µl/well. Cells were incubated for 9 days at 37°C and 10% CO_2. For 4OH-tamoxifen (Sigma Aldrich, H7904) treatment, the 4OH-tamoxifen was dissolved in 100% ethanol at 10mg/ml (25.8mM). 1µM 4OH-tamoxifen diluted in medium was added to cells in a 96-well plate at day 0 and cells were analysed at day 9.

2.4.3 Transwell Assay

The transwell assay was performed in 24-well plates with 5.0µm Pore Polycarbonate Membrane Inserts (Corning) with RPMI medium containing 0.5% BSA and 10mM Hepes. Recombinant CCL21 (R&D) was diluted in this medium to the appropriate concentration and 600µl was placed in each well. Single cell suspensions from pooled brachial, axillary and inguinal LNs were prepared, counted and resuspended in RPMI medium containing 0.5% BSA and 10mM Hepes, to a final concentration of $1*10^7$ cells/ml. Inserts were placed in the wells and 100µl of the cell suspension was placed in the insert. Plates were incubated for 3-4h at 37°C and 10% CO_2, after which cells from the well and insert were collected, stained for CD11c and MHCII and analysed by flow cytometry. The frequency of migrated cells was calculated by dividing cells in the well by cells in well plus insert.

2.4.4 Southern Blot

Genomic DNA was isolated by incubating about 5mm of tail in 700µl tail buffer (50mM Tris pH8.0, 100mM EDTA, 100mM NaCl ,1% SDS and 0.34mg/ml Proteinase K (Qiagen)) overnight at 55°C. Non-dissolved material was removed by centrifugation at 13000rpm for 10s. 300µl 5M NaCl was added to the supernatant and samples were centrifuged at 13000rpm for 10min. 800µl Supernatant was collected and 530µl isopropanol was added. Samples were centrifuged at 13000rpm for 10min and supernatant was discarded. 1ml 70% EtOH was added and samples were centrifuged at 13000rpm for 5min. Supernatant was discarded and the pellet was air-dried. The DNA was dissolved in 200µl H_2O and quantified on a Nanodrop (Thermo Scientific).

10µg of DNA per Southern Blot was digested overnight at 37°C with BamHI enzyme (NEB) and DNA was cleaned via phenol-chloroform extraction.

The digoxigenin (DIG) labelling system (Roche) was used for the southern blot analysis. Southern blot probes against the ‘5 homology arm and Neo cassette were DIG-labelled with the PCR DIG probe synthesis kit. Both probes were amplified from a pcDNA plasmid containing the 5’ probe sequence. The primers to amplify the 5’ probe are AAGTCTGACTTAGAAACCTCATT and AGCCTGGGCTTACAGCAT, and for the neo probe GATTGAACAAGATGGATTGCACGC and AATATCACGGGTAGCCAACG.

BamHI-digested DNA was run on a 0.8% agarose gel at 60V. The gel was briefly stained with ethidium bromide (Sigma) to check the loading. The gel was next incubated in hydrolysis buffer (0.25M HCl) for about 2 hours, then in denaturation buffer (1.5M NaOH, 0.5M NaCl) for 30min and finally in neutralisation buffer (1.5M NaCl, 0.5M Tris pH7.2, 10mM EDTA), all at room temperature. DNA was transferred to a nylon membrane overnight at room temperature in a Schleicher and Schuell transfer turboblotter. DNA was UV-cross-linked (1200 µJoules x100) to the membrane.
The membrane was prehybridised with DIG easy hyb solution (Roche) for 30min at 42°C in a hybridisation oven. DIG-labelled probes were denatured by boiling for 5min followed by rapid cooling on ice. The denatured probe was diluted in DIG easy hyb solution (2µl probe per 1ml) and the membrane was incubated in this solution overnight at 42°C.
The membrane was washed twice for 5min at room temperature with wash buffer I (2x SSC 0.1% SDS,), twice with wash buffer II (0.2x SSC, 0.1% SDS) for 15min at 68°C and once with wash buffer III (0.1M maleic acid pH7.5, 0.15M NaCl and 0.3% Tween 20 v/v) for 3min at room temperature.
The membrane was equilibrated by incubating for 2min in detection buffer (0.1M Tris pH9.5, 0.1M NaCl). The membrane was then transferred to a hybridisation bag and 10 drops of CSPD (Roche) were added before the bag was sealed. The membrane was incubated for 5min at room temperature and transferred to a new hybridisation bag, incubated for 10min at 37°C and exposed to a film.

2.4.5 Semi-quantitative RT-PCR

Cells were pelleted, resuspended in 1mL TRIzol (Invitrogen) and incubated for 5min at room temperature. 400µl Chloroform was added (Fisher Scientific), samples were vortexed for 15s and incubated for 2min at RT. Samples were centrifuged for 12500rpm/4°C/10min and the aqueous phase was transferred to a new tube. 800µl 100% isopropanol (Fisher Scientific) was added and samples were incubated for 15min at room temperature. Samples were centrifuged for 12500rpm/4°C/15min and the supernatant was removed. Samples were washed with 70% ethanol (Fisher Scientific) and centrifuged for 12500rpm/4°C/5min. Supernatant was removed and the RNA pellet was air-dried, before being resuspended in 20µl H_2O. Samples were incubated at 55°C for 10-15min to dissolve the RNA and quantified by Nanodrop (Thermo Scientific).
Any residual DNA was removed by DNA-free DNase Treatment and Removal Kit (Ambion). RNA was diluted to 10µg/44µl and 5µl buffer from the kit and 1µl DNase I were added. Samples were incubated for 30min at 37°C, after which 1µl DNase I was added and the samples were incubated for another 30min at 37°C. 10µl Inactivation buffer from the kit was added and the samples were incubated for 3min at room temperature while vortexing regularly. Samples were centrifuged for 10000rpm/4°C/5min and the supernatant containing the RNA was transferred to a new tube.
cDNA was generated using SuperScript II reverse transcriptase (Invitrogen). 7µl of DNA-free RNA was combined with 1µl oligo(dT) 12-18 primer (Invitrogen) and 1.5µl dNTPs PCR nucleotide mix (Promega) and incubated for 5min at 65°C followed by 5min on ice. 4µl 5x FS buffer, 2µl dithiothreitol, 1µl reverse transcriptase (all from kit) and 3.5µl H_2O were added. The sample was incubated for 10min at 25°C, 1h at 42°C and 15min at 70°C.
For the semi-quantitative RT-PCR, a neat, 10x diluted and 100x diluted sample were amplified with the indicated PCR primers using GoTaq Green Master Mix (Promega). PCR reactions were run in a total volume of 20µl and PCR primer concentrations of 0.125µM. The PCR programme was set to run for 3min at 95°C, perform 35 cycles of (30s at 95°C, 30s at 60°C, 40s at 72°C) and 10min at 72°C. 8µl Of the PCR product was run on a 2% agarose gel along with 5µl of 1kb plus DNA ladder (Invitrogen).

Target	Forward primer	Reverse primer	Product
hprt	TGAAGAGCTACTGTAATGATCAGTCAAC	AGCAAGCTTGCAACCTTAACCA	186bp
dta	CGTACCACGGGACTAAACCTGGT	TGCGAGAACCTTCGTCAGTCC	224bp
Creert2	GGTGCGCCTGCTGGAAGATG	TCCACAAAGCCTGGCACCCTCT	297bp

Table 5 Primers used for semi-quantitative RT-PCR

2.4.6 Statistical analyses

Statistical analyses were performed in Prism 6 (Graphpad). Results are shown as mean ± standard deviation. Unpaired student *t* tests were performed to calculate p-values, unless otherwise stated.

Chapter 3. A Novel Mouse Model to Inducibly Deplete Dendritic Cells

3.1 Introduction

Mouse models to deplete DCs have proven useful tools to elucidate DC function *in vivo*. The first such model exploited CD11c expression to drive expression of simian DTR fused to GFP in DCs (Jung et al., 2002). CD11c is commonly used as marker for DCs, but is also expressed by some macrophages, plasmablasts, Ly-6C^{low} monocytes, activated T cells and NK cells, resulting in DTR expression and DT-mediated depletion of these cell types (Jung *et al.*, 2002; Probst, Tschannen, *et al.*, 2005; Hochweller *et al.*, 2008). More recently, improved models have been developed in which DTR expresison is more highly restricted to DCs (CD11c-DOG and zDC-DTR mice) (Hochweller et al., 2008; Meredith, Liu, Darrasse-Jeze, et al., 2012) or is expressed selectively in specific DC subsets (Langerin-DTR, BDCA2-DTR, SiglecH-DTR, CD205-DTR and Clec9a-DTR mice) (Bennett et al., 2005; Kissenpfennig et al., 2005; Swiecki et al., 2010; Takagi et al., 2011; Fukaya et al., 2012; Piva et al., 2012). All these models allow for successful DT-mediated ablation of the target DC populations and have been instrumental in advancing DC research, despite suffering from limitations, predominantly due to misexpression of DTR, or side effects such as neutrophilia following DT-mediated DC ablation (Tittel *et al.*, 2012; van Blijswijk, Schraml and Reis e Sousa, 2013; Jiao *et al.*, 2014). Nevertheless, no immune abnormalities have been reported in any models expressing DTR on DCs in the absence of DT treatment, despite the fact that DTR, being an EGF family member, might potentially be able to engage murine EGF receptors.

DNGR-1 (also known as CLEC9A) is specifically expressed on CDPs and preDCs and as a consequence, mice expressing Cre recombinase under the control of the *Clec9a* locus can be used to fate map those precursors *in vivo* when crossed to a ROSA26-YFP reporter line (Schraml et al., 2013). In Clec9a$^{+/Cre}$ROSA^{YFP} mice YFP expression is largely restricted to DCs, even under inflammatory conditions. Clec9a$^{+/Cre}$ROSA^{YFP} mice can therefore be used to genetically trace the DC lineage

in vivo. Unfortunately, penetrance of YFP labelling is not complete in heterozygous Clec9a-Cre mice, possibly due to the rapid cycling of DC precursors. Therefore, only roughly half of the CD11b$^+$ DCs are labelled in Clec9a$^{+/Cre}$ROSA^{YFP} mice. Labelling of CD8α-like DCs is nearly complete, as these DC subsets also express DNGR-1, and consequently Cre, as differentiated cells.
To generate DT-sensitive DCs *in vivo*, Clec9a-Cre mice (Schraml et al., 2013) were crossed to a ROSA26-iDTR strain (Buch et al., 2005) to generate Clec9a$^{+/Cre}$ROSA^{iDTR} mice that express DTR on DCs . All mice used for experiments were heterozygous for Cre recombinase and, therefore, DNGR-1 sufficient, unless otherwise stated. No differences were observed between mice harbouring either one or two copies of DTR and therefore both were combined in experiments shown in this chapter.

3.2 DT injection efficiently depletes DCs but no other cells in spleens of Clec9a$^{+/Cre}$ROSA^{iDTR} mice

Clec9a$^{+/Cre}$ROSA^{iDTR} mice were first validated for DTR expression specifically on DCs and efficient depletion of DCs upon DT injection. Flow cytometry analysis using an antibody that recognises DTR revealed that in the spleen of Clec9a$^{+/Cre}$ROSA^{iDTR} animals 93±1% of CD8α$^+$ DCs and 59±5% of CD11b$^+$ DCs expressed DTR (Figure 3.1A). The fact that circa 40% of CD11b$^+$ splenic DCs were negative for DTR expression is in line with the previously observed incomplete penetrance of Cre activity in heterozygous Clec9a-Cre mice crossed to ROSA26-LSL-YFP mice (Schraml et al., 2013). In line with the observed DTR expression, virtually all splenic CD8α$^+$ DCs and most CD11b$^+$ DCs were depleted 24 hours post-treatment when Clec9a$^{+/Cre}$ROSA^{iDTR} mice were injected i.p. with one dose of DT (Figure 3.1B,C). In contrast, DT treatment did not have any effect on CD8α$^+$ DCs or CD11b$^+$ DCs in Clec9a$^{+/+}$ROSA^{iDTR} control mice (Figure 3.1C).

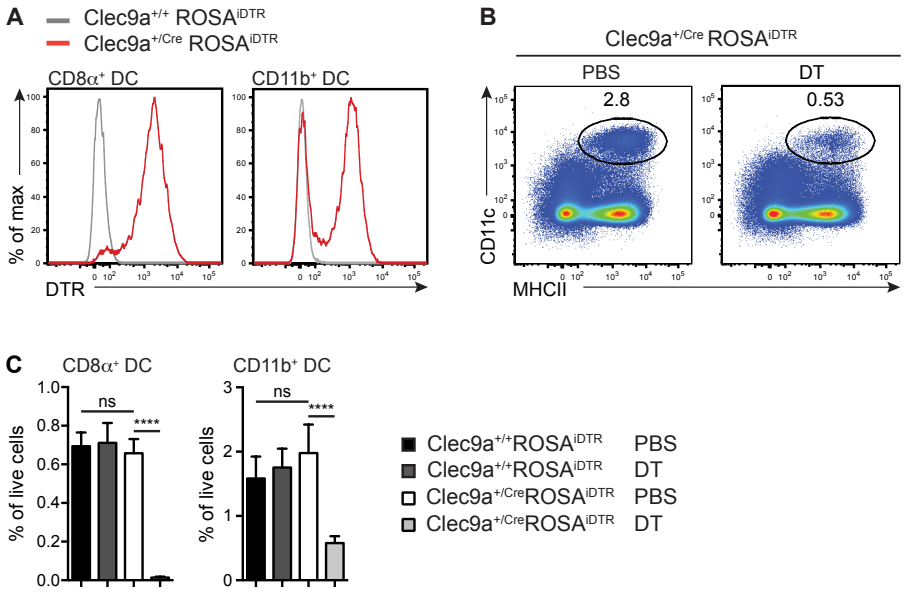

Figure 3.1 Efficient DC depletion in spleens of DT-injected Clec9a$^{+/Cre}$ROSA^{iDTR} mice

(A) CD8α^{+} DCs (CD11c^{+} MHCII^{+} CD8α^{+}) and CD11b^{+} DCs (CD11c^{+} MHCII^{+} CD11b^{+}) in spleen were stained with a polyclonal anti-DTR antibody and analysed by flow cytometry. Each plot is representative of at least 6 mice per group. **(B-C)** Mice were injected i.p. with DT or PBS and sacrificed 24h later. **(B)** Representative plots of spleen for PBS and DT treated Clec9a$^{+/Cre}$ROSA^{iDTR} mice (gated on live, autofluorescence^{-} cells). Frequency of gated population is shown. **(C)** Frequency of CD8α^{+} DCs and CD11b^{+} DCs in spleen of PBS- and DT-treated control and Clec9a$^{+/Cre}$ROSA^{iDTR} mice is shown. A one-way ANOVA with a Tukey's multiple comparisons post-test was performed to calculate p-values. Ns: non significant, ****: p≤0.0001. This experiment was performed twice with 4-7 mice per group. One representative experiment is shown.

One of the limitations that many of the current mouse models to inducibly deplete DCs suffer from, is the emergence of neutrophilia and monocytosis upon DT injection. In light of these observations, Clec9a$^{+/Cre}$ROSA^{iDTR} mice were assessed for increased neutrophil and monocyte frequencies upon DT injection. As expected, neutrophils and monocytes did not express DTR in Clec9a$^{+/Cre}$ROSA^{iDTR} mice (Figure 3.2A). Notably, DC depletion was not accompanied by neutrophilia and monocytosis 24 hours after DT administration (Figure 3.2B), in contrast to depletion in other models such as CD11c-DOG mice and CD11c-DTR mice. Clec9a$^{+/Cre}$ROSA^{iDTR} mice were not tested for the presence of a 'late' (72h after DT injection and onwards) wave of neutrophilia and monocytosis and therefore at present it is unknown if Clec9a$^{+/Cre}$ROSA^{iDTR} mice exhibit increased granulopoiesis upon DC depletion.

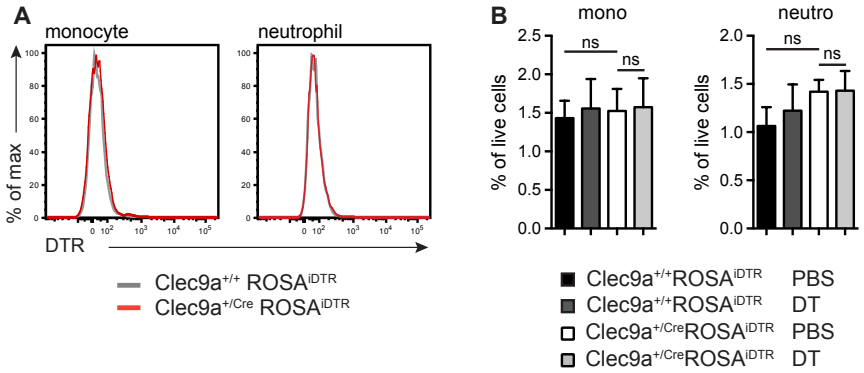

Figure 3.2 Clec9a$^{+/Cre}$ROSA^{iDTR} mice do not show neutrophilia or monocytosis upon DT injection

(A) Monocytes (CD11b^{+} Ly6c^{+} Ly6g^{-}) and neutrophils (CD11b^{+} Ly6g^{+}) in spleen were stained with a polyclonal anti-DTR antibody and analysed by flow cytometry. Each plot is representative of at least 6 mice per group. **(B)** Mice were injected i.p. with DT or PBS and sacrificed 24h later. Frequency of monocytes (mono) and neutrophils (neutro) in spleen of PBS- and DT-treated control and Clec9a$^{+/Cre}$ROSA^{iDTR} mice is shown. A one-way ANOVA with a Tukey's multiple comparisons post-test was performed to calculate p-values. Ns: non significant. This experiment was performed twice with 4-7 mice per group. One representative experiment is shown.

To interrogate if deletion is restricted to DCs in Clec9a$^{+/Cre}$ROSA^{iDTR} mice, other immune cell populations in the spleens of these mice were examined. As shown in Figure 3.3A, B cells, T cells, NK cells, NKT cells and red pulp macrophages did not express DTR in Clec9a$^{+/Cre}$ROSA^{iDTR} mice and these cell populations were not affected 24 hour after DT injection of Clec9a$^{+/Cre}$ROSA^{iDTR} mice (Figure 3.3B).

In summary, when Clec9a$^{+/Cre}$ROSA^{iDTR} mice were injected with DT, virtually all splenic CD8α^{+} DCs and most CD11b^{+} DCs were depleted 24 hours post-treatment while other immune cell populations in the spleen were spared. Notably, DT-mediated DC depletion in this strain was not accompanied by neutrophilia and monocytosis, at least at this time point, in contrast to depletion in other models such as CD11c-DOG mice and CD11c-DTR mice. Therefore, Clec9a$^{+/Cre}$ROSA^{iDTR} mice can be used to successfully and specifically deplete DCs in the spleen using DT with minimal side effects caused by DT treatment.

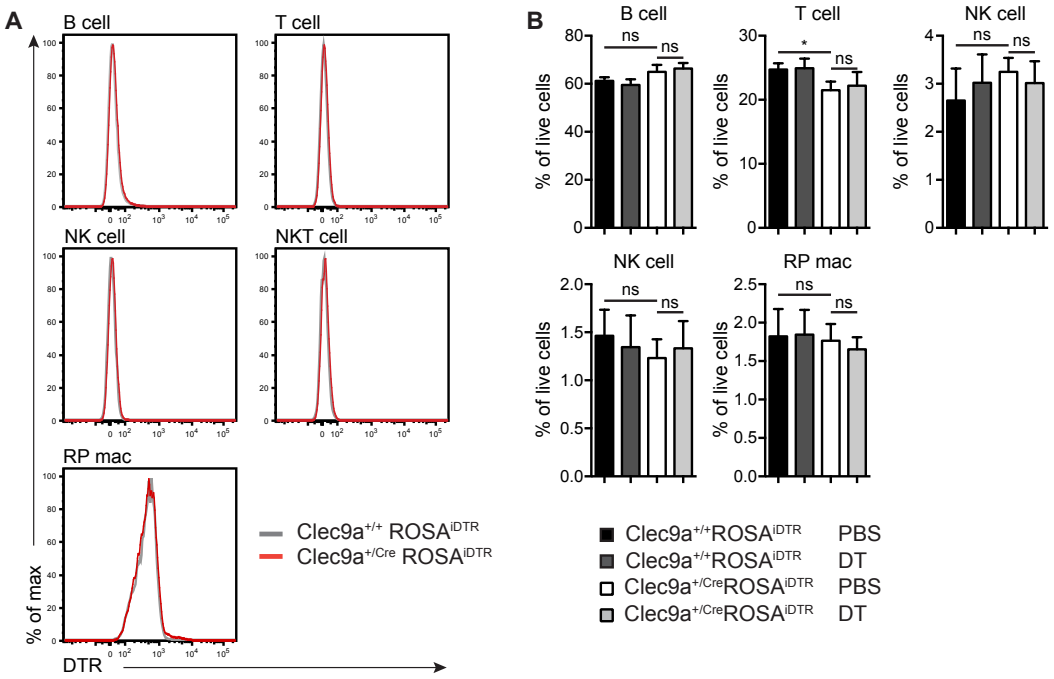

Figure 3.3 Other immune cells are not affected in the spleen of DT-injected Clec9a$^{+/Cre}$ROSA^{iDTR} mice

(A) B cells (MHCII^{+} CD11c^{-}), T cells (CD3^{+} NK1.1^{-} MHCII^{-}), NK cells (CD3^{-} NK1.1^{+} MHCII^{-}), NKT cells (CD3^{+} NK1.1^{+} MHCII^{-}) and red pulp macrophages (F4/80^{+} autofluorescent) in spleen were stained with a polyclonal anti-DTR antibody and analysed by flow cytometry. Each plot is representative of at least 6 mice per group. **(B)** Mice were injected with DT or PBS and sacrificed 24h later. B cells, T cells, NK cells, NKT cells and red pulp macrophages in spleen of PBS- and DT-treated control and Clec9a$^{+/Cre}$ROSA^{iDTR} mice were identified by flow cytometry. Frequencies of cell populations are shown. A one-way ANOVA with a Tukey's multiple comparisons post-test was performed to calculate p-values. Ns: non significant. This experiment was performed twice with 4-7 mice per group. One representative experiment is shown.

3.3 LNs of Clec9a$^{+/Cre}$ROSA^{iDTR} mice show hypocellularity and reduced frequencies of DCs

As expected, DTR was also expressed by both resDCs and migDCs in sdLNs of Clec9a$^{+/Cre}$ROSA^{iDTR} mice, but not by LCs (Figure 3.4A), which do not originate from DC precursors and were also not labelled in Clec9a$^{+/Cre}$ROSA^{YFP} mice (Schraml et al., 2013). The incomplete penetrance of DTR expression was also in line with previous findings in Clec9a$^{+/Cre}$ROSA^{YFP} mice (Schraml et al., 2013).

In accordance with DTR expression on resDCs, these cells were depleted in sdLNs upon DT injection (Figure 3.4B). However, when analysing sdLNs, it was noticed that both resDCs and migDCs were present at reduced frequency in PBS-treated Clec9a$^{+/Cre}$ROSA^{iDTR} mice compared to PBS-treated genetic control mice (Figure 3.4B).

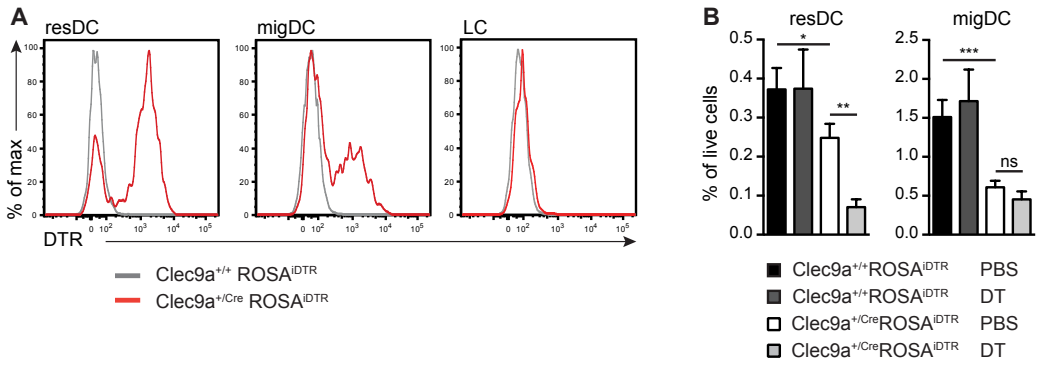

Figure 3.4 sdLNs of PBS-injected Clec9a$^{+/Cre}$ROSA^{iDTR} mice show a reduction in DCs

(A) resDCs (CD11c^{+} MHCII^{int}), migDCs (CD11c^{+} MHCII^{hi}) and LC (CD11c^{+} MHCII^{hi} CD207^{+} CD103^{-}) in sdLNs were stained with polyclonal anti-DTR antibody and analysed by flow cytometry. Each plot is representative of at least 6 mice per group. **(B)** Mice were injected with DT or PBS and sacrificed 24h later. ResDCs and migDCs in sdLNs of PBS- and DT-treated control and Clec9a$^{+/Cre}$ROSA^{iDTR} mice were identified by flow cytometry and DC subsets as percentage of live leukocytes are plotted. A one-way ANOVA with a Tukey's multiple comparisons post-test was performed to calculate p-values. Ns: non significant, *: p≤0.05, **: p≤0.01, ***: p≤0.001. This experiment was performed twice with 4-7 mice per group. One representative experiment is shown.

To follow-up on this unexpected observation, LNs, spleens and thymi of untreated Clec9a$^{+/Cre}$ROSA^{iDTR} mice were analysed in greater detail. Untreated Clec9a$^{+/Cre}$ROSA^{iDTR} mice indeed displayed a marked reduction in frequency of both resDCs and migDCs in sdLNs when compared to Cre-negative controls (Figure 3.5AB), confirming above-mentioned findings in PBS-treated Clec9a$^{+/Cre}$ROSA^{iDTR} and control mice. Both CD8α^{+} and CD11b^{+} resDC subsets and all migDC subsets (LC, CD103^{+} migDCs and DN migDCs) were reduced in frequency in Clec9a$^{+/Cre}$ROSA^{iDTR} mice (Figure 3.5B). A particularly intriguing observation was the reduced frequency of LCs, as these cells do not come from a

DC precursor and did not express DTR (Figure 3.4A). This result suggests that DTR does not merely act in a cell autonomous manner, but also exerts effects on DTR-negative cells.

A similar decrease in frequency of resDCs and migDC as in sdLNs of Clec9a$^{+/Cre}$ROSA^{iDTR} mice was observed in mesLNs (Figure 3.5C). In the mesLNs both CD8α^{+} and CD11b^{+} resDC subsets and all migDC subsets were reduced. In contrast, CD8α^{+} and CD11b^{+} DC frequency in the spleen and DC frequency in the thymus were identical between Clec9a$^{+/Cre}$ROSA^{iDTR} mice and Cre-negative controls (Figure 3.5D). Together, these observations suggest that only lymphoid organs with an afferent lymph supply and, consequently, possessing migDCs are affected.

As migDCs in LNs originate from non-lymphoid tissues, the next question to ask was if DC frequency is also reduced in skin and small intestine, from where DCs migrate to sdLNs and mesLNs, respectively. Interestingly, LC frequency in the epidermis and LC, CD103^{+} DC and DN DC frequencies in the dermis were identical in Clec9a$^{+/Cre}$ROSA^{iDTR} mice when compared to Cre-negative controls (Figure 3.6A), even though their migratory counterparts in sdLNs were reduced. A similar observation was made in the small intestine and Peyer's patches, were the frequency of CD64^{+} cells, CD103^{+} CD11b^{-} DCs, CD103^{+} CD11b^{+} DCs and CD103^{-} CD11b^{+} DCs or total DCs, respectively, was similar between Clec9a$^{+/Cre}$ROSA^{iDTR} and control mice (Figure 3.6B).

As Clec9a$^{+/Cre}$ROSA^{iDTR} mice only seem to show reduced DC frequencies in LNs, but not other lymphoid organs or non-lymphoid tissues, it is unlikely that Clec9a$^{+/Cre}$ROSA^{iDTR} mice have a defect at the level of DC precursors or their ability to seed tissues.

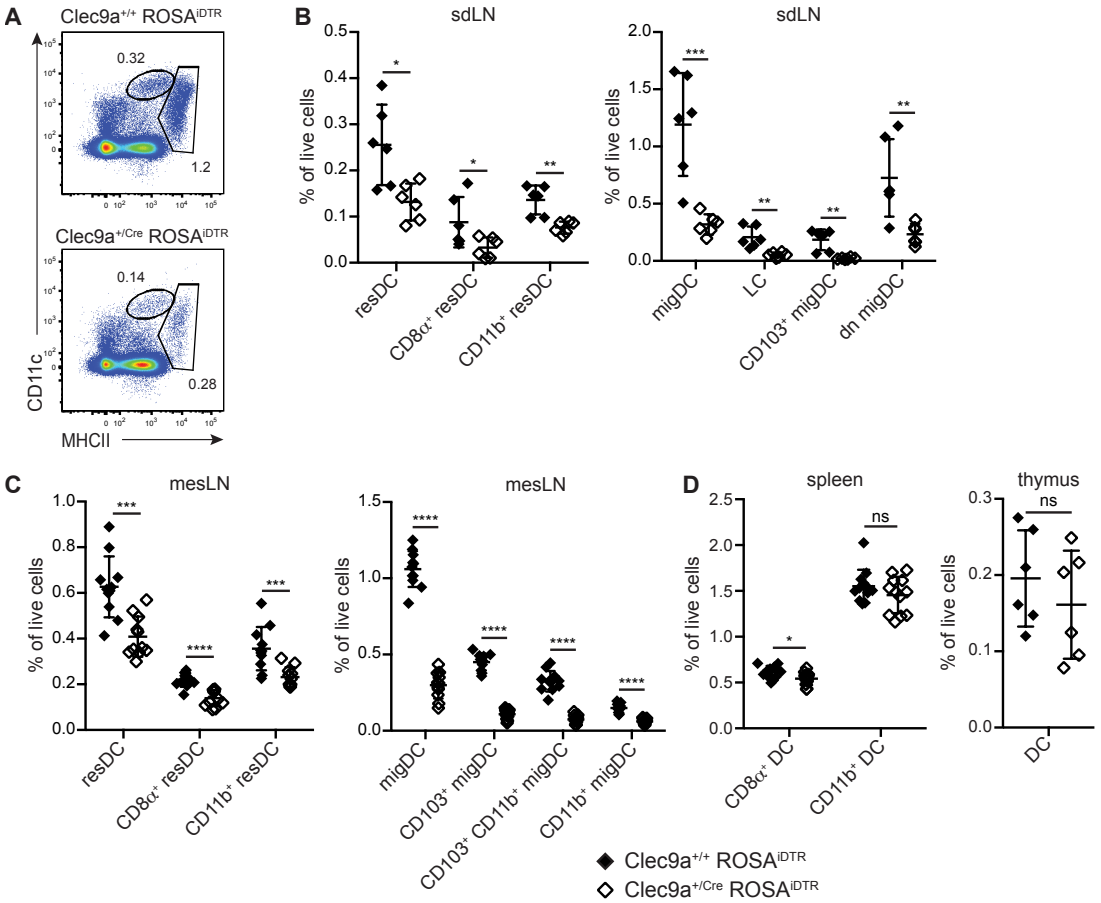

Figure 3.5 LNs but not spleen or thymus of Clec9a$^{+/Cre}$ROSA^{iDTR} mice display reduced DC frequencies

(A) Representative plots of sdLNs of control and Clec9a$^{+/Cre}$ROSA^{iDTR} mice, gated on live cells. **(B)** Total resDCs (CD11c^{+} MHCII^{int}), CD8α^{+} resDCs (CD11c^{+} MHCII^{int} CD8α^{+}) and CD11b^{+} resDCs (CD11c^{+} MHCII^{int} CD11b^{+}) (left panel), and total migDCs (CD11c^{+} MHCII^{hi}), LCs (CD11c^{+} MHCII^{hi} CD207^{+} CD103^{-}), CD103^{+} migDCs (CD11c^{+} MHCII^{hi} CD207^{+} CD103^{+}) and double negative (DN) migDCs (CD11c^{+} MHCII^{hi} CD207^{-} CD103^{-}) (right panel) in sdLNs of control and Clec9a$^{+/Cre}$ROSA^{iDTR} mice were identified by flow cytometry and DC subsets as percentage of live leukocytes are plotted. **(C)** Total resDCs (CD11c^{+} MHCII^{int}), CD8α^{+} resDCs (CD11c^{+} MHCII^{int} CD8α^{+}) and CD11b^{+} resDCs (CD11c^{+} MHCII^{int} CD11b^{+}) (left panel), and total migDCs (CD11c^{+} MHCII^{hi}), CD103^{+} migDCs (CD11c^{+} MHCII^{hi} CD11b^{-} CD103^{+}), CD103^{+} CD11b^{+} migDCs (CD11c^{+} MHCII^{hi} CD11b^{+} CD103^{+}) and CD11b^{+} migDCs (CD11c^{+} MHCII^{hi} CD11b^{+} CD103^{-}) (right panel) in mesLNs of control and Clec9a$^{+/Cre}$ROSA^{iDTR} mice were identified by flow cytometry and DC subsets as percentage of live leukocytes are plotted. **(D)** CD8α^{+} DCs (CD11c^{+} MHCII^{+} CD8α^{+}) and CD11b^{+} DCs (CD11c^{+} MHCII^{+} CD11b^{+}) in spleen and DCs in thymus (CD11c^{+} MHCII^{+}) were identified by flow cytometry and DC subsets as percentage of live leukocytes are plotted. Each dot represents one mouse. Ns: non significant, *: p≤0.05, **: p≤0.01, ***: p≤0.001, ****: p≤0.0001. Data are pooled from at least two independent experiments.

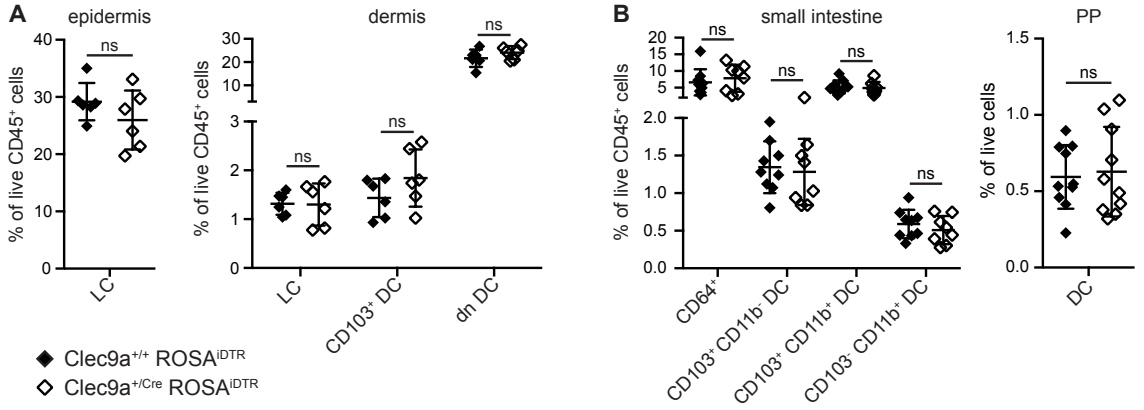

Figure 3.6 Epidermis, dermis, small intestine and Peyer's patches of Clec9a$^{+/Cre}$ROSA^{iDTR} mice do not have reduced frequencies of DCs

(A) LCs (MHCII^{+} CD64^{-} EpCAM^{hi}), CD103^{+} DCs (MHCII^{+} CD64^{-} CD103^{+}) and double negative DCs (DN DCs, MHCII^{+} CD64^{-} CD103^{-} EpCAM^{-}) in epidermis and dermis of control and Clec9a$^{+/Cre}$ROSA^{iDTR} mice were identified by flow cytometry and DC subsets as percentage of live CD45^{+} cells are plotted. **(B)** CD64^{+} cells (CD11c^{+} MHCII^{+} CD64^{+}), CD103^{+} CD11b^{-} DCs (CD11c^{+} MHCII^{+} CD64^{-} CD103^{+} CD11b^{-}), CD103^{+} CD11b^{+} DCs (CD11c^{+} MHCII^{+} CD64^{-} CD103^{+} CD11b^{+}) and CD103^{-} CD11b^{+} DCs (CD11c^{+} MHCII^{+} CD64^{-} CD103^{-} CD11b^{+}) in the small intestine and DCs (CD11c^{+} MHCII^{+}) in the Peyer's Patches (PP) of control and Clec9a$^{+/Cre}$ROSA^{iDTR} mice were identified by flow cytometry and DC subsets as percentage of live CD45^{+} cells (small intestine) or of live leukocytes (PP) are plotted. Each dot represents one mouse. Ns: non significant. Data are pooled from at least two independent experiments.

In addition to lower DC frequency, and equally unexpected, untreated Clec9a$^{+/Cre}$ROSA^{iDTR} mice also had a marked reduction in the cellularity of sdLNs and mesLNs (Figure 3.7) when compared to their genetic controls. This hypocellularity accentuated the dearth of LN DCs and was not seen in the spleen and thymus, which displayed normal cellularity (Figure 3.7). All immune cell populations were reduced in number in the LNs of Clec9a$^{+/Cre}$ROSA^{iDTR} mice, contributing to the overall hypocellularity, although the loss of T cells was most acute, leading to an increase in the ratio of B to T cells (Figure 3.8A). However, despite hypocellularity and increased B/T cell ratio, the overall LN architecture appeared intact (Figure 3.8B).

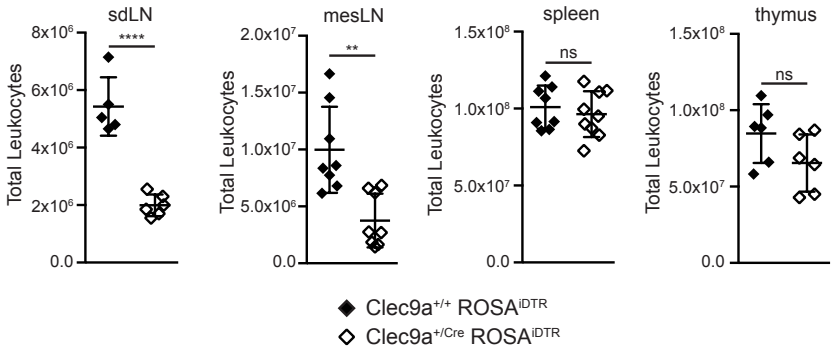

Figure 3.7 LNs, but not spleen or thymus, are hypocellular in Clec9a$^{+/Cre}$ROSA^{iDTR} mice

Single-cell suspensions of sdLNs, mesLNs, spleen and thymus from control and Clec9a$^{+/Cre}$ROSA^{iDTR} mice were counted and the number of total leukocytes is plotted. Each dot represents one mouse. Ns: non significant, **: p≤0.01, ****: p≤0.0001. Data are pooled from at least two independent experiments.

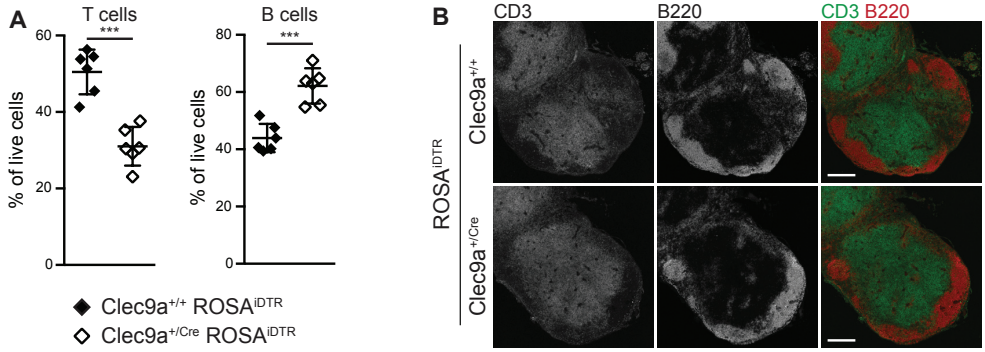

Figure 3.8 LNs of Clec9a$^{+/Cre}$ROSA^{iDTR} mice show an altered T/B cell ratio, but maintain LN organisation

(A) T cells (CD3^{+} MHCII^{-}) and B cells (MHCII^{+} CD11c^{-}) in mesLNs of control and Clec9a$^{+/Cre}$ROSA^{iDTR} mice were identified by flow cytometry and T cells and B cells as percentage of live leukocytes are plotted. **(B)** Frozen sections of sdLNs from control and Clec9a$^{+/cre}$ROSA^{iDTR} mice were stained with anti-CD3 and anti-B220 antibodies and imaged by confocal microscopy. Scale bar: 300µm. Images are representative of 3 mice per group.

To determine the influence of age on the observed phenotype, DC frequency and cellularity in spleen and sdLNs of one year old Clec9a$^{+/Cre}$ROSA^{iDTR} mice and Cre-negative controls were assessed. In line with the findings in younger mice, there was no difference in splenic DC frequency or spleen cellularity between Clec9a$^{+/Cre}$ROSA^{iDTR} and Cre-negative control mice (Figure 3.9AB). However, the frequency of migDCs in sdLNs of old Clec9a$^{+/Cre}$ROSA^{iDTR} mice was again reduced

compared with control mice (Figure 3.9A). Furthermore, cellularity was reduced in sdLNs of old Clec9a$^{+/Cre}$ROSA^{iDTR} mice (Figure 3.9B). No difference in resDC frequency was observed in this experiment, which may be due to the small number of mice analysed.

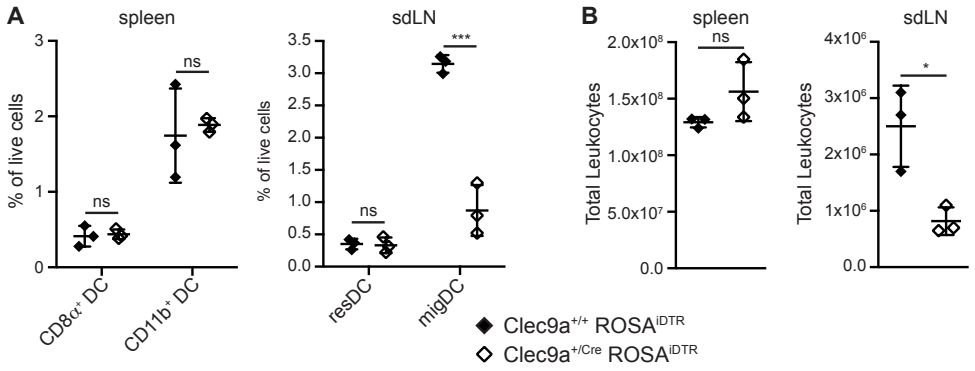

Figure 3.9 Reduced migDC frequency in LNs and LN hypocellularity is maintained in old Clec9a$^{+/Cre}$ROSA^{iDTR} mice

(A) CD8α$^+$ DCs (CD11c$^+$ MHCII$^+$ CD8α$^+$) and CD11b$^+$ DCs (CD11c$^+$ MHCII$^+$ CD11b$^+$) in spleen and resDCs (CD11c$^+$ MHCII^{int}) and migDCs (CD11c$^+$ MHCII^{hi}) in sdLNs of one year old control and Clec9a$^{+/Cre}$ROSA^{iDTR} mice were identified by flow cytometry and DC subsets as percentage of live leukocytes are plotted. **(B)** Single-cell suspensions of spleen and sdLNs from one year old control and Clec9a$^{+/Cre}$ROSA^{iDTR} mice were counted and the number of total leukocytes is plotted. Each dot represents one mouse. Ns: non significant, *: p≤0.05, ***: p≤0.001. Data are from one experiment.

3.4 In mixed bone marrow chimeras the phenotype of Clec9a$^{+/Cre}$ROSA^{iDTR} BM is dominant over WT BM

DTR expression could be toxic to DCs, acting in a cell-autonomous fashion to decrease survival or migration. Alternatively, expression of DTR on DCs might act in a non-cell-autonomous manner to broadly influence the environment and all DCs within it. To distinguish these possibilities, mixed BM chimeras were generated with a 1:1 mixture of CD45.1$^+$ WT BM and CD45.2$^+$ Clec9a$^{+/+}$ROSA^{iDTR} (Cre-negative) or Clec9a$^{+/Cre}$ROSA^{iDTR} (Cre-positive) BM. Full chimerism was confirmed by measuring the ratio of CD45.1 to CD45.2 in blood neutrophils (Figure 3.10A). Frequencies of resDCs and migDCs within the total CD45.1$^+$ or CD45.2$^+$ population in both sdLNs and mesLNs were first compared. Among CD45.2$^+$ cells, both resDC

and migDC frequencies were reduced in sdLNs and mesLNs of mice receiving Cre-positive BM compared to animals receiving control Cre-negative BM (Figure 3.10BC). These data indicated that the paucity of DCs in Clec9a$^{+/Cre}$ROSA^{iDTR} mice could not be rescued by the presence of WT cells.

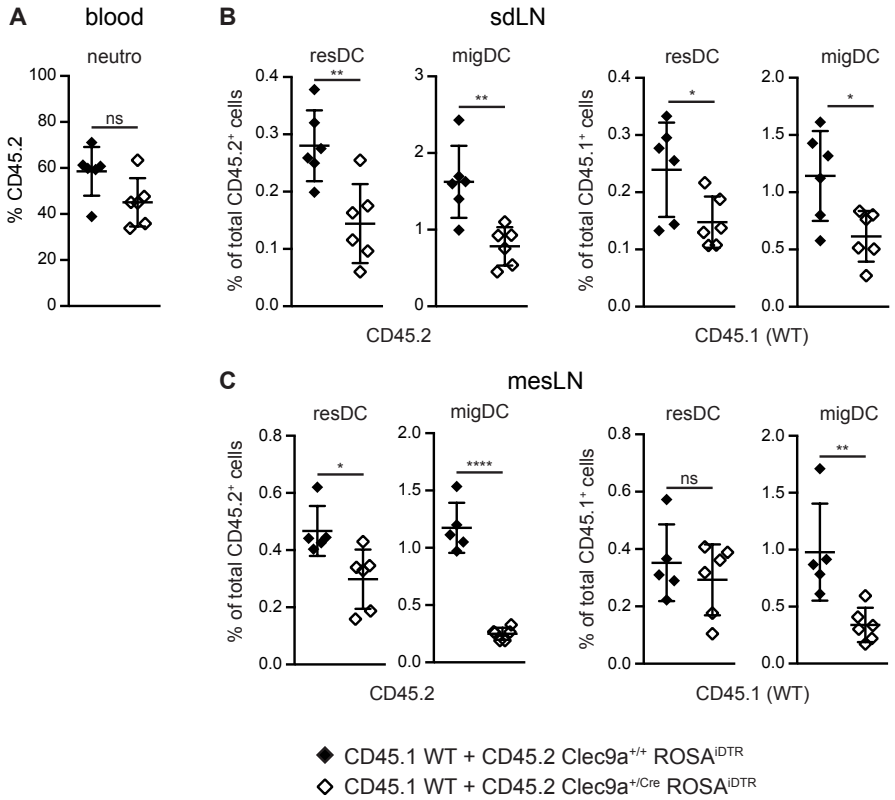

Figure 3.10 In mixed BM chimeras the phenotype conferred by Clec9a$^{+/Cre}$ROSA^{iDTR} BM is dominant

CD45.2$^+$ C57BL/6J hosts were lethally irradiated and reconstituted with a 1:1 mixture of CD45.1$^+$ WT and CD45.2$^+$ Clec9a$^{+/+}$ROSA^{iDTR} or Clec9a$^{+/Cre}$ROSA^{iDTR} BM. Mice were analysed 7 months after BM transfer.
(A) Peripheral blood was analysed by flow cytometry. Neutrophils (neutro; CD11b$^+$ Gr1$^+$) were identified and the frequency of CD45.2$^+$ neutrophils is plotted. **(B)** Single cell suspensions of sdLNs were analysed by flow cytometry. CD45.1$^+$ and CD45.2$^+$ cells were identified and within these fractions resDCs (CD11c$^+$ MHCII^{int}) and migDCs (CD11c$^+$ MHCII^{hi}) were gated. Frequencies of resDCs and migDCs within the CD45.2$^+$ or CD45.1$^+$ fraction are plotted. **(C)** Same analysis as in (B), but then for mesLNs. Each dot represents one mouse. Ns: non significant, *: p≤0.05, **: p≤0.01, ****: p≤0.0001. Data are representative of two independent experiments.

Even more intriguingly, the WT compartment in chimeras receiving Cre-positive BM was similarly affected. As shown in Figure 3.10BC, in the CD45.1^{+} WT compartment the frequencies of migDCs in both sdLNs and mesLNs, and resDCs in sdLNs were reduced in chimeras receiving Cre-positive BM, but not in chimeras receiving Cre-negative control BM. Therefore, DTR does not appear to merely affect in a cell autonomous manner those DCs that express it. Rather, Clec9a$^{+/Cre}$ROSA^{iDTR} BM-derived cells have a dominant effect that reduces the frequency of DCs derived from WT BM. These observations are reminiscent of the reduced frequency of LCs in Clec9a$^{+/Cre}$ROSA^{iDTR} mice (Figure 3.5B), as in both cases DCs that do not express DTR are reduced in frequency.
The dominance of Clec9a$^{+/Cre}$ROSA^{iDTR} BM was also reflected in the size of sdLNs and mesLNs, but not spleen, which was reduced in chimeras receiving Cre-positive BM when compared with control chimeras (Figure 3.11). In summary, the hypocellularity and relative reduction of DCs in LNs of Clec9a$^{+/Cre}$ROSA^{iDTR} mice are replicated in mixed chimeras containing Clec9a$^{+/Cre}$ROSA^{iDTR} BM.

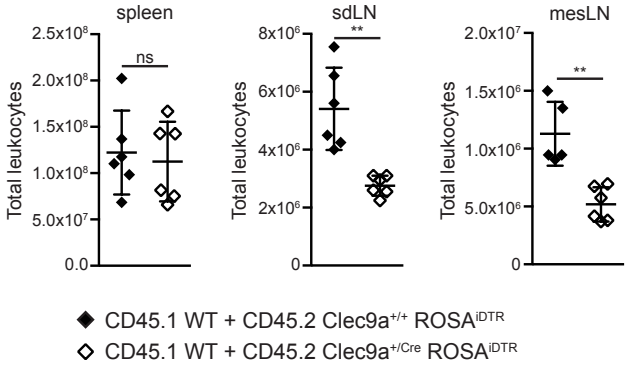

Figure 3.11 LNs of mixed BM chimeras reconstituted with Clec9a$^{+/Cre}$ROSA^{iDTR} and WT BM show hypocellularity

CD45.2^{+} C57BL/6J hosts were lethally irradiated and reconstituted with a 1:1 mixture of CD45.1^{+} WT and CD45.2^{+} Clec9a$^{+/+}$ROSA^{iDTR} or Clec9a$^{+/Cre}$ROSA^{iDTR} BM. Mice were analysed 7 months after BM transfer. Total leukocyte numbers of spleen, sdLNs and mesLNs are plotted. Each dot represents one mouse. Ns: non significant, **: p≤0.01. Data are representative of two independent experiments.

3.5 Other mice that express DTR on DCs also show LN hypocellularity and reduced DC frequencies

The LN hypocellularity and reduced frequencies of DC subsets in LNs could be the result of targeting the Clec9a locus, targeting the ROSA26-locus, or expressing DTR on DCs. Arguing against the first two possibilities, the original reporter mice in which the Clec9a-Cre strain was crossed to ROSA26-YFP mice, all had normal size LNs and unaltered LN composition (Figure 3.12). Nevertheless, to determine whether the phenotype was exclusive to the use of the Clec9a-Cre strain, CD11c-Cre mice (Caton, Smith-Raska and Reizis, 2007) were crossed to ROSA26-iDTR mice. CD11c-Cre^{+ve}ROSA^{iDTR} mice expressed DTR on a high proportion of DCs in sdLNs (Figure 3.13A). These mice also showed hypocellularity of sdLNs and mesLNs (Figure 3.13BC), and reduced frequencies of migDCs in sdLNs and mesLNs compared with littermate controls (Figure 3.13BC). ResDC frequency was reduced in mesLNs of CD11c-Cre^{+ve}ROSA^{iDTR} mice (Figure 3.13C) and there was a trend for reduced frequencies of resDCs in sdLNs, albeit not reaching statistically significance (Figure 3.13B). Thus, CD11c-Cre^{+ve}ROSA^{iDTR} mice largely phenocopy Clec9a$^{+/Cre}$ROSA^{iDTR} mice and also show LN hypocellularity and a reduced frequency of DCs.

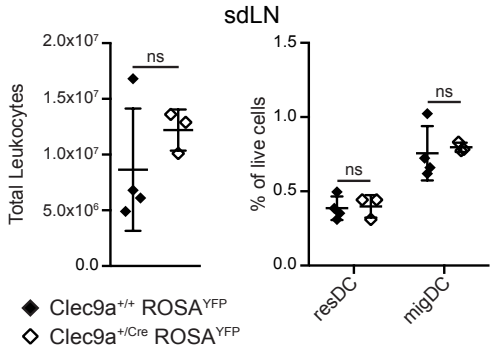

Figure 3.12 Clec9a$^{+/cre}$ROSA^{YFP} mice do not show hypocellularity or reduced DC frequency of LNs

SdLNs of Clec9a$^{+/cre}$ROSA^{YFP} mice were analysed for total cellularity (left panel) and frequency of resDCs (CD11c^{+} MHCII^{int}) and migDCs (CD11c^{+} MHCII^{hi}) (right panel). Each dot represents one mouse. Ns: non significant. Data are from one experiment.

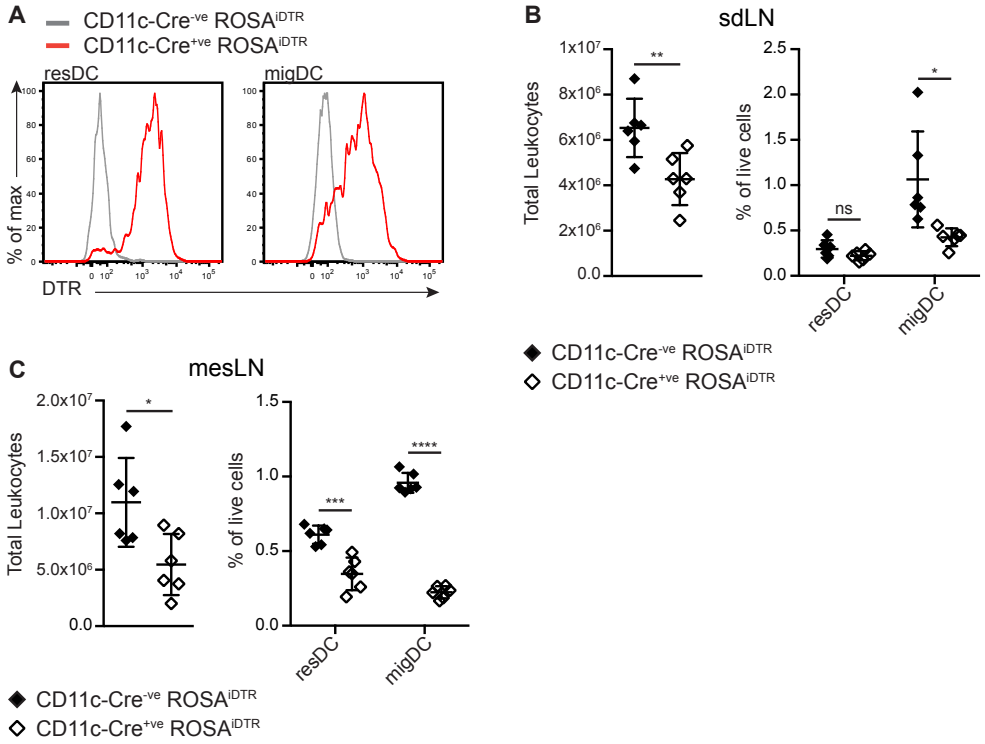

Figure 3.13 CD11c-Cre^{+ve}ROSA^{iDTR} mice show LN hypocellularity and reduced DC frequency in LNs

(A) ResDCs (CD11c^{+} MHCII^{int}) and migDCs (CD11c^{+} MHCII^{hi}) in sdLNs from CD11c-Cre^{+ve}ROSA^{iDTR} mice were stained with a polyclonal anti-DTR antibody and analysed by flow cytometry. Data are representative of at least six mice per group. **(B-C)** SdLNs (B) and mesLNs (C) of CD11c-Cre^{+ve}ROSA^{iDTR} mice were analysed for total cellularity (left panel) and frequency of resDCs (CD11c^{+} MHCII^{int}) and migDCs (CD11c^{+} MHCII^{hi}) (right panel). Each dot represents one mouse. Data are pooled from at least two independent experiments. Ns: non significant, *: p≤0.05, **: p≤0.01 ***: p≤0.001, ****: p≤0.0001.

Next, the original CD11c-DTR mice (Jung et al., 2002) were analysed, which have been widely used to study DC functions *in vivo* for over ten years. These mice expressed DTR on most DCs in sdLNs, although especially some of the resDCs did not stain positive with the polyclonal DTR antibody (Figure 3.14A). Similar to Clec9a$^{+/Cre}$ROSA^{iDTR} mice, CD11c-DTR mice showed reduced frequencies of resDCs and migDCs in sdLNs and mesLNs and hypocellularity of the same organs (Figure 3.14BC). As CD11c-DTR mice do not express DTR from the ROSA26-locus, this finding excludes the possibility that the ROSA26-iDTR strain is responsible for the observed phenotype. Together, these results indicate that paucity of LN DCs and hypocellularity of LNs is a feature common to Clec9a$^{+/Cre}$ROSA^{iDTR}, CD11c-Cre^{+ve}ROSA^{iDTR} and CD11c-DTR mice.

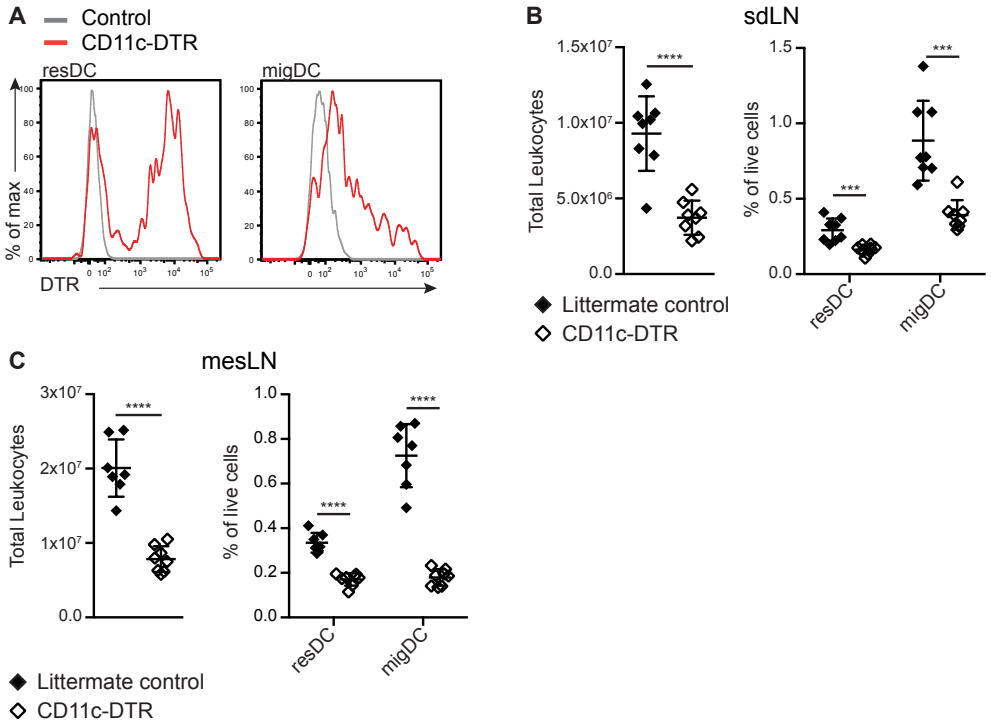

Figure 3.14 CD11c-DTR mice show LN hypocellularity and reduced DC frequency in LNs

(A) ResDCs (CD11c^{+} MHCII^{int}) and migDCs (CD11c^{+} MHCII^{hi}) in sdLNs from CD11c-DTR mice were stained with a polyclonal anti-DTR antibody and analysed by flow cytometry. Data are representative of at least six mice per group. **(B-C)** SdLNs (B) and mesLNs (C) of CD11c-DTR mice were analysed for total cellularity (left panel) and frequency of resDCs (CD11c^{+} MHCII^{int}) and migDCs (CD11c^{+} MHCII^{hi}) (right panel). Each dot represents one mouse. Data are pooled from at least two independent experiments. ***: p≤0.001, ****: p≤0.0001.

The above-mentioned strains all allow for expression of DTR on multiple DC subtypes. To test if expression of DTR on a subset of DCs is sufficient to induce the observed phenotype, Langerin-DTR mice (Kissenpfennig et al., 2005) were analysed. In Langerin-DTR mice, DTR expression is under control of the CD207 locus, which is active in LCs, CD103^{+} dermal DCs and some CD8α^{+} resDCs. As observed for the other mouse strains, Langerin-DTR mice displayed reduced frequencies of migDCs in sdLNs and hypocellularity of the same organ compared with littermate controls (Figure 3.15B). This phenotype was not observed in mesLNs, unlike in the other strains tested (Figure 3.15D). Further investigation revealed that the difference in phenotype between sdLNs and mesLNs in Langerin-DTR mice correlated with levels of DTR expression: very little DTR expression was observed on resDCs and migDCs from mesLNs (Figure 3.15C) while DTR was

expressed on both resDCs and migDCs subsets in sdLNs, although both expression levels and the frequency of cells stained positive were very low (Figure 3.15A). In sum, analysis of Langerin-DTR mice suggests that even low DTR expression on a subset of DCs is sufficient to induce reduced migDCs accumulation in LNs and LN hypocellularity. Moreover, the effects of DTR appear to be local and not systemic, as in Langerin-DTR mice the affected LNs are only those in which DTR expression is found on DCs.

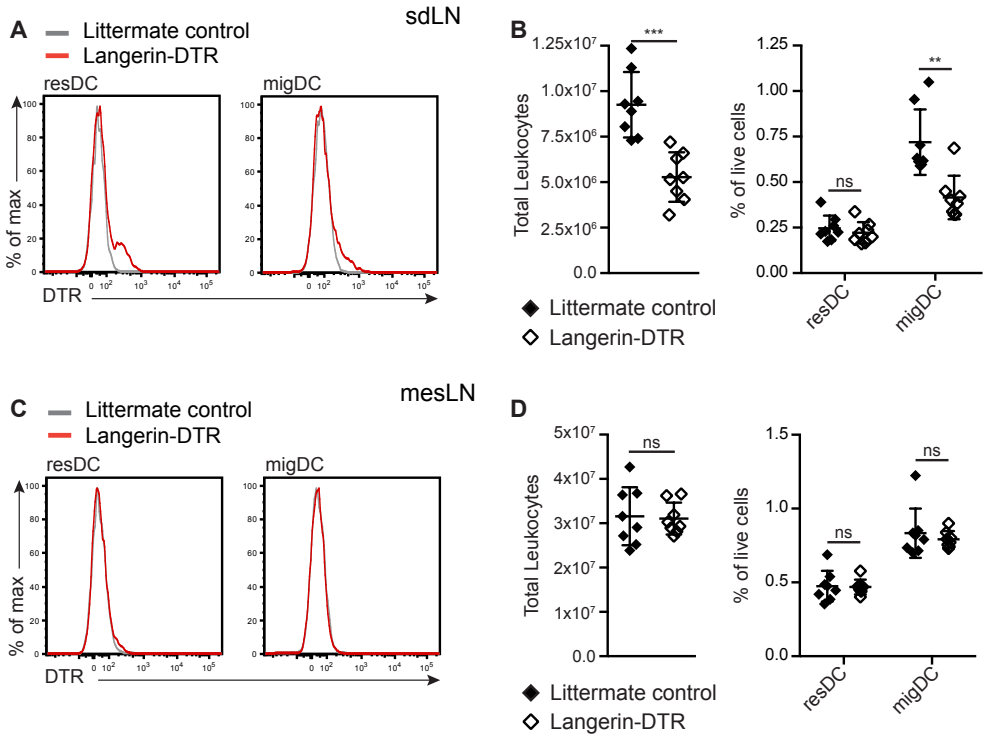

Figure 3.15 Langerin-DTR mice show hypocellularity and reduced DC frequency only in sdLNs

(A,C) ResDCs (CD11c^{+} MHCII^{int}) and migDCs (CD11c^{+} MHCII^{hi}) in sdLNs (A) or mesLNs (C) from Langerin-DTR mice were stained with a polyclonal anti-DTR antibody and analysed by flow cytometry. Data are representative of at least six mice per group. **(B,D)** SdLNs (B) and mesLNs (D) of Langerin-DTR mice were analysed for total cellularity (left panel) and frequency of resDCs (CD11c^{+} MHCII^{int}) and migDCs (CD11c^{+} MHCII^{hi}) (right panel). Each dot represents one mouse. Data are pooled from at least two independent experiments. Ns: non significant, **: p≤0.01 ***: p≤0.001.

Finally, CD11c-DOG mice were tested. Like CD11c-DTR mice, these mice also exploit CD11c expression to express DTR on DCs. However, CD11c-DOG mice utilise the CD11c locus control region instead of a minimal promoter to drive DTR expression (Jung et al., 2002; Hochweller et al., 2008). Surprisingly, no difference was found in sdLN and mesLN cellularity or DC frequencies in sdLNs and mesLNs between CD11c-DOG mice and controls (Figure 3.16BD). However, resDCs in sdLNs and mesLNs of CD11c-DOG mice expressed DTR at very low levels (Figure 3.16AC). Moreover, DTR expression on migDCs in sdLNs and mesLNs of CD11c-DOG mice was undetectable by antibody staining (Figure 3.16AC). These results suggest that low DTR expression on resDCs alone may not be not sufficient to confer the phenotype of LN hypocellularity and reduced frequencies of DCs in LNs.

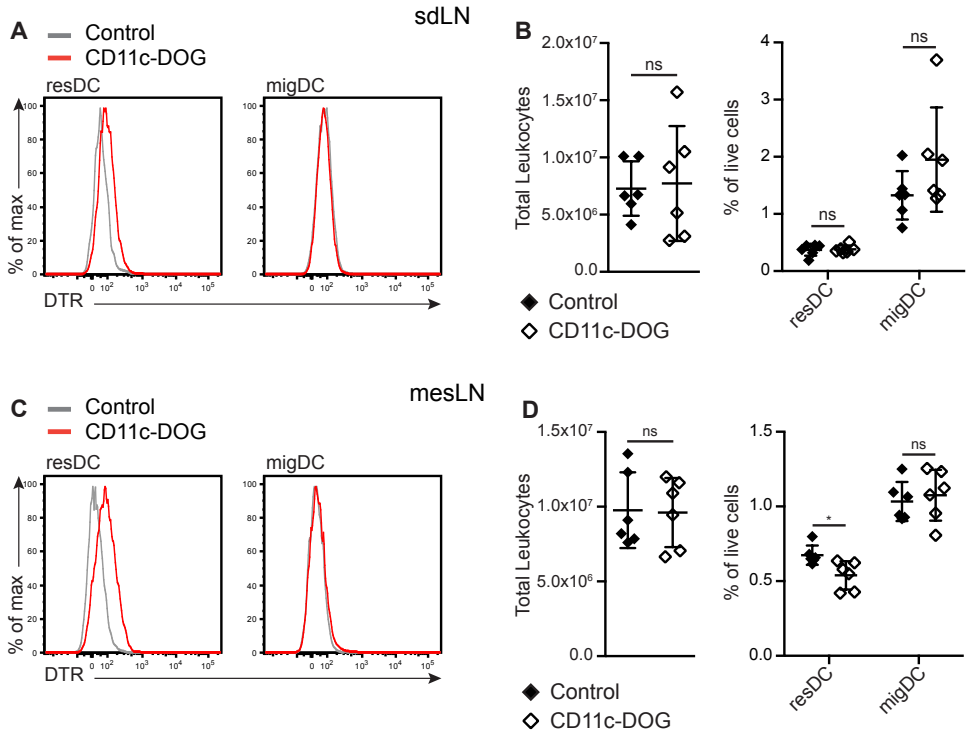

Figure 3.16 CD11c-DOG mice do not show LN hypocellularity or reduced frequency of LN DCs

(A,C) ResDCs (CD11c^{+} MHCII^{int}) and migDCs (CD11c^{+} MHCII^{hi}) in sdLNs (A) or mesLNs (C) from CD11c-DOG mice were stained with a polyclonal anti-DTR antibody and analysed by flow cytometry. Data are representative of at least six mice per group. **(B,D)** SdLNs (B) and mesLNs (D) of CD11c-DOG mice were analysed for total cellularity (left panel) and frequency of resDCs (CD11c^{+} MHCII^{int}) and migDCs (CD11c^{+} MHCII^{hi}) (right panel). Each dot represents one mouse. Data are pooled from at least two independent experiments. Ns: non significant, *: p≤0.05.

In sum, CD11c-Cre^{+ve}ROSA^{iDTR} and CD11c-DTR mice showed a similar phenotype of LN hypocellularity and reduced frequencies of DCs in LNs as Clec9a$^{+/Cre}$ROSA^{iDTR} mice, while Langerin-DTR mice only show this phenotype in the LNs were DTR expression could be observed by antibody staining. In contrast, CD11c-DOG mice did not show any aberrations in LNs, but also failed to show DTR expression on migDCs and had very low DTR expression on resDCs.

3.6 Mice that express DTR on B cells or Tregs do not show a profound LN hypocellularity or reduced DC frequencies

To address whether DTR expression on other immune cells than DCs leads to a similar LN phenotype, CD19-Cre mice (Rickert, Roes and Rajewsky, 1997) were crossed to ROSA26-iDTR mice, to drive expression of DTR on B cells. Notably, frequencies of B cells and resDCs were not decreased in sdLNs and mesLNs of CD19$^{+/Cre}$ROSA^{iDTR} mice compared with controls (Figure 3.17AB). MigDC frequencies were unaltered in sdLNs, but slightly decreased in mesLNs (Figure 3.17AB), although this decrease was much smaller than that observed in the DC-restricted DTR models tested here. CD8α$^+$ DCs in the spleen of CD19$^{+/Cre}$ROSA^{iDTR} mice were unaltered, while CD11b$^+$ DC frequency was increased in spleens of CD19$^{+/Cre}$ROSA^{iDTR} mice (Figure 3.17C) compared with controls. Furthermore, CD19$^{+/Cre}$ROSA^{iDTR} mice displayed only a mild reduction in cellularity of sdLNs, but not of the mesLNs or spleen (Figure 3.17A-C).
DEREG mice, in which DTR is expressed on Tregs (Lahl et al., 2007), were also analysed. DEREG mice displayed a mild decrease in the frequency of migDCs in both sdLNs and mesLNs compared with controls, while resDCs in LNs and DCs in the spleen were unaltered (Figure 3.18A-C). However, in contrast to mice expressing DTR on DCs, DEREG mice did not show signs of LN hypocellularity (Figure 3.18AB).

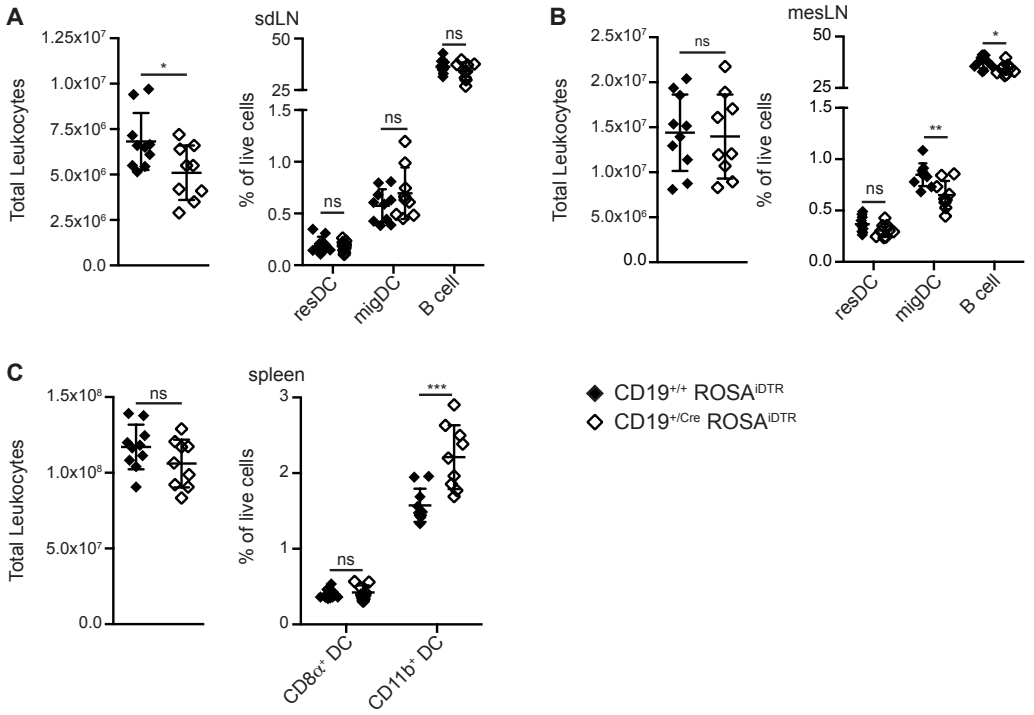

Figure 3.17 Expression of DTR on B cells does not lead to overall LN hypocellularity and reduced frequencies of LN DCs

Left panels: single-cell suspensions of sdLNs **(A)**, mesLNs **(B)** and spleen **(C)** from control and CD19$^{+/Cre}$ROSA^{iDTR} mice were counted and the number of total leukocytes is plotted. Right panels: resDCs (CD11c^{+} MHCII^{int}) and migDCs (CD11c^{+} MHCII^{hi}) in sdLNs **(A)** and mesLNs **(B)** and CD8α^{+} DCs (CD11c^{+} MHCII^{+} CD8α^{+}), CD11b^{+} DCs (CD11c^{+} MHCII^{+} CD11b^{+}) and B cells in spleen **(C)** of control and CD19$^{+/Cre}$ROSA^{iDTR} mice were identified by flow cytometry and DC subsets or B cells as percentage of live leukocytes are plotted. Each dot represents one mouse. Data are pooled from at least two independent experiments. Ns: non significant, *: p≤0.05, **: p≤0.01 ***: p≤0.001.

In summary, neither CD19$^{+/Cre}$ROSA^{iDTR} mice nor DEREG mice fully recapitulate the phenotype of dramatic hypocellularity of LNs and reduced frequencies of resDCs and migDCs in LNs. However, LNs of CD19$^{+/Cre}$ROSA^{iDTR} and DEREG mice are not identical to those in the respective controls, perhaps because of effects of DTR expression on B cells or Tregs or because of an unknown cause (e.g., haploinsufficiency of CD19 or aberrations due to BAC integration). Overall, these results suggest that expression of DTR on a large fraction of LN cells is not necessarily detrimental but that its expression specifically on DCs has unexpected consequences.

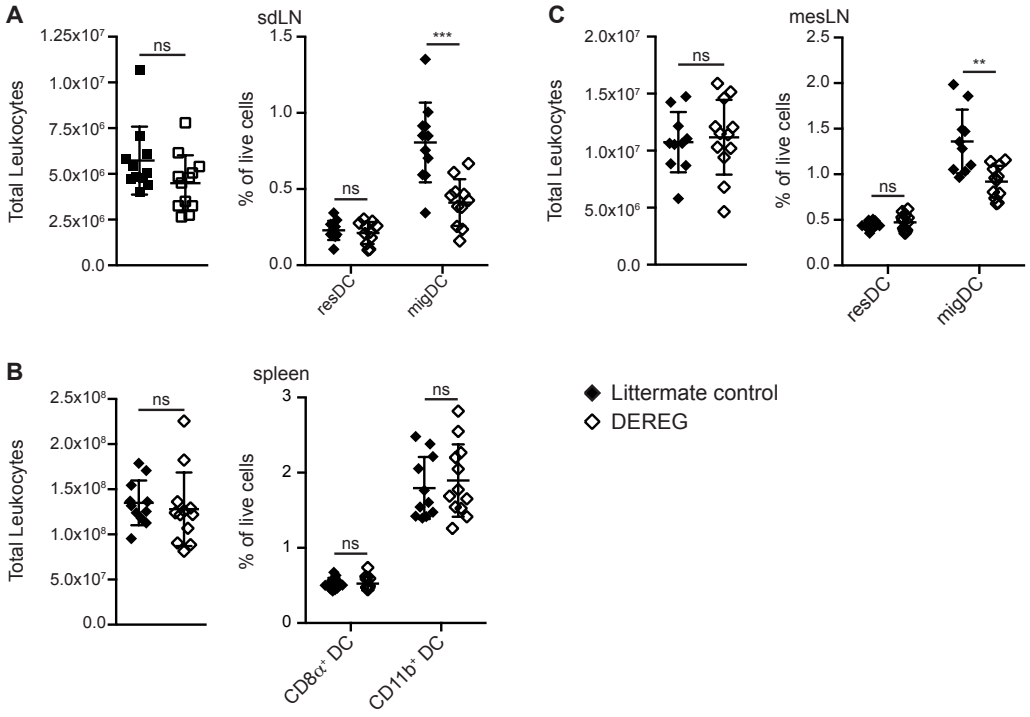

Figure 3.18 Expression of DTR on Tregs does not lead to overall LN hypocellularity and reduced frequencies of LN DCs

Left panels: single-cell suspensions of sdLNs **(A)**, mesLNs **(B)** and spleen **(C)** from control and DEREG mice were counted and the number of total leukocytes is plotted. Right panels: resDCs ($CD11c^+$ $MHCII^{int}$) and migDCs ($CD11c^+$ $MHCII^{hi}$) in sdLNs **(A)** and mesLNs **(B)** and $CD8\alpha^+$ DCs ($CD11c^+$ $MHCII^+$ $CD8\alpha^+$) and $CD11b^+$ DCs ($CD11c^+$ $MHCII^+$ $CD11b^+$) in spleen **(C)** of control and DEREG mice were identified by flow cytometry and DC subsets as percentage of live leukocytes are plotted. Each dot represents one mouse. Data are pooled from at least two independent experiments. Ns: non significant, **: p≤0.01, ***: p≤0.001.

3.7 $Clec9a^{+/Cre}ROSA^{iDTR}$ mice can mount normal immune responses upon immunisation or infection

Above-mentioned experiments investigated the unperturbed immune system of mice expressing DTR on DCs or other immune cells, and revealed that DTR expression specifically on DCs results in LN hypocellularity and reduced frequencies of DCs in LNs. As LNs are key sites for initiation and progression of local immune responses and DCs play a crucial role in these processes, $Clec9a^{Cre/Cre}ROSA^{iDTR}$ mice were next immunised with CFA/OVA or infected with influenza to study their ability to mount an immune response. Due to the limited availability of mice, homozygous $Clec9a^{Cre/Cre}ROSA^{iDTR}$ (and therefore DNGR-1

deficient) mice had to be used for these experiments, age and sex-matched with either control mice from the ROSA26-iDTR colony (CFA/OVA immunisation) or with Clec9a$^{+/+}$ROSA^{iDTR} mice from the same colony (influenza infection).
CFA/OVA immunisation led to expansion of draining LNs in both Clec9a$^{Cre/Cre}$ROSA^{iDTR} and control mice (Figure 3.19A). Surprisingly, the difference in LN size between naïve Clec9a$^{Cre/Cre}$ROSA^{iDTR} and control mice was lost upon immunisation (Figure 3.19A). In contrast, the difference in frequency of cells that fall in the resDC or migDC gates between Clec9a$^{Cre/Cre}$ROSA^{iDTR} and control mice was maintained upon immunisation (Figure 3.19B). At 12 days post immunisation OVA-specific pentamer^{+} CD8α^{+} CD44^{+} T cells were present in draining sdLNs of Clec9a$^{Cre/Cre}$ROSA^{iDTR} mice, although their numbers were lower than in draining sdLNs of control mice (Figure 3.20A). Likewise, in spleens of immunised control mice pentamer^{+} CD8α^{+} CD44^{+} T cells could be found, despite at a very low level, while in spleens of Clec9a$^{Cre/Cre}$ROSA^{iDTR} mice no specific pentamer stain could be detected (Figure 3.20B). Altogether, these results indicate that Clec9a$^{Cre/Cre}$ROSA^{iDTR} mice can mount a CD8^{+} T cell response, but that this response may be smaller than in control mice.

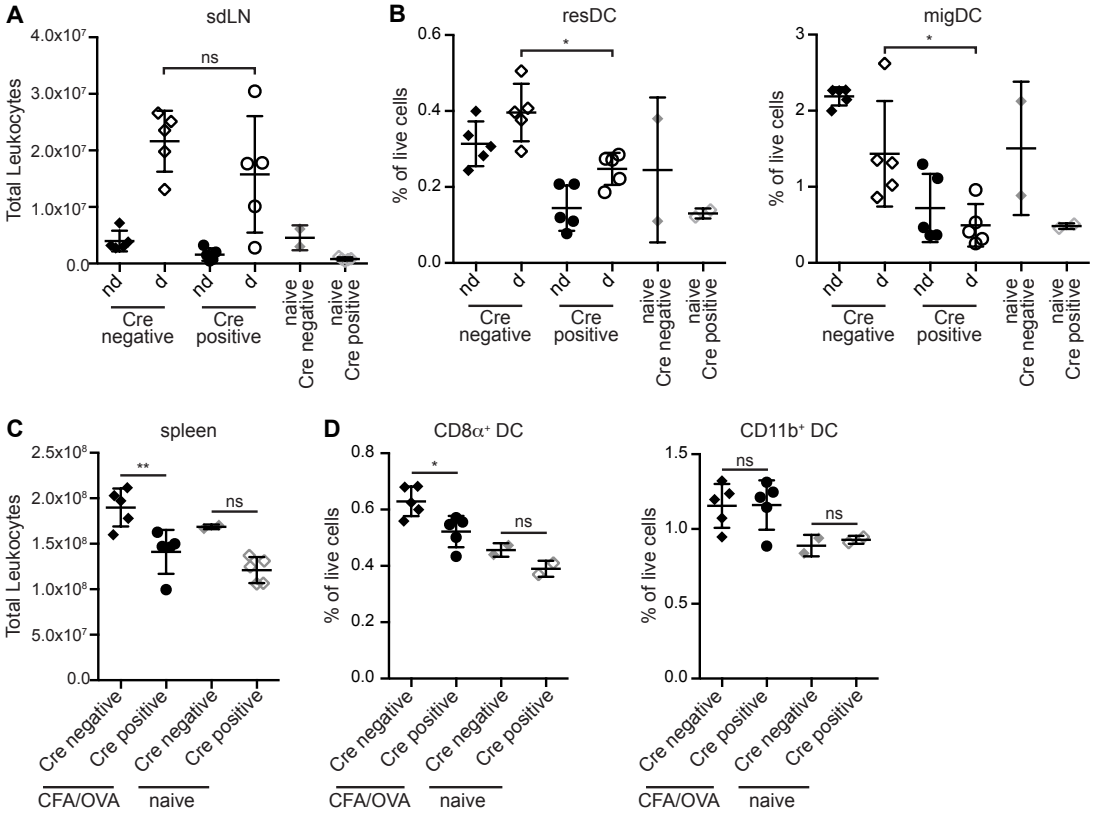

Figure 3.19 sdLNs expand normally in CFA/OVA immunised Clec9a$^{Cre/Cre}$ROSA^{iDTR} mice

ROSA26-iDTR control ('Cre negative') and Clec9a$^{Cre/Cre}$ROSA^{iDTR} ('Cre positive') mice were immunised s.c. in one flank with CFA/OVA (50µg OVA protein per mouse), draining to inguinal sdLN. Both draining and non-draining sdLNs and spleens were collected at day 12 post-immunisation, as well as LNs and spleens from non-immunised naïve mice. **(A)** Single cell suspensions from sdLNs were counted and the number of total leukocytes is plotted. **(B)** ResDCs (CD11c$^+$ MHCII^{int}) and migDCs (CD11c$^+$ MHCII^{hi}) in sdLNs were identified by flow cytometry and DC subsets as percentage of live leukocytes are plotted. **(C)** Single cell suspensions from spleens were counted and the number of total leukocytes is plotted. **(D)** CD8α$^+$ DCs (CD11c$^+$ MHCII$^+$ CD8α$^+$) and CD11b$^+$ DCs (CD11c$^+$ MHCII$^+$ CD11b$^+$) in spleen were identified by flow cytometry and DC subsets as percentage of live leukocytes are plotted. Each dot represents one mouse. Data are from one experiment. Ns: non significant, *: p≤0.05, **: p≤0.01.

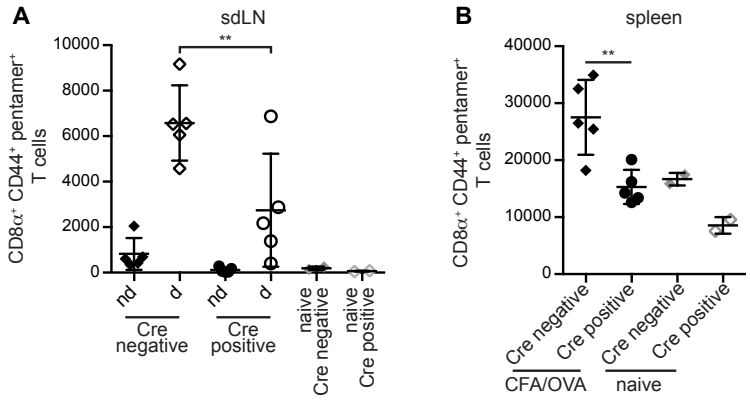

Figure 3.20 Clec9a$^{Cre/Cre}$ROSA^{iDTR} mice can mount a CD8$^+$ T cell response upon CFA/OVA immunisation

ROSA26-iDTR control ('Cre negative') and Clec9a$^{Cre/Cre}$ROSA^{iDTR} ('Cre positive') mice were immunised s.c. in one flank with CFA/OVA (50µg OVA protein per mouse), draining to inguinal sdLN. Both draining and non-draining sdLNs and spleens were collected at day 12 post-immunisation, as well as LNs and spleens from non-immunised naïve mice. Single cell suspensions from sdLNs **(A)** and spleens **(B)** were generated and CD8α$^+$ CD44$^+$ T cells (CD3$^+$ MHCII$^-$ CD8α$^+$ CD4$^-$ CD44$^+$) were identified by flow cytometry, total pentamer$^+$ CD8α$^+$ CD44$^+$ T cells are plotted. Each dot represents one mouse. Data are from one experiment. **: p≤0.01.

The influenza infection induced an influenza-specific CD8$^+$ T cell response in both Clec9a$^{Cre/Cre}$ROSA^{iDTR} and control mice, as exemplified by the presence of pentamer$^+$ CD8α$^+$ CD44$^+$ T cells in both medLNs and spleens (Figure 3.22AB) and IFNγ production by restimulated single cell suspensions from medLNs and spleens of infected mice (Figure 3.22CD). However, while the number of pentamer$^+$ CD8α$^+$ CD44$^+$ T cells was similar in medLNs of Clec9a$^{Cre/Cre}$ROSA^{iDTR} and control mice, there was a trend for reduced pentamer$^+$ CD8α$^+$ CD44$^+$ T cells in spleens of Clec9a$^{Cre/Cre}$ROSA^{iDTR} mice compared with controls (Figure 3.22AB). However, no difference in IFNγ production could be observed between cultures from spleens from Clec9a$^{Cre/Cre}$ROSA^{iDTR} and control mice when restimulated with CD8$^+$ T cell epitope peptides (Figure 3.22D).

To assess CD4$^+$ T cell priming upon influenza infection, single cell suspensions from medLNs and spleens of infected mice were restimulated with peptides representing CD4$^+$ T cell epitopes and IFNγ production was assessed. As shown in Figure 3.22CD, cultures from medLNs and spleens of infected Clec9a$^{Cre/Cre}$ROSA^{iDTR} mice may have produced more IFNγ upon restimulation.

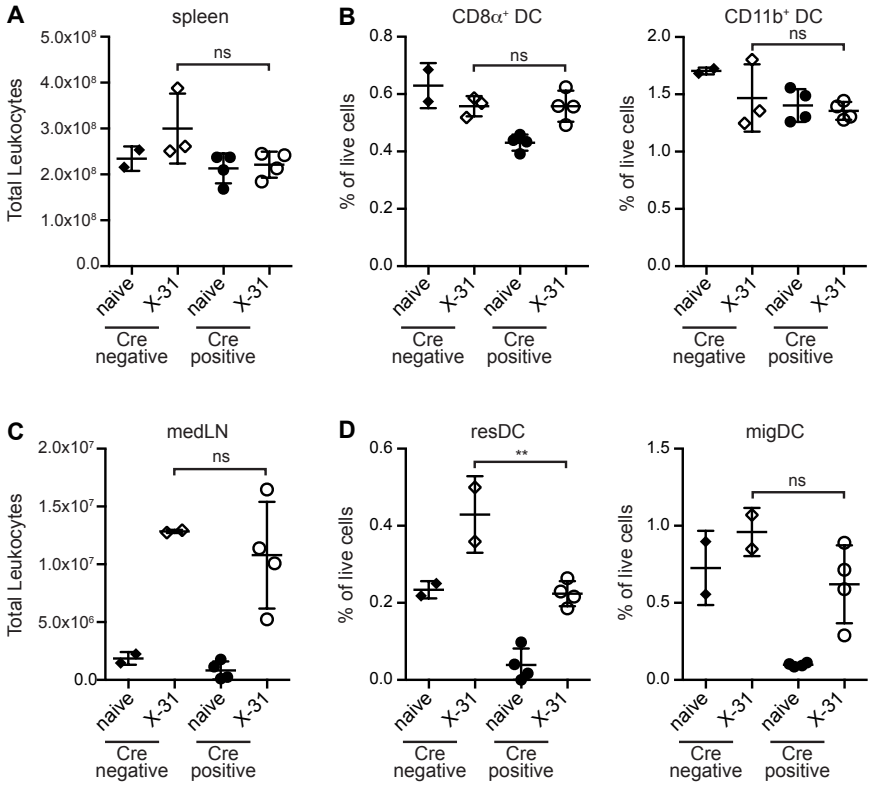

Figure 3.21 MedLNs expand normally in influenza X-31 infected Clec9a$^{Cre/Cre}$ROSA^{iDTR} mice

Clec9a$^{+/+}$ROSA^{iDTR} control ('Cre negative') and Clec9a$^{Cre/Cre}$ROSA^{iDTR} ('Cre positive') mice were infected i.n. with 1x10^4 pfu influenza X-31. MedLNs and spleens were collected at day 9 post infection, along with medLNs and spleens of naïve mice. **(A)** Single cell suspensions from spleens were counted and the number of total leukocytes is plotted. **(B)** CD8α$^+$ DCs (CD11c$^+$ MHCII$^+$ CD8α$^+$) and CD11b$^+$ DCs (CD11c$^+$ MHCII$^+$ CD11b$^+$) in spleen were identified by flow cytometry and DC subsets as percentage of live leukocytes are plotted. **(C)** Single cell suspensions from medLNs were counted and the number of total leukocytes is plotted. **(D)** ResDCs (CD11c$^+$ MHCII^{int}) and migDCs (CD11c$^+$ MHCII^{hi}) in LNs were identified by flow cytometry and DC subsets as percentage of live leukocytes are plotted. Each dot represents one mouse. Data are from one experiment. Ns: non significant, **: p≤0.01.

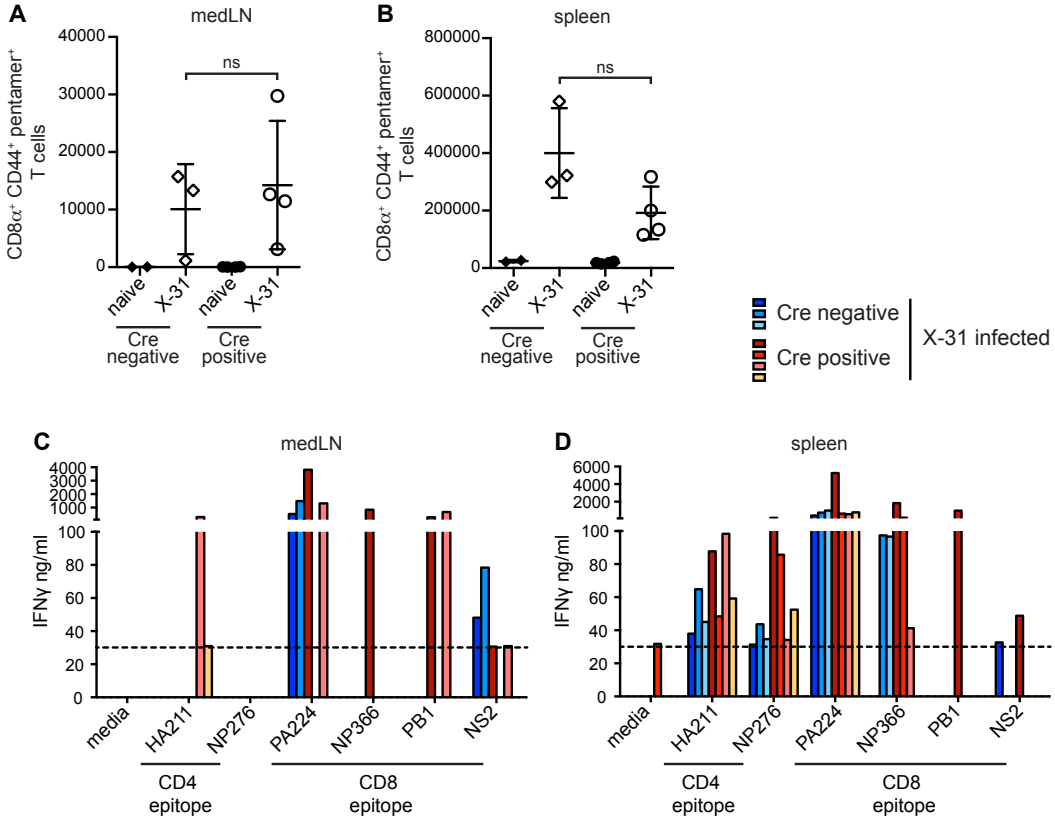

Figure 3.22 Clec9a$^{Cre/Cre}$ROSA^{iDTR} and control mice mount similar CD8$^+$ and CD4$^+$ T cell responses upon influenza X-31 infection

Clec9a$^{+/+}$ROSA^{iDTR} control ('Cre negative') and Clec9a$^{Cre/Cre}$ROSA^{iDTR} ('Cre positive') mice were infected i.n. with 1x10^4 pfu influenza X-31. MedLNs and spleens were collected at day 9 post infection, along with medLNs and spleens of non-infected naïve mice. Single cell suspensions from medLNs **(A)** and spleens **(B)** were generated, CD8α$^+$ CD44$^+$ T cells (CD3$^+$ MHCII$^-$ CD8α$^+$ CD4$^-$ CD44$^+$) were identified by flow cytometry and total pentamer$^+$ CD8α$^+$ CD44$^+$ T cells are plotted. Single cell suspensions (5x10^5 cells/well) from medLNs **(C)** and spleens **(D)** were restimulated overnight with the indicated peptides, after which IFNγ concentrations in the supernatants were determined by ELISA. Peptide names were shortened to their starting amino acid for brevity. Full peptide names and sequences are found in Table 4. Dashed line denotes detection limit of the ELISA. Only samples that reached the detection limit are shown with a bar. IFNγ from restimulated cultures from spleens of naïve mice (2 Cre negative and 3 Cre positive) or of naïve medLNs (one pooled sample for Cre negative and one pooled sample for Cre positive) were below detection limit and were not included in the graph for clarity. Each dot or bar represents one mouse. Data are from one experiment. Ns: non significant

Both upon immunisation with CFA/OVA and infection with influenza, draining LNs were able to increase in size to a similar extend as in control mice, indicating that LNs in Clec9a$^{+/Cre}$ROSA^{iDTR} mice can expand normally in an inflammatory setting.

However, both experiments also showed that cells that fall in the resDC or migDC gates were still reduced in frequencies in draining LNs of immunised or infected Clec9a$^{Cre/Cre}$ROSA^{iDTR} mice compared with controls. Both CFA/OVA immunisation and influenza infection induced antigen-specific CD8$^+$ T cells in Clec9a$^{Cre/Cre}$ROSA^{iDTR} mice. However, in the case of CFA/OVA immunisation the total numbers of pentamer$^+$ CD8$^+$ T cells in draining LNs was lower in Clec9a$^{Cre/Cre}$ROSA^{iDTR} mice compared with controls, while in the influenza setting no such difference was observed. Interestingly, both experiments revealed a trend for reduced pentamer$^+$ CD8$^+$ T cells in spleens of immunised or infected mice. Altogether, these results may indicate that although CD8$^+$ T cells can be efficiently primed in Clec9a$^{Cre/Cre}$ROSA^{iDTR} mice, the resulting antigen-specific CD8$^+$ T cells may not be fully functional.

In general, the results presented here should be interpreted with some caution, as both the CFA/OVA immunisation and the influenza X-31 infection were only performed once with mouse cohorts that were not perfectly matched. Furthermore, Clec9a$^{Cre/Cre}$ROSA^{iDTR} mice are deficient for DNGR-1, in addition to expressing DTR on DCs. Therefore the differences observed here may also be attributable to DNGR-1 deficiency instead of to DTR expression.

3.8 What is the mechanism by which DTR expression confers LN abnormalities?

The results presented thus far indicate that DTR expression on DCs confers LN hypocellularity and reduced DC frequencies in LNs. As only tissues with an afferent lymph supply seem to be affected and the paucity of migDCs in LNs may reflect an impairment in their migration from peripheral sites, the migratory ability of DTR-expressing DCs was assessed. To this extent, a transwell assay was performed with leukocytes isolated from sdLNs of Clec9a$^{+/Cre}$ROSA^{iDTR} and control mice. Interestingly, both resDCs and migDCs from Clec9a$^{+/Cre}$ROSA^{iDTR} mice were impaired in their migration towards the chemokine CCL21 in this *in vitro* assay (Figure 3.23). Therefore, CCR7 expression was assessed by flow cytometry on DC subpopulations in sdLNs. Both CD8α$^+$ resDCs and CD11b$^+$ resDCs from Clec9a$^{+/Cre}$ROSA^{iDTR} and control mice did not express detectable levels of CCR7, while all migDC populations and LCs in sdLNs expressed CCR7 (Figure 3.24).

However, there was no difference in CCR7 expression levels between Clec9a$^{+/Cre}$ROSA^{iDTR} and control mice (Figure 3.24) and therefore CCR7 expression could not explain the impaired migration of sdLN DCs from Clec9a$^{+/Cre}$ROSA^{iDTR} mice in the transwell assay, nor provide an explanation for the observed reduction in DC frequency in LNs of Clec9a$^{+/Cre}$ROSA^{iDTR} mice.

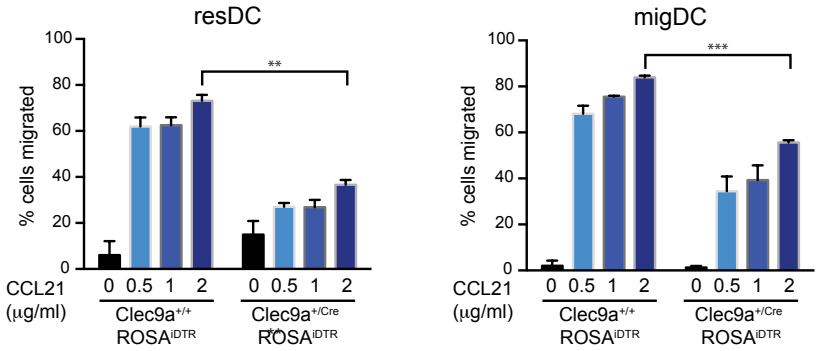

Figure 3.23 DCs from sdLNs of Clec9a$^{+/Cre}$ROSA^{iDTR} mice show impaired migration towards the chemokine CCL21

DCs were isolated from sdLNs of Clec9a$^{+/Cre}$ROSA^{iDTR} and control mice and exposed to the indicated concentrations CCL21 in a transwell assay. After 4h, cells from wells and inserts were collected and resDCs (CD11c^{+} MHCII^{int}) and migDCs (CD11c^{+} MHCII^{hi}) were identified by flow cytometry and the frequency of migrated cells was calculated. **: p≤0.01, ***: p≤0.001. This experiment was performed once with experimental duplicates for each concentration.

Flt3l is essential for DC homeostasis and mice lacking Flt3l or its receptor Flt3 (also called CD135) show a severe reduction in DCs (McKenna *et al.*, 2000; Waskow *et al.*, 2008). Hence, Flt3 expression was determined on sdLN DCs. Virtually all resDCs and migDCs isolated from sdLNs expressed Flt3, as did LCs. Expression levels varied per subset, but were similar between Clec9a$^{+/Cre}$ROSA^{iDTR} and control mice for any given subset (Figure 3.24).

In sum, DTR-expressing DCs are impaired in their migration in an *in vitro* transwell assay, which may explain why DCs are reduced in LNs of mice that express DTR on DCs. However, DTR-expressing DCs express normal levels of the chemokine receptor CCR7 and the receptor tyrosine kinase Flt3, which can therefore not explain why DC migration and/or survival is impaired in a DTR background.

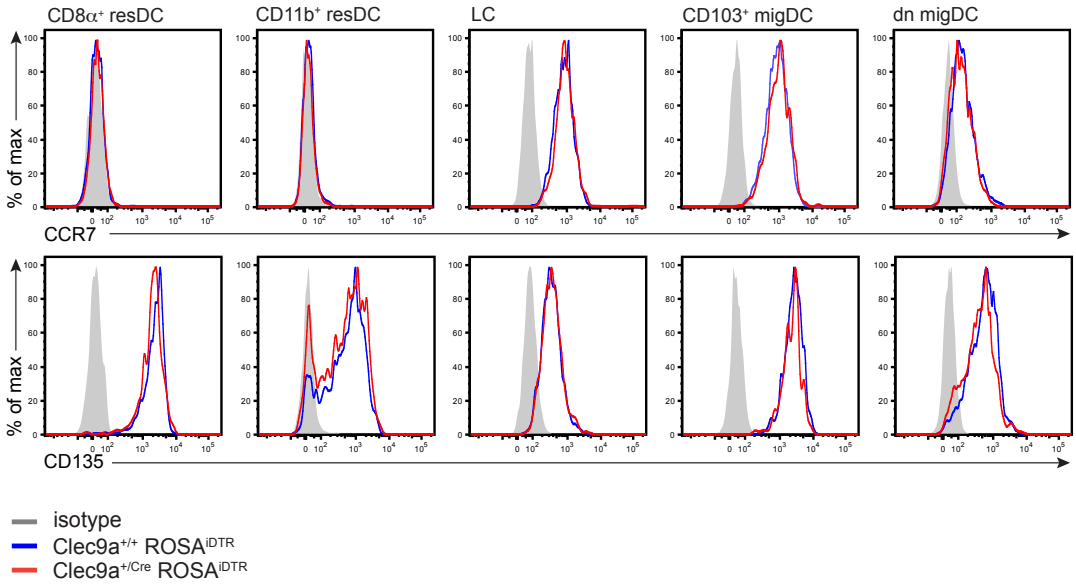

Figure 3.24 DC subsets in sdLNs of Clec9a$^{+/Cre}$ROSA^{iDTR} mice do not show differential CCR7 or CD135 (Flt3) expression compared with controls

CD8α^{+} resDCs (CD11c^{+} MHCII^{int} CD8α^{+}), CD11b^{+} resDCs (CD11c^{+} MHCII^{int} CD11b^{+}), LCs (CD11c^{+} MHCII^{hi} CD207^{+} CD103^{-}), CD103^{+} migDCs (CD11c^{+} MHCII^{hi} CD207^{+} CD103^{+}) and double negative (DN) migDCs (CD11c^{+} MHCII^{hi} CD207^{-} CD103^{-}) in sdLNs of control and Clec9a$^{+/Cre}$ROSA^{iDTR} mice were identified by flow cytometry and the levels of CCR7 and CD135 are shown for each subset. Grey shading represents isotype control. This experiment was performed once and each plot is representative of three mice.

Naïve lymphocytes enter LNs via HEVs and DCs have been shown to be essential for maintaining HEV function (Moussion and Girard, 2011). Therefore, the reduced LN size observed in mice that express DTR on DCs may be secondary to the reduction in DC frequency in LNs of these mice. To test this hypothesis, LN cryosections were stained with an antibody against the pan-endothelial marker CD31 and with the HEV-specific antibody MECA79 that recognises sulphated carbohydrate ligands for L-selectin, the homing receptor expressed by lymphocytes. However, neither the distribution and size of HEVs, nor the intensity of the MECA79 staining differed markedly between LNs from Clec9a$^{+/Cre}$ROSA^{iDTR} and control mice (Figure 3.25A), suggesting that a difference in HEV function cannot explain the LN hypocellularity in mice that express DTR on DCs.
HEVs express abundant amounts of CCL21 (Gunn et al., 1998; J. J. Campbell et al., 1998), while the most important source of CCL21 in T cell zones are FRCs (Link et al., 2007). In addition, FRCs form an elaborate network that supports leukocyte trafficking in the T cell zone (M. J. Miller *et al.*, 2002; Bajénoff *et al.*,

2006). As DCs are important for maintaining FRC function (Acton *et al.*, 2014; Astarita *et al.*, 2015), a paucity of DCs could lead to LN hypocellularity via malfunctioning FRCs and/or reduced CCL21 production. The FRC network and CCL21 expression were therefore examined in LN sections from Clec9a$^{+/Cre}$ROSA^{iDTR} and control mice. Interestingly, staining with the ER-TR7 antibody, which recognises an extracellular protein produced by FRCs, revealed a differential distribution of this FRC extracellular matrix protein in LN sections of Clec9a$^{+/Cre}$ROSA^{iDTR} and control mice (Figure 3.25B). LNs from Clec9a$^{+/Cre}$ROSA^{iDTR} mice showed a less pronounced ER-TR7 staining around HEVs (visualised by anti-CD31 staining), while the network was more prominent in the T cell zone, compared with LN sections from control mice (Figure 3.25B). Furthermore, anti-CCL21 staining showed a reduction in this chemokine in LN sections from Clec9a$^{+/Cre}$ROSA^{iDTR} mice (Figure 3.25B). Together these results indicate that the FRC network may be disrupted in LNs of Clec9a$^{+/Cre}$ROSA^{iDTR} mice.

In sum, DCs in Clec9a$^{+/Cre}$ROSA^{iDTR} mice may be impaired in their migration to LNs, leading to reduced frequencies of DCs in LNs, which in turn may impact on the FRC network in LNs and causing LN hypocellularity. However, the experiments presented here are not sufficient to fully confirm these conclusions. Firstly, it is still unclear why Clec9a$^{+/Cre}$ROSA^{iDTR} mice may be impaired in their migration and moreover, migration was only assessed *in vitro* and not in an *in vivo* setting. Moreover, the experiments presented here do not address the fundamental question of how DTR expression modulates the DC function and/or the DC microenvironment.

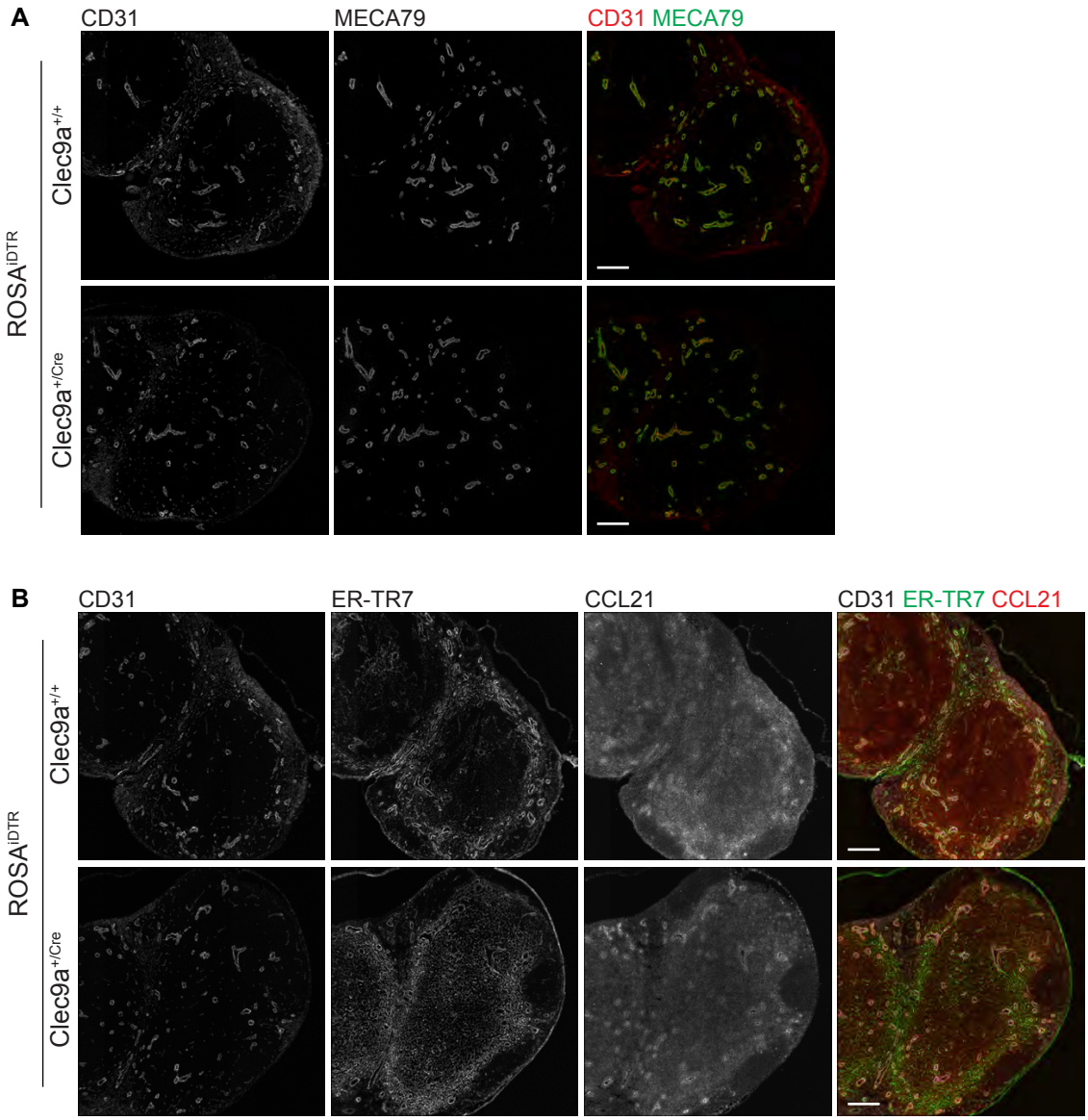

Figure 3.25 Clec9a$^{+/cre}$ROSA^{iDTR} mice appear to have normal HEVs, but may have an altered FRC network

Frozen sections of sdLNs from control and Clec9a$^{+/cre}$ROSA^{iDTR} mice were stained with anti-CD31 and anti-MECA79 antibodies **(A)** or with anti-CD31, ER-TR7 and anti-CCL21 antibodies **(B)** and imaged by confocal microscopy. Scale bar: 200µm. Images are representative of 3 mice per group.

3.9 Discussion

Mouse models to inducibly deplete DCs are useful tools to elucidate the role of DCs in immune functions. Many of these models rely on transgenic DTR expression driven by promoters more or less restricted to DCs. Despite the fact that the first such model, the CD11c-DTR mouse (Jung et al., 2002), was generated over ten years ago and has since been used extensively (van Blijswijk, Schraml and Reis e Sousa, 2013), mice in which simian or human DTR is forcibly expressed on DCs have not been reported to display immune abnormalities. Unexpectedly, the results presented in this chapter show that these models display reduced LN cellularity and a profound decrease in the relative frequency of DCs in LNs in the absence of DT treatment.

Five different mouse models were tested in which DTR is forcibly expressed in DCs (Clec9a$^{+/Cre}$ROSA^{iDTR}, CD11c-Cre^{+ve}ROSA^{iDTR}, CD11c-DTR, Langerin-DTR and CD11c-DOG mice). Although this list includes widely used models for DC depletion, it is not exhaustive. In particular, the recently described zDC-DTR mice (Meredith, Liu, Darrasse-Jeze, et al., 2012) were not investigated. Furthermore, the data presented here do not allow assessing whether it is necessary and/or sufficient for DTR to be expressed by a particular subset of DCs to confer the LN phenotype. In this regard, Clec9a-DTR mice (Piva et al., 2012), XCR1-DTR mice (Yamazaki et al., 2013), SiglecH-DTR and BDCA2-DTR mice (Swiecki et al., 2010) may be used to address the consequences of expressing DTR on CD8α-like cDCs or pDCs. In addition, it will be interesting to assess LN cellularity and phagocyte frequency in mice in which DTR is forcibly expressed on monocytes or macrophages, as these mononuclear phagocytes are found in similar niches and may perform similar functions as DCs.

The mechanistic basis for these findings is not fully elucidated, although the data presented here may provide some clues. As DC frequencies were unaltered in the spleen and non-lymphoid tissues in the mouse models examined here, and because in Langerin-DTR mice the sdLNs, but not mesLNs were affected, a defect at the level of DC precursors or their ability to seed tissues is unlikely. Rather, only tissues with an afferent lymph supply seem to be affected and the paucity of migDCs in LNs likely reflects an impairment in their migration from peripheral sites, or a reduced lifespan once in the LN. Reduced lifespan might also explain the

decrease in LN resDC frequencies. Furthermore, the alteration in LN composition and function in mice that express DTR on DCs is not imprinted during mouse development, as it can be conferred to adult mice by transplantation of BM from affected mice and, remarkably, acts dominantly over WT BM. It is therefore tempting to speculate that DCs expressing DTR modulate the LN microenvironment, either via a soluble factor or cell-cell contact, to make it unfavourable for DC immigration. This factor could be DTR itself, either shed from, or expressed on the DC surface, or another factor made by DCs or other cells, upon engagement of DTR on DCs and EGF receptors on adjacent cells. Within the LN, either the lack of DCs or, again, a modulation of the microenvironment by DTR-expressing DCs, may impair the homing to, or retention in the LN of lymphocytes, resulting in LN hypocellularity. In this regard, it is notable that paucity of DCs has been shown to cause shutdown of HEVs (Moussion and Girard, 2011). Furthermore, when DC migration to LNs is impaired due to a lack of CCR7, LNs also show a reduced number of HEVs, reduced LN size and T cell lymphopenia in LNs (Wendland et al., 2011).

A few of these possibilities were tested here. DCs isolated from LNs from Clec9a$^{+/Cre}$ROSA^{iDTR} mice were less able to migrate to the chemokine CCL21 in an *in vitro* transwell assay, and while HEVs looked normal, the FRC network was altered in LN sections from Clec9a$^{+/Cre}$ROSA^{iDTR} mice. However, none of these results can fully explain the phenotype observed and none address the fundamental question of how DTR expression on DCs exerts its biological effects. It may be that the phenotype observed is a consequence of a complex interaction with the external environment. In this regard, it will be of interest to analyse the same strains across multiple animal facilities or after rederivation into a gnotobiotic environment.

Whatever the underlying mechanism, these findings indicate a need for caution when interpreting results obtained with DTR-based mouse models to inducibly deplete DCs, as the steady-state immune system in such mice clearly differs from that of controls. In this regard, it is important to note that small LN size has been shown to markedly impact immune responses and resistance to infection (van de Pavert et al., 2014). Although the CFA/OVA immunisation and influenza X-31 infection experiments presented here did not show a marked impairment in immune response in mice expressing DTR on DCs, these experiments were not exhaustive

and mice expressing DTR on DCs may still show impaired immune responses in a different setting.

Why the phenotype described here appears to have passed unnoticed or at least unreported is unclear, but may in part be due to the tendency to use PBS-injected DTR-expressing mice (rather than littermates not expressing DTR) as controls for mice receiving DT. Based on the findings presented here, both types of controls are warranted and some of the changes in immune responses observed upon DT-mediated DC depletion might in fact be a composite caused by acute loss of DCs, superimposed on underlying LN defects. These findings also suggest that simian HB-EGF possesses biological activities in mice that cannot be ignored. As such, DTR expression on other cell types, including those outside the immune system, might alter their biology or, as shown here, that of their immediate environment. The latter may require shedding via the action of cell-specific metalloproteinases, explaining why expression on some cells (e.g., B cells or Tregs) is apparently innocuous while that is not the case for expression on DCs. Clearly, the use of DTR in mice has pitfalls that might impact on experimental approaches and need to be tempered with the great advantages awarded by the ability to ablate cells at will.

Chapter 4. A Novel Mouse Model to Constitutively Ablate Dendritic Cells

4.1 Introduction

DCs mediate both central and peripheral tolerance, which are crucial to avoid autoimmune reactions to develop. It was therefore hypothesised that constitutive ablation of DCs would lead to spontaneous autoimmunity. Both Ohmnacht et al. (Ohnmacht et al., 2009) and Birnberg et al. (Birnberg et al., 2008) have tested this hypothesis by crossing CD11c-Cre mice to two different strains of ROSA26-DTA mice, generating mice in which CD11c-expressing cells are ablated through expression of DTA. Remarkably, only the crosses generated by Ohmnacht et al. (Ohnmacht et al., 2009) developed spontaneous autoimmunity with increased Th1 and Th17 cells and the generation of autoantibodies, while Birnberg et al. (Birnberg et al., 2008) reported unaffected T cell homeostasis under steady state conditions. Furthermore, CD11c is not only expressed on DCs, but also on other immune cells, such as activated T cells and Ly-6C^{low} monocytes (Jung *et al.*, 2002; Probst, Tschannen, *et al.*, 2005; Hochweller *et al.*, 2008). Moreover, DCs also impact on processes beyond the regulation of T cell responses, such as the regulation of innate immune responses (Mashayekhi *et al.*, 2011; Satpathy *et al.*, 2013; Arora *et al.*, 2014; Whitney *et al.*, 2014) and stromal behaviour (Moussion and Girard, 2011; Acton et al., 2014).

In an attempt to address these outstanding issues, transgenic mice were generated that express the DTA protein under direct control of the endogenous *Clec9a* locus, following a similar knock-in strategy as was used to generate Clec9a-GFP (Sancho et al., 2009) and Clec9a-Cre mice (Schraml et al., 2013). In these Clec9a-DTA mice, DTA should be expressed in the CDP and preDCs, killing these DC precursors. Therefore, Clec9a-DTA mice should not harbour any DCs from very early in development. By utilising the *Clec9a* locus to drive DTA expression, ablation should be restricted to the DC lineage without affecting other (immune) cells, as opposed to models that use CD11c expression to manipulate DCs.

4.2 Generation of Clec9a-DTA mice to constitutively ablate DCs

The targeting construct to generate Clec9a-DTA mice was derived from the pFloxRI-C9a-EGFP vector that was used to generate Clec9a-GFP mice (Sancho et al., 2009). The *egfp* gene was replaced by the gene encoding DTA. Successful targeting by homologous recombination disrupts the *Clec9a* open reading frame abrogating DNGR-1 expression and leading to DTA expression under control of the endogenous *Clec9a* locus (Figure 4.1).

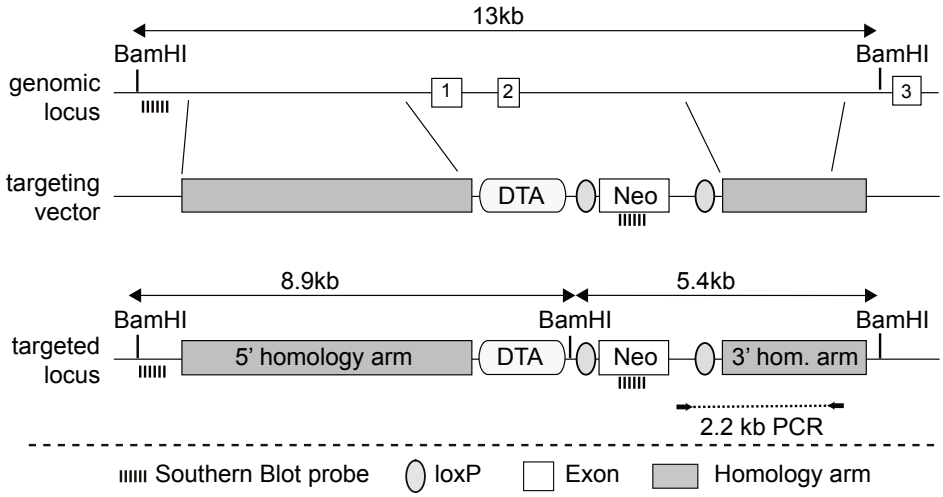

Figure 4.1 Targeting strategy to generate Clec9a-DTA mice

The endogenous genomic *Clec9a* locus is shown at the top, with the targeting vector to generate Clec9a-DTA mice below. The targeted allele is also depicted (bottom). The PCR product (2.2kb) to screen correctly targeted ES cells is shown. BamHI restriction enzyme target sites, the locations of the Neo probe and 5' probe and the size of the fragments detected by Southern blot screening are shown.

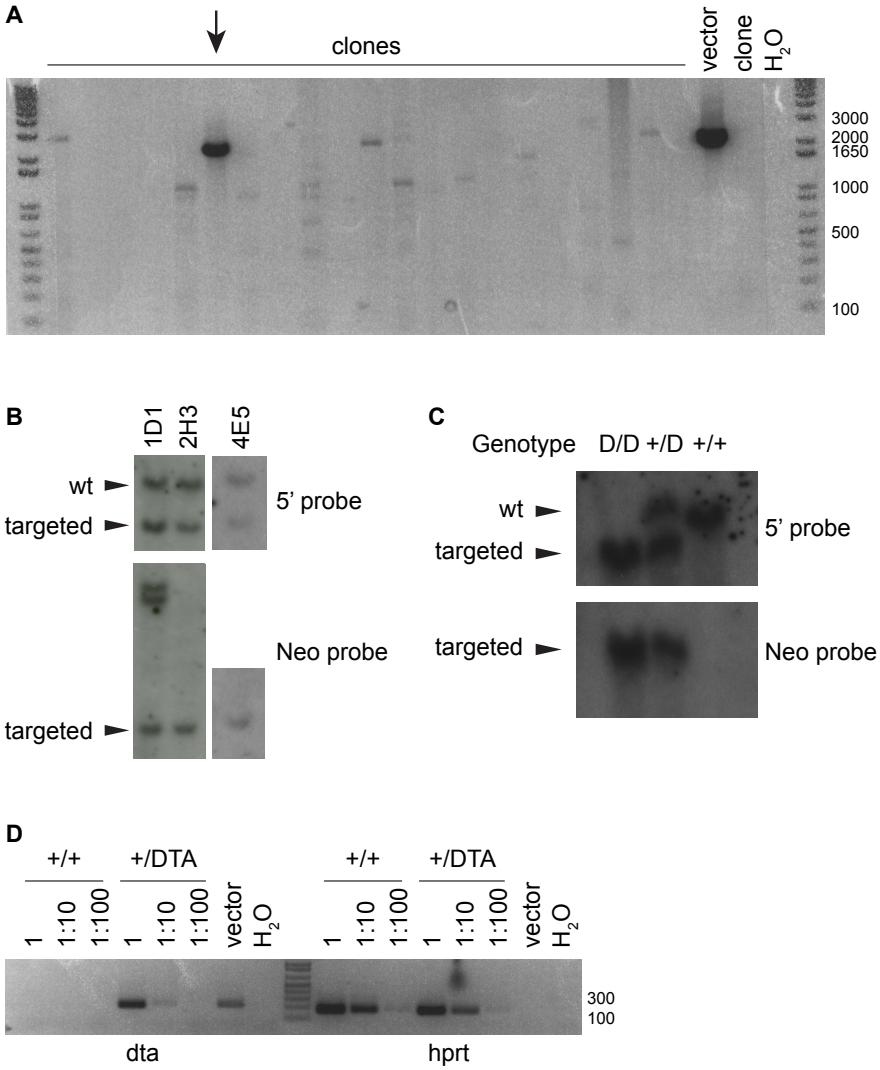

Figure 4.2 Generation of Clec9a-DTA mice

(A) ES cell clones were screened by a PCR that spans the 3' homology arm and results in a 2.2kb PCR product if the clone is correctly targeted (see Figure 4.1). 384 clones were screened, from which a selection is shown here. The arrow denotes clone 2H3. The targeting vector was used as positive control (vector) and a no-DNA sample (H_2O) was used as negative control. The size of the ladder fragments is denoted on the right in kb. **(B)** ES cell clones positive by PCR (clones 1D1, 2H3 and 4E5) were screened by Southern blot via digestion with BamHI and detection with neo and 5' probes (see Figure 4.1). **(C)** Genomic DNA from Clec9a-DTA 2H3 mice was screened by Southern blot as in (B). Genotype denotes homozygous (D/D), heterozygous (+/D) and WT (+/+) Clec9a-DTA 2H3 littermates. **(D)** A semi-quantitative RT-PCR was performed to assess DTA mRNA levels on CD11c MACS-enriched splenocytes from Clec9a$^{+/+}$ (+/+) and Clec9a$^{+/DTA}$ mice (+/DTA). cDNA was used undiluted or diluted 10 or 100 times before the PCR reaction was performed with primers for *dta* or *hprt* as control. The targeting vector used to generate the mice was used as a positive control. The size of the ladder fragments is denoted on the right in kb. All experiments were performed once.

A total of 384 ES cell clones were first screened for correct targeting by PCR, which resulted in three positive clones (1D1, 2H3 and 4E5) (Figure 4.2A). These clones were subsequently analysed by Southern blot analysis, confirming correct targeting of clones 2H3 and 4E5, but revealing multiple insertions of the targeting vector for clone 1D1 (Figure 4.2B). The two correctly targeted clones 2H3 and 4E5 were next used to generate chimeric mice and germline transmission was assessed by genotyping PCR of the offspring. Only clone 2H3 germline transmitted and established a colony of Clec9-DTA 2H3 mice, while clone 4E5 failed to transmit into the germline, despite numerous breeding attempts with different chimeric founders. For the remainder of this chapter 'Clec9a-DTA mice' will therefore refer to the colony established from the 2H3 ES cell clone.
To further validate the Clec9a-DTA mice, genomic DNA was screened by Southern blot. The Southern blot analysis confirmed correct and unique targeting of the *Clec9a* locus in a heterozygous and a homozygous Clec9a-DTA mouse (Figure 4.2C). The *dta* gene and proximal promoter were also sequenced from genomic DNA from a heterozygous Clec9a-DTA mouse to confirm that no mutations were introduced in the process of generating this mouse strain. Indeed, no mutations were found. In addition, the expression of *dta* mRNA was confirmed in CD11c-enriched splenocytes by semi-quantitative RT-PCR (Figure 4.2D).
In sum, out of 384 ES cell clones two clones were confirmed to be correctly targeted, one of which resulted in a Clec9a-DTA mouse colony. Correct targeting was reconfirmed in these mice by Southern blot analysis and *dta* mRNA expression could be detected in CD11c-enriched splenocytes from these mice.

4.3 Characterisation of Clec9a-DTA mice

The Clec9a-DTA mouse line bred well and Clec9a$^{+/DTA}$ and Clec9a$^{DTA/DTA}$ mice were born at the expected mendelian frequencies. These mice did not show any signs of illness and all survived into adulthood. Furthermore, adult Clec9a$^{+/DTA}$ and Clec9a$^{DTA/DTA}$ mice did not have monocytosis and neutrophilia in the spleen (Figure 4.3A) and also did not have increased spleen or mesLN cellularity (Figure 4.3B). These results indicate that they do not develop a myeloproliferative disorder, as opposed to what was reported for CD11c-Cre mice crossed to ROSA26-DTA mice (Birnberg *et al.*, 2008; Ohnmacht *et al.*, 2009).

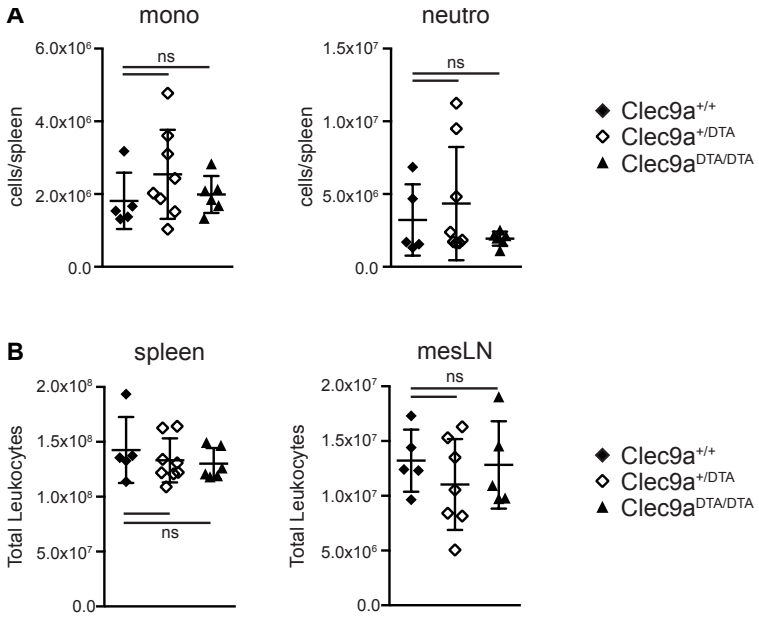

Figure 4.3 Clec9a$^{+/DTA}$ and Clec9a$^{DTA/DTA}$ mice do not show signs of myeloproliferative disorder

(A) Total numbers of monocytes (mono, CD11b^{+} Gr-1^{int}) and neutrophils (neutro, CD11b^{+} Gr-1^{hi}) in spleens of 8-12 week old Clec9a$^{+/+}$, Clec9a$^{+/DTA}$ and Clec9a$^{DTA/DTA}$ mice is shown. **(B)** Single-cell suspensions of spleens and mesLNs from 8-12 week old Clec9a$^{+/+}$, Clec9a$^{+/DTA}$ and Clec9a$^{DTA/DTA}$ mice were counted and the number of total leukocytes is plotted. A one-way ANOVA with a Tukey's multiple comparisons post-test was performed to calculate p-values. Each dot represents one mouse. Ns: non significant. Data are pooled from three independent experiments.

To address if DCs are actually ablated in Clec9a-DTA mice, spleens and mesLNs of Clec9a$^{+/+}$, Clec9a$^{+/DTA}$ and Clec9a$^{DTA/DTA}$ mice were analysed for the presence of DC subsets. Surprisingly, total DC frequency in the spleen was increased in Clec9a$^{+/DTA}$ and Clec9a$^{DTA/DTA}$ mice compared with controls, which was entirely attributable to an increase of the CD11b^{+} DC subset (Figure 4.4A). On the contrary, CD8α^{+} DC frequency was reduced in spleens of both Clec9a$^{+/DTA}$ and Clec9a$^{DTA/DTA}$ mice (Figure 4.4A). Similarly, the frequencies of CD8α^{+} resDCs and CD103^{+} migDCs were reduced in mesLNs of Clec9a$^{+/DTA}$ and Clec9a$^{DTA/DTA}$ mice compared with controls, while the frequencies of CD11b^{+} resDCs, CD103^{+} CD11b^{+} migDCs and CD11b^{+} migDCs remained unchanged or were slightly increased in Clec9a$^{+/DTA}$ and Clec9a$^{DTA/DTA}$ mice (Figure 4.4B).

Normal numbers of DCs can be identified in Clec9a-DTA mice, indicating that not all CDPs and preDCs were ablated. The precursor frequency in the bone marrow of Clec9a$^{+/DTA}$ and Clec9a$^{DTA/DTA}$ mice was therefore assessed. As shown in Figure

4.5, MDPs were unaltered in Clec9a$^{+/DTA}$ and Clec9a$^{DTA/DTA}$ mice, which is in line with earlier observations that MDPs do not express DNGR-1 (Schraml et al., 2013). Interestingly, CDPs and preDCs were unaffected in BM of Clec9a$^{+/DTA}$ and Clec9a$^{DTA/DTA}$ mice (Figure 4.5), indicating that the intended ablation of these precursor populations had failed.

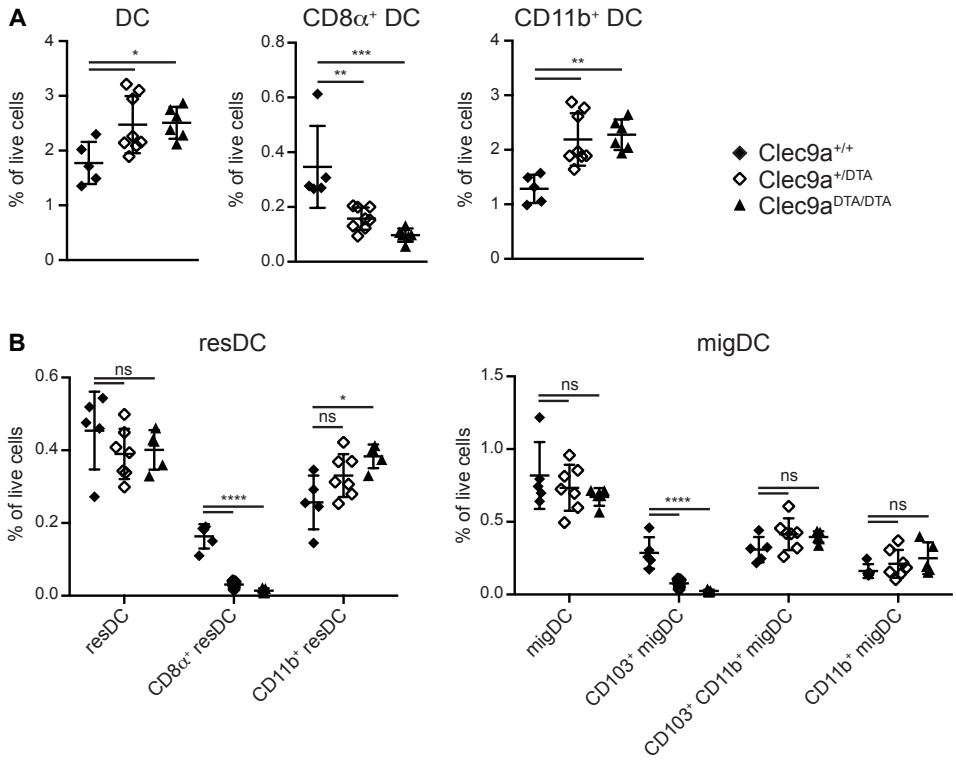

Figure 4.4 Clec9a$^{+/DTA}$ and Clec9a$^{DTA/DTA}$ mice show a reduction in CD8α-like DCs, but have increased frequencies of CD11b^{+} DCs in spleen and mesLNs

(A) Total DCs (CD11c^{+} MHCII$^{+)}$), CD8α^{+} DCs (CD11c^{+} MHCII^{+} CD8α^{+}) and CD11b^{+} DCs (CD11c^{+} MHCII^{+} CD11b^{+}) in spleens of 8-12 week old Clec9a$^{+/+}$, Clec9a$^{+/DTA}$ and Clec9a$^{DTA/DTA}$ mice were identified by flow cytometry and DC subsets as percentage of live leukocytes are plotted. **(B)** Total resDCs (CD11c^{+} MHCII^{int}), CD8α^{+} resDCs (CD11c^{+} MHCII^{int} CD8α^{+}) and CD11b^{+} resDCs (CD11c^{+} MHCII^{int} CD11b^{+}) (left panel), and total migDCs (CD11c^{+} MHCII^{hi}), CD103^{+} migDCs (CD11c^{+} MHCII^{hi} CD11b^{-} CD103^{+}), CD103^{+} CD11b^{+} migDCs (CD11c^{+} MHCII^{hi} CD11b^{+} CD103^{+}) and CD11b^{+} migDCs (CD11c^{+} MHCII^{hi} CD11b^{+} CD103^{-}) (right panel) in mesLNs of 8-12 week old Clec9a$^{+/+}$, Clec9a$^{+/DTA}$ and Clec9a$^{DTA/DTA}$ mice were identified by flow cytometry and DC subsets as percentage of live leukocytes are plotted. A one-way ANOVA with a Tukey's multiple comparisons post-test was performed to calculate p-values. Each dot represents one mouse. Ns: non significant, *: p≤0.05, **: p≤0.01, ***: p≤0.001, ****: p≤0.0001. Data are pooled from at least two independent experiments.

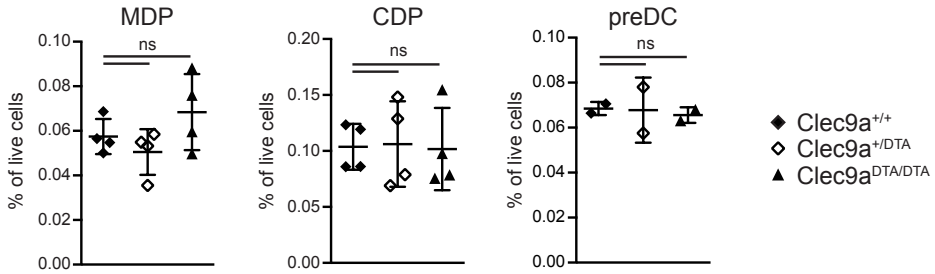

Figure 4.5 MDPs, CDPs and preDCs are unaffected in BM of Clec9a$^{+/DTA}$ and Clec9a$^{DTA/DTA}$ mice

MDPs (lin$^-$ MHCII$^-$ CD11c$^-$ CD115$^+$ CD135$^+$ CD117^{hi}), CDPs (lin$^-$ MHCII$^-$ CD11c$^-$ CD115$^+$ CD135$^+$ CD117^{low}) and preDCs (lin$^-$ MHCII$^-$ CD11c^{low}) in BM of 8-12 week old Clec9a$^{+/+}$, Clec9a$^{+/DTA}$ and Clec9a$^{DTA/DTA}$ mice were identified by flow cytometry and MDPs, CDPs and preDCs as percentage of live leukocytes are plotted. A one-way ANOVA with a Tukey's multiple comparisons post-test was performed to calculate p-values. Each dot represents one mouse. Ns: non significant. Data are from one experiment or pooled from two independent experiments.

To address if Clec9a-DTA mice develop any spontaneous autoimmunity with age, a cohort of Clec9a$^{+/+}$, Clec9a$^{+/DTA}$ and Clec9a$^{DTA/DTA}$ mice (5-10 per group) was aged for a year. However, none of the mice developed any signs of illness or died. In line with these results, one year old Clec9a$^{+/DTA}$ and Clec9a$^{DTA/DTA}$ mice had normal frequencies of CD11b$^+$ DCs in the spleen, while the CD8α$^+$ DC subset was reduced, but not absent (Figure 4.6A). MDP and CDP frequencies in the BM of old Clec9a$^{+/DTA}$ and Clec9a$^{DTA/DTA}$ mice were also similar to controls (Figure 4.6B) and the size of the spleens in Clec9a$^{+/DTA}$ and Clec9a$^{DTA/DTA}$ mice was normal (Figure 4.6C). In sum, Clec9a-DTA mice do not develop any spontaneous illnesses with age and the DC compartment is similar between old and young Clec9a-DTA mice.

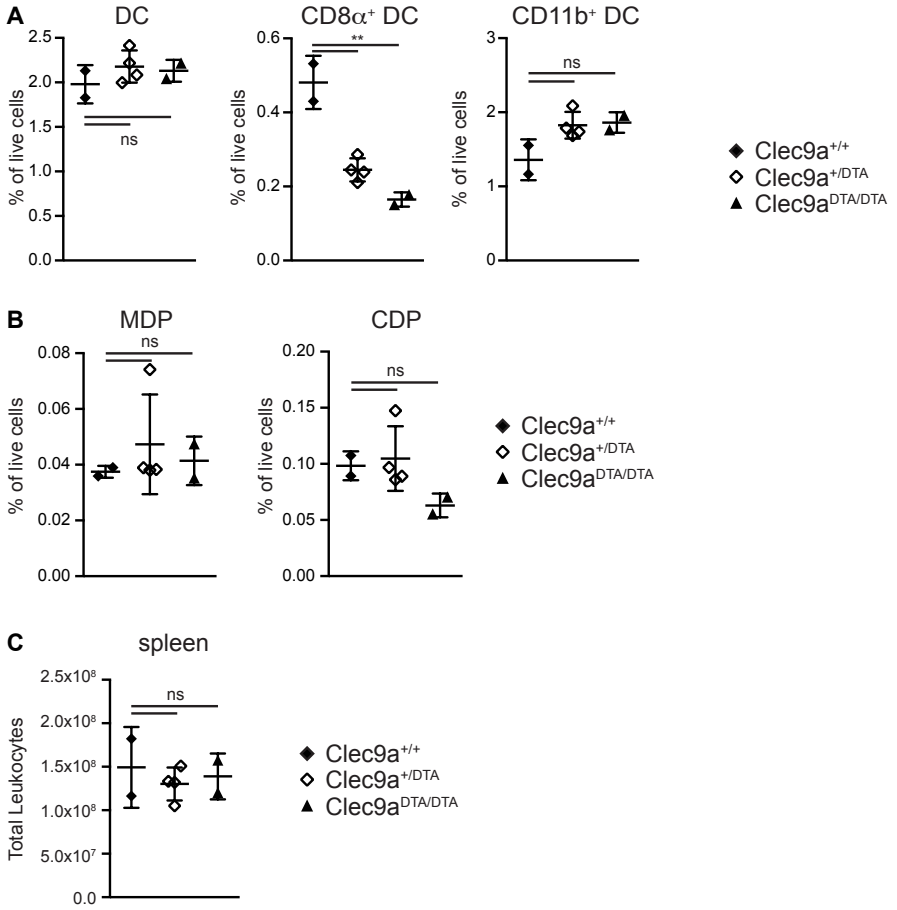

Figure 4.6 Old Clec9a$^{+/DTA}$ and Clec9a$^{DTA/DTA}$ mice show a similar phenotype as young mice

(A) Total DCs (CD11c$^+$ MHCII$^{+)}$), CD8α$^+$ DCs (CD11c$^+$ MHCII$^+$ CD8α$^+$) and CD11b$^+$ DCs (CD11c$^+$ MHCII$^+$ CD11b$^+$) in spleens of one year old Clec9a$^{+/+}$, Clec9a$^{+/DTA}$ and Clec9a$^{DTA/DTA}$ mice were identified by flow cytometry and DC subsets as percentage of live leukocytes are plotted. **(B)** MDPs (lin$^-$ MHCII$^-$ CD11c$^-$ CD115$^+$ CD135$^+$ CD117^{hi}) and CDPs (lin$^-$ MHCII$^-$ CD11c$^-$ CD115$^+$ CD135$^+$ CD117^{low}) in BM of one year old Clec9a$^{+/+}$, Clec9a$^{+/DTA}$ and Clec9a$^{DTA/DTA}$ mice were identified by flow cytometry and MDP and CDP as percentage of live leukocytes are plotted. **(C)** Single-cell suspensions of spleens from one year old Clec9a$^{+/+}$, Clec9a$^{+/DTA}$ and Clec9a$^{DTA/DTA}$ mice were counted and the number of total leukocytes is plotted. Each dot represents one mouse. Ns: non significant, **: p≤0.01. Data are from one experiment.

As CD8α$^+$ DCs in spleen and CD8α$^+$ resDCs and CD103$^+$ migDCs in mesLN express DNGR-1 in a WT mouse and DTA expression is under control of the *Clec9a* locus, DNGR-1 levels were assessed on the surviving CD8α-like DCs in Clec9a$^{+/DTA}$ mice (Clec9a$^{DTA/DTA}$ mice are knock out for DNGR-1, as the *dta* transgene disrupts the *Clec9a* gene). Surprisingly, the remaining CD8α$^+$ DCs in the spleen and CD8α$^+$ resDCs and CD103$^+$ migDCs in mesLNs of Clec9a$^{+/DTA}$ mice still

expressed DNGR-1 protein (Figure 4.7A). Furthermore, the CDP in BM also expressed DNGR-1 protein, while DNGR-1 expression was virtually absent on MDPs, even in Clec9a$^{+/+}$ control mice (Figure 4.7B). The lower expression levels of DNGR-1 in Clec9a$^{+/DTA}$ mice compared with Clec9a$^{+/+}$ control mice were expected, as Clec9a$^{+/DTA}$ mice only harbour one WT *Clec9a* allele, instead of two in Clec9a$^{+/+}$ control mice and a similar pattern was observed in Clec9a$^{+/Cre}$ mice (Schraml et al., 2013).

These results indicate that even though the *Clec9a* locus is actively transcribed and translated from the WT allele in Clec9a$^{+/DTA}$ mice, generating DNGR-1 protein, the transgenic DTA allele is not, as transcription and translation of DTA results in immediate death of the cell.

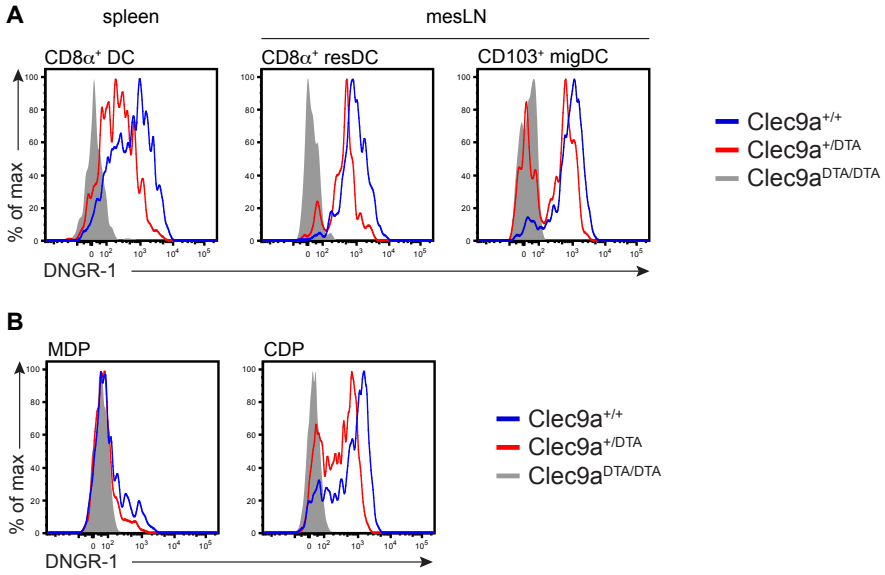

Figure 4.7 Clec9a$^{+/DTA}$ mice still express DNGR-1

(A) CD8α$^+$ DCs (CD11c$^+$ MHCII$^+$ CD8α$^+$) in the spleen and CD8α$^+$ resDCs (CD11c$^+$ MHCII^{int} CD8α$^+$) and CD103$^+$ migDCs (CD11c$^+$ MHCII^{hi} CD11b$^-$ CD103$^+$) in mesLNs from 8-12 week old Clec9a$^{+/+}$, Clec9a$^{+/DTA}$ and Clec9a$^{DTA/DTA}$ mice were stained with an anti-DNGR-1 antibody and analysed by flow cytometry. Data are representative of at least five mice per group. **(B)** MDPs (lin$^-$ MHCII$^-$ CD11c$^-$ CD115$^+$ CD135$^+$ CD117^{hi}) and CDPs (lin$^-$ MHCII$^-$ CD11c$^-$ CD115$^+$ CD135$^+$ CD117^{low}) in BM of 8-12 week old Clec9a$^{+/+}$, Clec9a$^{+/DTA}$ and Clec9a$^{DTA/DTA}$ mice were stained with an anti-DNGR-1 antibody and analysed by flow cytometry. Data are representative of four mice per group.

4.4 Discussion

Dendritic cells are key players in both innate and adaptive immune processes and can exert both immunostimulatory and immunomodulatory effects. So, to which side would the balance shift if DCs were taken out of the equation? On one hand a DC-less immune system could be largely immunodeficient, while on the other hand spontaneous autoimmunity could occur. In an attempt to answer this question, both Ohmnacht et al. (Ohnmacht et al., 2009) and Birnberg et al. (Birnberg et al., 2008) generated a DC-less mouse by crossing CD11c-Cre mice to two different strains of ROSA26-DTA mice. And although the results were mixed in terms of the development of autoimmunity, both groups reported that mice lacking DCs develop a myeloproliferative disorder, uncovering an unanticipated role for DCs in maintaining myeloid cell homeostasis.

Here, Clec9a-DTA mice were generated to re-address the question what influence a constitutive lack of DCs has on the immune system, using a model in which deletion should only affect the DC lineage. The restricted deletion is of importance, as CD11c is not only expressed on DCs, but also on other immune cells such as activated T cells and Ly-6C^{low} monocytes (Jung *et al.*, 2002; Probst, Tschannen, *et al.*, 2005; Hochweller *et al.*, 2008) and therefore these cells are likely to be affected in CD11c-Cre mice crossed to ROSA26-DTA mice. Especially the possible deletion of activated T cells is of importance here, as these cells are likely to play a role in autoimmune disorders. Differential deletion of activated T cells may explain why Ohmnacht et al. (Ohnmacht et al., 2009) observed spontaneous autoimmunity and Birnberg et al. (Birnberg et al., 2008) did not in similar mouse models.
The generation of DTA transgenic mouse lines is risky, as any leakiness of the regulatory elements that control DTA expression will lead to aberrant DTA expression and immediate death of the cell. If this happens at the ES cell stage or early during development, these cells or embryos will die and do not give rise to a transgenic mouse line. This may explain why only one of the two confirmed ES cell clones transmitted to the germline, as aberrant DTA expression may have rendered the chimeras generated from clone 4E5 infertile. Mice generated from clone 2H3 did not show the expected phenotype of a fully DC-less mouse. Instead, only DC subsets that express DNGR-1 as differentiated cells were reduced, while DNGR-1

negative DC subsets were unaffected, along with the CDP and preDC in the BM. Intriguingly, the surviving CD8α-like DCs in Clec9a$^{+/DTA}$ mice still expressed DNGR-1 protein on the cell surface and CDPs also clearly stained positive for DNGR-1 by flow cytometry.

An initial explanation for the observed phenotype of Clec9a-DTA mice could be that the *dta* gene is not functional in these mice. However, sequencing did not show any mutations in the gene itself or in the proximal promoter. In addition, Southern blot analysis confirmed correct integration in the genome. Moreover, CD8α-like DCs are reduced in Clec9a-DTA mice, indicating that DTA exerts some effects on the DC compartment in these mice. As any leakiness of the DTA construct will lead to immediate cell death, the whole process of generating Clec9a-DTA mice may have resulted in the selection of a hypomorph ES cell clone, giving rise to mice with reduced DTA expression. This event should occur either by epigenetic modifications of the locus, or by mutations in locus control regions outside of the proximal promoter that was sequenced. This hypothesis may explain why residual CD8α-like DCs still expressed DNGR-1 in Clec9a$^{+/DTA}$ mice, as the WT allele is unlikely to have been selected for an altered expression pattern. Furthermore, this hypothesis may also clarify why CDP and preDC frequencies were not affected, while CD8α-like DCs were reduced, as the *Clec9a* locus is likely to be regulated differently in DC precursors compared with differentiated CD8α-like DCs and (epi)genetic modifications of the *Clec9a-dta* allele may affect precursors and differentiated DCs differently.

As Clec9a-DTA mice still harbour plenty of DCs, they are not useful to address the original research proposal of studying a DC-less immune system. Furthermore, although CD8α-like DCs are reduced in both Clec9a$^{+/DTA}$ and Clec9a$^{DTA/DTA}$ mice, they are not completely absent. This feature renders this mouse strain not useful to study the immune system in the absence of CD8α-like DCs and use them as an alternative for Batf3$^{-/-}$ mice.

In summary, Clec9a-DTA mice were successfully generated, but did not show the intended phenotype of a DC-less mouse. These mice are therefore unlikely to be useful for future experiments.

Chapter 5. Fate Mapping of Single Dendritic Cell Precursors in the Small Intestine

5.1 Introduction

At a population level the progeny of CDPs and preDCs can be traced either by performing adoptive transfer studies, or by using lineage tracer mice. Both CDPs and preDCs express DNGR-1 and therefore mice expressing Cre recombinase under the control of the *Clec9a* locus can be used to trace the cDC lineage *in vivo*, when crossed to a fluorescent reporter line (Schraml et al., 2013). Both in adoptive transfer studies and in lineage tracer mice, DC precursor output is investigated at the population level and does not take into account cell-to-cell variations. Therefore, it is currently not known what is the clonal burst size of individual preDCs upon arrival in tissues, and if this changes under inflammatory conditions.
Assessment of the behaviour of single precursors has been complicated by their scarceness and lack of unique markers. Here, a novel system is proposed to study how individual DC precursors seed peripheral tissues, both in steady state and during inflammation. To trace DC precursor progeny, the multicolour fluorescent reporter line ROSA26-confetti was used (Snippert et al., 2010). As shown in Figure 5.1, ROSA26-confetti mice contain a strong promoter that allows for constitutive and ubiquitous gene expression, a loxP-flanked neomycin cassette that acts as STOP cassette preventing expression of downstream genes and the Brainbow-2.1 cassette that contains genes encoding nuclear GFP, cytoplasmic YFP, cytoplasmic RFP and membrane-bound CFP (Livet *et al.*, 2007; Snippert *et al.*, 2010). Expression of Cre results in the stochastic recombination of loxP sites, which will either remove the floxed region when the loxP sites are oriented in the same direction, or induces inversion of the region when the loxP sites are oriented in opposite directions. The outcome of Cre-mediated recombination of the ROSA26-confetti locus is the stochastic and heritable expression of one of the four fluorescent proteins. When Clec9a-Cre mice are crossed with ROSA26-confetti mice, Cre recombinase activity at the CDP and preDC stage is predicted to stochastically label these precursors with one of the four fluorescent proteins (Snippert *et al.*, 2010; Schraml *et al.*, 2013). The offspring of these precursors can

then be visualised in tissues by confocal microscopy. Ideally, this labelling should be done using temporal control of Cre activity, so that DC precursors are 'pulse-labelled', and their offspring can be 'chased' in the tissues. To achieve temporal control over precursor labelling, mice were generated that express an inducible form of Cre (CreERT2) under control of the *Clec9a* locus. In this chapter, the generation of such mice is reported, as well as the failure to use them to inducibly label DCs when crossed to fluorescent reporter mice. The remainder of the chapter therefore reports on the alternative strategy of using Clec9a-Cre mice crossed to ROSA26-confetti mice for DC fate mapping studies.

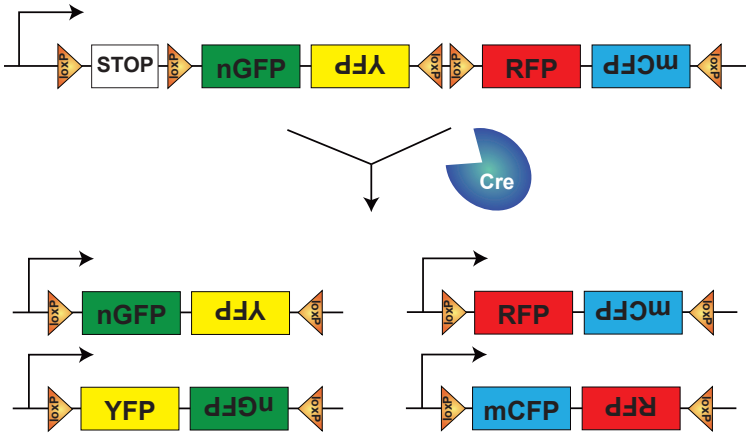

Figure 5.1 Schematic representation of ROSA26-confetti mice

Schematic overview of the ROSA26-confetti locus. LoxP sites in forward or reverse orientation, the Neo-containing STOP cassette and the genes encoding nuclear GFP (nGFP), cytoplasmic YFP (YFP), cytoplasmic RFP (RFP) and membrane-bound CFP (mCFP) are shown. A flipped font indicates that the gene is oriented in the opposite direction and will not be transcribed.

5.2 Generation of Clec9a-CreERT2 mice to allow for temporal control over Cre recombination

Clec9a-Cre mice have proven useful to trace the DC lineage, as Cre recombinase is expressed in CDPs and preDCs in these mice, in addition to pDCs and CD8α-like DCs (Schraml et al., 2013). However, in these mice the Cre recombinase is always active and continuously labels DC precursors. To trace the fate of single precursors, an inducible Cre system that allows for temporal control over DC

precursor labelling would be ideal. CreERT2 is a fusion protein of mutated hormone-binding domains of the oestrogen receptor and Cre, and is only functional when bound to 4OH-tamoxifen. Clec9a-CreERT2 mice were generated in a similar way to Clec9a-DTA (see Chapter 4) and to Clec9a-Cre mice (Schraml et al., 2013) by using the pFloxRI-C9a-EGFP vector that was originally used to generate Clec9a-GFP mice (Sancho et al., 2009). The *egfp* gene was replaced by the gene encoding CreERT2, generating the pFloxRI-C9a-CreERT2 targeting vector. This vector was used to replace exons one and two of the endogenous *Clec9a* locus with the gene encoding CreERT2 and a floxed Neo cassette, as depicted in Figure 5.2.

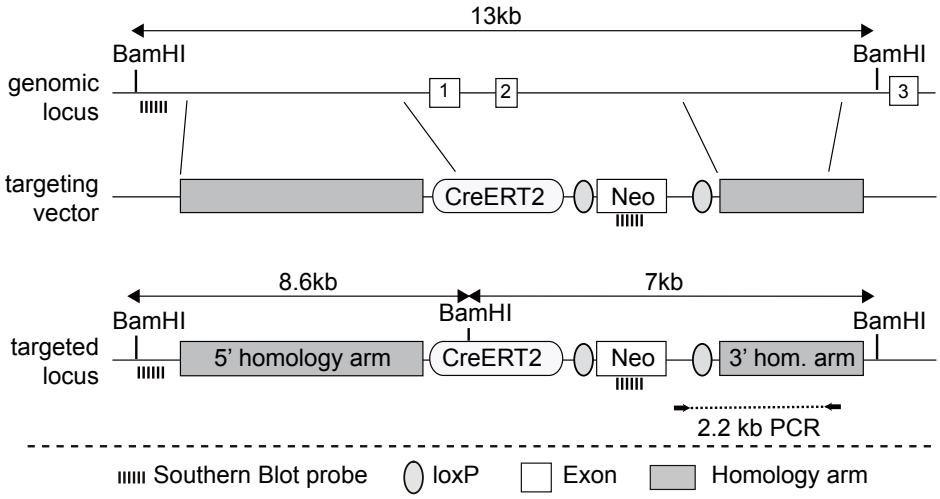

Figure 5.2 Targeting strategy to generate Clec9a-CreERT2 mice

The endogenous genomic *Clec9a* locus is shown at the top, with the targeting vector to generate Clec9a-CreERT2 mice below. The targeted allele is also depicted (bottom). The PCR product (2.2kb) to screen correctly targeted ES cells is shown. BamHI restriction enzyme target sites, the locations of the Neo probe and 5' probe and the size of the fragments detected by Southern blot screening are shown.

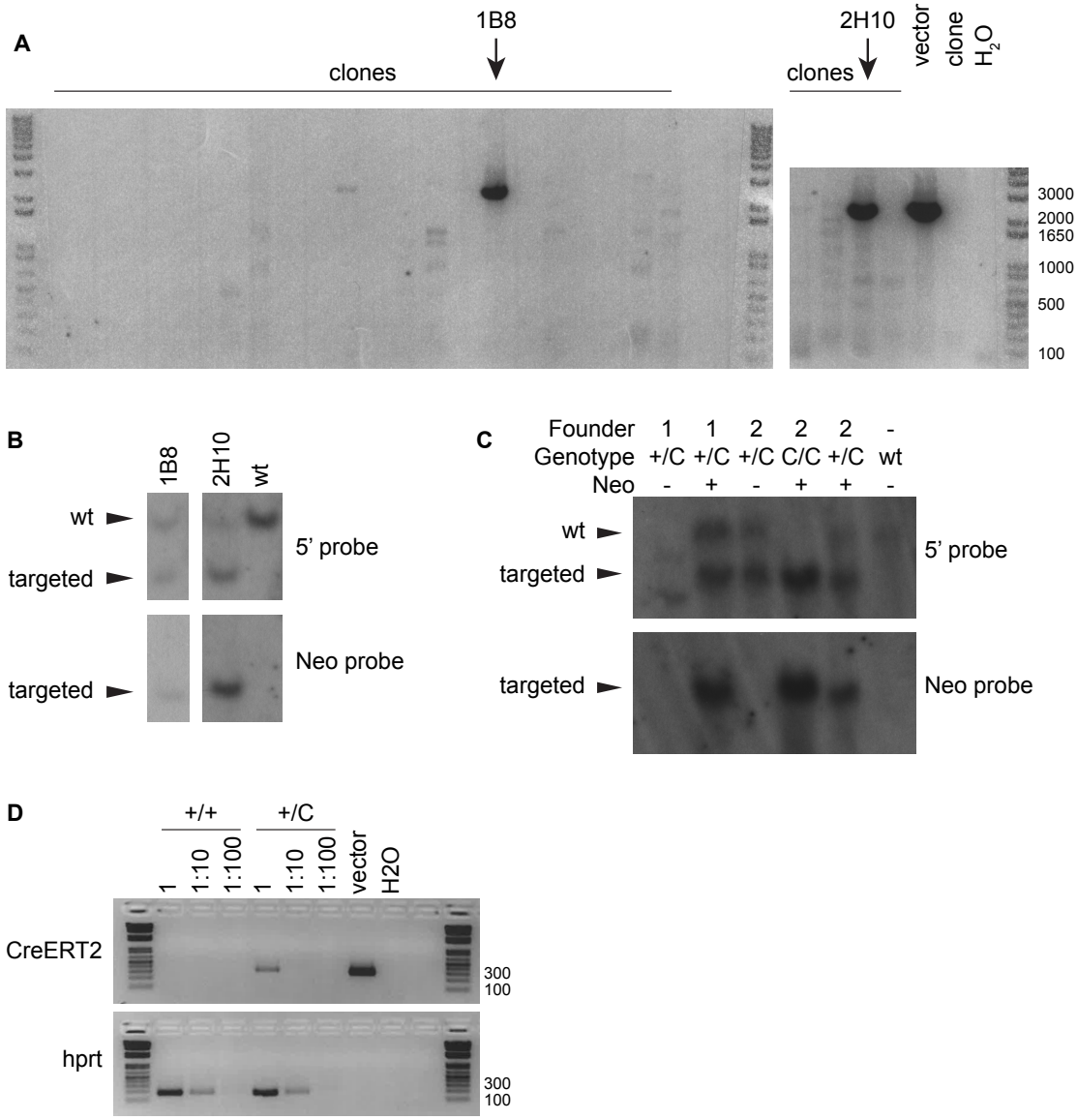

Figure 5.3 Generation of Clec9a-CreERT2 mice

(A) ES cell clones were screened by a PCR that spans the 3' homology arm and results in a 2.2kb PCR product if the clone is correctly targeted (see Figure 5.2). 384 clones were screened, from which examples are shown here. The arrows denote clones 1B8 and 2H10. The targeting vector to generate the mice was used as positive control (vector) and a no-DNA sample (H_2O) was used as negative control. The size of the ladder fragments is denoted on the right in kb. **(B)** ES cell clones positive by PCR were screened by Southern blot via digestion with BamHI and detection with neo and 5' probes (see Figure 5.2). Southern blots of two clones (clones 1B8 and 2H10) are shown. **(C)** Genomic DNA from two founder Clec9a-CreERT2 mice was screened by Southern blot as in (B). Mice originating from ES cell clone 1B8 are denoted as '1' and mice originating from ES cell clone 2H10 as '2' Genotype are homozygous (C/C), heterozygous (+/C) and WT (wt) Clec9a-CreERT2 mice. In some mice the Neo cassette was crossed out. **(D)** A semi-quantitative RT-PCR was performed to assess CreERT2 mRNA levels on Flt3l BM-

derived DCs from Clec9a$^{+/+}$ (+/+) and Clec9a$^{+/CreERT2}$ 2H10 mice (+/C). cDNA was used undiluted or diluted 10 or 100 times before the PCR reaction was performed with primers for *creert2* or *hprt* as control. The targeting vector was used as a positive control. The size of the ladder fragments is denoted on the right in kb. All experiments were performed once.

C57BL/6-derived ES cells were transfected with the linearized pFloxRI-C9a-CreERT2 targeting vector and selected for neomycin resistance. A total of 384 clones were initially screened by PCR for correct targeting and clones positive by PCR were additionally subjected to Southern blot analyses (Figure 5.3AB). Out of the 384 clones initially screened, six were correctly targeted and two of these, clones 1B8 and 2H10, were used to generate chimeric mice (Figure 5.3AB). Both clones transmitted to the germline and colonies of Clec9a-CreERT2 1B8 and Clec9a-CreERT2 2H10 mice were established. The floxed Neo cassette was removed by crossing these mice to PGK-Cre mice (Lallemand et al., 1998). To reconfirm correct targeting and removal of the Neo cassette, Southern blot analysis was performed on genomic DNA from Clec9a-CreERT2 1B8 and Clec9a-CreERT2 2H10 mice that either retained the Neo cassette or had the Neo cassette crossed out. As shown in Figure 5.3C, all mice tested showed correct targeting and predicted presence or absence of the Neo cassette. The *Creert2* gene and proximal promoter were also sequenced from genomic DNA of a heterozygous Clec9a-CreERT2 2H10 mouse to confirm the absence of mutations. As a final validation step, *Creert2* mRNA levels were measured via semi-quantitative PCR in Flt3l BMDCs. Indeed, *Creert2* mRNA was detected in BMDCs from heterozygous Clec9a-CreERT2 2H10 mice, but not in control BMDCs (Figure 5.3D).

In summary, two different Clec9a-CreERT2 founder lines, 1B8 and 2H10, were successfully generated. Correct targeting was confirmed by Southern blot and *Creert2* mRNA could be detected in Flt3l BM-derived DCs from Clec9a-CreERT2 2H10 mice.

5.3 Characterisation of Clec9a-CreERT2 mice

Both Clec9a-CreERT2 1B8 and Clec9a-CreERT2 2H10 mice were initially crossed to the ROSA26-YFP reporter line (Srinivas et al., 2001) to assess the efficiency of tamoxifen-induced CreERT2 activity. In a first experiment Clec9a$^{+/CreERT2\ 1B8}$ROSA$^{+/YFP}$ and Clec9a$^{+/CreERT2\ 2H10}$ROSA$^{+/YFP}$ mice were fed a tamoxifen-containing diet for six days. A ROSA26-CreERT2 mouse (that expresses CreERT2 in all cells) (Ventura et al., 2007) crossed to the ROSA26-YFP reporter line (Srinivas et al., 2001) was included as a positive control. Unfortunately, the tamoxifen-containing diet proved to be very inefficient in inducing Cre-mediated recombination, even in the ROSA$^{CreERT2/YFP}$ mice (Figure 5.4A). Similarly, oral gavage of tamoxifen failed to induce any YFP labelling in ROSA$^{CreERT2/YFP}$ mice (Figure 5.4B). The absence of YFP expression in splenic DCs from Clec9a$^{+/CreERT2\ 1B8}$ROSA$^{+/YFP}$ and Clec9a$^{+/CreERT2\ 2H10}$ROSA$^{+/YFP}$ mice in these experiments was therefore not interpretable (Figure 5.4).

ROSA26-based fluorescent reporter lines differ in the efficiency of reporter expression, even when crossed to the same Cre driver (J. Liu et al., 2013). It has been shown that ROSA26-mTmG mice, which express membrane-bound Tomato before recombination and membrane-bound GFP after recombination, and ROSA26-dTomato mice are much more efficient in recombining the loxP sites than ROSA26-YFP mice (Srinivas *et al.*, 2001; Muzumdar *et al.*, 2007; Madisen *et al.*, 2010; J. Liu *et al.*, 2013). Clec9a-CreERT2 1B8 and Clec9a-CreERT2 2H10 were therefore crossed to ROSA26-mTmG mice and to ROSA26-dTomato mice. These mice, along with ROSA$^{CreERT2/mTmG}$ mice as positive control, were injected i.p. with tamoxifen to induce recombination. Even though tamoxifen injection induced robust GFP expression in splenic DCs of ROSA$^{CreERT2/mTmG}$ mice, this treatment regime did not induce any recombination in Clec9a-CreERT2 1B8 and Clec9a-CreERT2 2H10 mice crossed to either ROSA26-mTmG mice or ROSA26-dTomato mice (Figure 5.5A). Subcutaneous injection of tamoxifen into Clec9a$^{+/CreERT2\ 1B8}$ROSA$^{+/mTmG}$ mice also failed to induce recombination, despite the fact that the same treatment induced robust GFP expression in ROSA$^{CreERT2/mTmG}$ mice (Figure 5.5B).

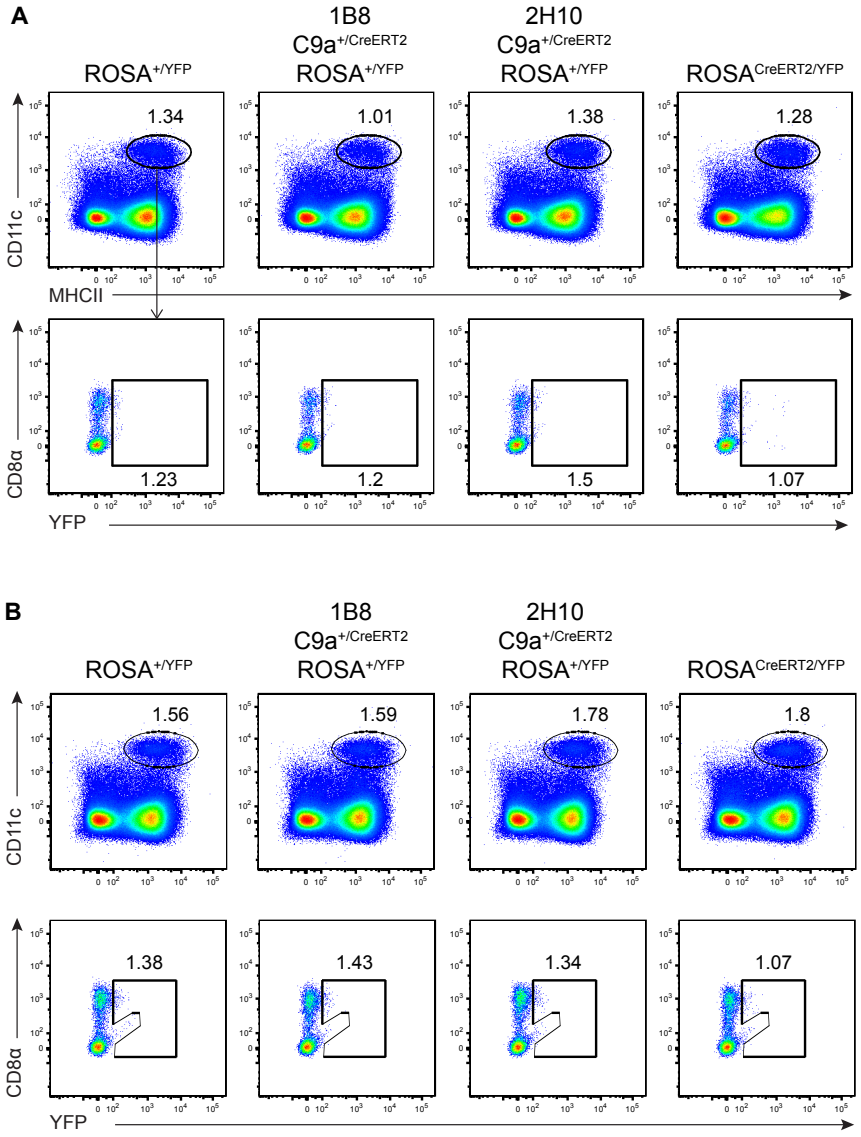

Figure 5.4 Tamoxifen-containing diet or oral gavage of tamoxifen does not induce labelling of DCs in the spleen of Clec9a$^{+/CreERT2}$ROSA$^{+/YFP}$ mice

(A) Mice were fed a tamoxifen-containing diet (TAM400) for six days. Spleens were analysed on day 6. Total DCs were identified as live, autofluorescent-negative CD11c^{+} MHCII^{+} cells and YFP expression was assessed in this population. **(B)** Mice were gavaged with 4mg tamoxifen for four days and analysed four days after the last gavage. Total DCs were identified as live, autofluorescent-negative CD11c^{+} MHCII^{+} cells and YFP expression was assessed in this population. These experiments were performed once with one mouse per group. 1B8 and 2H10 denote the different founder lines.

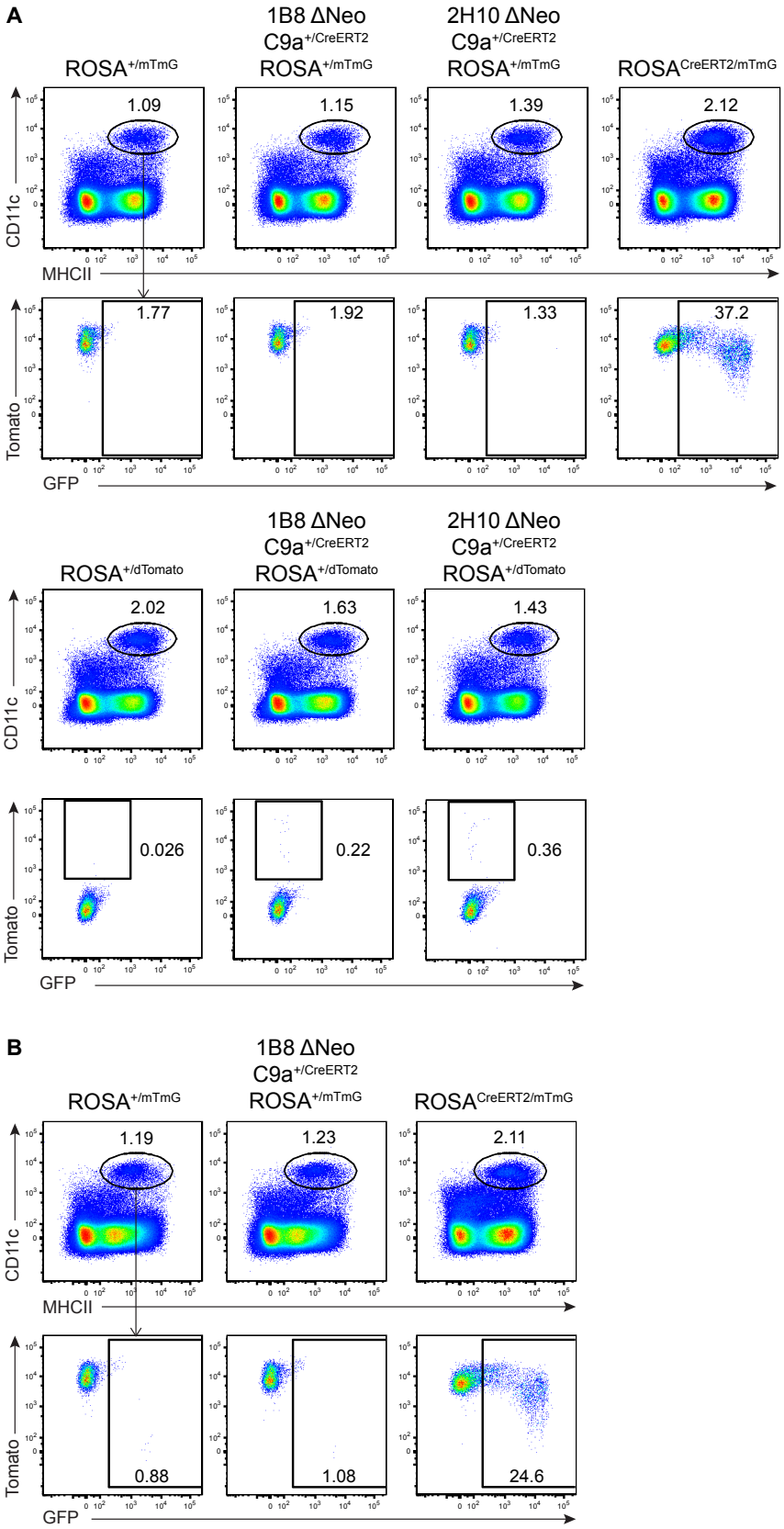
A
ROSA+/mTmG
1B8 ΔNeo C9a+/CreERT2 ROSA+/mTmG
2H10 ΔNeo C9a+/CreERT2 ROSA+/mTmG
ROSACreERT2/mTmG
1.09
1.15
1.39
2.12
CD11c
MHCII
1.77
1.92
1.33
37.2
Tomato
GFP
ROSA+/dTomato
1B8 ΔNeo C9a+/CreERT2 ROSA+/dTomato
2H10 ΔNeo C9a+/CreERT2 ROSA+/dTomato
2.02
1.63
1.43
CD11c
0.026
0.22
0.36
Tomato
GFP
B
ROSA+/mTmG
1B8 ΔNeo C9a+/CreERT2 ROSA+/mTmG
ROSACreERT2/mTmG
1.19
1.23
2.11
CD11c
MHCII
0.88
1.08
24.6
Tomato
GFP

Figure 5.5 I.p. or s.c. injection of tamoxifen does not induce labelling of DCs in the spleen of Clec9a$^{+/CreERT2}$ROSA$^{+/mTmG}$ mice

(A) Mice were injected i.p. on five consecutive days with 100µg tamoxifen per g body weight and analysed on day 6. Total DCs were identified as live, autofluorescent-negative CD11c^{+} MHCII^{+} cells and GFP (for ROSA26-mTmG crosses) or Tomato (for ROSA26-dTomato crosses) expression was assessed in this population. This experiment was performed twice with one mouse per group for ROSA26-mTmG crosses, once for ROSA26-dTomato crosses and once with Clec9a$^{+/CreERT2\ 1B8}$ROSA$^{+/YFP}$ and Clec9a$^{+/CreERT2\ 2H10}$ROSA$^{+/YFP}$ mice that still harboured the Neo cassette, with similar outcomes. **(B)** Mice were injected s.c. with 8mg tamoxifen on day 1, 3 and 5 and analysed on day 6. Total DCs were identified as live, autofluorescent-negative CD11c^{+} MHCII^{+} cells and GFP expression was assessed in this population. This experiment was performed once with one mouse per group. 1B8 and 2H10 denote the different founder lines and ΔNeo refers to a crossed-out Neo cassette

As tamoxifen is a prodrug that needs to be metabolised in the liver and *in vivo* administration might lead to poor bioavailability, CreERT2 activity was next tested in an *in vitro* setting. To this end Flt3l BM-derived DCs were generated from Clec9a$^{+/CreERT2\ 1B8}$ROSA$^{+/mTmG}$ and Clec9a$^{+/CreERT2\ 2H10}$ROSA$^{+/mTmG}$ mice in the presence of 4OH-tamoxifen. This setup generated a high degree of recombination in control Flt3l BMDC cultures generated from ROSA$^{CreERT2/mTmG}$ mice. However, no GFP expression was observed in Clec9a$^{+/CreERT2\ 1B8}$ROSA$^{+/mTmG}$ and Clec9a$^{+/CreERT2\ 2H10}$ROSA$^{+/mTmG}$ cultures, despite the fact that these cells express mRNA for *Creert2* (Figure 5.3D, Figure 5.6).

In sum, even though two Clec9a-CreERT2 founder lines were successfully generated, neither of them showed any sign of recombinase activity when crossed to various reporter lines, when tamoxifen was administered via oral or parental routes *in vivo*, or when Flt3l BMDC cultures were treated with 4OH-tamoxifen. Therefore, regrettably and for reasons that are unclear, the conclusion can only be that the Clec9a-CreERT2 1B8 and Clec9a-CreERT2 2H10 mice do not permit induction of Cre activity and labelling of DCs.

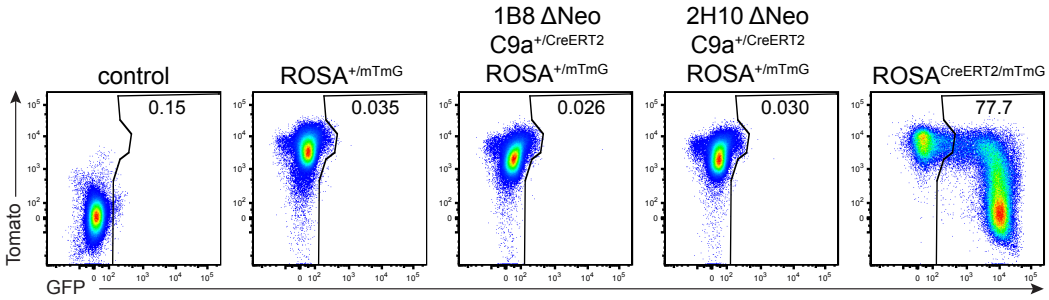

Figure 5.6 Treatment of Flt3l BMDC cultures from Clec9a$^{+/CreERT2}$ROSA$^{+/mTmG}$ BM with 4OH-tamoxifen does not induce labelling of DCs

Flt3l BMDCs were generated, 1µM 4OH-tamoxifen was added to the cultures on day 0 and the *in vitro* cultures were analysed on day 9. GFP expression was assessed in total live cells. This experiment was performed twice with BM cultures from one mouse per group. The same experiment was performed twice with Flt3l BMDCs generated from Clec9a$^{+/CreERT2\ 2H10}$ROSA$^{+/YFP}$ mice (with Neo) and once with Flt3l BMDCs generated from Clec9a$^{+/CreERT2\ 1B8}$ROSA$^{+/YFP}$ mice (with Neo), with similar outcomes. 1B8 and 2H10 denote the different founder lines and ΔNeo refers to a crossed-out Neo cassette

5.4 Histo-cytometric analysis of DC precursor fate in the small intestine using Clec9a$^{+/Cre}$ROSA$^{+/confetti}$ mice

As Clec9a-CreERT2 mice proved not to allow for DC labelling, analyses of how individual preDCs seed tissues and if preDC behaviour changes under inflammatory conditions were performed with Cleca9-Cre mice (Schraml et al., 2013). These mice were crossed to ROSA26-confetti mice, so that DC precursors were stochastically labelled with one of four fluorescent proteins: nuclear GFP, cytoplasmic YFP, cytoplasmic RFP or membrane-bound CFP (Snippert et al., 2010). All mice used here harboured one copy of *Cre* and one copy of the confetti locus and are called Clec9a$^{+/Cre}$ROSA$^{+/confetti}$ mice throughout.

Clec9a$^{+/Cre}$ROSA$^{+/confetti}$ mice were used to address the kinetics and dynamics of tissue seeding by DCs. Specifically, to test whether preDCs arrive in tissues and directly differentiate into a DC without prior division, or divide locally before differentiating into one or multiple DC subsets. In the former situation the pattern of DC labelling would be random, while in the latter situation the labelled DCs would form clusters of one colour. Therefore, a microscopy-based approach was developed in collaboration with Ronald Germain and Michael Gerner to analyse DC

precursor fate. The small intestine was chosen for the initial analysis, as its mononuclear phagocytes are well characterised and the villus-crypt structure imposes spatial restrictions to motile DCs, facilitating analysis. To this end, small intestines of Clec9a$^{+/Cre}$ROSA$^{+/confetti}$ mice were frozen according to the PLP protocol before sectioning (Bajénoff, Granjeaud and Guerder, 2003; Gerner et al., 2012). Tissue sections were rehydrated and analysed by confocal microscopy. As the emission spectra of CFP, GFP and YFP show considerable overlap, lambda mode scanning and subsequent unmixing were used to faithfully detect all confetti colours, using the 458nm, 514nm and 561nm lasers to excite the four fluorescent proteins (see Figure 5.7 for emission spectra and microscope setup). As shown in Figure 5.8 the PLP protocol worked well for preserving fluorescence and the lambda mode scanning and unmixing faithfully separated the four fluorescent proteins. The image of the small intestine in Figure 5.8A shows that the tissue autofluorescence can be used to identify the villi and that there are many confetti-labelled cells in isolated lymphoid follicles and mesLNs (Figure 5.8AB).

Even though the ROSA26-confetti locus is constructed in such a way that only one fluorescent protein can be transcribed at a time ((Snippert et al., 2010) and Figure 5.1), and the mice analysed here only had one copy of the ROSA26-confetti locus, cells double-positive for CFP and RFP could be identified in both the small intestine as well as the mesLNs (Figure 5.8AB). The most likely explanation for this phenomenon is that these cells continuously express Cre recombinase and therefore constantly ‘flip’ the CFP-RFP cassette of the confetti construct, as shown on the bottom right of Figure 5.1. Fluorescent proteins have a half-life of around one day and therefore cells that express Cre can accumulate both RFP and CFP protein, despite only transcribing and translating one of them at any given time. Interestingly, only CFP-RFP double-positive cells and not GFP-YFP cells were observed. This discrepancy probably reflects a preference of the GFP-YFP cassette for YFP, as was also reported in the original paper describing the ROSA26-confetti mice (Snippert et al., 2010). As Cre expression is regulated by the *clec9a* locus, it is expected that these CFP-RFP double-positive cells are the DNGR-1-expressing CD8α-like DCs, although this hypothesis remains to be tested.

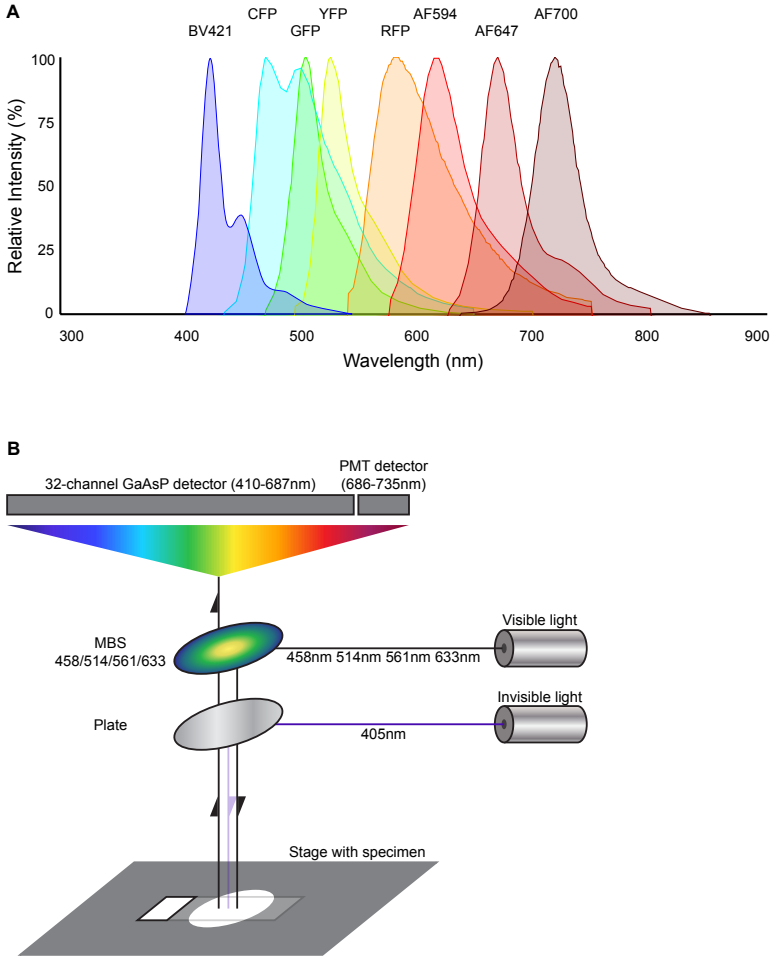

Figure 5.7 Overview of fluorophores and microscope setup

(A) Representation of the emission spectra of the fluorophores used in the analysis of Clec9a$^{+/Cre}$ROSA$^{+/confetti}$ mice by histo-cytometry. In some experiments APC was used instead of AF647 (which have similar emission spectra). **(B)** Schematic overview of the setup of the Zeiss LSM880 Invert confocal microscope for lambda mode scanning (32-channel GaAsP detector) with an additional PMT detector to acquire 686-735nm emission.

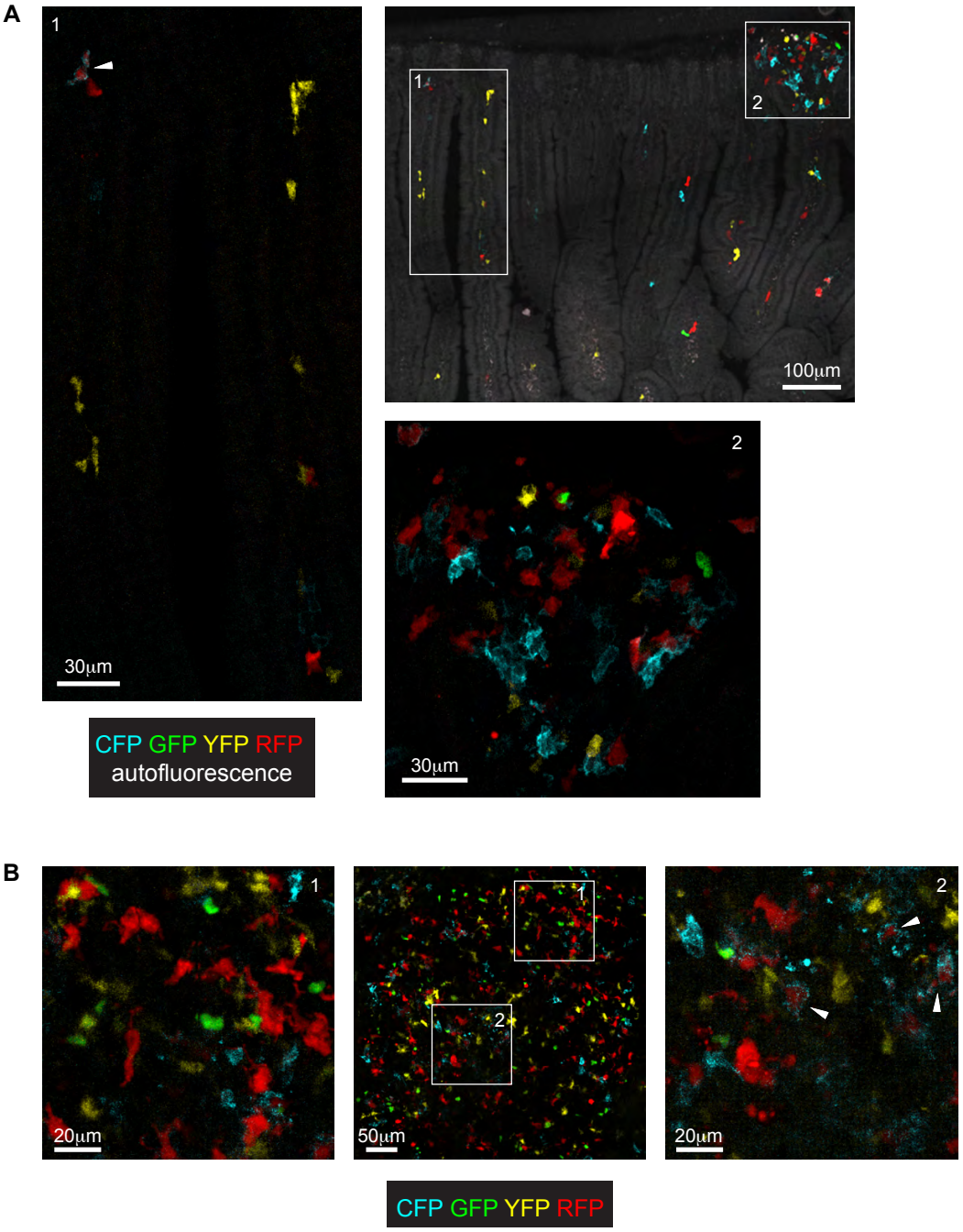

Figure 5.8 Visualisation of confetti colours in small intestine and mesLN of Clec9a$^{+/Cre}$ROSA$^{+/confetti}$ mice

30μm frozen sections of small intestine (A) and mesLN (B) of Clec9a$^{+/Cre}$ROSA$^{+/confetti}$ mice were rehydrated and analysed by microscopy using lambda mode scanning and unmixing. **(A)** Labelled cells in villi (insert 1) and isolated lymphoid follicle (insert 2) are shown. In the overview image autofluorescence of the tissue shows the villi. **(B)** The T cell zone of the mesLN is shown. Arrowheads in insert 2 identify cells that express both RFP and CFP.

As shown in Figure 5.8A, the tissues autofluorescence can give and idea of tissue organisation, but this signal is often faint and unreliable to be useful for quantification. So, ideally tissue sections should be stained with a marker identifying villi and crypts before analysis by microscopy. Additionally, further analysis of the confetti-positive cells would be greatly aided by an extra marker for DCs. To incorporate two antibody stains, the lambda mode scanning and unmixing protocol was expanded so that antibodies coupled to the fluorophores AF594 and AF647 or APC could be used to stain the confetti sections (Figure 5.7 for emission spectra). The 458/514/561nm lasers were still used to excite the confetti fluorophores. The 561nm laser additionally excited AF594, while the 633nm laser excited AF647. An antibody against E-cadherin (CD324) coupled to AF594 was delineated the villi and crypts and one against MHCII coupled to AF647 helped identifying confetti-positive DCs. As shown in Figure 5.9, this configuration allowed for the separation of all six fluorophores. As anticipated, the E-cadherin stain greatly aided the identification of villi and crypts and the MHCII stain mainly stained cells in the lamina propria. These $MHCII^{+}$ cells are DCs, but also other myeloid cells and B cells.

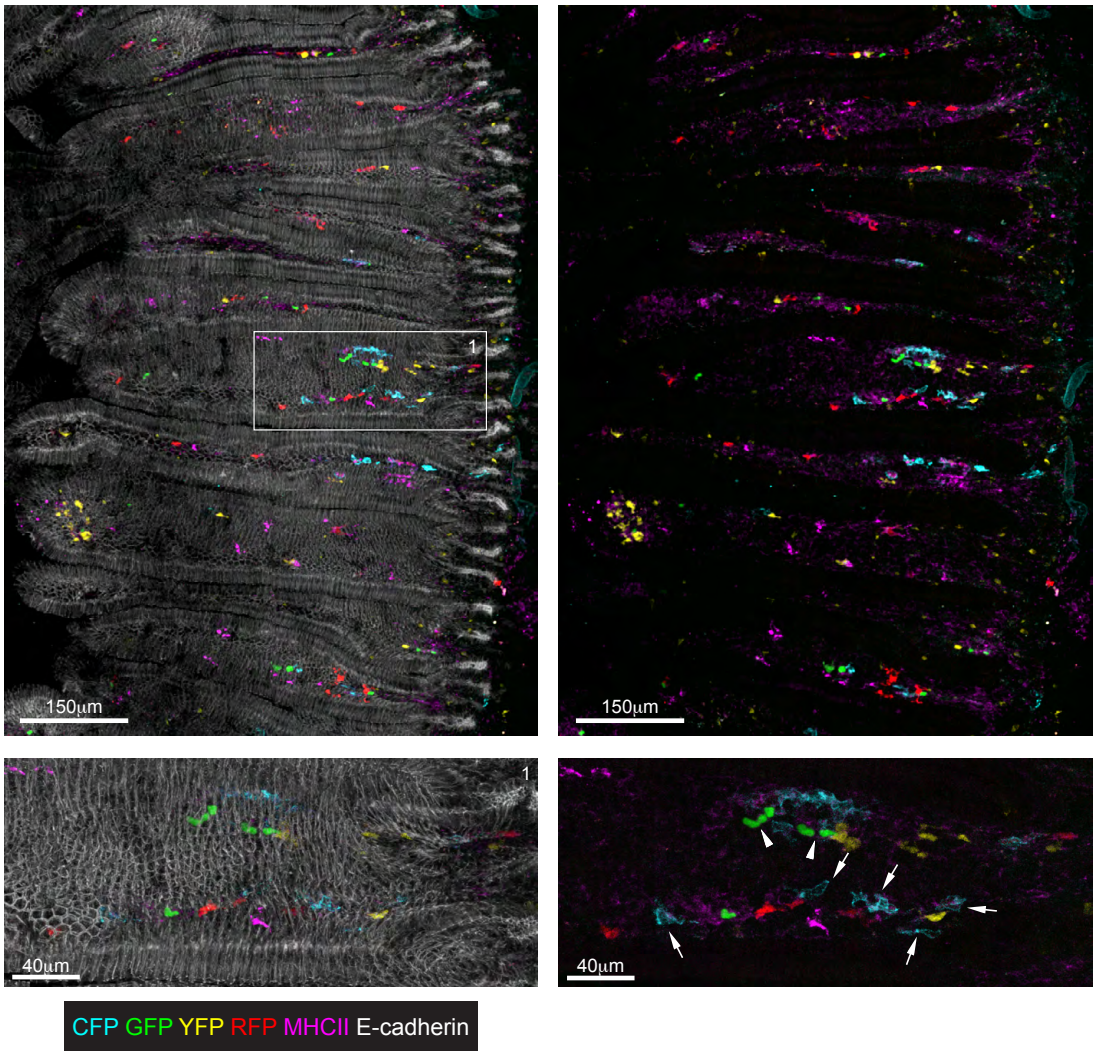

Figure 5.9 Analysis of small intestinal sections of Clec9a$^{+/Cre}$ROSA$^{+/confetti}$ mice for confetti colours, MHCII and E-cadherin

A 100μm frozen section of small intestine of Clec9a$^{+/Cre}$ROSA$^{+/confetti}$ mice was stained with antibodies against MHCII and E-cadherin, coupled to AF647 and AF594 respectively, and analysed by microscopy using lambda mode scanning and unmixing. In the insert arrows denote CFP-positive cells and arrowheads GFP-positive cells in a single villus.

Although the six-fluorophore panel used in Figure 5.9 was sufficient to identify MHCII^{+} confetti cells and the villus-crypt structure of the tissue, this panel was insufficient to identify different DC subsets within the confetti-positive population. This distinction is important to address if one DC precursor can give rise to only one or multiple DC subsets in the tissue. To identify DC subsets in the small intestine by flow cytometry, a combination of CD11c, MHCII, CD64, CD11b and

CD103 (or CD24) is normally used, with DCs being CD11c^{+} MHCII^{+} and CD64^{-}, and CD11b and CD103 (or CD24) identifying the three different DC subsets in the intestine (Figure 2.2). However, it is not feasible to perform confocal microscopy on five markers to identify DCs on top of four confetti colours and a structural marker. Therefore, it was decided to only use MHCII to help identifying confetti-positive DCs and find two markers that could be used for microscopy to identify the DC subsets in the intestine. The first obvious choice was to use CD11b and CD103 to stain DC subsets in tissues. Although an antibody against CD11b worked nicely for microscopy, antibodies against CD103 failed to show any staining (data not shown). Antibodies against CD24 and DNGR-1 also did not work (data not shown), but an antibody against the transcription factor IRF8 looked promising. Within the DC population, IRF8 expression was confirmed to be restricted to CD103^{+} CD11b^{-} DCs in the small intestine by flow cytometry (Figure 5.10A). A MHCII^{-} CD11c^{-} CD11b^{+} population also expresses IRF8 and these cells are likely to be eosinophils based on their scatter profile (data not shown). Nonetheless, within the DC population IRF8 and CD11b expression clearly separated CD103^{+} CD11b^{-} DCs from CD103^{+} CD11b^{+} DCs and CD103^{-} CD11b^{+} DCs (Figure 5.10A). Unfortunately, IRF8 and CD11b expression could not separate CD103^{+} CD11b^{+} DCs from CD103^{-} CD11b^{+} DCs, but at least CD8α-like and CD11b^{+} DCs could be identified via IRF8 and CD11b expression. Indeed, analysis of intestinal sections of Clec9a$^{+/Cre}$ROSA$^{+/confetti}$ mice stained with CD11b, IRF8 and MHCII revealed that confetti-positive cells could be found that were either positive for IRF8 or for CD11b (Figure 5.10B). So, staining for IRF8 and CD11b can identify CD8α-like and CD11b^{+} DCs in the intestine by microscopy.

For microscopy antibodies against IRF8 and CD11b coupled to AF594 or APC were used, which meant that antibodies against MHCII and a structural marker had to be conjugated to different fluorophores than in Figure 5.9. MHCII could be detected with an antibody coupled to AF700, when excited by the 633nm laser. However, the 32-channel GaAsP detector had a limit of detection of 687nm, which meant that AF700 emission could not be detected with the standard lambda mode setup. To solve this problem, a second, conventional channel was added that detected emitted light of 686-735nm and could therefore pick up the AF700 emission (see Figure 5.7 for emission spectra and microscope setup). This channel

was incorporated in the unmixing as a 33rd channel, in addition to the 32 channels from the GaAsP detector. To visualise the villus-crypt structure, an antibody against EpCAM was used instead of E-cadherin, as this antibody worked very well when coupled to BV421 and nicely stained the intestinal epithelium. BV421 was excited with the 405nm laser and detected via lambda mode scanning. However, when the 405nm dichroic was used, the laser power reaching the sample was too strong, leading to increased autofluorescence and imbalance between BV421 and CFP. Therefore, instead of the 405nm dichroic, a plate was used that reflected most of the laser light and only allowed a small percentage to reach the sample. This modification resulted in an artificially turned down laser power that was sufficient to excite the BV421 fluorophore, without increased autofluorescence or problems in detecting CFP (see Figure 5.7).

Indeed this configuration to simultaneously detect eight colours by confocal microscopy allowed for the visualisation of villi and crypts by EpCAM staining, showed confetti-positive cells and could refine the phenotypical analysis of these cells by MHCII, IRF8 and CD11b expression. Figure 5.11 and Figure 5.12 show two examples of images of intestinal sections of a Clec9a$^{+/Cre}$ROSA$^{+/confetti}$ mouse stained with anti-EpCAM-BV421, anti-CD11b-AF594, anti-IRF8-APC and anti-MHCII-AF700.

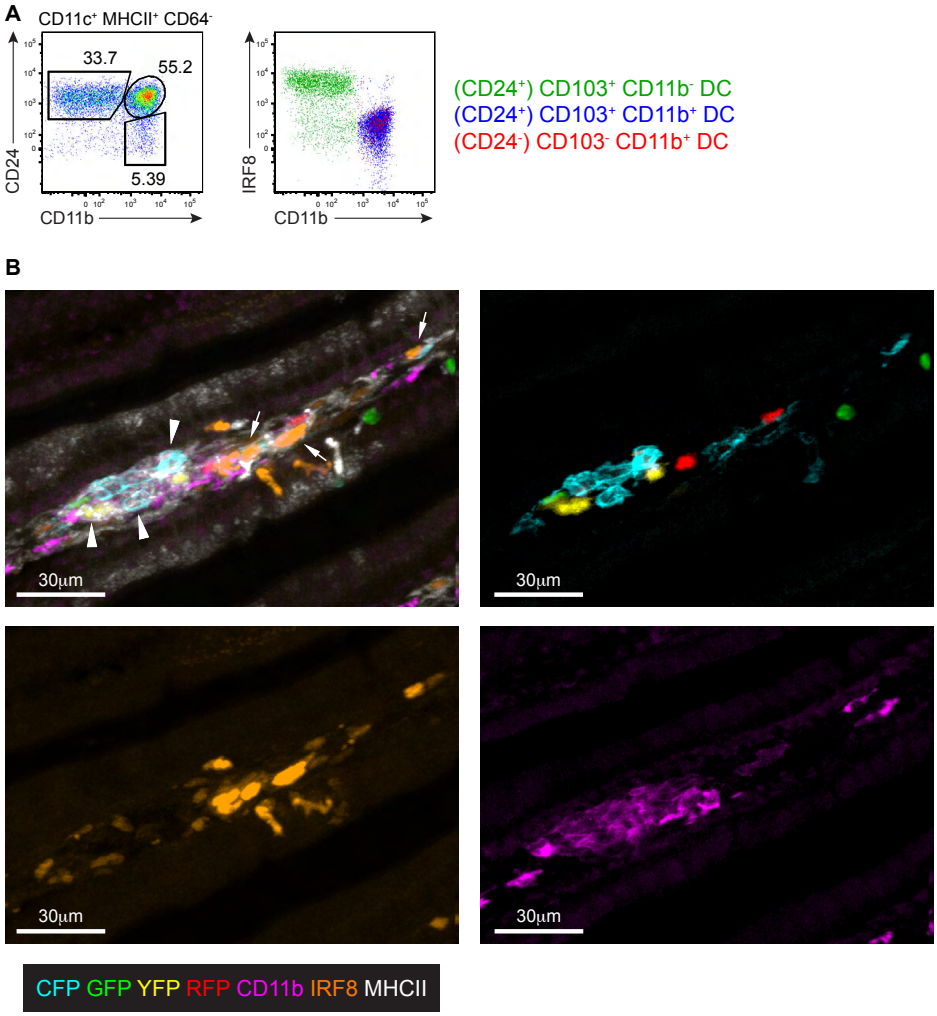

Figure 5.10 IRF8 and CD11b can be used to identify DC subsets in the small intestine by microscopy

(A) CD103^{+} CD11b^{-} DCs (CD11c^{+} MHCII^{+} CD64^{-} CD24^{+} CD11b^{-}), CD103^{+} CD11b^{+} DCs (CD11c^{+} MHCII^{+} CD64^{-} CD24^{+} CD11b^{+}) and CD103^{-} CD11b^{+} DCs (CD11c^{+} MHCII^{+} CD64^{-} CD24^{-} CD11b^{+}) in the small intestine of C57Bl/6J mice were identified by flow cytometry and expression of IRF8 and CD11b was assessed in an overlay graph. Plots are representative of three mice. **(B)** A 30µm frozen section of small intestine of Clec9a$^{+/Cre}$ROSA$^{+/confetti}$ mice was stained with antibodies against MHCII, CD11b and IRF8, and analysed by microscopy using lambda mode scanning and unmixing. The images shown here are close-ups of Figure 5.12. Arrows show confetti cells that are positive for CD11b and arrowheads show confetti cells positive for IRF8.

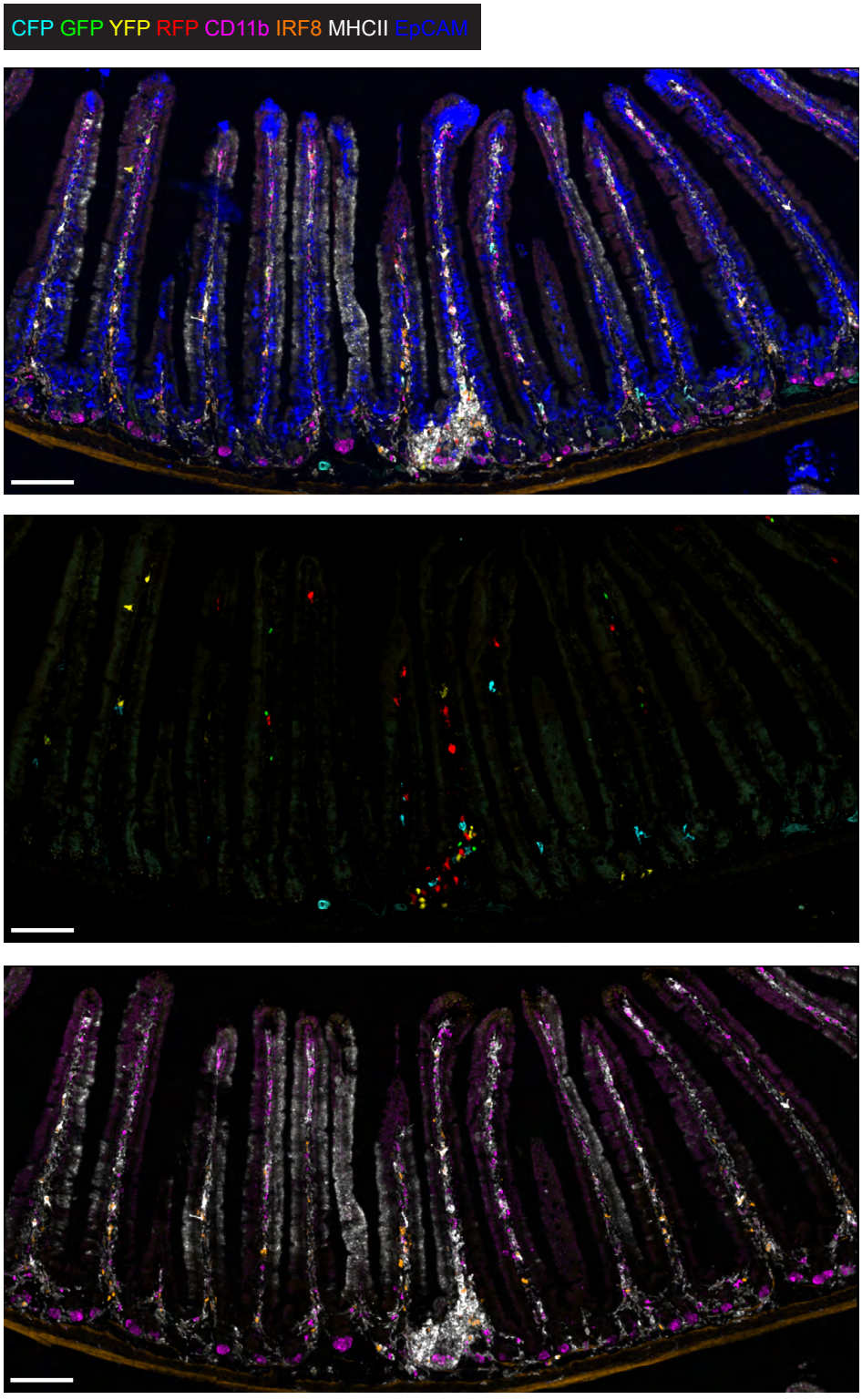

Figure 5.11 8-Colour analysis of the small intestine of Clec9a$^{+/Cre}$ROSA$^{+/confetti}$ mice (1)

A 30μm frozen section of small intestine of Clec9a$^{+/Cre}$ROSA$^{+/confetti}$ mice was stained with antibodies against MHCII, CD11b, IRF8 and EpCAM and analysed by microscopy using lambda mode scanning and unmixing. Scale bar is 100μm.

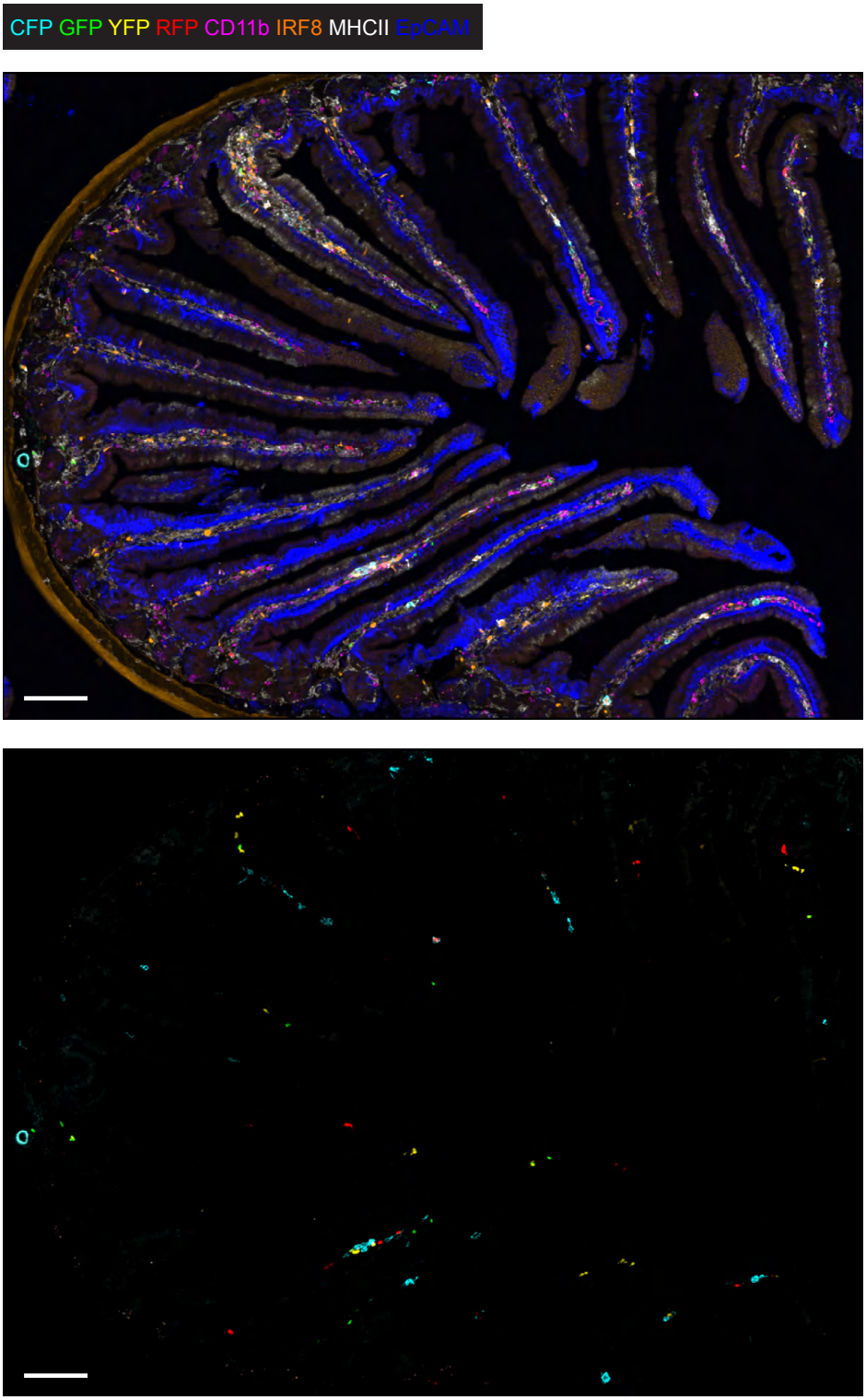

Figure 5.12 8-Colour analysis of the small intestine of Clec9a$^{+/Cre}$ROSA$^{+/confetti}$ mice (2)

A 30μm frozen section of small intestine of Clec9a$^{+/Cre}$ROSA$^{+/confetti}$ mice was stained with antibodies against MHCII, CD11b, IRF8 and EpCAM and analysed by microscopy using lambda mode scanning and unmixing. Scale bar is 100μm.

The images shown in Figure 5.10B, Figure 5.11 and Figure 5.12 already provide useful information on the clonality of confetti-positive cells within villi and their subset distribution. However, these 8-colour images are also difficult to interpret and additional information remains hidden in the complexity of the data. Furthermore, these images as such are not suitable for more quantitative analyses. Therefore, images were quantified by histo-cytometry (Gerner et al., 2012; Gerner, Torabi-Parizi and Germain, 2015). In order to quantify the confetti-positive cells, surfaces were generated on the individual cells by using the surface rendering tool built into Imaris imaging software. Surface rendering was performed subsequently on the CFP, GFP, YFP and RFP channel. An example of the surfaces generated in an isolated lymphoid follicle is shown in Figure 5.13A, while all surfaces for the image in Figure 5.11 are shown in Figure 5.13B. The software correctly identified all confetti cells that were visible by eye, however, it also assigned surfaces to autofluorescent structures such as the blood vessel in the bottom left corner of Figure 5.13A.

To further analyse these confetti surfaces, surface parameters (intensities of separate channels and location) were imported into FlowJo 10 to perform flow cytometry-like gating. The first step comprised of removing $MHCII^-$ surfaces from the analysis, as these surfaces likely correspond to autofluorescent structures (Figure 5.14A and Figure 5.15A). The original image was always used as a reference when performing gating. The XY-coordinates of these surfaces were then superimposed on a density plot of surfaces generated on the EpCAM channel to visualise the villi, as shown in Figure 5.14B and Figure 5.15B. Furthermore, the expression of IRF8 and CD11b by confetti surfaces could be visualised (Figure 5.14C and Figure 5.15C). Based on the flow cytometry data in Figure 5.10A, almost all confetti surfaces should be either $IRF8^+$ or $CD11b^+$, but cannot be positive for both or negative for both. Consistent with this notion, very few $IRF8^+$ $CD11b^+$ surfaces were identified. However, many surfaces appeared to be negative for both IRF8 and CD11b by histo-cytometry (Figure 5.14C and Figure 5.15C). For the GFP^+ surfaces this result is not surprising, as GFP is a nuclear marker and the surface generated on a GFP object will only capture the nucleus of the cell with very little cytoplasm or membrane, which means that a membrane marker such as CD11b would not be captured by the GFP surface. However, also many CFP^+,

YFP^+ and RFP^+ surfaces appeared to be negative for both IRF8 and CD11b, which exemplifies that histo-cytometry is less sensitive than flow cytometry to measure marker expression of cells. Unfortunately, a specific DC subset can only be attributed to surfaces that are either positive for IRF8 or for CD11b.

The images of small intestinal villi presented throughout this chapter clearly show the presence of cells of the same colour in individual villi. Examples can be found in insert 1 of Figure 5.8A and the GFP^+ cluster identified by arrowheads and the CFP^+ cluster identified by arrows in the insert of Figure 5.9. These clusters of cells of the same colour are even easier to identify in the FlowJo quantifications of Figure 5.11 and Figure 5.12. Cells of the same colour in individual villi can also be gated on and displayed in a plot showing their XY-coordinates and the outline of the villi (Figure 5.14D and Figure 5.15D). These groups of cells of the same colour and same villus suggest a clonal origin and as shown in Figure 5.14BD and Figure 5.15BD, many of these putative clones can be identified in a single image. Most putative clones are fairly small, only two or three cells, but some are larger and comprise up to six cells per clone for Figure 5.15D. Even larger putative clones can be identified in Figure 5.9. In FlowJo, these individual putative clones can also be analysed for IRF8 and CD11b expression (Figure 5.14E and Figure 5.15E). Despite the limitation that some surfaces appear to be negative for both IRF8 and CD11b, very few putative clones could be identified that harbour both $IRF8^+$ cells and $CD11b^+$ cells, These results indicate that DC precursors arriving in the small intestine divide locally before differentiating and that individual DC precursors may have a preference to differentiate into one subset or another. However, both for the clonal analysis and the subset distribution within clones more images have to be acquired and quantified. Moreover, the degree of clonality should be estimated using computational approaches.

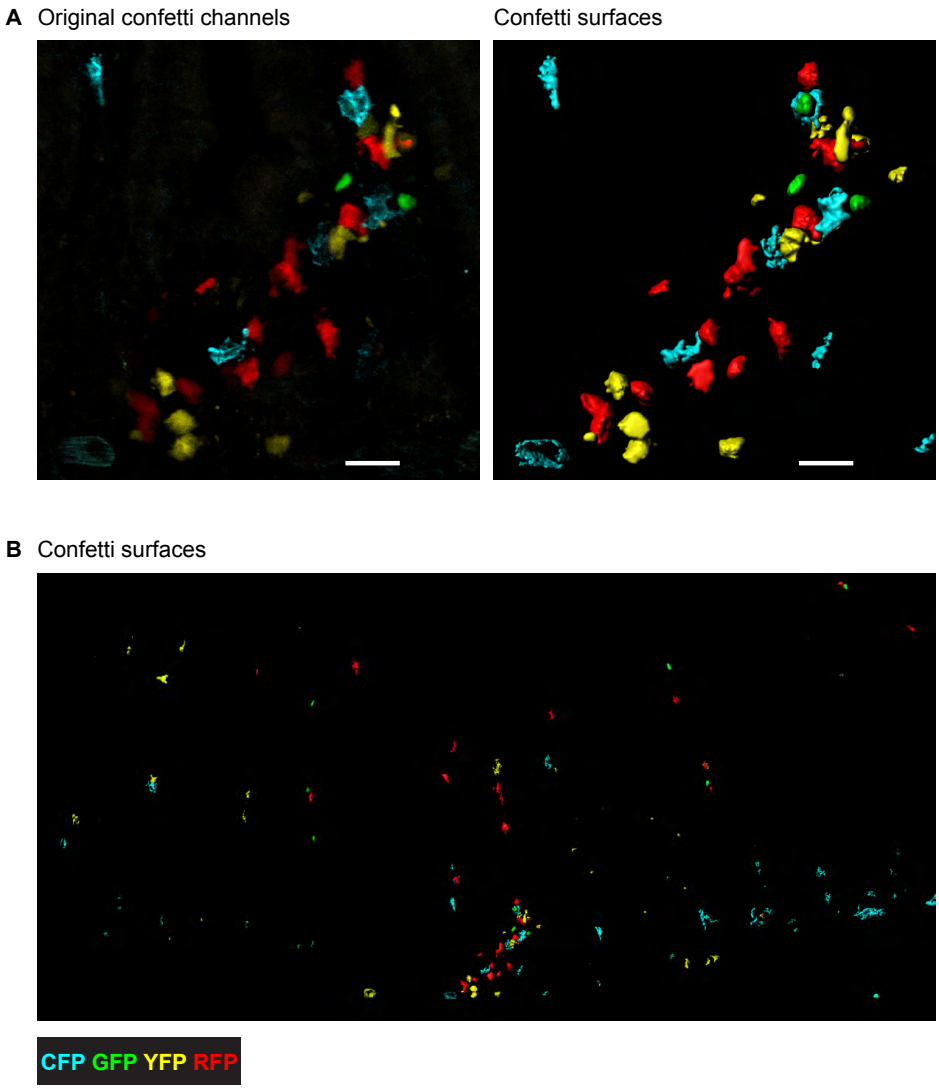

Figure 5.13 Surface rendering on confetti channels by Imaris

The surface rendering example shown here is based on the image in Figure 5.11. Surfaces were created for each of the four confetti channels using the built-in surface rendering tool in Bitplane Imaris software. **(A)** The left panel shows the original confetti channels for the isolated lymphoid follicle of Figure 5.11, the right panel shows the surfaces created on these channels. **(B)** Overview of all confetti surfaces generated for the image in Figure 5.11.

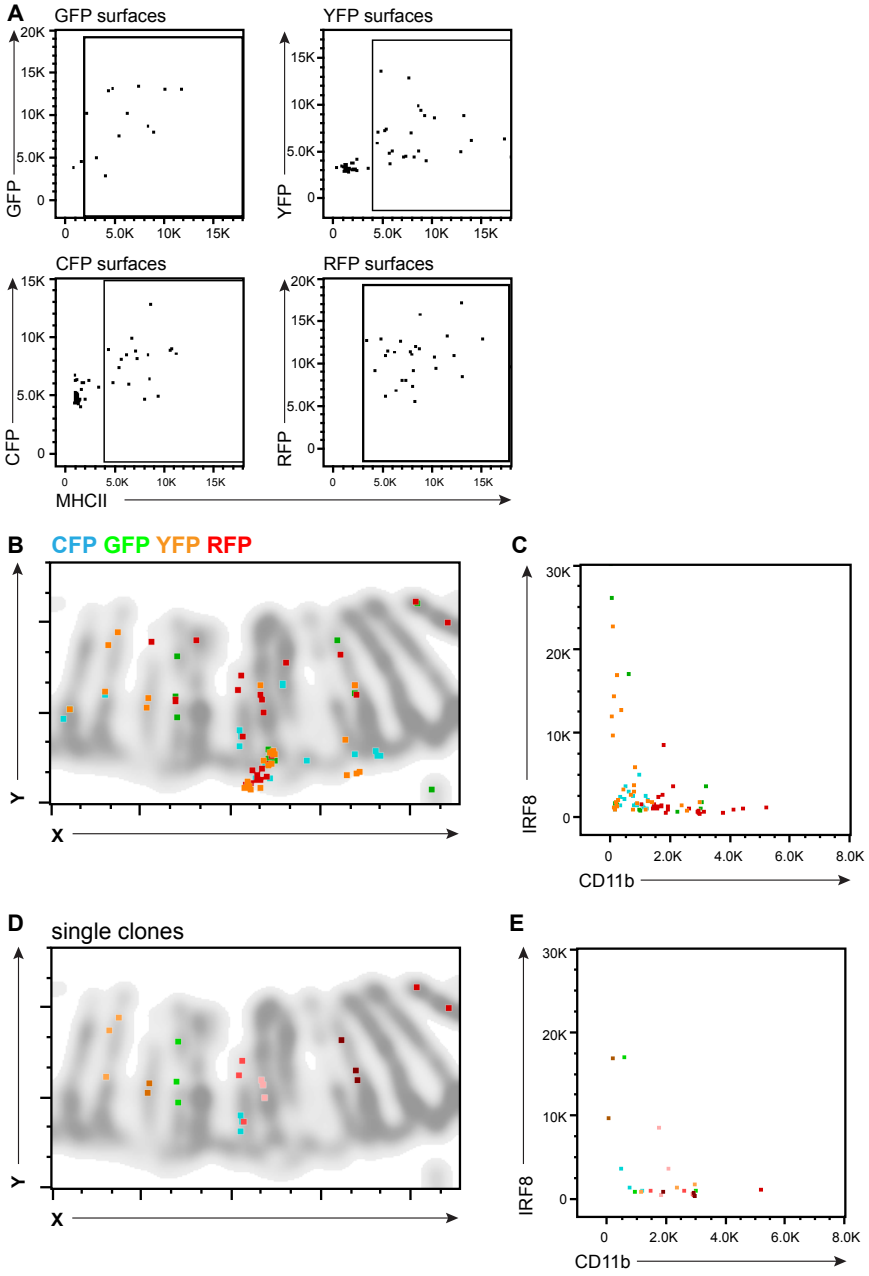

Figure 5.14 Analysis of confetti surfaces based on the images in Figure 5.11 by FlowJo

Statistics on confetti surfaces as identified in Figure 5.13 were exported from Imaris and imported into FlowJo 10. **(A)** $MHCII^+$ surfaces were selected. **(B)** XY coordinates of $MHCII^+$ confetti surfaces were plotted as dots, the outline of the villi was plotted as density plot of EpCAM surfaces and the two graphs were combined in Illustrator. **(C)** IRF8 and CD11b expression of $MHCII^+$ confetti surfaces. **(D)** Cells of the same confetti colour in a single villus were identified ('clone') and plotted as in (B). Each clone has its own colour. CFP clones are different shades of blue, GFP clones are different shades of green, YFP clones are different shades of orange and RFP clones are different shades of red. **(E)** IRF8 and CD11b expression of single clones as identified in (D). Colours correspond to the ones used in (D).

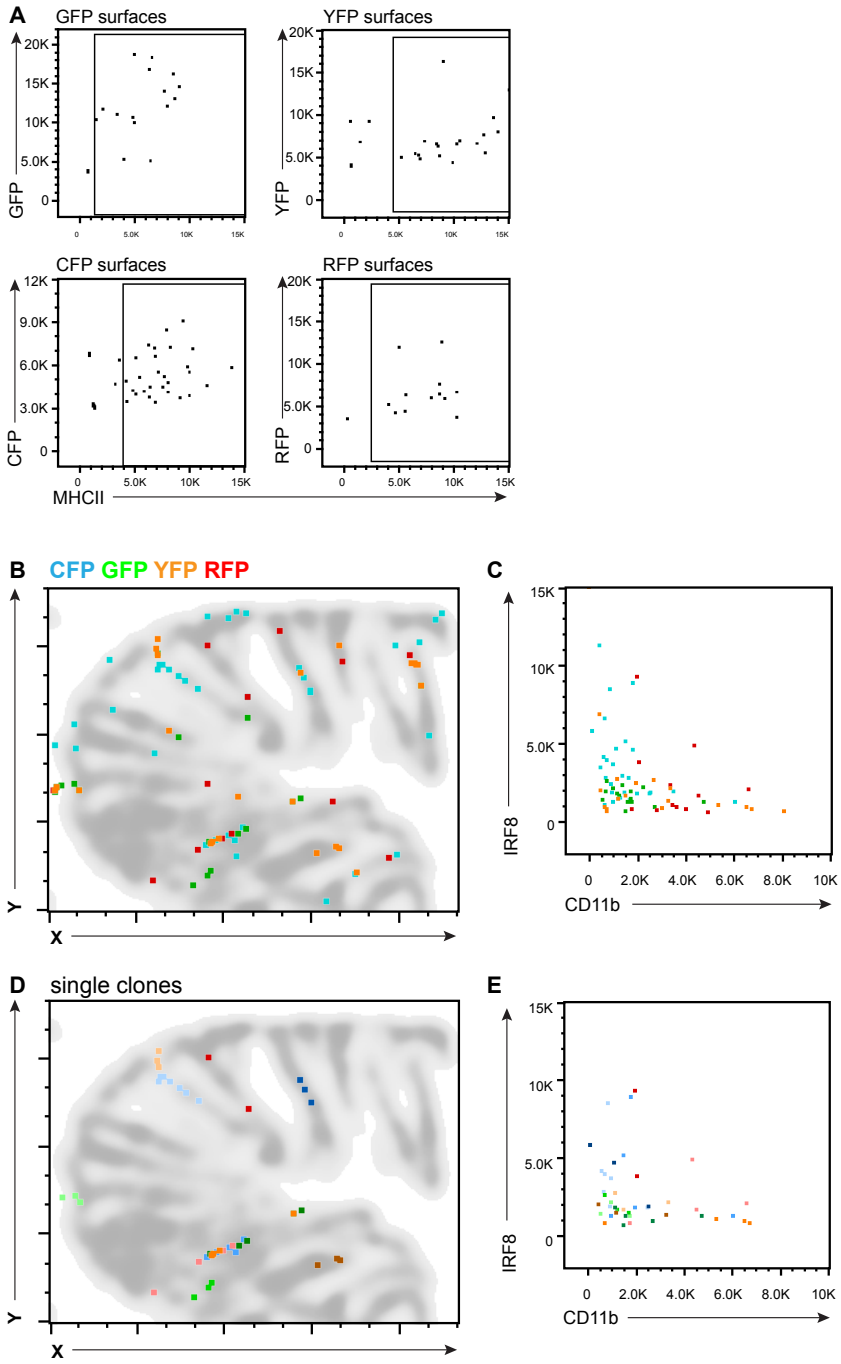

Figure 5.15 Analysis of confetti surfaces based on the images in Figure 5.12 by FlowJo

Same analysis as in Figure 5.14, but then for the image shown in Figure 5.12.

5.5 Discussion

In recent years our understanding of DC precursors has been substantially refined. CDPs were originally defined to exclusively give rise to both cDCs and pDCs, but more recent studies have shown that this population is heterogeneous and contains precursors that are either committed to generate either one or the other (Naik *et al.*, 2007; Onai *et al.*, 2007; K. Liu *et al.*, 2009; Satpathy, KC, *et al.*, 2012; Schraml *et al.*, 2013; Onai *et al.*, 2013). The same holds true for preDCs, where two subpopulations can be identified that generate either CD8α-like DCs or $CD11b^{+}$ DCs (Naik *et al.*, 2006; Schlitzer, McGovern and Ginhoux, 2015; Grajales-Reyes *et al.*, 2015). However, the vast majority of research on DC precursors has been done on bulk populations, precluding the analysis of the fate of single precursors and possibly masking heterogeneity within the studied population. Thus far, the fate of single precursors has only been studied in an *in vitro* culture setting, which may be of limited biological relevance (Schlitzer, McGovern and Ginhoux, 2015).
To overcome these limitations, a novel approach was devised to study DC precursor fate in vivo under physiological conditions. $Clec9a^{+/Cre}ROSA^{+/confetti}$ mice were employed to stochastically and irreversibly label precursors with one of four fluorescent proteins and chase their fate in peripheral tissues. Ideally, an inducible form of Cre is used in these types of experiments, so that labelling of DC precursors can be temporally controlled and the fate of one cohort of DC precursors can be chased *in vivo*. As these mice did not exist, mice were generated that express CreERT2 under control of the *Clec9a* locus via a knock-in approach that was previously employed to generate Clec9a-GFP and Clec9a-Cre mice (Sancho et al., 2009; Schraml et al., 2013). Two Clec9a-CreERT2 mouse lines were successfully established from two targeted ES cell clones. Unfortunately, when crossed to ROSA26 reporter lines, none of these mice induced reporter expression when tamoxifen was administered orally or parentally. Furthermore, treatment with 4OH-tamoxifen of Flt3l BMDC cultures from these mice also failed to induce Cre-mediated recombination. The reason why Clec9a-CreERT2 mice failed to work is unknown. The locus was correctly targeted, sequencing of the *Creert2* gene and proximal promoter failed to detect any aberrations and *Creert2* mRNA was expressed in Flt3l BMDCs, which makes it very unlikely that errors were introduced during the generation of these mice. Non-functional CreERT2 mouse

lines are not without precedent though. Tie2-CreERT2 mice were generated for the labelling of HSCs, but failed to show any signs of recombination (Busch et al., 2015). Interestingly, remaking these mice using a different type of inducible Cre solved the problem and resulted in a functional inducible Cre system (Busch et al., 2015). So, in principle chances are that newly generated mice expressing a different inducible version of Cre under control of the *Clec9a* locus will allow for tamoxifen-induced Cre recombination.

Unfortunately, remaking these mice was not feasible for the current study and therefore Clec9a-Cre mice were crossed to ROSA26-confetti mice to assess DC precursor fate *in vivo*. Clec9a-Cre mice continuously induce reporter expression in CDPs and preDCs when crossed to ROSA26-YFP mice, but labelling efficiency is not complete and therefore not all DCs are labelled in these mice (Schraml et al., 2013). The exception are CD8α-like DCs that express DNGR-1 and consequently Cre and therefore have an extra opportunity to recombine the ROSA26 locus (Schraml et al., 2013). Clec9a$^{+/Cre}$ROSA$^{+/confetti}$ mice have not been characterised by flow cytometry as it has proven to be difficult to detect CFP in these mice, due to a suboptimal laser configuration on flow cytometers.

Analysis of DC precursor fate in Clec9a$^{+/Cre}$ROSA$^{+/confetti}$ mice by microscopy was limited here to the small intestine. This tissue has a well-defined DC compartment and due to the villus architecture, DCs are naturally confined in their migration. This latter point is of particular importance, as DCs are motile cells and if daughter cells migrate away too quickly, they will not be recognisable as a clone. The villi of the small intestine naturally confine DCs in their movements, which makes it more likely that daughter cells stay together in the same villus and can be identified as one clone. In the mesLN for example, DC movement is much less restricted and there are also many more labelled cells, which makes it impossible to infer any information on DC precursor clonality from these images.

To analyse clonal burst size and DC subset distribution of clones in the small intestine of Clec9a$^{+/Cre}$ROSA$^{+/confetti}$ mice, a method was developed to perform 8-colour confocal microscopy and histo-cytometric analysis of the images (Gerner et al., 2012; Gerner, Torabi-Parizi and Germain, 2015). CFP, GFP, YFP and RFP

expressed in Clec9a$^{+/Cre}$ROSA$^{+/confetti}$ mice and four antibodies coupled to BV421, AF594, AF647 or APC and AF700 could be resolved by microscopy. Analysis of the images presented here revealed that groups of cells of the same colour could be identified in single villi, which suggest a clonal origin of these cells. Although most of these putative clones were fairly small, comprising two or three cells of the same colour, larger putative clones were also detected. Nevertheless, these images also revealed many cells that did not appear to belong to a putative clone. These single cells might be genuine events in which a precursor arrived in the tissue and differentiated into one DC, but may also reflect limitations in the experimental setup. The sections examined here are only 30μm thick and do not capture the whole villus, and therefore cells belonging to a genuine clone will be missed if they reside above or below the section examined. Furthermore, labelling of precursors is continuous with Clec9a-Cre mice and the images presented here give a snapshot of a mixed DC population, showing DCs that have recently differentiated, DC about to die or migrate out of the tissue and even a rare precursor itself that had just arrived. The cells not belonging to a putative clone may for example reflect events in which other daughter cells have already migrated out of the tissue, but one daugther is still present. These limitations may equally affect the observed size of putative clones. Finally, a small percentage of CD64^{+} intestinal macrophages is labelled in Clec9a$^{+/Cre}$ROSA$^{+/YFP}$ mice and will likely be labelled in Clec9a$^{+/Cre}$ROSA$^{+/confetti}$ mice (Schraml et al., 2013). These macrophages originate from different precursors and have different turnover kinetics from DCs, but are difficult to distinguish from DCs in the images, as CD64 is not used to stain tissue sections. So, the fact that single cells are observed in the images presented here may have various explanations and the size of the putative clones may be underestimated. Nonetheless, the fact that putative clones are present suggests that at least some preDCs divide locally upon arrival in the small intestine.

The analysis of putative clones can be further refined by assessing which DC subsets are found in an individual clone. This analysis will shed light on whether a preDC arriving in the small intestine can give rise to multiple subsets of DCs or is restricted to only one subset. Recent work has suggested that preDCs are already committed in the BM to give rise to either CD8α-like DCs or CD11b^{+} DCs when arriving in tissues (Schlitzer, McGovern and Ginhoux, 2015; Grajales-Reyes et al.,

2015). However, these analyses were either performed *in vitro* or by adoptively transferring sorted populations of preDCs and investigating their fate in the spleen. The microscopy-based approach described here provides a more refined way of assessing preDC commitment in the small intestine under physiological settings. Sadly, antibodies against CD103 did not work for microscopy, which meant that the CD11b- and CD103-based classification of intestinal DC subsets that is often used for flow cytometry could not be employed. Fortunately, an antibody against the transcription factor IRF8 did work for microscopy and a combination of IRF8 and CD11b expression could distinguish $CD103^+$ $CD11b^-$ DCs from $CD103^+$ $CD11b^+$ DCs and $CD103^-$ $CD11b^+$ DCs. Regrettably, the resolution of IRF8 and CD11b expression by microscopy was not as good as by flow cytometry and many confetti-positive cells appeared to be negative for both CD11b and IRF8. These cells would have to be excluded from the DC subset analysis.

The research project presented here will require future work to support firm conclusions. $Clec9a^{+/Cre}ROSA^{+/confetti}$ mice will need to be characterised by flow cytometry to quantify labelling efficiencies of DC subsets in the small intestine and to assess if other cell types, such as macrophages, are labelled. Furthermore, identification, quantification and phenotyping of cells expressing CFP and RFP, or GFP and YFP, are straightforward by flow cytometry. More images of small intestinal sections of $Clec9a^{+/Cre}ROSA^{+/confetti}$ mice will be generated, so that DC precursor fate can be quantified via computational methods. Furthermore, whole villi, instead of sections of villi, should be analysed by microscopy, to capture all confetti cells in a single villus and reduce the bias by missing confetti-positive cells that are below or above the section imaged. Recent advancements in tissue clarification techniques should aid the imaging of whole tissues while preserving fluorescence. Ideally though, the arrival of preDCs in the small intestine and their division and differentiation is followed over time. However, this approach is not feasible with currently available techniques, as microscopes cannot penetrate deep enough into the tissue to image the villi and the mice would have to be imaged for days by intravital microscopy.
Despite the failure of Clec9a-CreERT2 mice to induce recombination, temporal resolution of labelled cells may still be achieved in $Clec9a^{+/Cre}ROSA^{+/confetti}$ mice via different means. One promising approach is to treat mice with EdU, a BrdU

analogue, that gets incorporated into the DNA of dividing cells and can be visualised in tissue sections. A pulse of EdU administered to Clec9a$^{+/Cre}$ROSA$^{+/confetti}$ mice will label all dividing cells, including DC precursors, which can then be chased over the course of a few days. At time of analysis, cells that are both confetti- and EdU positive are known to have come from DC precursors that have divided during a specific time window and can be treated as a single cohort.
Once DC precursor fate is analysed in steady state, these analyses will be repeated under conditions of disturbed gut homeostasis, to assess if DC precursor behaviour changes when the intestinal environment changes. One method to alter the gut microenvironment is to treat the mice with a cocktail of antibiotics in the drinking water, which reduces the microbiota and changes its composition. Alternatively, mice can be orally infected with the natural mouse pathogen *Citrobacter rodentium* that causes a mild colitis in immunocompetent mice.

In the future Clec9a$^{+/Cre}$ROSA$^{+/confetti}$ mice can also be used to address DC precursor fate in other non-lymphoid tissues, such as the lung or skin, and compare results with the ones obtained in the small intestine. Furthermore, the influence of different types of infection, like influenza or *Candida albicans*, or inflammatory stimuli, on the behaviour of DC precursors can be assessed. Moreover, Clec9a$^{+/Cre}$ROSA$^{+/confetti}$ mice can be crossed to mouse strains constitutively or conditionally lacking transcription factors, signalling molecules, receptors etcetera, to address their influence on DC precursor biology. When Clec9a$^{+/Cre}$ROSA$^{+/confetti}$ mice are for example crossed with mice harbouring a floxed version of one of the genes encoding TLR receptors, or their adaptor protein MyD88, the influence of TLR signalling on DC precursor fate can be interrogated.

In summary, analysis of Clec9a$^{+/Cre}$ROSA$^{+/confetti}$ mice by 8-colour microscopy and histo-cytometry is a very useful tool to study DC precursor biology in a physiological *in vivo* setting. Preliminary results show that at least some preDCs divide a few times upon arrival in the small intestine, before differentiating into one or multiple DC subsets. However, further work needs to be done to confirm these observations.

Chapter 6. Discussion

6.1 How to classify mononuclear phagocytes?

Mononuclear phagocytes have historically been classified as monocytes, macrophages or DCs based on surface marker expression, morphology and functionality. However, many of these attributes overlap among the different mononuclear phagocytes, leading to considerable debates in the field as how to classify certain subsets of mononuclear phagocytes, and to the same subset having different names. Technical advancements, particularly in the field of flow cytometry, and the availability of transgenic mouse lines have brought novel insights into mononuclear phagocyte heterogeneity, function and ontogeny. Multicolour flow cytometry and mass cytometry, in combination with the identification of novel myeloid markers, have revealed increasing complexity and have permitted the identification of novel subsets of mononuclear phagocytes. For example, DCs in the spleen can be divided into CD8α^+ DCs and CD11b$^+$ DCs, but both of these subsets can be further separated into CD205$^+$ CX3CR1$^-$ CD8α^+ DCs and CD205$^-$ CX3CR1$^+$ CD8α^+ DCs, and ESAM^{hi} CD11b$^+$ DCs and ESAM^{low} CD11b$^+$ DCs, respectively (Bar-On and Jung, 2010; Lewis et al., 2011). Importantly, it is often unclear if this identification of subsets of subsets is biologically relevant, especially because surface marker expression is not immutable and can change during the life span of a cell. CD103 expression on CD8α-like DCs is for example induced by GM-CSF and CD103 levels may therefore differ depending on the strength of GM-CSF receptor signalling (Zhan et al., 2011; Sathe et al., 2011). Furthermore, in the spleen CD11b$^+$ DCs can be stratified into a CD4 negative and CD4 positive population, but it has been shown that both populations have similar expression patterns of other surface markers and transcription factor dependencies, arguing that CD4 negative and CD4 positive CD11b$^+$ DCs belong to the same subset (Edwards et al., 2003; Becher et al., 2014). On the contrary, studies have revealed that cells with similar surface marker expression and morphology may have different origins. One obvious example are CD11c$^+$ MHCII$^+$ cells, once almost synonymous for ‘dendritic cell’, but now understood to include also some monocyte-derived cells and macrophages.

Classifying mononuclear phagocytes based on functionality has its flaws. DCs have often been ascribed superior abilities to initiate T cell responses, while macrophages are described as highly phagocytic cells that can modulate inflammatory processes (Geissmann, Manz, *et al.*, 2010; Steinman and Idoyaga, 2010; Hashimoto, J. Miller and Merad, 2011; Merad *et al.*, 2013; Varol, Mildner and Jung, 2015). Yet, these descriptions ignore the fact that macrophages and monocytes can also present antigen and initiate T cell responses (see 1.1.4.1) and that DCs have functions that are independent of T cells, such as interacting with other innate immune cells or stromal cells (see 1.1.4.2 and 1.1.4.3). DCs can, like macrophages, also modulate inflammatory processes and phagocytose cargo (Inaba *et al.*, 1998; Roche and Furuta, 2015).

An alternative approach to distinguish monocytes, macrophages, DCs and their subsets is based on differential requirements for growth factors and transcription factors (see 1.1.2) (Satpathy, Wu, et al., 2012; Schraml and Reis e Sousa, 2014). The key growth factor regulating DC development is Flt3l and exogenous Flt3l administration expands DCs *in vivo*, while mice lacking Flt3l or its receptor Flt3 have strongly reduced DC numbers (Maraskovsky *et al.*, 1996; McKenna *et al.*, 2000; Manfra *et al.*, 2003; Waskow *et al.*, 2008; Kingston *et al.*, 2009). However, some DCs still develop in $Flt3l^{-/-}$ and $Flt3^{-/-}$ mice and loss of Flt3l signalling also impacts on NK cells, B cells and T cells (McKenna et al., 2000).
On the other hand, macrophages depend on signalling through the M-CSFR, either by M-CSF for most macrophage populations, or by the alternative ligand IL-34 for LCs (Pixley and Stanley, 2004; Y. Wang *et al.*, 2012; Greter, Lelios, *et al.*, 2012). However, analogous to Flt3l-dependency of DCs, some macrophages can still develop independently of M-CSFR signalling (Cecchini *et al.*, 1994; Pixley and Stanley, 2004). Macrophage development is dependent on the transcription factor Pu.1 and $Pu.1^{-/-}$ mice are devoid of macrophages (E. W. Scott *et al.*, 1994; McKercher *et al.*, 1996). However, Pu.1 deficiency affects many other haematopoietic lineages as well, and importantly has been argued to additionally affect DCs (E. W. Scott *et al.*, 1994; McKercher *et al.*, 1996; Guerriero *et al.*, 2000; Anderson *et al.*, 2000). Pu.1 dependency can therefore not be used to unambiguously distinguish macrophages from DCs.

A master regulator of the DC lineage has not been identified yet either. Although Zbtb46 expression is relatively restricted to DCs within the haematopoietic system, Zbtb46 expression can also be upregulated in activated monocytes, while it is downregulated upon DC stimulation and, importantly, absence of Zbtb46 does not negatively impact the development of DCs (Meredith, Liu, Darrasse-Jeze, et al., 2012; Satpathy, KC, et al., 2012; Meredith, Liu, Kamphorst, et al., 2012). Zbtb46 expression should therefore be used with caution when distinguishing DCs from monocytes and macrophages. Although growth factor and transcription factor dependency have thus far failed to unequivocally distinguish DCs from monocytes and macrophages, transcription factor dependency has been used more successfully to identify DC subsets. pDCs for example critically depend on the transcription factor E2-2, while CD8α-like DCs largely depend on Batf3 (Cisse *et al.*, 2008; Hildner *et al.*, 2008; Ghosh *et al.*, 2010).

A different approach relies on transcriptomics analysis of purified subsets of cells followed by supervised or unsupervised clustering to quantify relatedness of subsets and define key transcriptional profiles. This has been done for different mononuclear phagocyte subsets, for example by the Immgen consortium for DCs and macrophages (Robbins *et al.*, 2008; J. C. Miller *et al.*, 2012; Gautier *et al.*, 2012). However, as these analyses were performed on sorted populations of cells, they rely heavily on sample homogeneity. This limitation can be overcome by performing single-cell transcriptomics analyses, which are now becoming feasible due to recent technical advancements, and have indeed been performed on GM-CSF derived BMDCs (Shalek et al., 2013). Alternatively, high-dimension mass cytometry (or flow cytometry) can be used to analyse marker expression of single cells and classify mononuclear phagocyte subsets (Becher et al., 2014).

More recently, an ontogeny-based classification of DCs, monocytes and macrophages has been proposed (Guilliams et al., 2014). In this proposal mononuclear phagocytes are grouped according to the precursor from which they originate. Mononuclear phagocytes should only be called macrophages if they have an embryonic origin, while the term DC is restricted to cells derived from the CDP and cells originating from cMoPs should be called monocyte-derived cells. This approach has obvious advantages over classifications based on surface marker

expression, morphology and functionality. It may also complement transcription factor-based classifications, as precursors may depend on specific transcription factors. Furthermore, ontogeny from a common precursor does not define specific monocyte, macrophage or DC subsets, while transcription factor dependency differs for different subsets.

However, an ontogeny-based classification has its limitations as well, both in practical and more philosophical terms. Practically, the ontogeny-based approach critically depends on the unambiguous identification of dedicated precursors, either by flow cytometry to perform adoptive transfer experiments, or by selective expression of inducible or constitutive Cre recombinase for lineage tracing experiments. In the case of adoptive transfer experiments, precursor populations have to be sorted to high purity to avoid contamination with other cells and even then the sorted population may be heterogeneous. Furthermore, adoptive transfer studies are not always feasible due to low cell numbers, as may be the case with embryonic precursors, and the isolation and subsequent intravenous transfer may introduce artefacts. Lineage tracing experiments depend on the availability of transgenic mouse lines that express inducible or constitutive Cre recombinase specifically and efficiently in the precursor of interest, so that when crossed to a fluorescent reporter mouse strain all precursors and no other cells are irreversibly labelled. Labelling of cells other than the precursor of interest may lead to ambiguity in assessing the origin of labelled differentiated cells and if not all precursors are labelled, no formal conclusions can be drawn on unlabelled differentiated cells.

On a more philosophical level the ontogeny-based approach to classify mononuclear phagocytes assumes that precursors cannot substantially change their fate anymore once they are committed to a certain lineage and that a uniform population of cells cannot originate from multiple precursors. The first assumption that precursor fate is irreversible, is widely assumed and is in line with results from adoptive transfer experiments and single cell clonality assays performed with various haematopoietic precursors. However, haematopoiesis and lineage commitment is a gradual process, not a stochastic one. The grouping of haematopoietic cells into HSCs, GMPs, MDPs, CDPs etcetera is an arbitrary (albeit useful) process based on the expression of certain surface markers, while in reality it is a continuous transformation without defined boundaries. Cell fate choices

during haematopoiesis are regulated by a complex interplay of internal regulatory networks and external stimuli that allow for some plasticity. It is therefore possible that cells that have started to express a certain cell fate program, and may even show surface marker patters associated with this cell fate, could still change their fate, either stochastically or due to external factors. This reasoning may for example explain why Clec9a-Cre mice crossed to a fluorescent reporter strain also label a small fraction of macrophages, when some CDPs are not fully committed yet and can change their fate to generate other myeloid cells (Schraml et al., 2013). On the other hand, recent barcoding experiments suggested that DC commitment can take place much earlier during haematopoiesis, as a population of LMPPs can be identified that exclusively gives rise to DCs, apparently bypassing the classical GMP and MDP stages (Naik et al., 2013; Perié et al., 2014). Importantly, the LMPP fraction also contains more 'conventional' precursors that can still give rise to DCs and myeloid and/or B cells (Naik et al., 2013; Perié et al., 2014). These results suggest that lineage commitment is more complex than described by the classical haematopoietic 'tree' model, which complicates an ontogeny-based classification of mononuclear phagocytes.

Furthermore, highly similar cell populations may display multiple origins. For example, it has been suggested that DCs, especially thymic DCs and pDCs, can originate from lymphoid progenitors. Adoptive transfer of common lymphoid progenitors (CLPs) generated DCs in spleen and thymus and some pDCs show VDJ gene rearrangements, despite being functionally and phenotypically undistinguishable from CMP-derived cells (Traver et al., 2000; Corcoran et al., 2003; Sathe et al., 2013). Macrophage populations that are otherwise indistinguishable may have a dual origin in which embryonic macrophages are gradually replaced by monocyte-derived cells during life, as is for instance the case with alveolar macrophages (Ginhoux *et al.*, 2010; C Schulz *et al.*, 2012; Perdiguero *et al.*, 2014; Epelman *et al.*, 2014). For macrophages it was shown that the tissue microenvironment has a dominant role in defining macrophage identity (Lavin *et al.*, 2014; Gosselin *et al.*, 2014). Tissue imprinting is even strong enough to reprogram fully differentiated macrophages when they are transplanted from one tissue to another (Lavin *et al.*, 2014).

In these examples an ontogeny-based classification will classify CLP-derived DCs and MDP-derived DCs into separate lineages and embryonic macrophages and

macrophages with a monocytic origin into separate lineages, even though in both cases there is no functional, phenotypical or transcriptional evidence justifying such a division.

In summary, an ontogeny-based classification of mononuclear phagocytes overcomes many of the limitations of classifications based on surface marker expression, morphology and functionality. Practical limitations relating to the unambiguous identification of precursors may be addressed with time by technological innovation and a more detailed understanding of precursor biology. However, issues relating to precursor plasticity and cell populations originating from different precursors are fundamental limitations to the ontogeny-based approach and may require refining the ontogeny-based framework with transcription factor dependencies and/or single-cell transcriptomics or high-dimension cytometry data.

6.2 The perfect mouse model to study dendritic cell biology

To unravel the intricacies of DC biology, researchers increasingly rely on transgenic mouse models. Although current models are extremely useful, they are certainly not perfect. The perfect model should target only the DC population of interest with high efficiency and, depending on the research question, should constitutively or inducibly ablate this population, label it with a fluorescent protein or other tag, or delete or express a gene of interest. It is impossible to combine all these attributes into one single transgenic mouse and therefore it is probably more appropriate to talk about the ideal toolbox to study DC biology *in vivo*. This toolbox comprises of mice that target DC precursors (that can also be used to manipulate all DCs) or specific subsets of DCs, such as CD8α-like DCs or $CD11b^{+}$ DCs, and for each population of interest should at least consist of a constitutive and an inducible Cre recombinase, to improve the flexibility of the toolbox. The discovery of the genome-editing capabilities of the CRISPR-Cas9 system will greatly facilitate the generation of such novel transgenic strains (Pelletier, Gingras and Green, 2015).

Efficient DC-restricted expression of a transgene is crucially important in novel transgenic mice to study DC biology. Most transgenic mouse models currently available to target all DCs also target other cells and/or do not show complete penetrance. For example, transgenic mice that make use of the CD11c expression pattern additionally target many other immune cells and zbtb46 is also expressed on erythroid progenitors, endothelial cells and some activated monocytes (Jung *et al.*, 2002; Probst, Tschannen, *et al.*, 2005; Hochweller *et al.*, 2008; Meredith, Liu, Darrasse-Jeze, *et al.*, 2012; Satpathy, KC, *et al.*, 2012). Mice targeting the *Clec9a* locus, as used in the data presented here, are not ideal either, as DNGR-1 is expressed both on cDC precursors and on certain differentiated DCs (Sancho *et al.*, 2008; Caminschi *et al.*, 2008; Schraml *et al.*, 2013). Furthermore, in Clec9a-Cre mice the penetrance of Cre-mediated recombination in differentiated cDCs not expressing DNGR-1 is incomplete, while on the other hand a small proportion of macrophages is labelled (Schraml et al., 2013).

Unfortunately, the identification of good promoters to target DC precursors or specific DC subsets is not straightforward. The identification of transcription factors, if they exist, that specifically control DCs or DC subsets would be hugely beneficial, as the genetic loci encoding these transcription factors can then be exploited for the generation of transgenic lines to study DC biology. Identification of receptors or other proteins that are uniquely expressed on DCs or specific subsets could be used in a similar way. Alternatively, locus control regions of human genes whose expression is restricted to DCs or DC subsets can be used in the mouse, as long as the transcription factors binging the promoter are sufficiently conserved. This strategy has for example been successfully used for targeting pDCs or LCs via the human locus control region normally encoding BDCA-2 or langerin, respectively (Bursch *et al.*, 2007; Swiecki *et al.*, 2010; Bobr *et al.*, 2010). Promoters to specifically and efficiently target DC subsets have been identified in certain cases. CD8α-like DCs can for example be specifically manipulated via transgene expression under control of the *Xcr1* locus (Swiecki et al., 2010; Yamazaki et al., 2013). However, no promoters have currently been identified to specifically manipulate $CD11b^+$ DCs or subsets of CD8α-like DCs or $CD11b^+$ DCs, for example in certain tissues.

If no good promoter can be found to generate a transgenic mouse that specifically targets the cells of interest, an alternative is to use a combination of two less

specific promoters. Utilisation of LysM and Csf1R expression was for example used to generate LysM^{Cre}Csf1R^{iDTR} mice in which monocytes and macrophages can be inducibly depleted (Schreiber *et al.*, 2013). Similarly, CD11c^{Cre}CX3CR1^{iDTR} were generated to specifically deplete CD11c^{+} CX3CR1^{hi} cells via DT injection (Diehl *et al.*, 2013). Alternatively, a split-Cre or split-CreERT2 system can be used in combination with two less specific promoters (Hirrlinger, Scheller, et al., 2009; Hirrlinger, Requardt, et al., 2009; P. Wang et al., 2012). In this case two inactive Cre or CreERT2 fragments are expressed under the control of two different promoters, and only in cells in which both promoters are active the two fragments are expressed simultaneously, generating a working enzyme. This approach could be used to generate transgenic mice in which Cre activity is confined to DC precursors by expressing one fragment of the split-Cre under control of the *Clec9a* locus and the other part under control of the *Csf1r* locus (encoding M-CSFR or CD115). In Clec9a-Cre mice it has already been shown that Cre activity controlled by the *Clec9a* locus is confined to DC precursors, pDCs and CD8α-like DCs. Among these populations only DC precursors express detectable amounts of M-CSFR (Onai et al., 2007; K. Liu et al., 2009). The *Clec9a* and *Csf1r* loci are therefore likely to be only concomitantly active at the DC precursor stage, and therefore a split-Cre system using these two loci should only generate an active Cre recombinase at the DC precursor stage. However, as the penetrance of Cre-mediated recombination is incomplete in Clec9a-Cre mice, a split-Cre system using the *Clec9a* and *Csf1r* loci would likely suffer from the same limitation (Schraml et al., 2013). Other potentially interesting options for the split-Cre system are utilising expression patterns of both CD8α and CD11c to target resident CD8α^{+} DCs in lymphoid organs, CCR7 and CD11c to target migratory myeloid cells, or Zbtb46 and CD11c to more specifically target DCs than with either using CD11c or Zbtb46 expression alone.

However, the split-Cre system has not been extensively used yet for transgenic mouse generation and it is therefore at present unknown how the recombination efficiency of split-Cre compares to conventional Cre. Furthermore, the split-Cre system involves the generation of two transgenic mouse lines instead of one to obtain an active Cre recombinase in the desired cells, which doubles the amount of work to generate the mice and also considerably complicates breeding strategies.

In addition to identifying good promoters to target the intended DC subset, tools are needed to manipulate or label these cells. Many transgenic mice are already available that harbour floxed versions of genes that are of interest for DC biology, for example genes encoding TLRs, transcription factors or chemokine receptors. When crossed to mice expressing Cre or CreERT2 in the appropriate cell type, these mice are powerful tools to elucidate the function of such proteins in DCs.

Efficient and constitutive ablation of the desired cell population can be achieved via the expression of DTA, either via placing the gene encoding DTA under direct control of a cell-specific promoter, or by crossing mice expressing Cre recombinase in the desired population with ROSA26-DTA mice (Ivanova *et al.*, 2005; Voehringer, Liang and Locksley, 2008). To inducibly deplete cells *in vivo* the DTR system has been widely used, in which expression of simian or human DTR renders cells sensitive for DT-mediated depletion, while all other murine cells remain insensitive to DT. Although the DTR-mediated depletion has proven to be efficient and fast, data presented in Chapter 3 of this thesis show that human or simian DTR can be biologically active in mice, and when expressed on DCs leads to LN hypocellularity and reduced frequencies of DCs in the absence of DT administration. It has also been suggested that DT itself can be immunogenic irrespective of the presence of DTR (Chapman and Georas, 2013). Furthermore, long-term depletion cannot be achieved with the DTR system, as mice start generating neutralising antibodies against DT after around two weeks of treatment. Alternatively, inducible depletion can be achieved by crossing CreERT2-expressing mice with ROSA26-DTA mice (Ivanova *et al.*, 2005; Voehringer, Liang and Locksley, 2008). In this approach tamoxifen administration induces recombination of the ROSA26 locus and expression of DTA, killing the cells expressing CreERT2. Furthermore, mice do not generate neutralising antibodies against tamoxifen, which means that depletion should be achieved over longer periods of time. However, successful implementation of this approach relies on efficient CreERT2 recombination to ablate the whole cell population of interest, and most CreERT2 mouse lines currently available lack this high efficiency.
Inducible depletion can additionally be achieved by generating transgenic mice that express an inducible suicide gene in the cells of interest. MAFIA mice for instance express GFP and a drug-inducible suicide gene under control of the *c-fms*

promoter (encoding M-CSFR) that induces Fas-mediated apoptosis when the dimerising drug is administered (Burnett et al., 2004). However, depletion of macrophages in MAFIA mice required injections of the dimeriser during multiple days and the depletion was not complete, indicating that the use of inducible suicide genes for cell ablation *in vivo* may not be as efficient and fast as with a DTR-based system or CreERT2-DTA-based system (Burnett et al., 2004). Advantages and limitations of inducible depletion systems should therefore be carefully considered when generating novel transgenic mice to inducibly deplete cell populations.

To facilitate microscopic analyses of DC subsets, these cells should be labelled with fluorescent proteins. Many different fluorescent proteins are available and the decision on which one(s) to use will mainly be based on their respective intensities and excitation and emission spectra. Furthermore, fluorescent proteins can be localised in the cytoplasm or targeted to the nucleus or membrane. The gene encoding the fluorescent protein can be placed under direct control of a cell-specific promoter, or alternatively, mice expressing Cre or CreERT2 in the desired population can be crossed to ROSA26 mice harbouring one or multiple fluorescent proteins. When CreERT2-expressing mice are used, inducible labelling can be achieved via the administration of tamoxifen. Many ROSA26 mice have been generated that express one fluorescent protein, such as YFP or dTomato, upon Cre-mediated recombination (Srinivas et al., 2001; Madisen et al., 2010). More complex models have also been developed, such as the ROSA26-mTmG mice that constitutively express membrane-bound Tomato before recombination and membrane-bound GFP after recombination, or ROSA26-confetti mice that stochastically express one of four fluorescent proteins upon Cre-mediated recombination (Muzumdar et al., 2007; Snippert et al., 2010). However, loxP recombination efficiency differs for different ROSA26 reporter lines which should be taken into account when designing experiments, for example when different ROSA26 reporter lines crossed to the same Cre driver are compared (Madisen *et al.*, 2010; J. Liu *et al.*, 2013).

In summary, the perfect mouse model to study DC biology does not exist and will never be generated as such, as the ideal transgenic model will differ depending on

the research question. However, a good toolbox to study DC biology *in vivo* should at least comprise of mice expressing constitutive or inducible Cre exclusively in all DCs, or in specific DC subsets. These mice can then be crossed to the many floxed mouse strains already available, such as the ROSA26 lines expressing DTR, DTA or fluorescent proteins, generating a flexible and versatile toolbox that can be used to study DC biology. This strategy crucially depends on the identification of promoters that are specific for all DCs or the different DC subsets, or when split-Cre or split-CreERT2 are used, on the identification of a promoter pair that is unique for the population intended to be manipulated.

Chapter 7. Appendix

The following publications are included as appendix:

van Blijswijk, J., Schraml, B. U. and Reis e Sousa, C. (2013) 'Advantages and limitations of mouse models to deplete dendritic cells.', *European journal of immunology*, 43(1), pp. 22–26. doi: 10.1002/eji.201243022.

van Blijswijk, J., Schraml, B. U., Rogers, N. C., Whitney, P. G., Zelenay, S., Acton, S. E. and Reis e Sousa, C. (2015) 'Altered lymph node composition in diphtheria toxin receptor-based mouse models to ablate dendritic cells.', *Journal of immunology (Baltimore, Md : 1950)*, 194(1), pp. 307–315. doi: 10.4049/jimmunol.1401999.

Reference List

Acton, S. E., Astarita, J. L., Malhotra, D., Lukacs-Kornek, V., Franz, B., Hess, P. R., Jakus, Z., Kuligowski, M., Fletcher, A. L., Elpek, K. G., Bellemare-Pelletier, A., Sceats, L., Reynoso, E. D., Gonzalez, S. F., Graham, D. B., Chang, J., Peters, A., Woodruff, M., Kim, Y.-A., Swat, W., Morita, T., Kuchroo, V., Carroll, M. C., Kahn, M. L., Wucherpfennig, K. W. and Turley, S. J. (2012) 'Podoplanin-rich stromal networks induce dendritic cell motility via activation of the C-type lectin receptor CLEC-2.', *Immunity*, 37(2), pp. 276–289. doi: 10.1016/j.immuni.2012.05.022.

Acton, S. E., Farrugia, A. J., Astarita, J. L., Mourão-Sá, D., Jenkins, R. P., Nye, E., Hooper, S., van Blijswijk, J., Rogers, N. C., Snelgrove, K. J., Rosewell, I., Moita, L. F., Stamp, G., Turley, S. J., Sahai, E. and Reis e Sousa, C. (2014) 'Dendritic cells control fibroblastic reticular network tension and lymph node expansion', *Nature*. Nature Publishing Group, 514(7523), pp. 498–502. doi: 10.1038/nature13814.

Adolfsson, J., Borge, O. J., Bryder, D., Theilgaard-Mönch, K., Astrand-Grundström, I., Sitnicka, E., Sasaki, Y. and Jacobsen, S. E. (2001) 'Upregulation of Flt3 expression within the bone marrow Lin(-)Sca1(+)c-kit(+) stem cell compartment is accompanied by loss of self-renewal capacity.', *Immunity*, 15(4), pp. 659–669.

Adolfsson, J., Månsson, R., Buza-Vidas, N., Hultquist, A., Liuba, K., Jensen, C. T., Bryder, D., Yang, L., Borge, O.-J., Thoren, L. A. M., Anderson, K., Sitnicka, E., Sasaki, Y., Sigvardsson, M. and Jacobsen, S. E. W. (2005) 'Identification of Flt3+ lympho-myeloid stem cells lacking erythro-megakaryocytic potential a revised road map for adult blood lineage commitment.', *Cell*, 121(2), pp. 295–306. doi: 10.1016/j.cell.2005.02.013.

Aldridge, J. R., Moseley, C. E., Boltz, D. A., Negovetich, N. J., Reynolds, C., Franks, J., Brown, S. A., Doherty, P. C., Webster, R. G. and Thomas, P. G. (2009) 'TNF/iNOS-producing dendritic cells are the necessary evil of lethal influenza virus infection.', *Proceedings of the National Academy of Sciences*, 106(13), pp. 5306–5311. doi: 10.1073/pnas.0900655106.

Aliberti, J., Schulz, O., Pennington, D. J., Tsujimura, H., Reis e Sousa, C., Ozato, K. and Sher, A. (2003) 'Essential role for ICSBP in the in vivo development of murine CD8alpha + dendritic cells.', *Blood*, 101(1), pp. 305–310. doi: 10.1182/blood-2002-04-1088.

Allan, R. S., Waithman, J., Bedoui, S., Jones, C. M., Villadangos, J. A., Zhan, Y., Lew, A. M., Shortman, K., Heath, W. R. and Carbone, F. R. (2006) 'Migratory dendritic cells transfer antigen to a lymph node-resident dendritic cell population for efficient CTL priming.', *Immunity*, 25(1), pp. 153–162. doi: 10.1016/j.immuni.2006.04.017.

Alliot, F., Godin, I. and Pessac, B. (1999) 'Microglia derive from progenitors, originating from the yolk sac, and which proliferate in the brain.', *Brain research. Developmental brain research*, 117(2), pp. 145–152.

Alvarez, D., Vollmann, E. H. and Andrian, von, U. H. (2008) 'Mechanisms and consequences of dendritic cell migration.', *Immunity*, 29(3), pp. 325–342. doi: 10.1016/j.immuni.2008.08.006.

Anderson, K. L., Perkin, H., Surh, C. D., Venturini, S., Maki, R. A. and Torbett, B. E. (2000) 'Transcription factor PU.1 is necessary for development of thymic and myeloid progenitor-derived dendritic cells.', *Journal of immunology (Baltimore, Md : 1950)*, 164(4), pp. 1855–1861.

Anjuère, F., Luci, C., Lebens, M., Rousseau, D., Hervouet, C., Milon, G., Holmgren, J., Ardavín, C. and Czerkinsky, C. (2004) 'In vivo adjuvant-induced mobilization and maturation of gut dendritic cells after oral administration of cholera toxin.', *Journal of immunology (Baltimore, Md : 1950)*, 173(8), pp. 5103–5111.

Arora, P., Baena, A., Yu, K. O. A., Saini, N. K., Kharkwal, S. S., Goldberg, M. F., Kunnath-Velayudhan, S., Carreño, L. J., Venkataswamy, M. M., Kim, J., Lazar-Molnar, E., Lauvau, G., Chang, Y.-T., Liu, Z., Bittman, R., Al-Shamkhani, A., Cox, L. R., Jervis, P. J., Veerapen, N., Besra, G. S. and Porcelli, S. A. (2014) 'A Single Subset of Dendritic Cells Controls the Cytokine Bias of Natural Killer T Cell Responses to Diverse Glycolipid Antigens', *Immunity*. The Authors, 40(1), pp. 105–116. doi: 10.1016/j.immuni.2013.12.004.

Astarita, J. L., Cremasco, V., Fu, J., Darnell, M. C., Peck, J. R., Nieves-Bonilla, J. M., Song, K., Kondo, Y., Woodruff, M. C., Gogineni, A., Onder, L., Ludewig, B., Weimer, R. M., Carroll, M. C., Mooney, D. J., Xia, L. and Turley, S. J. (2015) 'The CLEC-2-podoplanin axis controls the contractility of fibroblastic reticular cells and lymph node microarchitecture.', *Nature Immunology*, 16(1), pp. 75–84. doi: 10.1038/ni.3035.

Bachem, A., Hartung, E., Güttler, S., Mora, A., Zhou, X., Hegemann, A., Plantinga, M., Mazzini, E., Stoitzner, P., Gurka, S., Henn, V., Mages, H. W. and Kroczek, R. A. (2012) 'Expression of XCR1 Characterizes the Batf3-Dependent Lineage of Dendritic Cells Capable of Antigen Cross-Presentation.', *Frontiers in immunology*, 3, p. 214. doi: 10.3389/fimmu.2012.00214.

Backer, R., van Leeuwen, F., Kraal, G. and Haan, den, J. M. M. (2008) 'CD8-dendritic cells preferentially cross-present Saccharomyces cerevisiae antigens.', *European journal of immunology*, 38(2), pp. 370–380. doi: 10.1002/eji.200737647.

Bain, C. C., Bravo-Blas, A., Scott, C. L., Gomez Perdiguero, E., Geissmann, F., Henri, S., Malissen, B., Osborne, L. C., Artis, D. and Mowat, A. M. (2014) 'Constant replenishment from circulating monocytes maintains the macrophage pool in the intestine of adult mice', *Nature Immunology*, 15(10), pp. 929–937. doi: 10.1038/ni.2967.

Bain, C. C., Scott, C. L., Uronen-Hansson, H., Gudjonsson, S., Jansson, O., Grip, O., Guilliams, M., Malissen, B., Agace, W. W. and Mowat, A. M. (2013) 'Resident and pro-inflammatory macrophages in the colon represent alternative context-dependent fates of the same Ly6Chi monocyte precursors.', *Mucosal Immunology*, 6(3), pp. 498–510. doi: 10.1038/mi.2012.89.

Bajana, S., Roach, K., Turner, S., Paul, J. and Kovats, S. (2012) 'IRF4 Promotes Cutaneous Dendritic Cell Migration to Lymph Nodes during Homeostasis and Inflammation', *The Journal of Immunology*. doi: 10.4049/jimmunol.1102613.

Bajénoff, M., Egen, J. G., Koo, L. Y., Laugier, J. P., Brau, F., Glaichenhaus, N. and Germain, R. N. (2006) 'Stromal Cell Networks Regulate Lymphocyte Entry, Migration, and Territoriality in Lymph Nodes', *Immunity*, 25(6), pp. 989–1001. doi: 10.1016/j.immuni.2006.10.011.

Bajénoff, M., Granjeaud, S. and Guerder, S. (2003) 'The strategy of T cell antigen-presenting cell encounter in antigen-draining lymph nodes revealed by imaging of initial T cell activation.', *The Journal of experimental medicine*, 198(5), pp. 715–724. doi: 10.1084/jem.20030167.

Ballesteros-Tato, A., León, B., Lund, F. E. and Randall, T. D. (2010) 'Temporal changes in dendritic cell subsets, cross-priming and costimulation via CD70 control CD8(+) T cell responses to influenza.', *Nature Immunology*, 11(3), pp. 216–224. doi: 10.1038/ni.1838.

Bar-On, L. and Jung, S. (2010) 'Defining dendritic cells by conditional and constitutive cell ablation', *Immunological reviews*, 234(1), pp. 76–89. doi: 10.1111/j.0105-2896.2009.00875.x.

Bar-On, L., Birnberg, T., Lewis, K. L., Edelson, B. T., Bruder, D., Hildner, K., Buer, J., Murphy, K. M., Reizis, B. and Jung, S. (2010) 'CX3CR1+ CD8alpha+ dendritic cells are a steady-state population related to plasmacytoid dendritic cells.', *Proceedings of the National Academy of Sciences*, 107(33), pp. 14745–14750. doi: 10.1073/pnas.1001562107.

Becher, B., Schlitzer, A., Chen, J., Mair, F., Sumatoh, H. R., Teng, K. W. W., Low, D., Ruedl, C., Riccardi-Castagnoli, P., Poidinger, M., Greter, M., Ginhoux, F. and Newell, E. W. (2014) 'High-dimensional analysis of the murine myeloid cell system.', *Nature Immunology*, 15(12), pp. 1181–1189. doi: 10.1038/ni.3006.

Bedoui, S., Prato, S., Mintern, J., Gebhardt, T., Zhan, Y., Lew, A. M., Heath, W. R., Villadangos, J. A. and Segura, E. (2009) 'Characterization of an immediate splenic precursor of CD8+ dendritic cells capable of inducing antiviral T cell responses', *Journal of immunology (Baltimore, Md : 1950)*, 182(7), pp. 4200–4207. doi: 10.4049/jimmunol.0802286.

Bedoui, S., Whitney, P. G., Waithman, J., Eidsmo, L., Wakim, L., Caminschi, I., Allan, R. S., Wojtasiak, M., Shortman, K., Carbone, F. R., Brooks, A. G. and Heath, W. R. (2009) 'Cross-presentation of viral and self antigens by skin-derived CD103+ dendritic cells', *Nature Immunology*, 10(5), pp. 488–495. doi: 10.1038/ni.1724.

Belz, G. T., Behrens, G. M. N., Smith, C. M., Miller, J. F. A. P., Jones, C., Lejon, K., Fathman, C. G., Mueller, S. N., Shortman, K., Carbone, F. R. and Heath, W. R. (2002) 'The CD8alpha(+) dendritic cell is responsible for inducing peripheral self-tolerance to tissue-associated antigens.', *The Journal of experimental medicine*, 196(8), pp. 1099–1104.

Bennett, C. L., van Rijn, E., Jung, S., Inaba, K., Steinman, R. M., Kapsenberg, M. L. and Clausen, B. E. (2005) 'Inducible ablation of mouse Langerhans cells diminishes but fails to abrogate contact hypersensitivity.', *The Journal of cell biology*, 169(4), pp. 569–576. doi: 10.1083/jcb.200501071.

Birbeck, M. S., Breathnach, A. S. and Everall, J. D. (1961) 'An Electron Microscope Study of Basal Melanocytes and High-Level Clear Cells (Langerhans Cells) in Vitiligo', *The Journal of investigative dermatology*, 37(1), pp. 51–63.

Birnberg, T., Bar-On, L., Sapoznikov, A., Caton, M. L., Cervantes-Barragán, L., Makia, D., Krauthgamer, R., Brenner, O., Ludewig, B., Brockschnieder, D., Riethmacher, D., Reizis, B. and Jung, S. (2008) 'Lack of conventional dendritic cells is compatible with normal development and T cell homeostasis, but causes myeloid proliferative syndrome.', *Immunity*, 29(6), pp. 986–997. doi: 10.1016/j.immuni.2008.10.012.

Blasius, A. L. (2006) 'Siglec-H is an IPC-specific receptor that modulates type I IFN secretion through DAP12', *Blood*, 107(6), pp. 2474–2476. doi: 10.1182/blood-2005-09-3746.

Blasius, A. L., Giurisato, E., Cella, M., Schreiber, R. D., Shaw, A. S. and Colonna, M. (2006) 'Bone marrow stromal cell antigen 2 is a specific marker of type I IFN-producing cells in the naive mouse, but a promiscuous cell surface antigen following IFN stimulation.', *Journal of immunology (Baltimore, Md : 1950)*, 177(5), pp. 3260–3265.

Bobr, A., Olvera-Gomez, I., Igyarto, B. Z., Haley, K. M., Hogquist, K. A. and Kaplan, D. H. (2010) 'Acute ablation of Langerhans cells enhances skin immune responses.', *The Journal of Immunology*, 185(8), pp. 4724–4728. doi: 10.4049/jimmunol.1001802.

Bogunovic, M., Ginhoux, F., Helft, J., Shang, L., Hashimoto, D., Greter, M., Liu, K., Jakubzick, C., Ingersoll, M. A., Leboeuf, M., Stanley, E. R., Nussenzweig, M., Lira, S. A., Randolph, G. J. and Merad, M. (2009) 'Origin of the lamina propria dendritic cell network.', *Immunity*, 31(3), pp. 513–525. doi: 10.1016/j.immuni.2009.08.010.

Boillée, S., Yamanaka, K., Lobsiger, C. S., Copeland, N. G., Jenkins, N. A., Kassiotis, G., Kollias, G. and Cleveland, D. W. (2006) 'Onset and progression in inherited ALS determined by motor neurons and microglia.', *Science (New York, NY)*, 312(5778), pp. 1389–1392. doi: 10.1126/science.1123511.

Bonifaz, L. C., Bonnyay, D. P., Charalambous, A., Darguste, D. I., Fujii, S.-I., Soares, H., Brimnes, M. K., Moltedo, B., Moran, T. M. and Steinman, R. M. (2004) 'In vivo targeting of antigens to maturing dendritic cells via the DEC-205 receptor improves T cell vaccination.', *The Journal of experimental medicine*, 199(6), pp. 815–824. doi: 10.1084/jem.20032220.

Bonifaz, L., Bonnyay, D., Mahnke, K., Rivera, M., Nussenzweig, M. C. and Steinman, R. M. (2002) 'Efficient targeting of protein antigen to the dendritic cell receptor DEC-205 in the steady state leads to antigen presentation on major histocompatibility complex class I products and peripheral CD8+ T cell tolerance.',

The Journal of experimental medicine, 196(12), pp. 1627–1638.

Borges da Silva, H., Fonseca, R., Cassado, A. D. A., Machado de Salles, É., de Menezes, M. N., Langhorne, J., Perez, K. R., Cuccovia, I. M., Ryffel, B., Barreto, V. M., Marinho, C. R. F., Boscardin, S. B., Álvarez, J. M., D'Império-Lima, M. R. and Tadokoro, C. E. (2015) 'In Vivo Approaches Reveal a Key Role for DCs in CD4+ T Cell Activation and Parasite Clearance during the Acute Phase of Experimental Blood-Stage Malaria.', *PLoS pathogens*, 11(2), p. e1004598. doi: 10.1371/journal.ppat.1004598.

Boring, L., Gosling, J., Chensue, S. W., Kunkel, S. L., Farese, R. V., Broxmeyer, H. E. and Charo, I. F. (1997) 'Impaired monocyte migration and reduced type 1 (Th1) cytokine responses in C-C chemokine receptor 2 knockout mice.', *The Journal of clinical investigation*, 100(10), pp. 2552–2561. doi: 10.1172/JCI119798.

Borkowski, T. A., Letterio, J. J., Farr, A. G. and Udey, M. C. (1996) 'A role for endogenous transforming growth factor beta 1 in Langerhans cell biology: the skin of transforming growth factor beta 1 null mice is devoid of epidermal Langerhans cells.', *The Journal of experimental medicine*, 184(6), pp. 2417–2422.

Boscardin, S. B., Hafalla, J. C. R., Masilamani, R. F., Kamphorst, A. O., Zebroski, H. A., Rai, U., Morrot, A., Zavala, F., Steinman, R. M., Nussenzweig, R. S. and Nussenzweig, M. C. (2006) 'Antigen targeting to dendritic cells elicits long-lived T cell help for antibody responses.', *The Journal of experimental medicine*, 203(3), pp. 599–606. doi: 10.1084/jem.20051639.

Brasel, K., De Smedt, T., Smith, J. L. and Maliszewski, C. R. (2000) 'Generation of murine dendritic cells from flt3-ligand-supplemented bone marrow cultures.', *Blood*, 96(9), pp. 3029–3039.

Buch, T., Heppner, F. L., Tertilt, C., Heinen, T. J. A. J., Kremer, M., Wunderlich, F. T., Jung, S. and Waisman, A. (2005) 'A Cre-inducible diphtheria toxin receptor mediates cell lineage ablation after toxin administration.', *Nature Methods*, 2(6), pp. 419–426. doi: 10.1038/nmeth762.

Burnett, S. H., Kershen, E. J., Zhang, J., Zeng, L., Straley, S. C., Kaplan, A. M. and Cohen, D. A. (2004) 'Conditional macrophage ablation in transgenic mice expressing a Fas-based suicide gene.', *Journal of leukocyte biology*, 75(4), pp. 612–623. doi: 10.1189/jlb.0903442.

Bursch, L. S., Wang, L., Igyarto, B., Kissenpfennig, A., Malissen, B., Kaplan, D. H. and Hogquist, K. A. (2007) 'Identification of a novel population of Langerin+ dendritic cells', 204(13), pp. 3147–3156. doi: 10.1084/jem.20071966.

Busch, K., Klapproth, K., Barile, M., Flossdorf, M., Holland-Letz, T., Schlenner, S. M., Reth, M., Höfer, T. and Rodewald, H.-R. (2015) 'Fundamental properties of unperturbed haematopoiesis from stem cells in vivo', *Nature*. doi: 10.1038/nature14242.

Caminschi, I., Proietto, A. I., Ahmet, F., Kitsoulis, S., Shin Teh, J., Lo, J. C. Y., Rizzitelli, A., Wu, L., Vremec, D., van Dommelen, S. L. H., Campbell, I. K.,

Maraskovsky, E., Braley, H., Davey, G. M., Mottram, P., van de Velde, N., Jensen, K., Lew, A. M., Wright, M. D., Heath, W. R., Shortman, K. and Lahoud, M. H. (2008) 'The dendritic cell subtype-restricted C-type lectin Clec9A is a target for vaccine enhancement.', *Blood*, 112(8), pp. 3264–3273. doi: 10.1182/blood-2008-05-155176.

Campbell, D. J. and Butcher, E. C. (2002) 'Rapid acquisition of tissue-specific homing phenotypes by CD4(+) T cells activated in cutaneous or mucosal lymphoid tissues.', *The Journal of experimental medicine*, 195(1), pp. 135–141.

Campbell, J. J., Bowman, E. P., Murphy, K., Youngman, K. R., Siani, M. A., Thompson, D. A., Wu, L., Zlotnik, A. and Butcher, E. C. (1998) '6-C-kine (SLC), a lymphocyte adhesion-triggering chemokine expressed by high endothelium, is an agonist for the MIP-3beta receptor CCR7.', *The Journal of cell biology*, 141(4), pp. 1053–1059.

Carotta, S., Dakic, A., D'Amico, A., Pang, S. H. M., Greig, K. T., Nutt, S. L. and Wu, L. (2010) 'The transcription factor PU.1 controls dendritic cell development and Flt3 cytokine receptor expression in a dose-dependent manner.', *Immunity*, 32(5), pp. 628–641. doi: 10.1016/j.immuni.2010.05.005.

Carter, P. B. and Collins, F. M. (1974) 'The route of enteric infection in normal mice.', *The Journal of experimental medicine*, 139(5), pp. 1189–1203.

Caton, M. L., Smith-Raska, M. R. and Reizis, B. (2007) 'Notch-RBP-J signaling controls the homeostasis of CD8- dendritic cells in the spleen.', *The Journal of experimental medicine*, 204(7), pp. 1653–1664. doi: 10.1084/jem.20062648.

Cecchini, M. G., Dominguez, M. G., Mocci, S., Wetterwald, A., Felix, R., Fleisch, H., Chisholm, O., Hofstetter, W., Pollard, J. W. and Stanley, E. R. (1994) 'Role of colony stimulating factor-1 in the establishment and regulation of tissue macrophages during postnatal development of the mouse.', *Development*, 120(6), pp. 1357–1372.

Cella, M., Engering, A., Pinet, V., Pieters, J. and Lanzavecchia, A. (1997) 'Inflammatory stimuli induce accumulation of MHC class II complexes on dendritic cells.', *Nature*, 388(6644), pp. 782–787. doi: 10.1038/42030.

Cerovic, V., Houston, S. A., Scott, C. L., Aumeunier, A., Yrlid, U., Mowat, A. M. and Milling, S. W. F. (2013) 'Intestinal CD103(-) dendritic cells migrate in lymph and prime effector T cells.', *Mucosal Immunology*, 6(1), pp. 104–113. doi: 10.1038/mi.2012.53.

Chapman, T. J. and Georas, S. N. (2013) 'Adjuvant effect of diphtheria toxin after mucosal administration in both wild type and diphtheria toxin receptor engineered mouse strains.', *Journal of Immunological Methods*, 400-401, pp. 122–126. doi: 10.1016/j.jim.2013.10.010.

Cheong, C., Matos, I., Choi, J.-H., Dandamudi, D. B., Shrestha, E., Longhi, M. P., Jeffrey, K. L., Anthony, R. M., Kluger, C., Nchinda, G., Koh, H., Rodriguez, A., Idoyaga, J., Pack, M., Velinzon, K., Park, C. G. and Steinman, R. M. (2010)

'Microbial stimulation fully differentiates monocytes to DC-SIGN/CD209(+) dendritic cells for immune T cell areas.', *Cell*, 143(3), pp. 416–429. doi: 10.1016/j.cell.2010.09.039.

Chieppa, M., Rescigno, M., Huang, A. Y. C. and Germain, R. N. (2006) 'Dynamic imaging of dendritic cell extension into the small bowel lumen in response to epithelial cell TLR engagement.', *The Journal of experimental medicine*, 203(13), pp. 2841–2852. doi: 10.1084/jem.20061884.

Choi, Y. S., Kageyama, R., Eto, D., Escobar, T. C., Johnston, R. J., Monticelli, L., Lao, C. and Crotty, S. (2011) 'ICOS receptor instructs T follicular helper cell versus effector cell differentiation via induction of the transcriptional repressor Bcl6.', *Immunity*, 34(6), pp. 932–946. doi: 10.1016/j.immuni.2011.03.023.

Chorro, L., Sarde, A., Li, M., Woollard, K. J., Chambon, P., Malissen, B., Kissenpfennig, A., Barbaroux, J.-B., Groves, R. and Geissmann, F. (2009) 'Langerhans cell (LC) proliferation mediates neonatal development, homeostasis, and inflammation-associated expansion of the epidermal LC network.', *The Journal of experimental medicine*, 206(13), pp. 3089–3100. doi: 10.1084/jem.20091586.

Chyou, S., Benahmed, F., Chen, J., Kumar, V., Tian, S., Lipp, M. and Lu, T. T. (2011) 'Coordinated regulation of lymph node vascular-stromal growth first by CD11c+ cells and then by T and B cells.', *The Journal of Immunology*, 187(11), pp. 5558–5567. doi: 10.4049/jimmunol.1101724.

Ciavarra, R. P., Stephens, A., Nagy, S., Sekellick, M. and Steel, C. (2006) 'Evaluation of immunological paradigms in a virus model: are dendritic cells critical for antiviral immunity and viral clearance?', *Journal of immunology (Baltimore, Md : 1950)*, 177(1), pp. 492–500.

Cisse, B., Caton, M. L., Lehner, M., Maeda, T., Scheu, S., Locksley, R., Holmberg, D., Zweier, C., Hollander, den, N. S., Kant, S. G., Holter, W., Rauch, A., Zhuang, Y. and Reizis, B. (2008) 'Transcription factor E2-2 is an essential and specific regulator of plasmacytoid dendritic cell development.', *Cell*, 135(1), pp. 37–48. doi: 10.1016/j.cell.2008.09.016.

Coombes, J. L., Siddiqui, K. R. R., Arancibia-Cárcamo, C. V., Hall, J., Sun, C.-M., Belkaid, Y. and Powrie, F. (2007) 'A functionally specialized population of mucosal CD103+ DCs induces Foxp3+ regulatory T cells via a TGF-beta and retinoic acid-dependent mechanism.', *The Journal of experimental medicine*, 204(8), pp. 1757–1764. doi: 10.1084/jem.20070590.

Copin, R., De Baetselier, P., Carlier, Y., Letesson, J.-J. and Muraille, E. (2007) 'MyD88-dependent activation of B220-CD11b+LY-6C+ dendritic cells during Brucella melitensis infection.', *Journal of immunology (Baltimore, Md : 1950)*, 178(8), pp. 5182–5191.

Corcoran, L., Ferrero, I., Vremec, D., Lucas, K., Waithman, J., O'Keeffe, M., Wu, L., Wilson, A. and Shortman, K. (2003) 'The lymphoid past of mouse plasmacytoid cells and thymic dendritic cells.', *Journal of immunology (Baltimore, Md : 1950)*, 170(10), pp. 4926–4932.

Crozat, K., Tamoutounour, S., Vu Manh, T.-P., Fossum, E., Luche, H., Ardouin, L., Guilliams, M., Azukizawa, H., Bogen, B., Malissen, B., Henri, S. and Dalod, M. (2011) 'Cutting Edge: Expression of XCR1 Defines Mouse Lymphoid-Tissue Resident and Migratory Dendritic Cells of the CD8 + Type', *Journal of immunology (Baltimore, Md : 1950)*, 187(9), pp. 4411–4415. doi: 10.4049/jimmunol.1101717.

Davey, G. M., Kurts, C., Miller, J. F. A. P., Bouillet, P., Strasser, A., Brooks, A. G., Carbone, F. R. and Heath, W. R. (2002) 'Peripheral deletion of autoreactive CD8 T cells by cross presentation of self-antigen occurs by a Bcl-2-inhibitable pathway mediated by Bim.', *The Journal of experimental medicine*, 196(7), pp. 947–955.

Davies, L. C., Jenkins, S. J., Allen, J. E. and Taylor, P. R. (2013) 'Tissue-resident macrophages', *Nature Immunology*, 14(10), pp. 986–995. doi: 10.1038/ni.2705.

de Heer, H. J. (2004) 'Essential Role of Lung Plasmacytoid Dendritic Cells in Preventing Asthmatic Reactions to Harmless Inhaled Antigen', *Journal of Experimental Medicine*, 200(1), pp. 89–98. doi: 10.1084/jem.20040035.

De Trez, C., Magez, S., Akira, S., Ryffel, B., Carlier, Y. and Muraille, E. (2009) 'iNOS-producing inflammatory dendritic cells constitute the major infected cell type during the chronic Leishmania major infection phase of C57BL/6 resistant mice.', *PLoS pathogens*, 5(6), p. e1000494. doi: 10.1371/journal.ppat.1000494.

del Rio, M.-L., Rodriguez-Barbosa, J.-I., Kremmer, E. and Förster, R. (2007) 'CD103- and CD103+ bronchial lymph node dendritic cells are specialized in presenting and cross-presenting innocuous antigen to CD4+ and CD8+ T cells.', *Journal of immunology (Baltimore, Md : 1950)*, 178(11), pp. 6861–6866.

Denning, T. L., Norris, B. A., Medina-Contreras, O., Manicassamy, S., Geem, D., Madan, R., Karp, C. L. and Pulendran, B. (2011) 'Functional specializations of intestinal dendritic cell and macrophage subsets that control Th17 and regulatory T cell responses are dependent on the T cell/APC ratio, source of mouse strain, and regional localization.', *The Journal of Immunology*, 187(2), pp. 733–747. doi: 10.4049/jimmunol.1002701.

Denning, T. L., Wang, Y.-C., Patel, S. R., Williams, I. R. and Pulendran, B. (2007) 'Lamina propria macrophages and dendritic cells differentially induce regulatory and interleukin 17-producing T cell responses.', *Nature Immunology*, 8(10), pp. 1086–1094. doi: 10.1038/ni1511.

Diehl, G. E., Longman, R. S., Zhang, J.-X., Breart, B., Galan, C., Cuesta, A., Schwab, S. R. and Littman, D. R. (2013) 'Microbiota restricts trafficking of bacteria to mesenteric lymph nodes by CX3CR1hi cells', *Nature*. Nature Publishing Group, 494(7435), pp. 116–120. doi: 10.1038/nature11809.

Dudda, J. C., Simon, J. C. and Martin, S. (2004) 'Dendritic cell immunization route determines CD8+ T cell trafficking to inflamed skin: role for tissue microenvironment and dendritic cells in establishment of T cell-homing subsets.', *Journal of immunology (Baltimore, Md : 1950)*, 172(2), pp. 857–863.

Dudziak, D., Kamphorst, A. O., Heidkamp, G. F., Buchholz, V. R., Trumpfheller, C.,

Yamazaki, S., Cheong, C., Liu, K., Lee, H.-W., Park, C. G., Steinman, R. M. and Nussenzweig, M. C. (2007) 'Differential antigen processing by dendritic cell subsets in vivo.', *Science (New York, NY)*, 315(5808), pp. 107–111. doi: 10.1126/science.1136080.

Duffield, J. S., Forbes, S. J., Constandinou, C. M., Clay, S., Partolina, M., Vuthoori, S., Wu, S., Lang, R. and Iredale, J. P. (2005) 'Selective depletion of macrophages reveals distinct, opposing roles during liver injury and repair.', *The Journal of clinical investigation*, 115(1), pp. 56–65. doi: 10.1172/JCI22675.

Edelson, B. T., Bradstreet, T. R., Kc, W., Hildner, K., Herzog, J. W., Sim, J., Russell, J. H., Murphy, T. L., Unanue, E. R. and Murphy, K. M. (2011) 'Batf3-dependent CD11b(low/-) peripheral dendritic cells are GM-CSF-independent and are not required for Th cell priming after subcutaneous immunization.', *PloS one*, 6(10), p. e25660. doi: 10.1371/journal.pone.0025660.

Edelson, B. T., Kc, W., Juang, R., Kohyama, M., Benoit, L. A., Klekotka, P. A., Moon, C., Albring, J. C., Ise, W., Michael, D. G., Bhattacharya, D., Stappenbeck, T. S., Holtzman, M. J., Sung, S.-S. J., Murphy, T. L., Hildner, K. and Murphy, K. M. (2010) 'Peripheral CD103+ dendritic cells form a unified subset developmentally related to CD8alpha+ conventional dendritic cells.', *Journal of Experimental Medicine*, 207(4), pp. 823–836. doi: 10.1084/jem.20091627.

Edwards, A. D., Chaussabel, D., Tomlinson, S., Schulz, O., Sher, A. and Reis e Sousa, C. (2003) 'Relationships among murine CD11c(high) dendritic cell subsets as revealed by baseline gene expression patterns.', *Journal of immunology (Baltimore, Md : 1950)*, 171(1), pp. 47–60.

Eidsmo, L., Allan, R., Caminschi, I., Van Rooijen, N., Heath, W. R. and Carbone, F. R. (2009) 'Differential Migration of Epidermal and Dermal Dendritic Cells during Skin Infection', *The Journal of Immunology*, 182(5), pp. 3165–3172. doi: 10.4049/jimmunol.0802950.

Epelman, S., Lavine, K. J., Beaudin, A. E., Sojka, D. K., Carrero, J. A., Calderon, B., Brija, T., Gautier, E. L., Ivanov, S., Satpathy, A. T., Schilling, J. D., Schwendener, R., Sergin, I., Razani, B., Forsberg, E. C., Yokoyama, W. M., Unanue, E. R., Colonna, M., Randolph, G. J. and Mann, D. L. (2014) 'Embryonic and adult-derived resident cardiac macrophages are maintained through distinct mechanisms at steady state and during inflammation.', *Immunity*, 40(1), pp. 91–104. doi: 10.1016/j.immuni.2013.11.019.

Farkas, L., Beiske, K., Lund-Johansen, F., Brandtzaeg, P. and Jahnsen, F. L. (2001) 'Plasmacytoid dendritic cells (natural interferon- alpha/beta-producing cells) accumulate in cutaneous lupus erythematosus lesions.', *The American Journal of Pathology*, 159(1), pp. 237–243.

Farrand, K. J., Dickgreber, N., Stoitzner, P., Ronchese, F., Petersen, T. R. and Hermans, I. F. (2009) 'Langerin+ CD8alpha+ dendritic cells are critical for cross-priming and IL-12 production in response to systemic antigens.', *The Journal of Immunology*, 183(12), pp. 7732–7742. doi: 10.4049/jimmunol.0902707.

Fei, M., Bhatia, S., Oriss, T. B., Yarlagadda, M., Khare, A., Akira, S., Saijo, S., Iwakura, Y., Fallert Junecko, B. A., Reinhart, T. A., Foreman, O., Ray, P., Kolls, J. and Ray, A. (2011) 'TNF-alpha from inflammatory dendritic cells (DCs) regulates lung IL-17A/IL-5 levels and neutrophilia versus eosinophilia during persistent fungal infection.', *Proceedings of the National Academy of Sciences*, 108(13), pp. 5360–5365. doi: 10.1073/pnas.1015476108.

Ferron, M. and Vacher, J. (2005) 'Targeted expression of Cre recombinase in macrophages and osteoclasts in transgenic mice.', *Genesis (New York, NY : 2000)*, 41(3), pp. 138–145. doi: 10.1002/gene.20108.

Fogg, D. K. (2006) 'A Clonogenic Bone Marrow Progenitor Specific for Macrophages and Dendritic Cells', *Science (New York, NY)*, 311(5757), pp. 83–87. doi: 10.1126/science.1117729.

Fossum, E., Grødeland, G., Terhorst, D., Tveita, A. A., Vikse, E., Mjaaland, S., Henri, S., Malissen, B. and Bogen, B. (2015) 'Vaccine molecules targeting Xcr1 on cross-presenting DCs induce protective CD8+ T-cell responses against influenza virus.', *European journal of immunology*, 45(2), pp. 624–635. doi: 10.1002/eji.201445080.

Förster, R. R., Schubel, A. A., Breitfeld, D. D., Kremmer, E. E., Renner-Müller, I. I., Wolf, E. E. and Lipp, M. M. (1999) 'CCR7 Coordinates the Primary Immune Response by Establishing Functional Microenvironments in Secondary Lymphoid Organs', *Cell*, 99(1), pp. 11–11. doi: 10.1016/S0092-8674(00)80059-8.

Förster, R., Davalos-Misslitz, A. C. and Rot, A. (2008) 'CCR7 and its ligands: balancing immunity and tolerance.', *Nature Reviews Immunology*, 8(5), pp. 362–371. doi: 10.1038/nri2297.

Fujimoto, K., Karuppuchamy, T., Takemura, N., Shimohigoshi, M., Machida, T., Haseda, Y., Aoshi, T., Ishii, K. J., Akira, S. and Uematsu, S. (2011) 'A new subset of CD103+CD8alpha+ dendritic cells in the small intestine expresses TLR3, TLR7, and TLR9 and induces Th1 response and CTL activity.', *The Journal of Immunology*, 186(11), pp. 6287–6295. doi: 10.4049/jimmunol.1004036.

Fukaya, T., Murakami, R., Takagi, H., Sato, K., Sato, Y., Otsuka, H., Ohno, M., Hijikata, A., Ohara, O., Hikida, M., Malissen, B. and Sato, K. (2012) 'Conditional ablation of CD205+ conventional dendritic cells impacts the regulation of T-cell immunity and homeostasis in vivo.', *Proceedings of the National Academy of Sciences*, 109(28), pp. 11288–11293. doi: 10.1073/pnas.1202208109.

Gaboriau-Routhiau, V., Rakotobe, S., Lécuyer, E., Mulder, I., Lan, A., Bridonneau, C., Rochet, V., Pisi, A., De Paepe, M., Brandi, G., Eberl, G., Snel, J., Kelly, D. and Cerf-Bensussan, N. (2009) 'The key role of segmented filamentous bacteria in the coordinated maturation of gut helper T cell responses.', *Immunity*, 31(4), pp. 677–689. doi: 10.1016/j.immuni.2009.08.020.

Gao, Y., Nish, S. A., Jiang, R., Hou, L., Licona-Limón, P., Weinstein, J. S., Zhao, H. and Medzhitov, R. (2013) 'Control of T Helper 2 Responses by Transcription Factor IRF4-Dependent Dendritic Cells', *Immunity*. Elsevier Inc., 39(4), pp. 722–732. doi:

10.1016/j.immuni.2013.08.028.

Gascoyne, D. M., Long, E., Veiga-Fernandes, H., de Boer, J., Williams, O., Seddon, B., Coles, M., Kioussis, D. and Brady, H. J. M. (2009) 'The basic leucine zipper transcription factor E4BP4 is essential for natural killer cell development.', *Nature Immunology*, 10(10), pp. 1118–1124. doi: 10.1038/ni.1787.

Gautier, E. L., Shay, T., Miller, J., Greter, M., Jakubzick, C., Ivanov, S., Helft, J., Chow, A., Elpek, K. G., Gordonov, S., Mazloom, A. R., Ma'ayan, A., Chua, W.-J., Hansen, T. H., Turley, S. J., Merad, M., Randolph, G. J., Gautier, E. L., Jakubzick, C., Randolph, G. J., Best, A. J., Knell, J., Goldrath, A., Miller, J., Brown, B., Merad, M., Jojic, V., Koller, D., Cohen, N., Brennan, P., Brenner, M., Shay, T., Regev, A., Fletcher, A., Elpek, K., Bellemare-Pelletier, A., Malhotra, D., Turley, S., Jianu, R., Laidlaw, D., Collins, J., Narayan, K., Sylvia, K., Kang, J., Gazit, R., Garrison, B. S., Rossi, D. J., Kim, F., Rao, T. N., Wagers, A., Shinton, S. A., Hardy, R. R., Monach, P., Bezman, N. A., Sun, J. C., Kim, C. C., Lanier, L. L., Heng, T., Kreslavsky, T., Painter, M., Ericson, J., Davis, S., Mathis, D. and Benoist, C. (2012) 'Gene-expression profiles and transcriptional regulatory pathways that underlie the identity and diversity of mouse tissue macrophages', *Nature Immunology*, 13(11), pp. 1118–1128. doi: 10.1038/ni.2419.

Gaya, M., Castello, A., Montaner, B., Rogers, N., Reis e Sousa, C., Bruckbauer, A. and Batista, F. D. (2015) 'Host response. Inflammation-induced disruption of SCS macrophages impairs B cell responses to secondary infection.', *Science (New York, NY)*, 347(6222), pp. 667–672. doi: 10.1126/science.aaa1300.

Gazzinelli, R. T., Hieny, S., Wynn, T. A., Wolf, S. and Sher, A. (1993) 'Interleukin 12 is required for the T-lymphocyte-independent induction of interferon gamma by an intracellular parasite and induces resistance in T-cell-deficient hosts.', *Proceedings of the National Academy of Sciences of the United States of America*, 90(13), pp. 6115–6119.

Geissmann, F., Gordon, S., Hume, D. A., Mowat, A. M. and Randolph, G. J. (2010) 'Unravelling mononuclear phagocyte heterogeneity.', *Nature Reviews Immunology*, 10(6), pp. 453–460. doi: 10.1038/nri2784.

Geissmann, F., Manz, M. G., Jung, S., Sieweke, M. H., Merad, M. and Ley, K. (2010) 'Development of monocytes, macrophages, and dendritic cells.', *Science (New York, NY)*, 327(5966), pp. 656–661. doi: 10.1126/science.1178331.

Gerner, M. Y., Kastenmuller, W., Ifrim, I., Kabat, J. and Germain, R. N. (2012) 'Histo-Cytometry: A Method for Highly Multiplex Quantitative Tissue Imaging Analysis Applied to Dendritic Cell Subset Microanatomy in Lymph Nodes', *Immunity*. Elsevier Inc., 37(2), pp. 364–376. doi: 10.1016/j.immuni.2012.07.011.

Gerner, M. Y., Torabi-Parizi, P. and Germain, R. N. (2015) 'Strategically Localized Dendritic Cells Promote Rapid T Cell Responses to Lymph-Borne Particulate Antigens', *Immunity*. Elsevier Inc., 42(1), pp. 172–185. doi: 10.1016/j.immuni.2014.12.024.

GeurtsvanKessel, C. H., Willart, M. A. M., van Rijt, L. S., Muskens, F., Kool, M.,

Baas, C., Thielemans, K., Bennett, C., Clausen, B. E., Hoogsteden, H. C., Osterhaus, A. D. M. E., Rimmelzwaan, G. F. and Lambrecht, B. N. (2008) 'Clearance of influenza virus from the lung depends on migratory langerin+CD11b- but not plasmacytoid dendritic cells', *The Journal of experimental medicine*, 205(7), pp. 1621–1634. doi: 10.1084/jem.20071365.

Ghigo, C., Mondor, I., Jorquera, A., Nowak, J., Wienert, S., Zahner, S. P., Clausen, B. E., Luche, H., Malissen, B., Klauschen, F. and Bajénoff, M. (2013) 'Multicolor fate mapping of Langerhans cell homeostasis.', *Journal of Experimental Medicine*, 210(9), pp. 1657–1664. doi: 10.1084/jem.20130403.

Ghosh, H. S., Cisse, B., Bunin, A., Lewis, K. L. and Reizis, B. (2010) 'Continuous expression of the transcription factor e2-2 maintains the cell fate of mature plasmacytoid dendritic cells.', *Immunity*, 33(6), pp. 905–916. doi: 10.1016/j.immuni.2010.11.023.

Ginhoux, F., Collin, M. P., Bogunovic, M., Abel, M., Leboeuf, M., Helft, J., Ochando, J., Kissenpfennig, A., Malissen, B., Grisotto, M., Snoeck, H., Randolph, G. and Merad, M. (2007) 'Blood-derived dermal langerin+ dendritic cells survey the skin in the steady state.', *Journal of Experimental Medicine*, 204(13), pp. 3133–3146. doi: 10.1084/jem.20071733.

Ginhoux, F., Greter, M., Leboeuf, M., Nandi, S., See, P., Gokhan, S., Mehler, M. F., Conway, S. J., Ng, L. G., Stanley, E. R., Samokhvalov, I. M. and Merad, M. (2010) 'Fate mapping analysis reveals that adult microglia derive from primitive macrophages.', *Science (New York, NY)*, 330(6005), pp. 841–845. doi: 10.1126/science.1194637.

Ginhoux, F., Liu, K., Helft, J., Bogunovic, M., Greter, M., Hashimoto, D., Price, J., Yin, N., Bromberg, J., Lira, S. A., Stanley, E. R., Nussenzweig, M. and Merad, M. (2009) 'The origin and development of nonlymphoid tissue CD103+ DCs.', *Journal of Experimental Medicine*, 206(13), pp. 3115–3130. doi: 10.1084/jem.20091756.

Ginhoux, F., Tacke, F., Angeli, V., Bogunovic, M., Loubeau, M., Dai, X.-M., Stanley, E. R., Randolph, G. J. and Merad, M. (2006) 'Langerhans cells arise from monocytes in vivo.', *Nature Immunology*, 7(3), pp. 265–273. doi: 10.1038/ni1307.

Goenka, R., Barnett, L. G., Silver, J. S., O'Neill, P. J., Hunter, C. A., Cancro, M. P. and Laufer, T. M. (2011) 'Cutting edge: dendritic cell-restricted antigen presentation initiates the follicular helper T cell program but cannot complete ultimate effector differentiation.', *The Journal of Immunology*, 187(3), pp. 1091–1095. doi: 10.4049/jimmunol.1100853.

Gosselin, D., Link, V. M., Romanoski, C. E., Fonseca, G. J., Eichenfield, D. Z., Spann, N. J., Stender, J. D., Chun, H. B., Garner, H., Geissmann, F. and Glass, C. K. (2014) 'Environment Drives Selection and Function of Enhancers Controlling Tissue-Specific Macrophage Identities', *Cell*. Elsevier Inc., 159(6), pp. 1327–1340. doi: 10.1016/j.cell.2014.11.023.

Goto, Y., Panea, C., Nakato, G., Cebula, A., Lee, C., Diez, M. G., Laufer, T. M., Ignatowicz, L. and Ivanov, I. I. (2014) 'Segmented Filamentous Bacteria Antigens

Presented by Intestinal Dendritic Cells Drive Mucosal Th17 Cell Differentiation', *Immunity*. Elsevier Inc., pp. 1–14. doi: 10.1016/j.immuni.2014.03.005.

Grajales-Reyes, G. E., Iwata, A., Albring, J. O. R., Wu, X., Tussiwand, R., Kc, W., Kretzer, N. M., o, C. G. B. N., Durai, V., Bagadia, P., Haldar, M., nheit, J. O. R. S. O., Rosenbauer, F., Murphy, T. L. and Murphy, K. M. (2015) 'Batf3 maintains autoactivation of Irf8 for commitment of a CD8a', *Nature Immunology*. Nature Publishing Group, pp. 1–12. doi: 10.1038/ni.3197.

Gray, E. E. and Cyster, J. G. (2012) 'Lymph Node Macrophages', *Journal of innate immunity*, 4(5-6), pp. 424–436. doi: 10.1159/000337007.

Greter, M., Helft, J., Chow, A., Hashimoto, D., Mortha, A., Agudo-Cantero, J., Bogunovic, M., Gautier, E. L., Miller, J., Leboeuf, M., Lu, G., Aloman, C., Brown, B. D., Pollard, J. W., Xiong, H., Randolph, G. J., Chipuk, J. E., Frenette, P. S. and Merad, M. (2012) 'GM-CSF Controls Nonlymphoid Tissue Dendritic Cell Homeostasis but Is Dispensable for the Differentiation of Inflammatory Dendritic Cells', *Immunity*. Elsevier Inc., 36(6), pp. 1031–1046. doi: 10.1016/j.immuni.2012.03.027.

Greter, M., Lelios, I., Pelczar, P., Hoeffel, G., Price, J., Leboeuf, M., Kündig, T. M., Frei, K., Ginhoux, F., Merad, M. and Becher, B. (2012) 'Stroma-derived interleukin-34 controls the development and maintenance of langerhans cells and the maintenance of microglia.', *Immunity*, 37(6), pp. 1050–1060. doi: 10.1016/j.immuni.2012.11.001.

Guerriero, A., Langmuir, P. B., Spain, L. M. and Scott, E. W. (2000) 'PU.1 is required for myeloid-derived but not lymphoid-derived dendritic cells.', *Blood*, 95(3), pp. 879–885.

Guilliams, M., Crozat, K., Henri, S., Tamoutounour, S., Grenot, P., Devilard, E., de Bovis, B., Alexopoulou, L., Dalod, M. and Malissen, B. (2010) 'Skin-draining lymph nodes contain dermis-derived CD103(-) dendritic cells that constitutively produce retinoic acid and induce Foxp3(+) regulatory T cells.', *Blood*, 115(10), pp. 1958–1968. doi: 10.1182/blood-2009-09-245274.

Guilliams, M., Ginhoux, F., Jakubzick, C., Naik, S. H., Onai, N., Schraml, B. U., Segura, E., Tussiwand, R. and Yona, S. (2014) 'Dendritic cells, monocytes and macrophages: a unified nomenclature based on ontogeny.', *Nature Reviews Immunology*. doi: 10.1038/nri3712.

Gunn, M. D., Kyuwa, S., Tam, C., Kakiuchi, T., Matsuzawa, A., Williams, L. T. and Nakano, H. (1999) 'Mice lacking expression of secondary lymphoid organ chemokine have defects in lymphocyte homing and dendritic cell localization.', *The Journal of experimental medicine*, 189(3), pp. 451–460.

Gunn, M. D., Tangemann, K., Tam, C., Cyster, J. G., Rosen, S. D. and Williams, L. T. (1998) 'A chemokine expressed in lymphoid high endothelial venules promotes the adhesion and chemotaxis of naive T lymphocytes.', *Proceedings of the National Academy of Sciences of the United States of America*, 95(1), pp. 258–263.

Haan, den, J. M. M. and Kraal, G. (2012) 'Innate immune functions of macrophage subpopulations in the spleen.', *Journal of innate immunity*, 4(5-6), pp. 437–445. doi: 10.1159/000335216.

Haan, den, J. M., Lehar, S. M. and Bevan, M. J. (2000) 'CD8(+) but not CD8(-) dendritic cells cross-prime cytotoxic T cells in vivo.', *The Journal of experimental medicine*, 192(12), pp. 1685–1696.

Hacker, C., Kirsch, R. D., Ju, X.-S., Hieronymus, T., Gust, T. C., Kuhl, C., Jorgas, T., Kurz, S. M., Rose-John, S., Yokota, Y. and Zenke, M. (2003) 'Transcriptional profiling identifies Id2 function in dendritic cell development', *Nature Immunology*, 4(4), pp. 380–386. doi: 10.1038/ni903.

Hadis, U., Wahl, B., Schulz, O., Hardtke-Wolenski, M., Schippers, A., Wagner, N., Müller, W., Sparwasser, T., Förster, R. and Pabst, O. (2011) 'Intestinal tolerance requires gut homing and expansion of FoxP3+ regulatory T cells in the lamina propria.', *Immunity*, 34(2), pp. 237–246. doi: 10.1016/j.immuni.2011.01.016.

Hammad, H., de Heer, H. J., Soullie, T., Hoogsteden, H. C., Trottein, F. and Lambrecht, B. N. (2003) 'Prostaglandin D2 inhibits airway dendritic cell migration and function in steady state conditions by selective activation of the D prostanoid receptor 1.', *Journal of immunology (Baltimore, Md : 1950)*, 171(8), pp. 3936–3940.

Hammad, H., Plantinga, M., Deswarte, K., Pouliot, P., Willart, M. A. M., Kool, M., Muskens, F. and Lambrecht, B. N. (2010) 'Inflammatory dendritic cells--not basophils--are necessary and sufficient for induction of Th2 immunity to inhaled house dust mite allergen.', *Journal of Experimental Medicine*, 207(10), pp. 2097–2111. doi: 10.1084/jem.20101563.

Hartung, E., Becker, M., Bachem, A., Reeg, N., Jäkel, A., Hutloff, A., Weber, H., Weise, C., Giesecke, C., Henn, V., Gurka, S., Anastassiadis, K., Mages, H. W. and Kroczek, R. A. (2015) 'Induction of potent CD8 T cell cytotoxicity by specific targeting of antigen to cross-presenting dendritic cells in vivo via murine or human XCR1.', *The Journal of Immunology*, 194(3), pp. 1069–1079. doi: 10.4049/jimmunol.1401903.

Hashimoto, D., Chow, A., Noizat, C., Teo, P., Beasley, M. B., Leboeuf, M., Becker, C. D., See, P., Price, J., Lucas, D., Greter, M., Mortha, A., Boyer, S. W., Forsberg, E. C., Tanaka, M., Van Rooijen, N., García-Sastre, A., Stanley, E. R., Ginhoux, F., Frenette, P. S. and Merad, M. (2013) 'Tissue-resident macrophages self-maintain locally throughout adult life with minimal contribution from circulating monocytes.', *Immunity*, 38(4), pp. 792–804. doi: 10.1016/j.immuni.2013.04.004.

Hashimoto, D., Miller, J. and Merad, M. (2011) 'Dendritic Cell and Macrophage Heterogeneity In Vivo', *Immunity*, 35(3), pp. 323–335. doi: 10.1016/j.immuni.2011.09.007.

Hawiger, D., Inaba, K., Dorsett, Y., Guo, M., Mahnke, K., Rivera, M., Ravetch, J. V., Steinman, R. M. and Nussenzweig, M. C. (2001) 'Dendritic cells induce peripheral T cell unresponsiveness under steady state conditions in vivo.', *The Journal of experimental medicine*, 194(6), pp. 769–779.

Helft, J., Böttcher, J., Chakravarty, P., Zelenay, S., Huotari, J., Schraml, B. U., Goubau, D. and Reis e Sousa, C. (2015) 'GM-CSF Mouse Bone Marrow Cultures Comprise a Heterogeneous Population of CD11c', *Immunity*. Elsevier Inc., 42(6), pp. 1197–1211. doi: 10.1016/j.immuni.2015.05.018.

Helft, J., Manicassamy, B., Guermonprez, P., Hashimoto, D., Silvin, A., Agudo, J., Brown, B. D., Schmolke, M., Miller, J. C., Leboeuf, M., Murphy, K. M., García-Sastre, A. and Merad, M. (2012) 'Cross-presenting CD103+ dendritic cells are protected from influenza virus infection.', *The Journal of clinical investigation*, 122(11), pp. 4037–4047. doi: 10.1172/JCI60659.

Henri, S., Poulin, L. F., Tamoutounour, S., Ardouin, L., Guilliams, M., de Bovis, B., Devilard, E., Viret, C., Azukizawa, H., Kissenpfennig, A. and Malissen, B. (2010) 'CD207+ CD103+ dermal dendritic cells cross-present keratinocyte-derived antigens irrespective of the presence of Langerhans cells.', *Journal of Experimental Medicine*, 207(1), pp. 189–206. doi: 10.1084/jem.20091964.

Hettinger, J., Richards, D. M., Hansson, J., Barra, M. M., Joschko, A.-C., Krijgsveld, J. and Feuerer, M. (2013) 'Origin of monocytes and macrophages in a committed progenitor', *Nature Immunology*. Nature Publishing Group, pp. 1–12. doi: 10.1038/ni.2638.

Higashiyama, S., Iwabuki, H., Morimoto, C., Hieda, M., Inoue, H. and Matsushita, N. (2008) 'Membrane-anchored growth factors, the epidermal growth factor family: Beyond receptor ligands', *Cancer Science*, 99(2), pp. 214–220. doi: 10.1111/j.1349-7006.2007.00676.x.

Hildner, K., Edelson, B. T., Purtha, W. E., Diamond, M., Matsushita, H., Kohyama, M., Calderon, B., Schraml, B. U., Unanue, E. R., Diamond, M. S., Schreiber, R. D., Murphy, T. L. and Murphy, K. M. (2008) 'Batf3 deficiency reveals a critical role for CD8alpha+ dendritic cells in cytotoxic T cell immunity', *Science (New York, NY)*, 322(5904), pp. 1097–1100. doi: 10.1126/science.1164206.

Hirrlinger, J., Requardt, R. P., Winkler, U., Wilhelm, F., Schulze, C. and Hirrlinger, P. G. (2009) 'Split-CreERT2: temporal control of DNA recombination mediated by split-Cre protein fragment complementation.', *PloS one*, 4(12), p. e8354. doi: 10.1371/journal.pone.0008354.

Hirrlinger, J., Scheller, A., Hirrlinger, P. G., Kellert, B., Tang, W., Wehr, M. C., Goebbels, S., Reichenbach, A., Sprengel, R., Rossner, M. J. and Kirchhoff, F. (2009) 'Split-cre complementation indicates coincident activity of different genes in vivo.', *PloS one*, 4(1), p. e4286. doi: 10.1371/journal.pone.0004286.

Hochweller, K., Striegler, J., Hämmerling, G. J. and Garbi, N. (2008) 'A novel CD11c.DTR transgenic mouse for depletion of dendritic cells reveals their requirement for homeostatic proliferation of natural killer cells.', *European journal of immunology*, 38(10), pp. 2776–2783. doi: 10.1002/eji.200838659.

Hoeffel, G., Chen, J., Lavin, Y., Low, D., Almeida, F. F., See, P., Beaudin, A. E., Lum, J., Low, I., Forsberg, E. C., Poidinger, M., Zolezzi, F., Larbi, A., Ng, L. G., Chan, J. K. Y., Greter, M., Becher, B., Samokhvalov, I. M., Merad, M. and Ginhoux,

F. (2015) ‘Erythro-Myeloid Progenitor-Derived Fetal Monocytes Give Rise to Adult Tissue-Resident Macrophages’, *Immunity*. Elsevier Inc., 42(4), pp. 665–678. doi: 10.1016/j.immuni.2015.03.011.

Hoeffel, G., Wang, Y., Greter, M., See, P., Teo, P., Malleret, B., Leboeuf, M., Low, D., Oller, G., Almeida, F., Choy, S. H. Y., Grisotto, M., Renia, L., Conway, S. J., Stanley, E. R., Chan, J. K. Y., Ng, L. G., Samokhvalov, I. M., Merad, M. and Ginhoux, F. (2012) ‘Adult Langerhans cells derive predominantly from embryonic fetal liver monocytes with a minor contribution of yolk sac-derived macrophages’, *The Journal of experimental medicine*, 209(6), pp. 1167–1181. doi: 10.1084/jem.20120340.

Holtschke, T. T., Löhler, J. J., Kanno, Y. Y., Fehr, T. T., Giese, N. N., Rosenbauer, F. F., Lou, J. J., Knobeloch, K. P. K., Gabriele, L. L., Waring, J. F. J., Bachmann, M. F. M., Zinkernagel, R. M. R., Morse, H. C. H., Ozato, K. K. and Horak, I. I. (1996) ‘Immunodeficiency and Chronic Myelogenous Leukemia-like Syndrome in Mice with a Targeted Mutation of the ICSBP Gene’, *Cell*, 87(2), pp. 11–11. doi: 10.1016/S0092-8674(00)81348-3.

Hsieh, C. S., Macatonia, S. E., Tripp, C. S., Wolf, S. F., O'Garra, A. and Murphy, K. M. (1993) ‘Development of TH1 CD4+ T cells through IL-12 produced by Listeria-induced macrophages.’, *Science (New York, NY)*, 260(5107), pp. 547–549.

Ichikawa, E., Hida, S., Omatsu, Y., Shimoyama, S., Takahara, K., Miyagawa, S., Inaba, K. and Taki, S. (2004) ‘Defective development of splenic and epidermal CD4+ dendritic cells in mice deficient for IFN regulatory factor-2.’, *Proceedings of the National Academy of Sciences of the United States of America*, 101(11), pp. 3909–3914. doi: 10.1073/pnas.0400610101.

Idoyaga, J., Lubkin, A., Fiorese, C., Lahoud, M. H., Caminschi, I., Huang, Y., Rodriguez, A., Clausen, B. E., Park, C. G., Trumpfheller, C. and Steinman, R. M. (2011) ‘Comparable T helper 1 (Th1) and CD8 T-cell immunity by targeting HIV gag p24 to CD8 dendritic cells within antibodies to Langerin, DEC205, and Clec9A.’, *Proceedings of the National Academy of Sciences*, 108(6), pp. 2384–2389. doi: 10.1073/pnas.1019547108.

Idoyaga, J., Suda, N., Suda, K., Park, C. G. and Steinman, R. M. (2009) ‘Antibody to Langerin/CD207 localizes large numbers of CD8alpha+ dendritic cells to the marginal zone of mouse spleen.’, *Proceedings of the National Academy of Sciences*, 106(5), pp. 1524–1529. doi: 10.1073/pnas.0812247106.

Igyarto, B. Z., Haley, K., Ortner, D., Bobr, A., Gerami-Nejad, M., Edelson, B. T., Zurawski, S. M., Malissen, B., Zurawski, G., Berman, J. and Kaplan, D. H. (2011) ‘Skin-resident murine dendritic cell subsets promote distinct and opposing antigen-specific T helper cell responses.’, *Immunity*, 35(2), pp. 260–272. doi: 10.1016/j.immuni.2011.06.005.

Inaba, K., Inaba, M., Romani, N., Aya, H., Deguchi, M., Ikehara, S., Muramatsu, S. and Steinman, R. M. (1992) ‘Generation of large numbers of dendritic cells from mouse bone marrow cultures supplemented with granulocyte/macrophage colony-stimulating factor.’, *The Journal of experimental medicine*, 176(6), pp. 1693–1702.

Inaba, K., Turley, S., Yamaide, F., Iyoda, T., Mahnke, K., Inaba, M., Pack, M., Subklewe, M., Sauter, B., Sheff, D., Albert, M., Bhardwaj, N., Mellman, I. and Steinman, R. M. (1998) 'Efficient presentation of phagocytosed cellular fragments on the major histocompatibility complex class II products of dendritic cells.', *The Journal of experimental medicine*, 188(11), pp. 2163–2173.

Indra, A. K., Warot, X., Brocard, J., Bornert, J. M., Xiao, J. H., Chambon, P. and Metzger, D. (1999) 'Temporally-controlled site-specific mutagenesis in the basal layer of the epidermis: comparison of the recombinase activity of the tamoxifen-inducible Cre-ER(T) and Cre-ER(T2) recombinases.', *Nucleic Acids Research*, 27(22), pp. 4324–4327. doi: 10.1093/nar/27.22.4324.

Ivanov, I. I., Atarashi, K., Manel, N., Brodie, E. L., Shima, T., Karaoz, U., Wei, D., Goldfarb, K. C., Santee, C. A., Lynch, S. V., Tanoue, T., Imaoka, A., Itoh, K., Takeda, K., Umesaki, Y., Honda, K. and Littman, D. R. (2009) 'Induction of intestinal Th17 cells by segmented filamentous bacteria.', *Cell*, 139(3), pp. 485–498. doi: 10.1016/j.cell.2009.09.033.

Ivanova, A., Signore, M., Caro, N., Greene, N. D. E., Copp, A. J. and Martinez-Barbera, J. P. (2005) 'In vivo genetic ablation by Cre-mediated expression of diphtheria toxin fragment A', *Genesis (New York, NY : 2000)*, 43(3), pp. 129–135. doi: 10.1002/gene.20162.

Iwasaki, A. and Kelsall, B. L. (2000) 'Localization of distinct Peyer's patch dendritic cell subsets and their recruitment by chemokines macrophage inflammatory protein (MIP)-3alpha, MIP-3beta, and secondary lymphoid organ chemokine.', *The Journal of experimental medicine*, 191(8), pp. 1381–1394.

Iyoda, T., Shimoyama, S., Liu, K., Omatsu, Y., Akiyama, Y., Maeda, Y., Takahara, K., Steinman, R. M. and Inaba, K. (2002) 'The CD8+ dendritic cell subset selectively endocytoses dying cells in culture and in vivo.', *The Journal of experimental medicine*, 195(10), pp. 1289–1302.

Jaensson, E., Uronen-Hansson, H., Pabst, O., Eksteen, B., Tian, J., Coombes, J. L., Berg, P.-L., Davidsson, T., Powrie, F., Johansson-Lindbom, B. and Agace, W. W. (2008) 'Small intestinal CD103+ dendritic cells display unique functional properties that are conserved between mice and humans.', *Journal of Experimental Medicine*, 205(9), pp. 2139–2149. doi: 10.1084/jem.20080414.

Jaensson-Gyllenbäck, E., Kotarsky, K., Zapata, F., Persson, E. K., Gundersen, T. E., Blomhoff, R. and Agace, W. W. (2011) 'Bile retinoids imprint intestinal CD103+ dendritic cells with the ability to generate gut-tropic T cells.', *Mucosal Immunology*, 4(4), pp. 438–447. doi: 10.1038/mi.2010.91.

Jakob, T. and Udey, M. C. (1998) 'Regulation of E-cadherin-mediated adhesion in Langerhans cell-like dendritic cells by inflammatory mediators that mobilize Langerhans cells in vivo.', *Journal of immunology (Baltimore, Md : 1950)*, 160(8), pp. 4067–4073.

Jakubzick, C., Gautier, E. L., Gibbings, S. L., Sojka, D. K., Schlitzer, A., Johnson, T. E., Ivanov, S., Duan, Q., Bala, S., Condon, T., Van Rooijen, N., Grainger, J. R.,

Belkaid, Y., Ma'ayan, A., Riches, D. W. H., Yokoyama, W. M., Ginhoux, F., Henson, P. M. and Randolph, G. J. (2013) 'Minimal differentiation of classical monocytes as they survey steady-state tissues and transport antigen to lymph nodes.', *Immunity*, 39(3), pp. 599–610. doi: 10.1016/j.immuni.2013.08.007.

Jakubzick, C., Tacke, F., Llodra, J., Van Rooijen, N. and Randolph, G. J. (2006) 'Modulation of dendritic cell trafficking to and from the airways.', *Journal of immunology (Baltimore, Md : 1950)*, 176(6), pp. 3578–3584.

Jang, M. H., Sougawa, N., Tanaka, T., Hirata, T., Hiroi, T., Tohya, K., Guo, Z., Umemoto, E., Ebisuno, Y., Yang, B.-G., Seoh, J.-Y., Lipp, M., Kiyono, H. and Miyasaka, M. (2006) 'CCR7 is critically important for migration of dendritic cells in intestinal lamina propria to mesenteric lymph nodes.', *Journal of immunology (Baltimore, Md : 1950)*, 176(2), pp. 803–810.

Jiang, W., Swiggard, W. J., Heufler, C., Peng, M., Mirza, A., Steinman, R. M. and Nussenzweig, M. C. (1995) 'The receptor DEC-205 expressed by dendritic cells and thymic epithelial cells is involved in antigen processing.', *Nature*, 375(6527), pp. 151–155. doi: 10.1038/375151a0.

Jiao, J., Dragomir, A.-C., Kocabayoglu, P., Rahman, A. H., Chow, A., Hashimoto, D., Leboeuf, M., Kraus, T., Moran, T., Carrasco-Avino, G., Friedman, S. L., Merad, M. and Aloman, C. (2014) 'Central Role of Conventional Dendritic Cells in Regulation of Bone Marrow Release and Survival of Neutrophils.', *The Journal of Immunology*. doi: 10.4049/jimmunol.1300237.

Joffre, O. P., Sancho, D., Zelenay, S., Keller, A. M. and Reis e Sousa, C. (2010) 'Efficient and versatile manipulation of the peripheral CD4+ T-cell compartment by antigen targeting to DNGR-1/CLEC9A.', *European journal of immunology*, 40(5), pp. 1255–1265. doi: 10.1002/eji.201040419.

Johansson-Lindbom, B. (2005) 'Functional specialization of gut CD103+ dendritic cells in the regulation of tissue-selective T cell homing', *Journal of Experimental Medicine*, 202(8), pp. 1063–1073. doi: 10.1084/jem.20051100.

Jung, S., Unutmaz, D., Wong, P., Sano, G.-I., De los Santos, K., Sparwasser, T., Wu, S., Vuthoori, S., Ko, K., Zavala, F., Pamer, E. G., Littman, D. R. and Lang, R. A. (2002) 'In Vivo Depletion of CD11c+ Dendritic Cells Abrogates Priming of CD8+ T Cells by Exogenous Cell-Associated Antigens', *Immunity*. Elsevier, 17(2), pp. 211–220. doi: 10.1016/S1074-7613(02)00365-5.

Kabashima, K., Banks, T. A., Ansel, K. M., Lu, T. T., Ware, C. F. and Cyster, J. G. (2005) 'Intrinsic lymphotoxin-beta receptor requirement for homeostasis of lymphoid tissue dendritic cells.', *Immunity*, 22(4), pp. 439–450. doi: 10.1016/j.immuni.2005.02.007.

Kabashima, K., Shiraishi, N., Sugita, K., Mori, T., Onoue, A., Kobayashi, M., Sakabe, J.-I., Yoshiki, R., Tamamura, H., Fujii, N., Inaba, K. and Tokura, Y. (2007) 'CXCL12-CXCR4 engagement is required for migration of cutaneous dendritic cells.', *The American Journal of Pathology*, 171(4), pp. 1249–1257. doi: 10.2353/ajpath.2007.070225.

Kamath, A. T., Henri, S., Battye, F., Tough, D. F. and Shortman, K. (2002) 'Developmental kinetics and lifespan of dendritic cells in mouse lymphoid organs.', *Blood*, 100(5), pp. 1734–1741.

Kamizono, S., Duncan, G. S., Seidel, M. G., Morimoto, A., Hamada, K., Grosveld, G., Akashi, K., Lind, E. F., Haight, J. P., Ohashi, P. S., Look, A. T. and Mak, T. W. (2009) 'Nfil3/E4bp4 is required for the development and maturation of NK cells in vivo.', *Journal of Experimental Medicine*, 206(13), pp. 2977–2986. doi: 10.1084/jem.20092176.

Kaplan, D. H., Jenison, M. C., Saeland, S., Shlomchik, W. D. and Shlomchik, M. J. (2005) 'Epidermal langerhans cell-deficient mice develop enhanced contact hypersensitivity.', *Immunity*, 23(6), pp. 611–620. doi: 10.1016/j.immuni.2005.10.008.

Kaplan, D. H., Li, M. O., Jenison, M. C., Shlomchik, W. D., Flavell, R. A. and Shlomchik, M. J. (2007) 'Autocrine/paracrine TGFbeta1 is required for the development of epidermal Langerhans cells.', *Journal of Experimental Medicine*, 204(11), pp. 2545–2552. doi: 10.1084/jem.20071401.

Karsunky, H., Merad, M., Cozzio, A., Weissman, I. L. and Manz, M. G. (2003) 'Flt3 ligand regulates dendritic cell development from Flt3+ lymphoid and myeloid-committed progenitors to Flt3+ dendritic cells in vivo.', *The Journal of experimental medicine*, 198(2), pp. 305–313. doi: 10.1084/jem.20030323.

Kashem, S. W., Igyarto, B. Z., Gerami-Nejad, M., Kumamoto, Y., Mohammed, J., Jarrett, E., Drummond, R. A., Zurawski, S. M., Zurawski, G., Berman, J., Iwasaki, A., Brown, G. D. and Kaplan, D. H. (2015) 'Candida albicans Morphology and Dendritic Cell Subsets Determine T Helper Cell Differentiation.', *Immunity*, 42(2), pp. 356–366. doi: 10.1016/j.immuni.2015.01.008.

Kashiwada, M., Levy, D. M., McKeag, L., Murray, K., Schröder, A. J., Canfield, S. M., Traver, G. and Rothman, P. B. (2010) 'IL-4-induced transcription factor NFIL3/E4BP4 controls IgE class switching.', *Proceedings of the National Academy of Sciences*, 107(2), pp. 821–826. doi: 10.1073/pnas.0909235107.

Kashiwada, M., Pham, N.-L. L., Pewe, L. L., Harty, J. T. and Rothman, P. B. (2011) 'NFIL3/E4BP4 is a key transcription factor for CD8α□ dendritic cell development.', *Blood*, 117(23), pp. 6193–6197. doi: 10.1182/blood-2010-07-295873.

Kautz-Neu, K., Noordegraaf, M., Dinges, S., Bennett, C. L., John, D., Clausen, B. E. and Stebut, von, E. (2011) 'Langerhans cells are negative regulators of the anti-Leishmania response.', *The Journal of experimental medicine*, 208(5), pp. 885–891. doi: 10.1084/jem.20102318.

Kawano, T., Cui, J., Koezuka, Y., Toura, I., Kaneko, Y., Motoki, K., Ueno, H., Nakagawa, R., Sato, H., Kondo, E., Koseki, H. and Taniguchi, M. (1997) 'CD1d-restricted and TCR-mediated activation of valpha14 NKT cells by glycosylceramides.', *Science (New York, NY)*, 278(5343), pp. 1626–1629.

Kc, W., Satpathy, A. T., Rapaport, A. S., Briseño, C. G., Wu, X., Albring, J. C.,

Russler-Germain, E. V., Kretzer, N. M., Durai, V., Persaud, S. P., Edelson, B. T., Loschko, J., Cella, M., Allen, P. M., Nussenzweig, M. C., Colonna, M., Sleckman, B. P., Murphy, T. L. and Murphy, K. M. (2014) 'L-Myc expression by dendritic cells is required for optimal T-cell priming.', *Nature*. doi: 10.1038/nature12967.

Kim, T. S. and Braciale, T. J. (2009) 'Respiratory dendritic cell subsets differ in their capacity to support the induction of virus-specific cytotoxic CD8+ T cell responses.', *PloS one*, 4(1), p. e4204. doi: 10.1371/journal.pone.0004204.

Kim, T. S., Hufford, M. M., Sun, J., Fu, Y.-X. and Braciale, T. J. (2010) 'Antigen persistence and the control of local T cell memory by migrant respiratory dendritic cells after acute virus infection.', *Journal of Experimental Medicine*, 207(6), pp. 1161–1172. doi: 10.1084/jem.20092017.

King, I. L., Kroenke, M. A. and Segal, B. M. (2010) 'GM-CSF-dependent, CD103+ dermal dendritic cells play a critical role in Th effector cell differentiation after subcutaneous immunization.', *Journal of Experimental Medicine*, 207(5), pp. 953–961. doi: 10.1084/jem.20091844.

Kingston, D., Schmid, M. A., Onai, N., Obata-Onai, A., Baumjohann, D. and Manz, M. G. (2009) 'The concerted action of GM-CSF and Flt3-ligand on in vivo dendritic cell homeostasis', *Blood*, 114(4), pp. 835–843. doi: 10.1182/blood-2009-02-206318.

Kinnebrew, M. A., Buffie, C. G., Diehl, G. E., Zenewicz, L. A., Leiner, I., Hohl, T. M., Flavell, R. A., Littman, D. R. and Pamer, E. G. (2012) 'Interleukin 23 production by intestinal CD103(+)CD11b(+) dendritic cells in response to bacterial flagellin enhances mucosal innate immune defense.', *Immunity*, 36(2), pp. 276–287. doi: 10.1016/j.immuni.2011.12.011.

Kissenpfennig, A., Henri, S., Dubois, B., Laplace-Builhé, C., Perrin, P., Romani, N., Tripp, C. H., Douillard, P., Leserman, L., Kaiserlian, D., Saeland, S., Davoust, J. and Malissen, B. (2005) 'Dynamics and function of Langerhans cells in vivo: dermal dendritic cells colonize lymph node areas distinct from slower migrating Langerhans cells.', *Immunity*, 22(5), pp. 643–654. doi: 10.1016/j.immuni.2005.04.004.

Kobayashi, T., Walsh, P. T., Walsh, M. C., Speirs, K. M., Chiffoleau, E., King, C. G., Hancock, W. W., Caamano, J. H., Hunter, C. A., Scott, P., Turka, L. A. and Choi, Y. (2003) 'TRAF6 is a critical factor for dendritic cell maturation and development.', *Immunity*, 19(3), pp. 353–363.

Kobayashi, Y., Matsumoto, M., Kotani, M. and Makino, T. (1999) 'Possible involvement of matrix metalloproteinase-9 in Langerhans cell migration and maturation.', *Journal of immunology (Baltimore, Md : 1950)*, 163(11), pp. 5989–5993.

Kumamoto, Y., Denda-Nagai, K., Aida, S., Higashi, N. and Irimura, T. (2009) 'MGL2+ Dermal Dendritic Cells Are Sufficient to Initiate Contact Hypersensitivity In Vivo', *PloS one*. Edited by D. Unutmaz, 4(5), p. e5619. doi: 10.1371/journal.pone.0005619.g007.

Kurts, C., Heath, W. R., Kosaka, H., Miller, J. F. and Carbone, F. R. (1998) 'The peripheral deletion of autoreactive CD8+ T cells induced by cross-presentation of self-antigens involves signaling through CD95 (Fas, Apo-1).', *The Journal of experimental medicine*, 188(2), pp. 415–420.

Kurts, C., Kosaka, H., Carbone, F. R., Miller, J. F. and Heath, W. R. (1997) 'Class I-restricted cross-presentation of exogenous self-antigens leads to deletion of autoreactive CD8(+) T cells.', *The Journal of experimental medicine*, 186(2), pp. 239–245.

Kuziel, W. A., Morgan, S. J., Dawson, T. C., Griffin, S., Smithies, O., Ley, K. and Maeda, N. (1997) 'Severe reduction in leukocyte adhesion and monocyte extravasation in mice deficient in CC chemokine receptor 2.', *Proceedings of the National Academy of Sciences of the United States of America*, 94(22), pp. 12053–12058.

Lahl, K., Loddenkemper, C., Drouin, C., Freyer, J., Arnason, J., Eberl, G., Hamann, A., Wagner, H., Huehn, J. and Sparwasser, T. (2007) 'Selective depletion of Foxp3+ regulatory T cells induces a scurfy-like disease', *The Journal of experimental medicine*, 204(1), pp. 57–63. doi: 10.1084/jem.20061852.

Lahoud, M. H., Ahmet, F., Kitsoulis, S., Wan, S. S., Vremec, D., Lee, C.-N., Phipson, B., Shi, W., Smyth, G. K., Lew, A. M., Kato, Y., Mueller, S. N., Davey, G. M., Heath, W. R., Shortman, K. and Caminschi, I. (2011) 'Targeting antigen to mouse dendritic cells via Clec9A induces potent CD4 T cell responses biased toward a follicular helper phenotype.', *The Journal of Immunology*, 187(2), pp. 842–850. doi: 10.4049/jimmunol.1101176.

Lallemand, Y., Luria, V., Haffner-Krausz, R. and Lonai, P. (1998) 'Maternally expressed PGK-Cre transgene as a tool for early and uniform activation of the Cre site-specific recombinase.', *Transgenic research*, 7(2), pp. 105–112.

Laouar, Y., Welte, T., Fu, X.-Y. and Flavell, R. A. (2003) 'STAT3 is required for Flt3L-dependent dendritic cell differentiation.', *Immunity*, 19(6), pp. 903–912.

Lavin, Y., Winter, D., Blecher-Gonen, R., David, E., Keren-Shaul, H., Merad, M., Jung, S. and Amit, I. (2014) 'Tissue-Resident Macrophage Enhancer Landscapes Are Shaped by the Local Microenvironment', *Cell*. Elsevier Inc., 159(6), pp. 1312–1326. doi: 10.1016/j.cell.2014.11.018.

Legge, K. L. and Braciale, T. J. (2003) 'Accelerated migration of respiratory dendritic cells to the regional lymph nodes is limited to the early phase of pulmonary infection.', *Immunity*, 18(2), pp. 265–277. doi: 10.1016/S1074-7613(03)00023-2.

Lécuyer, E., Rakotobe, S., Lengliné-Garnier, H., Lebreton, C., Picard, M., Juste, C., Fritzen, R., Eberl, G., McCoy, K. D., Macpherson, A. J., Reynaud, C.-A., Cerf-Bensussan, N. and Gaboriau-Routhiau, V. (2014) 'Segmented filamentous bacterium uses secondary and tertiary lymphoid tissues to induce gut IgA and specific T helper 17 cell responses.', *Immunity*, 40(4), pp. 608–620. doi: 10.1016/j.immuni.2014.03.009.

León, B., Ballesteros-Tato, A., Browning, J. L., Dunn, R., Randall, T. D. and Lund, F. E. (2012) 'Regulation of T(H)2 development by CXCR5+ dendritic cells and lymphotoxin-expressing B cells.', *Nature Immunology*, 13(7), pp. 681–690. doi: 10.1038/ni.2309.

León, B., López-Bravo, M. and Ardavín, C. (2007) 'Monocyte-derived dendritic cells formed at the infection site control the induction of protective T helper 1 responses against Leishmania.', *Immunity*, 26(4), pp. 519–531. doi: 10.1016/j.immuni.2007.01.017.

Lewis, K. L., Caton, M. L., Bogunovic, M., Greter, M., Grajkowska, L. T., Ng, D., Klinakis, A., Charo, I. F., Jung, S., Gommerman, J. L., Ivanov, I. I., Liu, K., Merad, M. and Reizis, B. (2011) 'Notch2 receptor signaling controls functional differentiation of dendritic cells in the spleen and intestine.', *Immunity*, 35(5), pp. 780–791. doi: 10.1016/j.immuni.2011.08.013.

Li, J., Ahmet, F., Sullivan, L. C., Brooks, A. G., Kent, S. J., De Rose, R., Salazar, A. M., Reis e Sousa, C., Shortman, K., Lahoud, M. H., Heath, W. R. and Caminschi, I. (2015) 'Antibodies targeting Clec9A promote strong humoral immunity without adjuvant in mice and non-human primates.', *European journal of immunology*, 45(3), pp. 854–864. doi: 10.1002/eji.201445127.

Lighvani, A. A., Frucht, D. M., Jankovic, D., Yamane, H., Aliberti, J., Hissong, B. D., Nguyen, B. V., Gadina, M., Sher, A., Paul, W. E. and O'Shea, J. J. (2001) 'T-bet is rapidly induced by interferon-gamma in lymphoid and myeloid cells.', *Proceedings of the National Academy of Sciences of the United States of America*, 98(26), pp. 15137–15142. doi: 10.1073/pnas.261570598.

Lindquist, R. L., Shakhar, G., Dudziak, D., Wardemann, H., Eisenreich, T., Dustin, M. L. and Nussenzweig, M. C. (2004) 'Visualizing dendritic cell networks in vivo.', *Nature Immunology*, 5(12), pp. 1243–1250. doi: 10.1038/ni1139.

Link, A., Vogt, T. K., Favre, S., Britschgi, M. R., Acha-Orbea, H., Hinz, B., Cyster, J. G. and Luther, S. A. (2007) 'Fibroblastic reticular cells in lymph nodes regulate the homeostasis of naive T cells', *Nature Immunology*, 8(11), pp. 1255–1265. doi: 10.1038/ni1513.

Liu, C.-H., Fan, Y.-T., Dias, A., Esper, L., Corn, R. A., Bafica, A., Machado, F. S. and Aliberti, J. (2006) 'Cutting edge: dendritic cells are essential for in vivo IL-12 production and development of resistance against Toxoplasma gondii infection in mice.', *Journal of immunology (Baltimore, Md : 1950)*, 177(1), pp. 31–35.

Liu, J., Willet, S. G., Bankaitis, E. D., Xu, Y., Wright, C. V. E. and Gu, G. (2013) 'Non-parallel recombination limits cre-loxP-based reporters as precise indicators of conditional genetic manipulation', *Genesis (New York, NY : 2000)*, 51(6), pp. 436–442. doi: 10.1002/dvg.22384.

Liu, K., Victora, G. D., Schwickert, T. A., Guermonprez, P., Meredith, M. M., Yao, K., Chu, F.-F., Randolph, G. J., Rudensky, A. Y. and Nussenzweig, M. (2009) 'In vivo analysis of dendritic cell development and homeostasis', *Science (New York, NY)*, 324(5925), pp. 392–397. doi: 10.1126/science.1170540.

Liu, K., Waskow, C., Liu, X., Yao, K., Hoh, J. and Nussenzweig, M. (2007) 'Origin of dendritic cells in peripheral lymphoid organs of mice.', *Nature Immunology*, 8(6), pp. 578–583. doi: 10.1038/ni1462.

Livet, J., Weissman, T. A., Kang, H., Draft, R. W., Lu, J., Bennis, R. A., Sanes, J. R. and Lichtman, J. W. (2007) 'Transgenic strategies for combinatorial expression of fluorescent proteins in the nervous system.', *Nature*, 450(7166), pp. 56–62. doi: 10.1038/nature06293.

Longman, R. S., Diehl, G. E., Victorio, D. A., Huh, J. R., Galan, C., Miraldi, E. R., Swaminath, A., Bonneau, R., Scherl, E. J. and Littman, D. R. (2014) 'CX3CR1+ mononuclear phagocytes support colitis-associated innate lymphoid cell production of IL-22.', *Journal of Experimental Medicine*, 211(8), pp. 1571–1583. doi: 10.1084/jem.20140678.

Luber, C. A., Cox, J., Lauterbach, H., Fancke, B., Selbach, M., Tschopp, J., Akira, S., Wiegand, M., Hochrein, H., O'Keeffe, M. and Mann, M. (2010) 'Quantitative proteomics reveals subset-specific viral recognition in dendritic cells.', *Immunity*, 32(2), pp. 279–289. doi: 10.1016/j.immuni.2010.01.013.

Luther, S. A., Tang, H. L., Hyman, P. L., Farr, A. G. and Cyster, J. G. (2000) 'Coexpression of the chemokines ELC and SLC by T zone stromal cells and deletion of the ELC gene in the plt/plt mouse.', *Proceedings of the National Academy of Sciences of the United States of America*, 97(23), pp. 12694–12699. doi: 10.1073/pnas.97.23.12694.

Lutz, M. B., Kukutsch, N., Ogilvie, A. L., Rössner, S., Koch, F., Romani, N. and Schuler, G. (1999) 'An advanced culture method for generating large quantities of highly pure dendritic cells from mouse bone marrow.', *Journal of Immunological Methods*, 223(1), pp. 77–92.

MacDonald, A. S., Straw, A. D., Bauman, B. and Pearce, E. J. (2001) 'CD8- dendritic cell activation status plays an integral role in influencing Th2 response development.', *Journal of immunology (Baltimore, Md : 1950)*, 167(4), pp. 1982–1988.

Mackarehtschian, K., Hardin, J. D., Moore, K. A., Boast, S., Goff, S. P. and Lemischka, I. R. (1995) 'Targeted disruption of the flk2/flt3 gene leads to deficiencies in primitive hematopoietic progenitors.', *Immunity*, 3(1), pp. 147–161.

Madisen, L., Zwingman, T. A., Sunkin, S. M., Oh, S. W., Zariwala, H. A., Gu, H., Ng, L. L., Palmiter, R. D., Hawrylycz, M. J., Jones, A. R., Lein, E. S. and Zeng, H. (2010) 'A robust and high-throughput Cre reporting and characterization system for the whole mouse brain.', *Nature neuroscience*, 13(1), pp. 133–140. doi: 10.1038/nn.2467.

Magalhaes, J. G., Rubino, S. J., Travassos, L. H., Le Bourhis, L., Duan, W., Sellge, G., Geddes, K., Reardon, C., Lechmann, M. and Carneiro, L. A. (2011) 'Nucleotide oligomerization domain-containing proteins instruct T cell helper type 2 immunity through stromal activation', *Proceedings of the National Academy of Sciences of the United States of America*. National Acad Sciences, 108(36), pp. 14896–14901.

Maillard, I., Fang, T. and Pear, W. S. (2005) 'Regulation of lymphoid development, differentiation, and function by the Notch pathway.', *Annual Review of Immunology*, 23, pp. 945–974. doi: 10.1146/annurev.immunol.23.021704.115747.

Maldonado-López, R., De Smedt, T., Michel, P., Godfroid, J., Pajak, B., Heirman, C., Thielemans, K., Leo, O., Urbain, J. and Moser, M. (1999) 'CD8alpha+ and CD8alpha- subclasses of dendritic cells direct the development of distinct T helper cells in vivo.', *The Journal of experimental medicine*, 189(3), pp. 587–592.

Malissen, B., Tamoutounour, S. and Henri, S. (2014) 'The origins and functions of dendritic cells and macrophages in the skin', *Nature Reviews Immunology*. Nature Publishing Group, 14(6), pp. 417–428. doi: 10.1038/nri3683.

Manfra, D. J., Chen, S.-C., Jensen, K. K., Fine, J. S., Wiekowski, M. T. and Lira, S. A. (2003) 'Conditional expression of murine Flt3 ligand leads to expansion of multiple dendritic cell subsets in peripheral blood and tissues of transgenic mice.', *Journal of immunology (Baltimore, Md : 1950)*, 170(6), pp. 2843–2852.

Manicassamy, S., Reizis, B., Ravindran, R., Nakaya, H., Salazar-Gonzalez, R. M., Wang, Y.-C. and Pulendran, B. (2010) 'Activation of beta-catenin in dendritic cells regulates immunity versus tolerance in the intestine.', *Science (New York, NY)*, 329(5993), pp. 849–853. doi: 10.1126/science.1188510.

Maraskovsky, E., Brasel, K., Teepe, M., Roux, E. R., Lyman, S. D., Shortman, K. and McKenna, H. J. (1996) 'Dramatic increase in the numbers of functionally mature dendritic cells in Flt3 ligand-treated mice: multiple dendritic cell subpopulations identified.', *The Journal of experimental medicine*, 184(5), pp. 1953–1962.

Mashayekhi, M., Sandau, M. M., Dunay, I. R., Frickel, E. M., Khan, A., Goldszmid, R. S., Sher, A., Ploegh, H. L., Murphy, T. L., Sibley, L. D. and Murphy, K. M. (2011) 'CD8α+ Dendritic Cells Are the Critical Source of Interleukin-12 that Controls Acute Infection by Toxoplasma gondii Tachyzoites', *Immunity*, 35(2), pp. 249–259. doi: 10.1016/j.immuni.2011.08.008.

Mattei, F., Schiavoni, G., Belardelli, F. and Tough, D. F. (2001) 'IL-15 is expressed by dendritic cells in response to type I IFN, double-stranded RNA, or lipopolysaccharide and promotes dendritic cell activation.', *Journal of immunology (Baltimore, Md : 1950)*, 167(3), pp. 1179–1187.

Mayer-Barber, K. D., Andrade, B. B., Barber, D. L., Hieny, S., Feng, C. G., Caspar, P., Oland, S., Gordon, S. and Sher, A. (2011) 'Innate and Adaptive Interferons Suppress IL-1aand IL-1b Production by Distinct Pulmonary Myeloid Subsets during Mycobacterium tuberculosis Infection', *Immunity*. Elsevier Inc., 35(6), pp. 1023–1034. doi: 10.1016/j.immuni.2011.12.002.

McDole, J. R., Wheeler, L. W., McDonald, K. G., Wang, B., Konjufca, V., Knoop, K. A., Newberry, R. D. and Miller, M. J. (2012) 'Goblet cells deliver luminal antigen to CD103+ dendritic cells in the small intestine.', *Nature*, 483(7389), pp. 345–349. doi: 10.1038/nature10863.

McGrath, K. E., Koniski, A. D., Malik, J. and Palis, J. (2003) 'Circulation is established in a stepwise pattern in the mammalian embryo.', *Blood*, 101(5), pp. 1669–1676. doi: 10.1182/blood-2002-08-2531.

McKenna, H. J., Stocking, K. L., Miller, R. E., Brasel, K., De Smedt, T., Maraskovsky, E., Maliszewski, C. R., Lynch, D. H., Smith, J., Pulendran, B., Roux, E. R., Teepe, M., Lyman, S. D. and Peschon, J. J. (2000) 'Mice lacking flt3 ligand have deficient hematopoiesis affecting hematopoietic progenitor cells, dendritic cells, and natural killer cells.', *Blood*, 95(11), pp. 3489–3497.

McKercher, S. R., Torbett, B. E., Anderson, K. L., Henkel, G. W., Vestal, D. J., Baribault, H., Klemsz, M., Feeney, A. J., Wu, G. E., Paige, C. J. and Maki, R. A. (1996) 'Targeted disruption of the PU.1 gene results in multiple hematopoietic abnormalities.', *The EMBO Journal*, 15(20), pp. 5647–5658.

McLachlan, J. B., Catron, D. M., Moon, J. J. and Jenkins, M. K. (2009) 'Dendritic cell antigen presentation drives simultaneous cytokine production by effector and regulatory T cells in inflamed skin.', *Immunity*, 30(2), pp. 277–288. doi: 10.1016/j.immuni.2008.11.013.

Merad, M., Manz, M. G., Karsunky, H., Wagers, A., Peters, W., Charo, I., Weissman, I. L., Cyster, J. G. and Engleman, E. G. (2002) 'Langerhans cells renew in the skin throughout life under steady-state conditions', *Nature Immunology*, 3(12), pp. 1135–1141. doi: 10.1038/ni852.

Merad, M., Sathe, P., Helft, J., Miller, J. and Mortha, A. (2013) 'The Dendritic Cell Lineage: Ontogeny and Function of Dendritic Cells and Their Subsets in the Steady State and the Inflamed Setting', *Annual Review of Immunology*, 31(1), pp. 563–604. doi: 10.1146/annurev-immunol-020711-074950.

Meredith, M. M., Liu, K., Darrasse-Jeze, G., Kamphorst, A. O., Schreiber, H. A., Guermonprez, P., Idoyaga, J., Cheong, C., Yao, K. H., Niec, R. E. and Nussenzweig, M. C. (2012) 'Expression of the zinc finger transcription factor zDC (Zbtb46, Btbd4) defines the classical dendritic cell lineage', *The Journal of experimental medicine*. doi: 10.1084/jem.20112675.

Meredith, M. M., Liu, K., Kamphorst, A. O., Idoyaga, J., Yamane, A., Guermonprez, P., Rihn, S., Yao, K. H., Silva, I. T., Oliveira, T. Y., Skokos, D., Casellas, R. and Nussenzweig, M. C. (2012) 'Zinc finger transcription factor zDC is a negative regulator required to prevent activation of classical dendritic cells in the steady state', *The Journal of experimental medicine*. doi: 10.1084/jem.20121003.

Mesnil, C., Sabatel, C. M., Marichal, T., Toussaint, M., Cataldo, D., Drion, P.-V., Lekeux, P., Bureau, F. and Desmet, C. J. (2012) 'Resident CD11b+Ly6C− Lung Dendritic Cells Are Responsible for Allergic Airway Sensitization to House Dust Mite in Mice', *PloS one*. Edited by B. Ryffel, 7(12), p. e53242. doi: 10.1371/journal.pone.0053242.g009.

Metcalf, D. (2008) 'Hematopoietic cytokines.', *Blood*, 111(2), pp. 485–491. doi: 10.1182/blood-2007-03-079681.

Miller, J. C., Brown, B. D., Shay, T., Gautier, E. L., Jojic, V., Cohain, A., Pandey, G., Leboeuf, M., Elpek, K. G., Helft, J., Hashimoto, D., Chow, A., Price, J., Greter, M., Bogunovic, M., Bellemare-Pelletier, A., Frenette, P. S., Randolph, G. J., Turley, S. J. and Merad, M. (2012) 'Deciphering the transcriptional network of the dendritic cell lineage', *Nature Immunology*. Nature Publishing Group, pp. 1–14. doi: 10.1038/ni.2370.

Miller, M. J., Wei, S. H., Parker, I. and Cahalan, M. D. (2002) 'Two-photon imaging of lymphocyte motility and antigen response in intact lymph node.', *Science (New York, NY)*, 296(5574), pp. 1869–1873. doi: 10.1126/science.1070051.

Miteva, D. O., Rutkowski, J. M., Dixon, J. B., Kilarski, W., Shields, J. D. and Swartz, M. A. (2010) 'Transmural flow modulates cell and fluid transport functions of lymphatic endothelium.', *Circulation research*, 106(5), pp. 920–931. doi: 10.1161/CIRCRESAHA.109.207274.

Mittrücker, H. W., Matsuyama, T., Grossman, A., Kündig, T. M., Potter, J., Shahinian, A., Wakeham, A., Patterson, B., Ohashi, P. S. and Mak, T. W. (1997) 'Requirement for the transcription factor LSIRF/IRF4 for mature B and T lymphocyte function.', *Science (New York, NY)*, 275(5299), pp. 540–543.

Mollah, S. A., Dobrin, J. S., Feder, R. E., Tse, S.-W., Matos, I. G., Cheong, C., Steinman, R. M. and Anandasabapathy, N. (2014) 'Flt3L dependence helps define an uncharacterized subset of murine cutaneous dendritic cells.', *The Journal of investigative dermatology*, 134(5), pp. 1265–1275. doi: 10.1038/jid.2013.515.

Mora, J. R., Bono, M. R., Manjunath, N., Weninger, W., Cavanagh, L. L., Rosemblatt, M. and Andrian, von, U. H. (2003) 'Selective imprinting of gut-homing T cells by Peyer's patch dendritic cells.', *Nature*, 424(6944), pp. 88–93. doi: 10.1038/nature01726.

Morgan, D. J., Kreuwel, H. T. and Sherman, L. A. (1999) 'Antigen concentration and precursor frequency determine the rate of CD8+ T cell tolerance to peripherally expressed antigens.', *Journal of immunology (Baltimore, Md : 1950)*, 163(2), pp. 723–727.

Moussion, C. and Girard, J.-P. (2011) 'Dendritic cells control lymphocyte entry to lymph nodes through high endothelial venules', *Nature*, 479(7374), pp. 542–546. doi: 10.1038/nature10540.

Mowat, A. M. and Agace, W. W. (2014) 'Regional specialization within the intestinal immune system.', *Nature Reviews Immunology*, 14(10), pp. 667–685. doi: 10.1038/nri3738.

Mucida, D., Park, Y., Kim, G., Turovskaya, O., Scott, I., Kronenberg, M. and Cheroutre, H. (2007) 'Reciprocal TH17 and regulatory T cell differentiation mediated by retinoic acid.', *Science (New York, NY)*, 317(5835), pp. 256–260. doi: 10.1126/science.1145697.

Murakami, R., Denda-Nagai, K., Hashimoto, S.-I., Nagai, S., Hattori, M. and Irimura, T. (2013) 'A Unique Dermal Dendritic Cell Subset That Skews the Immune

Response toward Th2', *PloS one*. Edited by G. Kassiotis, 8(9), p. e73270. doi: 10.1371/journal.pone.0073270.s005.

Muzumdar, M. D., Tasic, B., Miyamichi, K., Li, L. and Luo, L. (2007) 'A global double-fluorescent Cre reporter mouse.', *Genesis (New York, NY : 2000)*, 45(9), pp. 593–605. doi: 10.1002/dvg.20335.

Nagao, K., Kobayashi, T., Moro, K., Ohyama, M., Adachi, T., Kitashima, D. Y., Ueha, S., Horiuchi, K., Tanizaki, H., Kabashima, K., Kubo, A., Cho, Y.-H., Clausen, B. E., Matsushima, K., Suematsu, M., Furtado, G. C., Lira, S. A., Farber, J. M., Udey, M. C. and Amagai, M. (2012) 'Stress-induced production of chemokines by hair follicles regulates the trafficking of dendritic cells in skin', *Nature Immunology*, 13(8), pp. 744–752. doi: 10.1038/ni.2353.

Naik, S. H., Metcalf, D., van Nieuwenhuijze, A., Wicks, I., Wu, L., O'Keeffe, M. and Shortman, K. (2006) 'Intrasplenic steady-state dendritic cell precursors that are distinct from monocytes.', *Nature Immunology*, 7(6), pp. 663–671. doi: 10.1038/ni1340.

Naik, S. H., Perié, L., Swart, E., Gerlach, C., van Rooij, N., de Boer, R. J. and Schumacher, T. N. (2013) 'Diverse and heritable lineage imprinting of early haematopoietic progenitors.', *Nature*, 496(7444), pp. 229–232. doi: 10.1038/nature12013.

Naik, S. H., Proietto, A. I., Wilson, N. S., Dakic, A., Schnorrer, P., Fuchsberger, M., Lahoud, M. H., O'Keeffe, M., Shao, Q.-X., Chen, W.-F., Villadangos, J. A., Shortman, K. and Wu, L. (2005) 'Cutting edge: generation of splenic CD8+ and CD8- dendritic cell equivalents in Fms-like tyrosine kinase 3 ligand bone marrow cultures.', *Journal of immunology (Baltimore, Md : 1950)*, 174(11), pp. 6592–6597.

Naik, S. H., Sathe, P., Park, H.-Y., Metcalf, D., Proietto, A. I., Dakic, A., Carotta, S., O'Keeffe, M., Bahlo, M., Papenfuss, A., Kwak, J.-Y., Wu, L. and Shortman, K. (2007) 'Development of plasmacytoid and conventional dendritic cell subtypes from single precursor cells derived in vitro and in vivo.', *Nature Immunology*, 8(11), pp. 1217–1226. doi: 10.1038/ni1522.

Nakano, H. and Gunn, M. D. (2001) 'Gene duplications at the chemokine locus on mouse chromosome 4: multiple strain-specific haplotypes and the deletion of secondary lymphoid-organ chemokine and EBI-1 ligand chemokine genes in the plt mutation.', *Journal of immunology (Baltimore, Md : 1950)*, 166(1), pp. 361–369.

Nakano, H., Lin, K. L., Yanagita, M., Charbonneau, C., Cook, D. N., Kakiuchi, T. and Gunn, M. D. (2009) 'Blood-derived inflammatory dendritic cells in lymph nodes stimulate acute T helper type 1 immune responses.', *Nature Immunology*, 10(4), pp. 394–402. doi: 10.1038/ni.1707.

Nestle, F. O., Conrad, C., Tun-Kyi, A., Homey, B., Gombert, M., Boyman, O., Burg, G., Liu, Y.-J. and Gilliet, M. (2005) 'Plasmacytoid predendritic cells initiate psoriasis through interferon-alpha production.', *The Journal of experimental medicine*, 202(1), pp. 135–143. doi: 10.1084/jem.20050500.

Nolte, M. A., Hoen, E. N., van Stijn, A., Kraal, G. and Mebius, R. E. (2000) 'Isolation of the intact white pulp. Quantitative and qualitative analysis of the cellular composition of the splenic compartments.', *European journal of immunology*, 30(2), pp. 626–634. doi: 10.1002/1521-4141(200002)30:2<626::AID-IMMU626>3.0.CO;2-H.

Ohl, L., Mohaupt, M., Czeloth, N., Hintzen, G., Kiafard, Z., Zwirner, J., Blankenstein, T., Henning, G. and Förster, R. (2004) 'CCR7 governs skin dendritic cell migration under inflammatory and steady-state conditions.', *Immunity*, 21(2), pp. 279–288. doi: 10.1016/j.immuni.2004.06.014.

Ohnmacht, C., Pullner, A., King, S. B. S., Drexler, I., Meier, S., Brocker, T. and Voehringer, D. (2009) 'Constitutive ablation of dendritic cells breaks self-tolerance of CD4 T cells and results in spontaneous fatal autoimmunity', *The Journal of experimental medicine*, 206(3), pp. 549–559. doi: 10.1084/jem.20082394.

Okuyama, M., Kayama, H., Atarashi, K., Saiga, H., Kimura, T., Waisman, A., Yamamoto, M. and Takeda, K. (2010) 'A novel in vivo inducible dendritic cell ablation model in mice.', *Biochemical and Biophysical Research Communications*. doi: 10.1016/j.bbrc.2010.05.157.

Onai, N., Kurabayashi, K., Hosoi-Amaike, M., Toyama-Sorimachi, N., Matsushima, K., Inaba, K. and Ohteki, T. (2013) 'A Clonogenic Progenitor with Prominent Plasmacytoid Dendritic Cell Developmental Potential.', *Immunity*. doi: 10.1016/j.immuni.2013.04.006.

Onai, N., Obata-Onai, A., Schmid, M. A., Ohteki, T., Jarrossay, D. and Manz, M. G. (2007) 'Identification of clonogenic common Flt3+M-CSFR+ plasmacytoid and conventional dendritic cell progenitors in mouse bone marrow.', *Nature Immunology*, 8(11), pp. 1207–1216. doi: 10.1038/ni1518.

Osterholzer, J. J., Chen, G.-H., Olszewski, M. A., Curtis, J. L., Huffnagle, G. B. and Toews, G. B. (2009) 'Accumulation of CD11b+ lung dendritic cells in response to fungal infection results from the CCR2-mediated recruitment and differentiation of Ly-6Chigh monocytes.', *The Journal of Immunology*, 183(12), pp. 8044–8053. doi: 10.4049/jimmunol.0902823.

Otero, K., Vecchi, A., Hirsch, E., Kearley, J., Vermi, W., Del Prete, A., Gonzalvo-Feo, S., Garlanda, C., Azzolino, O., Salogni, L., Lloyd, C. M., Facchetti, F., Mantovani, A. and Sozzani, S. (2010) 'Nonredundant role of CCRL2 in lung dendritic cell trafficking.', *Blood*, 116(16), pp. 2942–2949. doi: 10.1182/blood-2009-12-259903.

Ouwehand, K., Santegoets, S. J. A. M., Bruynzeel, D. P., Scheper, R. J., de Gruijl, T. D. and Gibbs, S. (2008) 'CXCL12 is essential for migration of activated Langerhans cells from epidermis to dermis', *European journal of immunology*, 38(11), pp. 3050–3059. doi: 10.1002/eji.200838384.

Pelletier, S., Gingras, S. and Green, D. R. (2015) 'Mouse Genome Engineering via CRISPR-Cas9 for Study of Immune Function', *Immunity*. Elsevier Inc., 42(1), pp. 18–27. doi: 10.1016/j.immuni.2015.01.004.

Perdiguero, E. G., Klapproth, K., Schulz, C., Busch, K., Azzoni, E., Crozet, L., Garner, H., Trouillet, C., de Bruijn, M. F., Geissmann, F. and Rodewald, H.-R. (2014) 'Tissue-resident macrophages originate from yolk-sac-derived erythro-myeloid progenitors', *Nature*. Nature Publishing Group, pp. 1–17. doi: 10.1038/nature13989.

Perié, L., Hodgkin, P. D., Naik, S. H., Schumacher, T. N., de Boer, R. J. and Duffy, K. R. (2014) 'Determining Lineage Pathways from Cellular Barcoding Experiments.', *CellReports*. doi: 10.1016/j.celrep.2014.01.016.

Persson, E. K., Scott, C. L., Mowat, A. M. and Agace, W. W. (2013) 'Dendritic cell subsets in the intestinal lamina propria: Ontogeny and function.', *European journal of immunology*. doi: 10.1002/eji.201343740.

Persson, E. K., Uronen-Hansson, H., Semmrich, M., Rivollier, A., Hägerbrand, K., Marsal, J., Gudjonsson, S., Håkansson, U., Reizis, B., Kotarsky, K. and Agace, W. W. (2013) 'IRF4 Transcription-Factor-Dependent CD103(+)CD11b(+) Dendritic Cells Drive Mucosal T Helper 17 Cell Differentiation.', *Immunity*, 38(5), pp. 958–969. doi: 10.1016/j.immuni.2013.03.009.

Pflicke, H. and Sixt, M. (2009) 'Preformed portals facilitate dendritic cell entry into afferent lymphatic vessels.', *Journal of Experimental Medicine*, 206(13), pp. 2925–2935. doi: 10.1084/jem.20091739.

Phythian-Adams, A. T., Cook, P. C., Lundie, R. J., Jones, L. H., Smith, K. A., Barr, T. A., Hochweller, K., Anderton, S. M., Hämmerling, G. J., Maizels, R. M. and MacDonald, A. S. (2010) 'CD11c depletion severely disrupts Th2 induction and development in vivo.', *Journal of Experimental Medicine*, 207(10), pp. 2089–2096. doi: 10.1084/jem.20100734.

Pierre, P., Turley, S. J., Gatti, E., Hull, M., Meltzer, J., Mirza, A., Inaba, K., Steinman, R. M. and Mellman, I. (1997) 'Developmental regulation of MHC class II transport in mouse dendritic cells.', *Nature*, 388(6644), pp. 787–792. doi: 10.1038/42039.

Piva, L., Tetlak, P., Claser, C., Karjalainen, K., Renia, L. and Ruedl, C. (2012) 'Cutting Edge: Clec9A+ Dendritic Cells Mediate the Development of Experimental Cerebral Malaria.', *The Journal of Immunology*, pp. –. doi: 10.4049/jimmunol.1201171.

Pixley, F. J. and Stanley, E. R. (2004) 'CSF-1 regulation of the wandering macrophage: complexity in action.', *Trends in cell biology*, 14(11), pp. 628–638. doi: 10.1016/j.tcb.2004.09.016.

Plantinga, M., Guilliams, M., Vanheerswynghels, M., Deswarte, K., Branco-Madeira, F., Toussaint, W., Vanhoutte, L., Neyt, K., Killeen, N., Malissen, B., Hammad, H. and Lambrecht, B. N. (2013) 'Conventional and monocyte-derived CD11b(+) dendritic cells initiate and maintain T helper 2 cell-mediated immunity to house dust mite allergen.', *Immunity*, 38(2), pp. 322–335. doi: 10.1016/j.immuni.2012.10.016.

Poholek, A. C., Hansen, K., Hernandez, S. G., Eto, D., Chandele, A., Weinstein, J. S., Dong, X., Odegard, J. M., Kaech, S. M., Dent, A. L., Crotty, S. and Craft, J. (2010) 'In vivo regulation of Bcl6 and T follicular helper cell development.', *The Journal of Immunology*, 185(1), pp. 313–326. doi: 10.4049/jimmunol.0904023.

Poltorak, M. P. and Schraml, B. U. (2015) 'Fate mapping of dendritic cells.', *Frontiers in immunology*, 6, p. 199. doi: 10.3389/fimmu.2015.00199.

Pooley, J. L., Heath, W. R. and Shortman, K. (2001) 'Cutting edge: intravenous soluble antigen is presented to CD4 T cells by CD8- dendritic cells, but cross-presented to CD8 T cells by CD8+ dendritic cells.', *Journal of immunology (Baltimore, Md : 1950)*, 166(9), pp. 5327–5330.

Poulin, L. F., Henri, S., de Bovis, B., Devilard, E., Kissenpfennig, A. and Malissen, B. (2007) 'The dermis contains langerin+ dendritic cells that develop and function independently of epidermal Langerhans cells', *The Journal of experimental medicine*, 204(13), pp. 3119–3131. doi: 10.1084/jem.20071724.

Probst, H. C., Lagnel, J., Kollias, G. and van den Broek, M. (2003) 'Inducible transgenic mice reveal resting dendritic cells as potent inducers of CD8+ T cell tolerance.', *Immunity*, 18(5), pp. 713–720.

Probst, H. C., McCoy, K., Okazaki, T., Honjo, T. and van den Broek, M. (2005) 'Resting dendritic cells induce peripheral CD8+ T cell tolerance through PD-1 and CTLA-4.', *Nature Immunology*, 6(3), pp. 280–286. doi: 10.1038/ni1165.

Probst, H. C., Tschannen, K., Odermatt, B., Schwendener, R., Zinkernagel, R. M. and Van Den Broek, M. (2005) 'Histological analysis of CD11c-DTR/GFP mice after in vivo depletion of dendritic cells.', *Clinical and experimental immunology*, 141(3), pp. 398–404. doi: 10.1111/j.1365-2249.2005.02868.x.

Qiu, C.-H., Miyake, Y., Kaise, H., Kitamura, H., Ohara, O. and Tanaka, M. (2009) 'Novel subset of CD8{alpha}+ dendritic cells localized in the marginal zone is responsible for tolerance to cell-associated antigens.', *The Journal of Immunology*, 182(7), pp. 4127–4136. doi: 10.4049/jimmunol.0803364.

Radtke, A. J., Kastenmuller, W., Espinosa, D. A., Gerner, M. Y., Tse, S.-W., Sinnis, P., Germain, R. N., Zavala, F. P. and Cockburn, I. A. (2015) 'Lymph-Node Resident CD8α+ Dendritic Cells Capture Antigens from Migratory Malaria Sporozoites and Induce CD8+ T Cell Responses.', *PLoS pathogens*, 11(2), p. e1004637. doi: 10.1371/journal.ppat.1004637.

Rathinam, C., Geffers, R., Yücel, R., Buer, J., Welte, K., Möröy, T. and Klein, C. (2005) 'The transcriptional repressor Gfi1 controls STAT3-dependent dendritic cell development and function.', *Immunity*, 22(6), pp. 717–728. doi: 10.1016/j.immuni.2005.04.007.

Ratzinger, G., Stoitzner, P., Ebner, S., Lutz, M. B., Layton, G. T., Rainer, C., Senior, R. M., Shipley, J. M., Fritsch, P., Schuler, G. and Romani, N. (2002) 'Matrix metalloproteinases 9 and 2 are necessary for the migration of Langerhans cells and dermal dendritic cells from human and murine skin.', *Journal of immunology*

(Baltimore, Md : 1950), 168(9), pp. 4361–4371.

Reis e Sousa, C. (2004) 'Toll-like receptors and dendritic cells: for whom the bug tolls.', *Seminars in Immunology*, 16(1), pp. 27–34.

Reis e Sousa, C., Hieny, S., Scharton-Kersten, T., Jankovic, D., Charest, H., Germain, R. N. and Sher, A. (1997) 'In vivo microbial stimulation induces rapid CD40 ligand-independent production of interleukin 12 by dendritic cells and their redistribution to T cell areas.', *The Journal of experimental medicine*, 186(11), pp. 1819–1829.

Rickert, R. C., Roes, J. and Rajewsky, K. (1997) 'B lymphocyte-specific, Cre-mediated mutagenesis in mice.', *Nucleic Acids Research*, 25(6), pp. 1317–1318.

Rivollier, A., He, J., Kole, A., Valatas, V. and Kelsall, B. L. (2012) 'Inflammation switches the differentiation program of Ly6Chi monocytes from antiinflammatory macrophages to inflammatory dendritic cells in the colon.', *The Journal of experimental medicine*, 209(1), pp. 139–155. doi: 10.1084/jem.20101387.

Robbiani, D. F., Finch, R. A., Jäger, D., Muller, W. A., Sartorelli, A. C. and Randolph, G. J. (2000) 'The leukotriene C(4) transporter MRP1 regulates CCL19 (MIP-3beta, ELC)-dependent mobilization of dendritic cells to lymph nodes.', *Cell*, 103(5), pp. 757–768.

Robbins, S. H., Walzer, T., Dembélé, D., Thibault, C., Defays, A., Bessou, G., Xu, H., Vivier, E., Sellars, M., Pierre, P., Sharp, F. R., Chan, S., Kastner, P. and Dalod, M. (2008) 'Novel insights into the relationships between dendritic cell subsets in human and mouse revealed by genome-wide expression profiling.', *Genome Biology*, 9(1), p. R17. doi: 10.1186/gb-2008-9-1-r17.

Roche, P. A. and Furuta, K. (2015) 'The ins and outs of MHC class II-mediated antigen processing and presentation.', *Nature Reviews Immunology*. doi: 10.1038/nri3818.

Rodero, M. P., Licata, F., Poupel, L., Hamon, P., Khosrotehrani, K., Combadière, C. and Boissonnas, A. (2014) 'In vivo imaging reveals a pioneer wave of monocyte recruitment into mouse skin wounds.', *PloS one*, 9(10), p. e108212. doi: 10.1371/journal.pone.0108212.

Saito, M., Iwawaki, T., Taya, C., Yonekawa, H., Noda, M., Inui, Y., Mekada, E., Kimata, Y., Tsuru, A. and Kohno, K. (2001) 'Diphtheria toxin receptor-mediated conditional and targeted cell ablation in transgenic mice.', *Nature biotechnology*, 19(8), pp. 746–750. doi: 10.1038/90795.

Samokhvalov, I. M., Samokhvalova, N. I. and Nishikawa, S.-I. (2007) 'Cell tracing shows the contribution of the yolk sac to adult haematopoiesis.', *Nature*, 446(7139), pp. 1056–1061. doi: 10.1038/nature05725.

Sancho, D., Joffre, O. P., Keller, A. M., Rogers, N. C., Martínez, D., Hernanz-Falcón, P., Rosewell, I. and Reis e Sousa, C. (2009) 'Identification of a dendritic cell receptor that couples sensing of necrosis to immunity.', *Nature*, 458(7240), pp.

899–903. doi: 10.1038/nature07750.

Sancho, D., Mourão-Sá, D., Joffre, O. P., Schulz, O., Rogers, N. C., Pennington, D. J., Carlyle, J. R. and Reis e Sousa, C. (2008) 'Tumor therapy in mice via antigen targeting to a novel, DC-restricted C-type lectin.', *The Journal of clinical investigation*, 118(6), pp. 2098–2110. doi: 10.1172/JCI34584.

Sathe, P., Metcalf, D., Vremec, D., Naik, S. H., Langdon, W. Y., Huntington, N. D., Wu, L. and Shortman, K. (2014) 'Lymphoid Tissue and Plasmacytoid Dendritic Cells and Macrophages Do Not Share a Common Macrophage-Dendritic Cell-Restricted Progenitor', *Immunity*. Elsevier Inc., 41(1), pp. 104–115. doi: 10.1016/j.immuni.2014.05.020.

Sathe, P., Pooley, J., Vremec, D., Mintern, J., Jin, J.-O., Wu, L., Kwak, J.-Y., Villadangos, J. A. and Shortman, K. (2011) 'The acquisition of antigen cross-presentation function by newly formed dendritic cells.', *The Journal of Immunology*, 186(9), pp. 5184–5192. doi: 10.4049/jimmunol.1002683.

Sathe, P., Vremec, D., Wu, L., Corcoran, L. and Shortman, K. (2013) 'Convergent differentiation: myeloid and lymphoid pathways to murine plasmacytoid dendritic cells.', *Blood*, 121(1), pp. 11–19. doi: 10.1182/blood-2012-02-413336.

Satpathy, A. T., Briseño, C. G., Cai, X., Michael, D. G., Chou, C., Hsiung, S., Bhattacharya, D., Speck, N. A. and Egawa, T. (2014) 'Runx1 and Cbfβ regulate the development of Flt3+ dendritic cell progenitors and restrict myeloproliferative disorder.', *Blood*, 123(19), pp. 2968–2977. doi: 10.1182/blood-2013-11-539643.

Satpathy, A. T., Briseño, C. G., Lee, J. S., Ng, D., Manieri, N. A., Kc, W., Wu, X., Thomas, S. R., Lee, W.-L., Turkoz, M., McDonald, K. G., Meredith, M. M., Song, C., Guidos, C. J., Newberry, R. D., Ouyang, W., Murphy, T. L., Stappenbeck, T. S., Gommerman, J. L., Nussenzweig, M. C., Colonna, M., Kopan, R. and Murphy, K. M. (2013) 'Notch2-dependent classical dendritic cells orchestrate intestinal immunity to attaching-and-effacing bacterial pathogens.', *Nature Immunology*, 14(9), pp. 937–948. doi: 10.1038/ni.2679.

Satpathy, A. T., KC, W., Albring, J. C., Edelson, B. T., Kretzer, N. M., Bhattacharya, D., Murphy, T. L. and Murphy, K. M. (2012) 'Zbtb46 expression distinguishes classical dendritic cells and their committed progenitors from other immune lineages', *The Journal of experimental medicine*. doi: 10.1084/jem.20120030.

Satpathy, A. T., Wu, X., Albring, J. C. and Murphy, K. M. (2012) 'Re(de)fining the dendritic cell lineage', *Nature Immunology*, 13(12), pp. 1145–1154. doi: 10.1038/ni.2467.

Sauer, B. and Henderson, N. (1988) 'Site-specific DNA recombination in mammalian cells by the Cre recombinase of bacteriophage P1.', *Proceedings of the National Academy of Sciences of the United States of America*, 85(14), pp. 5166–5170.

Savina, A., Jancic, C., Hugues, S., Guermonprez, P., Vargas, P., Moura, I. C., Lennon-Dumenil, A.-M., Seabra, M. C., Raposo, G. and Amigorena, S. (2006)

'NOX2 controls phagosomal pH to regulate antigen processing during crosspresentation by dendritic cells.', *Cell*, 126(1), pp. 205–218. doi: 10.1016/j.cell.2006.05.035.

Scheinecker, C., McHugh, R., Shevach, E. M. and Germain, R. N. (2002) 'Constitutive presentation of a natural tissue autoantigen exclusively by dendritic cells in the draining lymph node.', *The Journal of experimental medicine*, 196(8), pp. 1079–1090.

Schiavoni, G., Mattei, F., Borghi, P., Sestili, P., Venditti, M., Morse, H. C., Belardelli, F. and Gabriele, L. (2004) 'ICSBP is critically involved in the normal development and trafficking of Langerhans cells and dermal dendritic cells.', *Blood*, 103(6), pp. 2221–2228. doi: 10.1182/blood-2003-09-3007.

Schlitzer, A., McGovern, N. and Ginhoux, F. (2015) 'Dendritic cells and monocyte-derived cells: Two complementary and integrated functional systems.', *Seminars in cell & developmental biology*. doi: 10.1016/j.semcdb.2015.03.011.

Schlitzer, A., McGovern, N., Teo, P., Zelante, T., Atarashi, K., Low, D., Ho, A. W. S., See, P., Shin, A., Wasan, P. S., Hoeffel, G., Malleret, B., Heiseke, A., Chew, S., Jardine, L., Purvis, H. A., Hilkens, C. M. U., Tam, J., Poidinger, M., Stanley, E. R., Krug, A. B., Renia, L., Sivasankar, B., Ng, L. G., Collin, M., Ricciardi-Castagnoli, P., Honda, K., Haniffa, M. and Ginhoux, F. (2013) 'IRF4 Transcription Factor-Dependent CD11b(+) Dendritic Cells in Human and Mouse Control Mucosal IL-17 Cytokine Responses.', *Immunity*, 38(5), pp. 970–983. doi: 10.1016/j.immuni.2013.04.011.

Schnorrer, P., Behrens, G. M. N., Wilson, N. S., Pooley, J. L., Smith, C. M., El-Sukkari, D., Davey, G., Kupresanin, F., Li, M., Maraskovsky, E., Belz, G. T., Carbone, F. R., Shortman, K., Heath, W. R. and Villadangos, J. A. (2006) 'The dominant role of CD8+ dendritic cells in cross-presentation is not dictated by antigen capture.', *Proceedings of the National Academy of Sciences of the United States of America*, 103(28), pp. 10729–10734. doi: 10.1073/pnas.0601956103.

Schnupf, P., Gaboriau-Routhiau, V., Gros, M., Friedman, R., Moya-Nilges, M., Nigro, G., Cerf-Bensussan, N. and Sansonetti, P. J. (2015) 'Growth and host interaction of mouse segmented filamentous bacteria in vitro.', *Nature*, 520(7545), pp. 99–103. doi: 10.1038/nature14027.

Schraml, B. U. and Reis e Sousa, C. (2014) 'Defining dendritic cells.', *Current opinion in immunology*, 32C, pp. 13–20. doi: 10.1016/j.coi.2014.11.001.

Schraml, B. U., van Blijswijk, J., Zelenay, S., Whitney, P. G., Filby, A., Acton, S. E., Rogers, N. C., Moncaut, N., Carvajal, J. J. and Reis e Sousa, C. (2013) 'Genetic Tracing via DNGR-1 Expression History Defines Dendritic Cells as a Hematopoietic Lineage', *Cell*. Elsevier Inc., 154(4), pp. 843–858. doi: 10.1016/j.cell.2013.07.014.

Schreiber, H. A., Loschko, J., Karssemeijer, R. A., Escolano, A., Meredith, M. M., Mucida, D., Guermonprez, P. and Nussenzweig, M. C. (2013) 'Intestinal monocytes and macrophages are required for T cell polarization in response to Citrobacter rodentium', *Journal of Experimental Medicine*, 210(10), pp. 2025–2039. doi:

10.1038/nm1720.

Schulz, C, Perdiguero, E. G., Chorro, L., Szabo-Rogers, H., Cagnard, N., Kierdorf, K., Prinz, M., Wu, B., Jacobsen, S. E. W., Pollard, J. W., Frampton, J., Liu, K. J. and Geissmann, F. (2012) 'A Lineage of Myeloid Cells Independent of Myb and Hematopoietic Stem Cells', *Science (New York, NY)*, 336(6077), pp. 86–90. doi: 10.1126/science.1219179.

Schulz, O, Edwards, A. D., Schito, M., Aliberti, J., Manickasingham, S., Sher, A. and Reis e Sousa, C. (2000) 'CD40 triggering of heterodimeric IL-12 p70 production by dendritic cells in vivo requires a microbial priming signal.', *Immunity*, 13(4), pp. 453–462.

Schulz, Olga, Jaensson, E., Persson, E. K., Liu, X., Worbs, T., Agace, W. W. and Pabst, O. (2009) 'Intestinal CD103+, but not CX3CR1+, antigen sampling cells migrate in lymph and serve classical dendritic cell functions.', *Journal of Experimental Medicine*, 206(13), pp. 3101–3114. doi: 10.1084/jem.20091925.

Schulz, Oliver and Reis e Sousa, C. (2002) 'Cross-presentation of cell-associated antigens by CD8alpha+ dendritic cells is attributable to their ability to internalize dead cells.', *Immunology*, 107(2), pp. 183–189.

Scott, C. L., Bain, C. C., Wright, P. B., Sichien, D., Kotarsky, K., Persson, E. K., Luda, K., Guilliams, M., Lambrecht, B. N., Agace, W. W., Milling, S. W. and Mowat, A. M. (2015) 'CCR2(+)CD103(-) intestinal dendritic cells develop from DC-committed precursors and induce interleukin-17 production by T cells.', *Mucosal Immunology*, 8(2), pp. 327–339. doi: 10.1038/mi.2014.70.

Scott, E. W., Simon, M. C., Anastasi, J. and Singh, H. (1994) 'Requirement of transcription factor PU.1 in the development of multiple hematopoietic lineages.', *Science (New York, NY)*, 265(5178), pp. 1573–1577.

Seillet, C., Jackson, J. T., Markey, K. A., Brady, H. J. M., Hill, G. R., Macdonald, K. P. A., Nutt, S. L. and Belz, G. T. (2013) 'CD8α+ DCs can be induced in the absence of transcription factors Id2, Nfil3, and Batf3.', *Blood*, 121(9), pp. 1574–1583. doi: 10.1182/blood-2012-07-445650.

Serbina, N. V. and Pamer, E. G. (2006) 'Monocyte emigration from bone marrow during bacterial infection requires signals mediated by chemokine receptor CCR2.', *Nature Immunology*, 7(3), pp. 311–317. doi: 10.1038/ni1309.

Serbina, N. V., Kuziel, W., Flavell, R., Akira, S., Rollins, B. and Pamer, E. G. (2003) 'Sequential MyD88-independent and -dependent activation of innate immune responses to intracellular bacterial infection.', *Immunity*, 19(6), pp. 891–901. doi: 10.4103/2045-8932.109921?ref=no-x-route:7b18466ca0d0bb05b5bddff5e700051f.

Serbina, N. V., Salazar-Mather, T. P., Biron, C. A., Kuziel, W. A. and Pamer, E. G. (2003) 'TNF/iNOS-producing dendritic cells mediate innate immune defense against bacterial infection.', *Immunity*, 19(1), pp. 59–70.

Shalek, A. K., Satija, R., Adiconis, X., Gertner, R. S., Gaublomme, J. T.,

Raychowdhury, R., Schwartz, S., Yosef, N., Malboeuf, C., Lu, D., Trombetta, J. T., Gennert, D., Gnirke, A., Goren, A., Hacohen, N., Levin, J. Z., Park, H. and Regev, A. (2013) 'Single-cell transcriptomics reveals bimodality in expression and splicing in immune cells.', *Nature*. doi: 10.1038/nature12172.

Sheng, J., Ruedl, C. and Karjalainen, K. (2015) 'Most Tissue-Resident Macrophages Except Microglia Are Derived from Fetal Hematopoietic Stem Cells', *Immunity*. Elsevier Inc., 43(2), pp. 382–393. doi: 10.1016/j.immuni.2015.07.016.

Sitnicka, E., Bryder, D., Theilgaard-Mönch, K., Buza-Vidas, N., Adolfsson, J. and Jacobsen, S. E. W. (2002) 'Key role of flt3 ligand in regulation of the common lymphoid progenitor but not in maintenance of the hematopoietic stem cell pool.', *Immunity*, 17(4), pp. 463–472.

Smith, C. M., Wilson, N. S., Waithman, J., Villadangos, J. A., Carbone, F. R., Heath, W. R. and Belz, G. T. (2004) 'Cognate CD4(+) T cell licensing of dendritic cells in CD8(+) T cell immunity.', *Nature Immunology*, 5(11), pp. 1143–1148. doi: 10.1038/ni1129.

Smith, K. A., Harcus, Y., Garbi, N., Hämmerling, G. J., MacDonald, A. S. and Maizels, R. M. (2012) 'Type 2 innate immunity in helminth infection is induced redundantly and acts autonomously following CD11c(+) cell depletion.', *Infection and immunity*, 80(10), pp. 3481–3489. doi: 10.1128/IAI.00436-12.

Smith, K. A., Hochweller, K., Hämmerling, G. J., Boon, L., MacDonald, A. S. and Maizels, R. M. (2011) 'Chronic helminth infection promotes immune regulation in vivo through dominance of CD11cloCD103- dendritic cells.', *The Journal of Immunology*, 186(12), pp. 7098–7109. doi: 10.4049/jimmunol.1003636.

Snippert, H. J., van der Flier, L. G., Sato, T., van Es, J. H., van den Born, M., Kroon-Veenboer, C., Barker, N., Klein, A. M., van Rheenen, J., Simons, B. D. and Clevers, H. (2010) 'Intestinal crypt homeostasis results from neutral competition between symmetrically dividing Lgr5 stem cells.', *Cell*, 143(1), pp. 134–144. doi: 10.1016/j.cell.2010.09.016.

Srinivas, S., Watanabe, T., Lin, C. S., William, C. M., Tanabe, Y., Jessell, T. M. and Costantini, F. (2001) 'Cre reporter strains produced by targeted insertion of EYFP and ECFP into the ROSA26 locus.', *BMC developmental biology*, 1, p. 4.

Steinman, R. M. and Cohn, Z. A. (1973) 'Identification of a novel cell type in peripheral lymphoid organs of mice. I. Morphology, quantitation, tissue distribution', *The Journal of experimental medicine*, 137(5), pp. 1142–1162.

Steinman, R. M. and Cohn, Z. A. (1974) 'Identification of a novel cell type in peripheral lymphoid organs of mice. II. Functional properties in vitro.', *The Journal of experimental medicine*, 139(2), pp. 380–397.

Steinman, R. M. and Idoyaga, J. (2010) 'Features of the dendritic cell lineage.', *Immunological reviews*, 234(1), pp. 5–17. doi: 10.1111/j.0105-2896.2009.00888.x.

Steinman, R. M. and Witmer, M. D. (1978) 'Lymphoid dendritic cells are potent

stimulators of the primary mixed leukocyte reaction in mice.', *Proceedings of the National Academy of Sciences of the United States of America*, 75(10), pp. 5132–5136.

Steinman, R. M., Adams, J. C. and Cohn, Z. A. (1975) 'Identification of a novel cell type in peripheral lymphoid organs of mice. IV. Identification and distribution in mouse spleen.', *The Journal of experimental medicine*, 141(4), pp. 804–820.

Steinman, R. M., Gutchinov, B., Witmer, M. D. and Nussenzweig, M. C. (1983) 'Dendritic cells are the principal stimulators of the primary mixed leukocyte reaction in mice', *The Journal of experimental medicine*, 157(2), pp. 613–627.

Steinman, R. M., Lustig, D. S. and Cohn, Z. A. (1974) 'Identification of a novel cell type in peripheral lymphoid organs of mice. 3. Functional properties in vivo.', *The Journal of experimental medicine*, 139(6), pp. 1431–1445.

Sternberg, N. and Hamilton, D. (1981) 'Bacteriophage P1 site-specific recombination. I. Recombination between loxP sites.', *Journal of molecular biology*, 150(4), pp. 467–486.

Sun, C.-M., Hall, J. A., Blank, R. B., Bouladoux, N., Oukka, M., Mora, J. R. and Belkaid, Y. (2007) 'Small intestine lamina propria dendritic cells promote de novo generation of Foxp3 T reg cells via retinoic acid.', *The Journal of experimental medicine*, 204(8), pp. 1775–1785. doi: 10.1084/jem.20070602.

Sung, S. S. J., Fu, S. M., Rose, C. E., Gaskin, F., Ju, S. T. and Beaty, S. R. (2006) 'A Major Lung CD103 (E)- 7 Integrin-Positive Epithelial Dendritic Cell Population Expressing Langerin and Tight Junction Proteins', *The Journal of Immunology*, 176(4), pp. 2161–2172. doi: 10.4049/jimmunol.176.4.2161.

Suzuki, S., Honma, K., Matsuyama, T., Suzuki, K., Toriyama, K., Akitoyo, I., Yamamoto, K., Suematsu, T., Nakamura, M., Yui, K. and Kumatori, A. (2004) 'Critical roles of interferon regulatory factor 4 in CD11bhighCD8alpha- dendritic cell development.', *Proceedings of the National Academy of Sciences of the United States of America*, 101(24), pp. 8981–8986. doi: 10.1073/pnas.0402139101.

Swiecki, M., Gilfillan, S., Vermi, W., Wang, Y. and Colonna, M. (2010) 'Plasmacytoid dendritic cell ablation impacts early interferon responses and antiviral NK and CD8(+) T cell accrual', *Immunity*, 33(6), pp. 955–966. doi: 10.1016/j.immuni.2010.11.020.

Swiecki, M., Wang, Y., Riboldi, E., Kim, A. H. J., Dzutsev, A., Gilfillan, S., Vermi, W., Ruedl, C., Trinchieri, G. and Colonna, M. (2014) 'Cell Depletion in Mice That Express Diphtheria Toxin Receptor under the Control of SiglecH Encompasses More Than Plasmacytoid Dendritic Cells', *The Journal of Immunology*. doi: 10.4049/jimmunol.1303135.

Swirski, F. K., Nahrendorf, M., Etzrodt, M., Wildgruber, M., Cortez-Retamozo, V., Panizzi, P., Figueiredo, J.-L., Kohler, R. H., Chudnovskiy, A., Waterman, P., Aikawa, E., Mempel, T. R., Libby, P., Weissleder, R. and Pittet, M. J. (2009) 'Identification of splenic reservoir monocytes and their deployment to inflammatory

sites.', *Science (New York, NY)*, 325(5940), pp. 612–616. doi: 10.1126/science.1175202.

Tailor, P., Tamura, T., Morse, H. C. and Ozato, K. (2008) 'The BXH2 mutation in IRF8 differentially impairs dendritic cell subset development in the mouse.', *Blood*, 111(4), pp. 1942–1945. doi: 10.1182/blood-2007-07-100750.

Takagi, H., Fukaya, T., Eizumi, K., Sato, Y., Sato, K., Shibazaki, A., Otsuka, H., Hijikata, A., Watanabe, T., Ohara, O., Kaisho, T., Malissen, B. and Sato, K. (2011) 'Plasmacytoid Dendritic Cells Are Crucial for the Initiation of Inflammation and T Cell Immunity In Vivo', *Immunity*, 35(6), pp. 958–971. doi: 10.1016/j.immuni.2011.10.014.

Tal, O., Lim, H. Y., Gurevich, I., Milo, I., Shipony, Z., Ng, L. G., Angeli, V. and Shakhar, G. (2011) 'DC mobilization from the skin requires docking to immobilized CCL21 on lymphatic endothelium and intralymphatic crawling.', *The Journal of experimental medicine*, 208(10), pp. 2141–2153. doi: 10.1084/jem.20102392.

Tamoutounour, S., Guilliams, M., Montanana Sanchis, F., Liu, H., Terhorst, D., Malosse, C., Pollet, E., Ardouin, L., Luche, H., Sanchez, C., Dalod, M., Malissen, B. and Henri, S. (2013) 'Origins and functional specialization of macrophages and of conventional and monocyte-derived dendritic cells in mouse skin.', *Immunity*, 39(5), pp. 925–938. doi: 10.1016/j.immuni.2013.10.004.

Tamoutounour, S., Henri, S., Lelouard, H., de Bovis, B., de Haar, C., van der Woude, C. J., Woltman, A. M., Reyal, Y., Bonnet, D., Sichien, D., Bain, C. C., Mcl Mowat, A., Reis e Sousa, C., Poulin, L. F., Malissen, B. and Guilliams, M. (2012) 'CD64 distinguishes macrophages from dendritic cells in the gut and reveals the Th1-inducing role of mesenteric lymph node macrophages during colitis', *European journal of immunology*, pp. n/a–n/a. doi: 10.1002/eji.201242847.

Tamura, T. T., Nagamura-Inoue, T. T., Shmeltzer, Z. Z., Kuwata, T. T. and Ozato, K. K. (2000) 'ICSBP Directs Bipotential Myeloid Progenitor Cells to Differentiate into Mature Macrophages', *Immunity*, 13(2), pp. 11–11. doi: 10.1016/S1074-7613(00)00016-9.

Tang, A., Amagai, M., Granger, L. G., Stanley, J. R. and Udey, M. C. (1993) 'Adhesion of epidermal Langerhans cells to keratinocytes mediated by E-cadherin.', *Nature*, 361(6407), pp. 82–85. doi: 10.1038/361082a0.

Tang, H., Cao, W., Kasturi, S. P., Ravindran, R., Nakaya, H. I., Kundu, K., Murthy, N., Kepler, T. B., Malissen, B. and Pulendran, B. (2010) 'The T helper type 2 response to cysteine proteases requires dendritic cell-basophil cooperation via ROS-mediated signaling.', *Nature Immunology*, 11(7), pp. 608–617. doi: 10.1038/ni.1883.

Terhorst, D., Fossum, E., Baranska, A., Tamoutounour, S., Malosse, C., Garbani, M., Braun, R., Lechat, E., Crameri, R., Bogen, B., Henri, S. and Malissen, B. (2015) 'Laser-assisted intradermal delivery of adjuvant-free vaccines targeting XCR1+ dendritic cells induces potent antitumoral responses.', *The Journal of Immunology*, 194(12), pp. 5895–5902. doi: 10.4049/jimmunol.1500564.

Tittel, A. P., Heuser, C., Ohliger, C., Llanto, C., Yona, S., Hämmerling, G. J., Engel, D. R., Garbi, N. and Kurts, C. (2012) 'Functionally relevant neutrophilia in CD11c diphtheria toxin receptor transgenic mice', *Nature Methods*. Nature Publishing Group, 9(4), pp. 385–390. doi: 10.1038/nmeth.1905.

Traver, D., Akashi, K., Manz, M., Merad, M., Miyamoto, T., Engleman, E. G. and Weissman, I. L. (2000) 'Development of CD8alpha-positive dendritic cells from a common myeloid progenitor.', *Science (New York, NY)*, 290(5499), pp. 2152–2154.

Trombetta, E. S., Ebersold, M., Garrett, W., Pypaert, M. and Mellman, I. (2003) 'Activation of lysosomal function during dendritic cell maturation.', *Science (New York, NY)*, 299(5611), pp. 1400–1403. doi: 10.1126/science.1080106.

Tsujimura, H. H., Nagamura-Inoue, T. T., Tamura, T. T. and Ozato, K. K. (2002) 'IFN consensus sequence binding protein/IFN regulatory factor-8 guides bone marrow progenitor cells toward the macrophage lineage.', *Journal of immunology (Baltimore, Md : 1950)*, 169(3), pp. 1261–1269.

Tsujimura, H., Tamura, T. and Ozato, K. (2003) 'Cutting edge: IFN consensus sequence binding protein/IFN regulatory factor 8 drives the development of type I IFN-producing plasmacytoid dendritic cells.', *Journal of immunology (Baltimore, Md : 1950)*, 170(3), pp. 1131–1135.

Tussiwand, R., Everts, B., Grajales-Reyes, G. E., Kretzer, N. M., Iwata, A., Bagaitkar, J., Wu, X., Wong, R., Anderson, D. A., Murphy, T. L., Pearce, E. J. and Murphy, K. M. (2015) 'Klf4 expression in conventional dendritic cells is required for T helper 2 cell responses.', *Immunity*, 42(5), pp. 916–928. doi: 10.1016/j.immuni.2015.04.017.

Tussiwand, R., Lee, W.-L., Murphy, T. L., Mashayekhi, M., Kc, W., Albring, J. C., Satpathy, A. T., Rotondo, J. A., Edelson, B. T., Kretzer, N. M., Wu, X., Weiss, L. A., Glasmacher, E., Li, P., Liao, W., Behnke, M., Lam, S. S. K., Aurthur, C. T., Leonard, W. J., Singh, H., Stallings, C. L., Sibley, L. D., Schreiber, R. D. and Murphy, K. M. (2012) 'Compensatory dendritic cell development mediated by BATF-IRF interactions', *Nature*. Nature Publishing Group, pp. 1–9. doi: 10.1038/nature11531.

Uematsu, S., Fujimoto, K., Jang, M. H., Yang, B.-G., Jung, Y.-J., Nishiyama, M., Sato, S., Tsujimura, T., Yamamoto, M., Yokota, Y., Kiyono, H., Miyasaka, M., Ishii, K. J. and Akira, S. (2008) 'Regulation of humoral and cellular gut immunity by lamina propria dendritic cells expressing Toll-like receptor 5.', *Nature Immunology*, 9(7), pp. 769–776. doi: 10.1038/ni.1622.

Valladeau, J., Ravel, O., Dezutter-Dambuyant, C., Moore, K., Kleijmeer, M., Liu, Y., Duvert-Frances, V., Vincent, C., Schmitt, D., Davoust, J., Caux, C., Lebecque, S. and Saeland, S. (2000) 'Langerin, a novel C-type lectin specific to Langerhans cells, is an endocytic receptor that induces the formation of Birbeck granules.', *Immunity*, 12(1), pp. 71–81.

van Blijswijk, J., Schraml, B. U. and Reis e Sousa, C. (2013) 'Advantages and limitations of mouse models to deplete dendritic cells.', *European journal of*

immunology, 43(1), pp. 22–26. doi: 10.1002/eji.201243022.

van de Pavert, S. A., Ferreira, M., Domingues, R. G., Ribeiro, H., Molenaar, R., Moreira-Santos, L., Almeida, F. F., Ibiza, S., Barbosa, I., Goverse, G., Labão-Almeida, C., Godinho-Silva, C., Konijn, T., Schooneman, D., O'Toole, T., Mizee, M. R., Habani, Y., Haak, E., Santori, F. R., Littman, D. R., Schulte-Merker, S., Dzierzak, E., Simas, J. P., Mebius, R. E. and Veiga-Fernandes, H. (2014) 'Maternal retinoids control type 3 innate lymphoid cells and set the offspring immunity', *Nature*. Nature Publishing Group, 508(7494), pp. 123–127. doi: 10.1038/nature13158.

van der Fits, L., Mourits, S., Voerman, J. S. A., Kant, M., Boon, L., Laman, J. D., Cornelissen, F., Mus, A.-M., Florencia, E., Prens, E. P. and Lubberts, E. (2009) 'Imiquimod-induced psoriasis-like skin inflammation in mice is mediated via the IL-23/IL-17 axis.', *The Journal of Immunology*, 182(9), pp. 5836–5845. doi: 10.4049/jimmunol.0802999.

van Rijt, L. S., Jung, S., Kleinjan, A., Vos, N., Willart, M., Duez, C., Hoogsteden, H. C. and Lambrecht, B. N. (2005) 'In vivo depletion of lung CD11c+ dendritic cells during allergen challenge abrogates the characteristic features of asthma.', *The Journal of experimental medicine*, 201(6), pp. 981–991. doi: 10.1084/jem.20042311.

Vander Lugt, B., Khan, A. A., Hackney, J. A., Agrawal, S., Lesch, J., Zhou, M., Lee, W. P., Park, S., Xu, M., Devoss, J., Spooner, C. J., Chalouni, C., Delamarre, L., Mellman, I. and Singh, H. (2014) 'Transcriptional programming of dendritic cells for enhanced MHC class II antigen presentation.', *Nature Immunology*, 15(2), pp. 161–167. doi: 10.1038/ni.2795.

Varol, C., Mildner, A. and Jung, S. (2015) 'Macrophages: development and tissue specialization.', *Annual Review of Immunology*, 33, pp. 643–675. doi: 10.1146/annurev-immunol-032414-112220.

Varol, C., Vallon-Eberhard, A., Elinav, E., Aychek, T., Shapira, Y., Luche, H., Fehling, H. J., Hardt, W.-D., Shakhar, G. and Jung, S. (2009) 'Intestinal lamina propria dendritic cell subsets have different origin and functions.', *Immunity*, 31(3), pp. 502–512. doi: 10.1016/j.immuni.2009.06.025.

Vassileva, G., Soto, H., Zlotnik, A., Nakano, H., Kakiuchi, T., Hedrick, J. A. and Lira, S. A. (1999) 'The reduced expression of 6Ckine in the plt mouse results from the deletion of one of two 6Ckine genes.', *The Journal of experimental medicine*, 190(8), pp. 1183–1188.

Ventura, A., Kirsch, D. G., McLaughlin, M. E., Tuveson, D. A., Grimm, J., Lintault, L., Newman, J., Reczek, E. E., Weissleder, R. and Jacks, T. (2007) 'Restoration of p53 function leads to tumour regression in vivo.', *Nature*, 445(7128), pp. 661–665. doi: 10.1038/nature05541.

Voehringer, D., Liang, H.-E. and Locksley, R. M. (2008) 'Homeostasis and effector function of lymphopenia-induced "memory-like" T cells in constitutively T cell-depleted mice.', *Journal of immunology (Baltimore, Md : 1950)*, 180(7), pp. 4742–

4753.

Waithman, J., Zanker, D., Xiao, K., Oveissi, S., Wylie, B., Ng, R., Tögel, L. and Chen, W. (2013) 'Resident CD8(+) and migratory CD103(+) dendritic cells control CD8 T cell immunity during acute influenza infection.', *PloS one*, 8(6), p. e66136. doi: 10.1371/journal.pone.0066136.

Wakim, L. M. and Bevan, M. J. (2011) 'Cross-dressed dendritic cells drive memory CD8+ T-cell activation after viral infection.', *Nature*, 471(7340), pp. 629–632. doi: 10.1038/nature09863.

Wakim, L. M., Waithman, J., Van Rooijen, N., Heath, W. R. and Carbone, F. R. (2008) 'Dendritic cell-induced memory T cell activation in nonlymphoid tissues.', *Science (New York, NY)*, 319(5860), pp. 198–202. doi: 10.1126/science.1151869.

Wang, P., Chen, T., Sakurai, K., Han, B.-X., He, Z., Feng, G. and Wang, F. (2012) 'Intersectional Cre Driver Lines Generated Using Split-Intein Mediated Split-Cre Reconstitution', *Scientific reports*, 2. doi: 10.1038/srep00497.

Wang, Y., Szretter, K. J., Vermi, W., Gilfillan, S., Rossini, C., Cella, M., Barrow, A. D., Diamond, M. S. and Colonna, M. (2012) 'IL-34 is a tissue-restricted ligand of CSF1R required for the development of Langerhans cells and microglia.', *Nature Immunology*, 13(8), pp. 753–760. doi: 10.1038/ni.2360.

Wang, Y.-G., Kim, K. D., Wang, J., Yu, P. and Fu, Y.-X. (2005) 'Stimulating lymphotoxin beta receptor on the dendritic cells is critical for their homeostasis and expansion.', *Journal of immunology (Baltimore, Md : 1950)*, 175(10), pp. 6997–7002.

Waskow, C., Liu, K., Darrasse-Jèze, G., Guermonprez, P., Ginhoux, F., Merad, M., Shengelia, T., Yao, K. and Nussenzweig, M. (2008) 'The receptor tyrosine kinase Flt3 is required for dendritic cell development in peripheral lymphoid tissues', *Nature Immunology*. Nature Publishing Group, 9(6), pp. 676–683. doi: 10.1038/ni.1615.

Weber, M., Hauschild, R., Schwarz, J., Moussion, C., de Vries, I., Legler, D. F., Luther, S. A., Bollenbach, T. and Sixt, M. (2013) 'Interstitial dendritic cell guidance by haptotactic chemokine gradients.', *Science (New York, NY)*, 339(6117), pp. 328–332. doi: 10.1126/science.1228456.

Welty, N. E., Staley, C., Ghilardi, N., Sadowsky, M. J., Igyarto, B. Z. and Kaplan, D. H. (2013) 'Intestinal lamina propria dendritic cells maintain T cell homeostasis but do not affect commensalism.', *Journal of Experimental Medicine*, 210(10), pp. 2011–2024. doi: 10.1084/jem.20130728.

Wendland, M., Czeloth, N., Mach, N., Malissen, B., Kremmer, E., Pabst, O. and Förster, R. (2007) 'CCR9 is a homing receptor for plasmacytoid dendritic cells to the small intestine.', *Proceedings of the National Academy of Sciences of the United States of America*, 104(15), pp. 6347–6352. doi: 10.1073/pnas.0609180104.

Wendland, M., Willenzon, S., Kocks, J., Davalos-Misslitz, A. C., Hammerschmidt,

S. I., Schumann, K., Kremmer, E., Sixt, M., Hoffmeyer, A., Pabst, O. and Förster, R. (2011) 'Lymph node T cell homeostasis relies on steady state homing of dendritic cells.', *Immunity*, 35(6), pp. 945–957. doi: 10.1016/j.immuni.2011.10.017.

West, M. A., Wallin, R. P. A., Matthews, S. P., Svensson, H. G., Zaru, R., Ljunggren, H.-G., Prescott, A. R. and Watts, C. (2004) 'Enhanced dendritic cell antigen capture via toll-like receptor-induced actin remodeling.', *Science (New York, NY)*, 305(5687), pp. 1153–1157. doi: 10.1126/science.1099153.

Westphalen, K., Gusarova, G. A., Islam, M. N., Subramanian, M., Cohen, T. S., Prince, A. S. and Bhattacharya, J. (2014) 'Sessile alveolar macrophages communicate with alveolar epithelium to modulate immunity.', *Nature*, 506(7489), pp. 503–506. doi: 10.1038/nature12902.

Whitney, P. G., Bär, E., Osorio, F., Rogers, N. C., Schraml, B. U., Deddouche, S., Leibundgut-Landmann, S. and Reis e Sousa, C. (2014) 'Syk signaling in dendritic cells orchestrates innate resistance to systemic fungal infection.', *PLoS pathogens*, 10(7), p. e1004276. doi: 10.1371/journal.ppat.1004276.

Williams, J. W., Tjota, M. Y., Clay, B. S., Vander Lugt, B., Bandukwala, H. S., Hrusch, C. L., Decker, D. C., Blaine, K. M., Fixsen, B. R., Singh, H., Sciammas, R. and Sperling, A. I. (2013) 'Transcription factor IRF4 drives dendritic cells to promote Th2 differentiation.', *Nature Communications*, 4, p. 2990. doi: 10.1038/ncomms3990.

Wolff, K. (1967) 'The fine structure of the Langerhans cell granule.', *The Journal of cell biology*, 35(2), pp. 468–473.

Wollenberg, A., Wagner, M., Günther, S., Towarowski, A., Tuma, E., Moderer, M., Rothenfusser, S., Wetzel, S., Endres, S. and Hartmann, G. (2002) 'Plasmacytoid dendritic cells: a new cutaneous dendritic cell subset with distinct role in inflammatory skin diseases.', *The Journal of investigative dermatology*, 119(5), pp. 1096–1102. doi: 10.1046/j.1523-1747.2002.19515.x.

Worbs, T., Mempel, T. R., Bölter, J., Andrian, von, U. H. and Förster, R. (2007) 'CCR7 ligands stimulate the intranodal motility of T lymphocytes in vivo.', *The Journal of experimental medicine*, 204(3), pp. 489–495. doi: 10.1084/jem.20061706.

Wu, L., D'Amico, A., Winkel, K. D., Suter, M., Lo, D. and Shortman, K. (1998) 'RelB is essential for the development of myeloid-related CD8alpha- dendritic cells but not of lymphoid-related CD8alpha+ dendritic cells.', *Immunity*, 9(6), pp. 839–847.

Wu, L., Nichogiannopoulou, A., Shortman, K. and Georgopoulos, K. (1997) 'Cell-autonomous defects in dendritic cell populations of Ikaros mutant mice point to a developmental relationship with the lymphoid lineage.', *Immunity*, 7(4), pp. 483–492.

Wu, Q., Wang, Y., Wang, J., Hedgeman, E. O., Browning, J. L. and Fu, Y. X. (1999) 'The requirement of membrane lymphotoxin for the presence of dendritic cells in lymphoid tissues.', *The Journal of experimental medicine*, 190(5), pp. 629–

638.

Xu, R.-H., Remakus, S., Ma, X., Roscoe, F. and Sigal, L. J. (2010) 'Direct presentation is sufficient for an efficient anti-viral CD8+ T cell response.', *PLoS pathogens*, 6(2), p. e1000768. doi: 10.1371/journal.ppat.1000768.

Yamazaki, C., Sugiyama, M., Ohta, T., Hemmi, H., Hamada, E., Sasaki, I., Fukuda, Y., Yano, T., Nobuoka, M., Hirashima, T., Iizuka, A., Sato, K., Tanaka, T., Hoshino, K. and Kaisho, T. (2013) 'Critical Roles of a Dendritic Cell Subset Expressing a Chemokine Receptor, XCR1', *The Journal of Immunology*. doi: 10.4049/jimmunol.1202798.

Yang, C. Y., Vogt, T. K., Favre, S., Scarpellino, L., Huang, H. Y., Tacchini-Cottier, F. and Luther, S. A. (2014) 'Trapping of naive lymphocytes triggers rapid growth and remodeling of the fibroblast network in reactive murine lymph nodes', *Proceedings of the National Academy of Sciences*, 111(1), pp. E109–E118. doi: 10.1073/pnas.1312585111.

Yao, C., Zurawski, S. M., Jarrett, E. S., Chicoine, B., Crabtree, J., Peterson, E. J., Zurawski, G., Kaplan, D. H. and Igyarto, B. Z. (2015) 'Skin dendritic cells induce follicular helper T cells and protective humoral immune responses.', *The Journal of allergy and clinical immunology*. doi: 10.1016/j.jaci.2015.04.001.

Yokota, Y., Mansouri, A., Mori, S., Sugawara, S., Adachi, S., Nishikawa, S. and Gruss, P. (1999) 'Development of peripheral lymphoid organs and natural killer cells depends on the helix-loop-helix inhibitor Id2.', *Nature*, 397(6721), pp. 702–706. doi: 10.1038/17812.

Yona, S., Kim, K.-W., Wolf, Y., Mildner, A., Varol, D., Breker, M., Strauss-Ayali, D., Viukov, S., Guilliams, M., Misharin, A., Hume, D. A., Perlman, H., Malissen, B., Zelzer, E. and Jung, S. (2012) 'Fate Mapping Reveals Origins and Dynamics of Monocytes and Tissue Macrophages under Homeostasis.', *Immunity*. doi: 10.1016/j.immuni.2012.12.001.

Zaft, T., Sapoznikov, A., Krauthgamer, R., Littman, D. R. and Jung, S. (2005) 'CD11chigh dendritic cell ablation impairs lymphopenia-driven proliferation of naive and memory CD8+ T cells.', *Journal of immunology (Baltimore, Md : 1950)*, 175(10), pp. 6428–6435.

Zahner, S. P., Kel, J. M., Martina, C. A. E., Brouwers-Haspels, I., van Roon, M. A. and Clausen, B. E. (2011) 'Conditional deletion of TGF-βR1 using Langerin-Cre mice results in Langerhans cell deficiency and reduced contact hypersensitivity.', *Journal of immunology (Baltimore, Md : 1950)*, 187(10), pp. 5069–5076. doi: 10.4049/jimmunol.1101880.

Zhan, Y., Carrington, E. M., van Nieuwenhuijze, A., Bedoui, S., Seah, S., Xu, Y., Wang, N., Mintern, J. D., Villadangos, J. A., Wicks, I. P. and Lew, A. M. (2011) 'GM-CSF increases cross-presentation and CD103 expression by mouse CD8□ spleen dendritic cells.', *European journal of immunology*, 41(9), pp. 2585–2595. doi: 10.1002/eji.201141540.

Zhang, J., Raper, A., Sugita, N., Hingorani, R., Salio, M., Palmowski, M. J., Cerundolo, V. and Crocker, P. R. (2006) 'Characterization of Siglec-H as a novel endocytic receptor expressed on murine plasmacytoid dendritic cell precursors', *Blood*, 107(9), pp. 3600–3608. doi: 10.1182/blood-2005-09-3842.

Zigmond, E., Varol, C., Farache, J., Elmaliah, E., Satpathy, A. T., Friedlander, G., Mack, M., Shpigel, N., Boneca, I. G., Murphy, K. M., Shakhar, G., Halpern, Z. and Jung, S. (2012) 'Ly6C hi monocytes in the inflamed colon give rise to proinflammatory effector cells and migratory antigen-presenting cells.', *Immunity*, 37(6), pp. 1076–1090. doi: 10.1016/j.immuni.2012.08.026.